INFORMATION TO USERS

This manuscript has been reproduced from the microfilm master. UMI films the text directly from the original or copy submitted. Thus, some thesis and dissertation copies are in typewriter face, while others may be from any type of computer printer.

The quality of this reproduction is dependent upon the quality of the copy submitted. Broken or indistinct print, colored or poor quality illustrations and photographs, print bleedthrough, substandard margins, and improper alignment can adversely affect reproduction.

In the unlikely event that the author did not send UMI a complete manuscript and there are missing pages, these will be noted. Also, if unauthorized copyright material had to be removed, a note will indicate the deletion.

Oversize materials (e.g., maps, drawings, charts) are reproduced by sectioning the original, beginning at the upper left-hand corner and continuing from left to right in equal sections with small overlaps. Each original is also photographed in one exposure and is included in reduced form at the back of the book.

Photographs included in the original manuscript have been reproduced xerographically in this copy. Higher quality 6" x 9" black and white photographic prints are available for any photographs or illustrations appearing in this copy for an additional charge. Contact UMI directly to order.

UMI

A Bell & Howell Information Company
300 North Zeeb Road, Ann Arbor MI 48106-1346 USA
313/761-4700 800/521-0600

A NESTED WATERSHED STUDY IN THE KUPARUK RIVER BASIN, ARCTIC ALASKA: STREAMFLOW, SCALING, AND DRAINAGE BASIN STRUCTURE

A THESIS

Presented to the Faculty

of the University of Alaska Fairbanks

in Partial Fulfillment of the Requirements

for the degree of

Doctor of Philosophy

By

James P. McNamara, B.S., M.S.

Fairbanks, Alaska

May 1997

A NESTED WATERSHED STUDY IN THE KUPARUK RIVER BASIN, ARCTIC ALASKA: STREAMFLOW, SCALING, AND DRAINAGE BASIN STRUCTURE

By

James P. McNamara

Recommended:

Advisory Committee Chair

Department Head

Approved:

Dean, College of Science, Engineering, and Mathematics

Dean of the Graduate School

4-14-97

Date

ABSTRACT

The central hypothesis of this dissertation is that permafrost influences the form, function, and scaling of hydrologic and geomorphologic characteristics in the Kuparuk River basin in Northern Alaska. This problem was addressed using three approaches: field hydrologic studies, statistical scaling studies, and geomorphology studies using digital elevation models.

Permafrost and snow exert significant controls on hydrologic processes in the Kuparuk River basin. Storm hydrographs show fast responses, long time lags, extended recessions, and high runoff/precipitation ratios. These features arise from the diminished storage capacity caused by permafrost. Summer storm flow compositions in the are dominated by old water, as is commonly observed in basins without permafrost. However, the thawing active layer imposes seasonal trends on storm flow composition and other streamflow characteristics. These seasonal trends are often masked by precipitation patterns.

Significant differences exist in the spatial variability and scaling of streamflow between arctic and temperate basins. Streamflow in arctic basins is subject to simple scaling, whereas streamflow in temperate regions is subject to multiscaling. Since the variability of streamflow downstream results from the timing of storm hydrographs upstream, regional scaling differences may result from the differences in runoff generation mechanisms in basins with and without permafrost.

Fractal analysis of channel networks, and the scaling of mass distribution suggest that channel networks in the Kuparuk River basin are underdeveloped.

Hillslope water tracks convey water off slopes, but the organization of water tracks lacks universal characteristics of mass and energy distribution common to other rivers, and hence can not be considered fluvial channels. However, the heads of water tracks are located where some theoretical models of channel initiation predict that channels should occur. A likely scenario is that a rudimentary channel network was formed soon after deglaciation, but was never allowed to develop into a mature network due to the limits that permafrost imposes on erosion.

An encompassing conclusion is that the Kuparuk River basin is adjusted to arctic conditions in both form and function. Consequently, thermal changes to the existing permafrost condition may impose significant changes in the erosional development of channel networks and in the subsequent hydrologic response.

Table of Contents

LIST OF FIGURES

List of Tables

ACKNOWLEDGEMENTS

This work was supported by the National Science Foundation grant numbers OPP-931858 and OPP-9214927. My first thanks go to Dr. Douglas Kane for conception of the greater project and acquisition of funds, with which he was very generous throughout my studies. Dr. Kane also served as my research advisor and paddling partner, and performed admirably in both roles. Dr. Larry Hinzman served as an unofficial co-advisor, and his commitment to excellence in research, tenacity in the field, and academic excellence were inspiring. Additional thanks go to the remaining members of my committee, Dr. Carl Benson and Dr. Donald Schell, for direction in selecting my coursework and critical reviews of this manuscript.

This research was field intensive, and involved many weeks each year working in all kinds of arctic weather. The success of the field campaign rests almost entirely on the tireless efforts of Robert Gieck. His commitment to quality and getting the job done despite the circumstances will always be a model for which I will strive. Several others assisted with the field work including Ronald Rovansek, David Robinson, Bill Coughlin, Johnny Mendez, Neil Meade, Ziya Zhang, Jennifer Clark, Richard Smith, and Melissa Tendick. George "Bub" Mueller assisted with data loggers and other electronic tools. Elizabeth Lilly assisted with the handling of data, production of figures, and field work. Huan Luong assissted whenever needed. Ignacio Rodriguez-Iturbe provided constructive comments at a serendipitous meeting at a conference.

I thank my parents, Dan and Gail McNamara, for their support early in my education, which laid the foundation for my subsequent graduate school experiences.

My wife Laurie has been with me since the very first weekend of my undergraduate experience. To her I owe my deepest thanks for her tireless support. Finally, I owe the motivation for completing this project to my son Nolan, whose arrival sparked an urgency for timely completion.

Chapter 1

INTRODUCTION

1.1 Scope

A drainage basin is essentially a collage of slopes connected by a channel network. The physics governing the hydrologic processes in channels and slopes independently is well understood, but when integrated as a system at the basin scale our understanding is less complete. This is a scale problem. Our knowledge of processes at one scale do not readily translate to processes at other scales. This gap in knowledge has become increasingly evident as the scientific community has placed considerable attention on regional and global scale processes to understand the causes and consequences of global climate change. A demand has been placed on hydrologists to generate information at scales much larger than the hillslope or individual channel. Hence, there is a great need to understand the hydrologic behavior of whole watersheds. This is particularly critical in the Arctic where it has been predicted that global climate change will be most pronounced.

Consequently, an effort is in progress in the Kuparuk River Basin on the North Slope of Alaska as part of the Arctic System Science NSF-LAII Flux Study to determine the controls on mass and energy flux to and from an entire river basin (Weller et al., 1995). Problems of this magnitude transcend the boundaries of any one discipline and require collaborative efforts from many disciplines. Hydrology is the integrating science that links the atmosphere to the landscape, the landscape to the

ocean, and the ocean to the atmosphere. Hence, the success of the flux study requires a comprehensive examination of the hydrologic processes operating at the basin-scale. To meet this need, a hydrologic monitoring and modeling program was initiated in the Kuparuk River basin. This dissertation is a compilation of hydrologic field studies to support the objectives of the LAII flux study.

The theme of this dissertation is basin-scale hydrology of an Arctic river system. A few key concepts in that statement exemplify some important areas of research. The most obvious keyword is "hydrology". Hydrology is the study of the occurrence and movement of water on earth. Its importance to the flux study is obvious; the hydrologic cycle encompasses the major transport mechanisms of mass and energy into and out of the watershed. Each component of the hydrologic cycle warrants intensive research on its own, but this dissertation focuses on streamflow hydrology.

A second key concept in the theme statement is "basin-scale". Basin hydrology is the science that integrates the hillslopes and the channels to understand how the whole system cycles mass and energy. Until quite recently, the hydrologic response at the basin scale was treated as a black box through techniques such as the unit hydrograph and lumped parameter modeling. Few attempts were made to understand the distributed processes collectively that dictate the hydrologic response at the basin scale. Most complications in basin-scale hydrology arise from the integration of spatially heterogeneous variables. Basins are composed of several hillslopes acting independently. Precipitation is not uniformly distributed over a basin. Geologic

heterogeneities produce different soil types and therefore different hydrologic characteristics across a basin. These complications constitute problems of scale. With all these integrating factors, how do we apply the physics that we understand at the hillslope and channel scale to successively larger scales? This is partly a statistical problem, but mostly it is a problem of understanding the physics of mass and energy transport, and of understanding scales of representation. When we collect data as point measurements, what is the scale of representation that is carried by that data - the surrounding plot, the hillslope, the watershed, and so on? Scaling studies have become a part of nearly every basin-scale hydrologic study with objectives that typically center around identifying natural process scales, or developing techniques to extrapolate information across modeling scales. Of particular interest to this study, researchers are finding connections between landscape form and drainage basin function through the use of scaling studies and fractal analysis.

A third key concept in the theme statement is "Arctic". The motivation for the flux study was that in the advent of anthropogenically induced global climatic change, it is suspected that circumpolar regions will undergo the most pronounced changes, and that these changes will produce certain feedbacks, both positive and negative, on the global climate system. Hence, an enhanced understanding of the mechanisms and pathways by which mass and energy are exchanged between arctic systems is crucial. The term "Arctic" has further significance in that a unique set of physical conditions exist that dominate nearly all physical and biological processes in a watershed. Foremost among these conditions, from a hydrologic perspective, is the ubiquitous

presence of permafrost. Hydrologic studies in basins with permafrost are relatively rare, although a growing number of studies have shown that significant differences exist between the hydrologic mechanisms operating in basins with and without permafrost. These differences arise primarily from the influence that permafrost has on the structure of the drainage basin.

The central hypothesis of this dissertation is that the presence of permafrost in an arctic watershed has significant influences on the form, function, and scaling of hydrologic and geomorphologic characteristics. Three approaches were used to address this problem. First, a series of mass transport studies was implemented at a nest of scales in the Kuparuk River basin. A nested watershed study involves investigating a cascade of basins, thereby providing a framework for studying how the physics of hydrologic processes are related across scales. The scales in this study included four basins: a hillslope water track (drainage area = 0.026 km^2), Imnavait Creek (drainage area = 2.2 km^2), the Upper Kuparuk River (drainage area = 142 km^2), and the entire Kuparuk River (drainage area = 8140 km^2) (Figure 1.1). Descriptive field studies at these scales permitted comparison of hydrologic characteristics of these arctic basins to "typical" basins in non-permafrost regions. Second, field and modeling studies of drainage basin geomorphology were initiated to identify characteristic landscape scales. Third, scaling studies of hydrologic processes, particularly streamflow, were performed. This combination of approaches yielded two papers concerning the physical characteristics of streamflow in the Kuparuk River basin, a third paper addressing the scaling of streamflow in Arctic basins, and a fourth paper

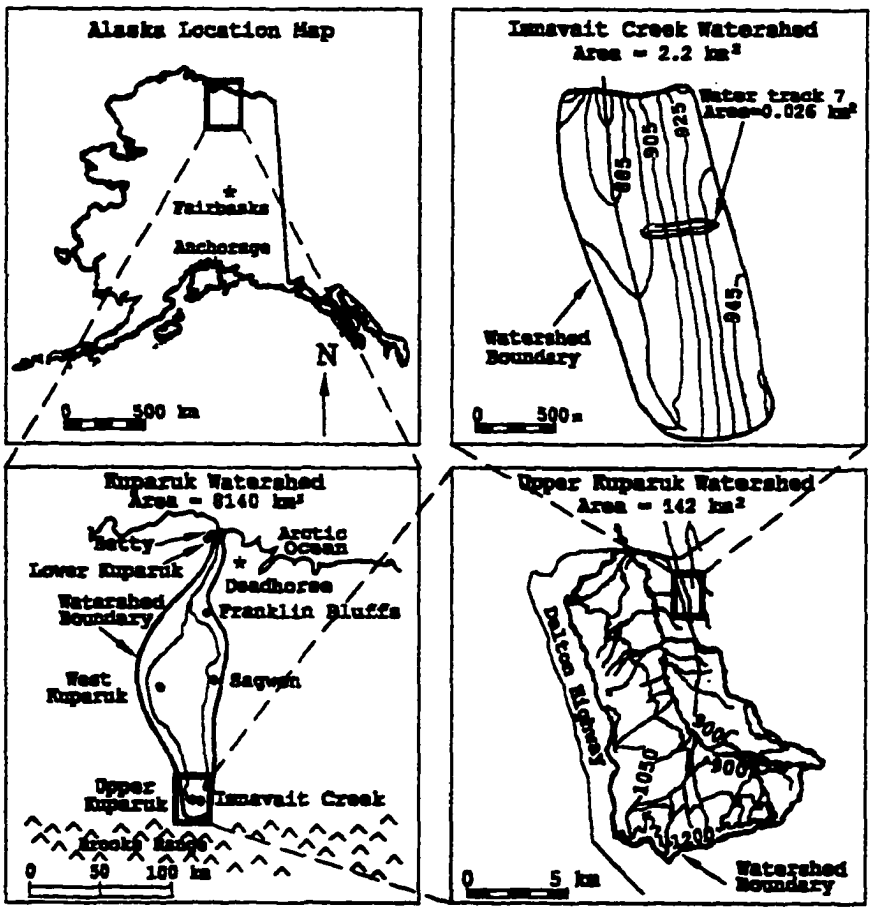

Figure 1.1. Map showing the locations of the drainage basins in this study. The locations of meteorological stations are shown as dots on the map of the entire basin.

that investigated the scaling of drainage basin form.

1.2 Outline

This dissertation is a collection of four technical papers (chapters four through seven) that address different aspects of basin hydrology in the Kuparuk River drainage, in addition to supporting chapters. The technical papers were originally written to be published independent of one another. To avoid repetition, site descriptions were removed from each paper and placed in chapter three. Additional descriptions are included in chapter introductions where necessary. There is some unavoidable repetition in the introductory comments and methods in each chapter.

Each of the four technical papers has its own pertinent literature review. A general literature review is contained in chapter two, which covers more detailed background information than could be included in the chapters intended for publication. The description of methods is included in the individual chapters.

Chapter four, entitled "An Analysis of Streamflow Hydrology in the Kuparuk River Basin, Arctic Alaska: A Nested Watershed Approach," is a descriptive hydrology paper that has been accepted for publication in the *Journal of Hydrology*. This paper treats the hydrograph as a fundamental signature of a basin, identifies distinctive features of hydrographs from permafrost dominated basins, and makes comparisons between hydrographs from arctic and temperate regions.

Chapter five, entitled "Hydrograph Separations in an Arctic Watershed Using Chemical and Graphical Techniques," has been accepted for publication in *Water Resources Research*. This paper further examines storm flow hydrographs using

various techniques to determine the sources of streamflow during storms, and evaluates the role of the thawing active layer on flow sources.

Chapter six entitled, "Scaling of River Flows in the Alaskan Arctic," has been submitted to *Water Resources Research*. This paper addresses the variability of streamflow across a range of scales in the Kuparuk River basin. It identifies a significant difference between the scaling of river flows between arctic and temperate regions, and speculates that the differences are due to the mechanisms by which the landscapes transfer precipitation into runoff.

Chapter seven entitled, "A Geomorphologic Analysis of an Arctic Drainage Basin Using a DEM," has been prepared for submission to *Geomorphology*. The premise of this paper is that since landscape processes and patterns are intricately connected, studying the spatial variability and scaling of landscape forms will enhance our knowledge of the scaling of hydrological processes. The paper uses several techniques to evaluate the form of drainage basins extracted from digital elevation models.

Chapter eight is a summary of the conclusions from each paper, and draws some integrated conclusions from the overall study.

Chapter 2

LITERATURE REVIEW

2.1 Hydrology of Arctic Regions

The discipline of hydrology has not always been recognized as a science in its own right, but has been an emphasis of geology, civil engineering, agricultural engineering, or forestry. Much of the early research concerning the movement and occurrence of water on earth was not directed towards addressing fundamental questions of a scientific nature, but was focused on solving water resource problems. Consequently, the primary tools of hydrologic analysis to this day are based on empiricisms and engineering approximations, as opposed to theory. In recent times, hydrology has risen to become its own scientific discipline, and considerable emphasis is being placed on basic research (NRC, 1991). For example, watershed hydrology models were once dominated by black box type systems models where attention is paid to bulk inputs and outputs with little regard for the physics governing the system. Lately, there has been a trend to develop physically based watershed hydrology models that are firmly rooted in the physics governing the movement of mass and energy.

This surge of growth in scientific hydrology has arisen primarily from the interdisciplinary nature of the significant environmental research efforts of the day. Many questions being addressed by environmental scientists today transcend discipline boundaries and require interdisciplinary approaches. Hydrology is the communicating link between the land, the atmosphere, and the oceans. Therefore, the science of

hydrology is by nature interdisciplinary, and the demand for interdisciplinary environmental research demands fundamental hydrologic research.

Because early hydrologic research focused on water resource problems for humans, there is a paucity of data in arctic regions where few humans live. Occasional hydrologic studies were performed to support development projects such as the trans-Alaska pipeline, but very few watershed scale hydrologic studies have been performed in arctic regions, and those that did occur were short term. Hence, there are very few long term records from which to decipher long term hydrologic trends in the Arctic. For example, in the entire Alaskan Arctic, the United States Geological Survey (USGS) operates only four stream gauging stations.

Early hydrologic research in the Alaskan Arctic occurred along the Arctic coast (Brown et al., 1968; Carlson et al., 1974). The USGS performed occasional reconnaissance studies on Arctic rivers using channel morphology to estimate the hydrologic regime (Childers et al., 1979; Lamke, 1979), but little actual hydrologic data was obtained. The construction of the trans-Alaskan pipeline in the mid-1970's prompted a flurry of hydrology related research for the purpose of bridge and pipeline crossing design (Sloane et al., 1975), and subsequent research on runoff regime of rivers crossing potential oil fields (Kane and Carlson, 1973; Scott, 1978). Wherever limited development occurred, engineers performed various hydrologic studies (Seagel and Parish, 1974). However, none of these studies focused on collecting continuous hydrologic data even through one season.

Perhaps the first comprehensive, long term hydrologic study in the Alaskan Arctic was initiated in 1984 in Imnavait Creek in the foothills of the Brooks Range as part of an interdisciplinary study to investigate the response of tundra ecosystems to disturbances (Kane and Hinzman, 1988; Kane et al., 1989). These studies demonstrated the interactive dependence between thermal and hydrologic processes in arctic watersheds. Because of the paucity of basic hydrologic data to build upon, the Imnavait Creek study required years of baseline research before disturbance studies could commence. This was a fortunate boon for hydrologic science in the Arctic, because it launched an extensive data gathering campaign that is continuing still to produce the longest running watershed-scale hydrology study in the Alaskan Arctic.

Considerable hydrologic research has been performed in the Canadian Arctic (see the many references by Woo and Woo et al. as examples). Woo, in his many publications, investigated the influence that permafrost has on individual components of the watershed hydrologic cycle. For example, Woo and Steer (1982) showed that runoff generation in permafrost dominated wetlands occurs as a threshold response to saturation of the soil storage capacity, as opposed to runoff that results from precipitation intensity exceeding infiltration.

An observation held in common amongst all of these studies is that snow, ice, and permafrost have profound influences on terrestrial hydrologic processes in the Arctic. Permafrost is any earth material that remains frozen for at least two consecutive years (Mueller, 1943). A few notable reviews concerning hydrology in

permafrost-dominated basins exist (Church, 1974; Dingman, 1973; Kane et al., 1992; and Woo, 1986).

Woo (1986) summarized the works of several permafrost hydrology studies and arrived at the following generalizations: 1) Frozen ground has negligible permeability and acts as a barrier to vertical movement of groundwater. 2) Most hydrologic activities are confined to the active layer, which is the shallow surface zone that undergoes annual thawing and freezing. 3) Most hydrologic processes become dormant during the winter. 4) Energy and water fluxes are strongly linked. 5) Permafrost hydrology is tightly coupled with the hydrology of snow and ice.

2.1.1 Water Balance in Arctic Regions

Each component of the simplified water balance equation

$$P = Q + E + dS \qquad (2.1)$$

is influenced by arctic conditions, where P = precipitation, Q = runoff, E = evapotranspiration, and dS = change in storage. Rainfall in the Arctic is typically low in both magnitude and intensity. The highest amounts of precipitation typically occur between late July and mid-September (Kane and Hinzman, 1988). The percentage of annual precipitation that occurs as snow varies considerably across the Arctic, and has been estimated to range between 30 and 80% (Haugen, 1980; Benson, 1982). However, the measurement of snowfall is a difficult problem in the Arctic due to the redistribution by wind (Benson, 1982; Black, 1954; Clagget, 1988; Woo and Marsh, 1978). Benson (1982) suggested that the National Weather Service precipitation gauges underestimate snowfall in the Arctic by up to 50% or more. Although the

redistribution of snow by wind creates a measurement problem, it is an important component of the hydrologic cycle. Much of the snow that falls on flat terrain gets re-deposited in bluffs along the stream margin. Consequently, water that would otherwise evaporate from the flat regions melts directly into the channels and contributes to runoff. As a result, the runoff/precipitation ratios during snowmelt can be up to 70% (Woo et al., 1996).

The runoff term in Equation 2.1 encompasses both hillslope runoff and channel flow, each of which have evolved as considerable topics of research. Runoff can occur from hillslopes as a result of overland flow, or subsurface storm flow. Several different kinds of overland flow have been identified, but foremost are Hortonian overland flow, and saturation overland flow.

Hortonian overland flow occurs when precipitation intensity exceeds the soils infiltration capacity. The mechanism is named for Robert E. Horton, who originally described the process (Horton, 1933, 1945). For many years it was believed that Hortonian overland flow was the only mechanism responsible for overland flow, and was used exclusively in many hydrologic models of watershed response. Horton (1933, 1945) suggested that overland flow due to exceedence of infiltration capacity by rainfall would occur over an entire watershed at nearly the same time. Betson (1964) noted that the contributing area of Hortonian overland flow may be only a small portion of the basin. This became know as the partial-area concept of storm runoff. However, beginning in the 1960's, several field studies showed that Hortonian

overland flow was not the only form (see Kirkby, 1978 for examples), and not even the most common form.

Saturation overland flow occurs when the soil storage capacity is exceeded. Runoff results either from precipitation onto previously saturated regions, or from infiltrated water returning to the surface upon saturation. Dingman (1994) differentiates between Hortonian and saturation overland flow as saturation from above and saturation from below, respectively. Dunne and Black (1970) first identified saturation overland flow as an important source of streamflow during storms. This typically occurs near the stream margins, first where the water table is close to the surface, then the saturated area expands through the storm as the valley bottoms saturate. However, saturation can occur wherever depressions or convergences exist in the watershed. Thus, the saturated area of a basin varies widely in time depending upon watershed wetness. This is known as the variable-source-area concept of runoff generation (Hewlett and Hibbert, 1967). A number of studies have concluded that saturation overland flow is far more important than Hortonian overland flow in humid regions (see Chorley, 1978 for a review).

In the Arctic, rainfall intensities are typically low, and surface organic soils have high infiltration capacities when thawed. These conditions dictate that overland flow in arctic watersheds occurs almost exclusively as saturation overland flow (Woo and Steer, 1982). Since the occurrence of saturation overland flow depends upon the storage capacity of the soil, the active layer has considerable influence on the generation of saturation overland flow (Woo and Steer, 1983; Wright, 1983). During

snowmelt and early summer, the active layer is very thin. Consequently, the storage capacity is low and even small storms can generate overland flow. As the summer progresses, the active layer thaws and the storage capacity increases. This unsteady storage term is unique to arctic basins. Evapotranspiration demands increase simultaneously so that in the late summer, more precipitation is required to saturate the active layer and generate runoff (Woo and Steer, 1983). However, permanent water tracks that remain saturated most of the summer exist on slopes with permafrost (Kane et al. 1989), which create a fairly constant saturated area from which to generate saturation overland flow.

Permafrost also has considerable influence on the timing of stream response. Early in the thawing season, streams respond quickly to precipitation events (Woo and Steer, 1982). As the season progresses, response times increase, and the recession constants of the falling limb of hydrographs increase (Anderson, 1974; Anderson and Neuman, 1984; Wright, 1983).

Lewkowicz and French (1982) suggested that subsurface storm flow is more important than surface flow contributions to streams in a permafrost basin on Banks Island. Hinzman et al., (1993) concurred that the most common mechanism of downslope movement of water from the hillslopes (excluding water tracks) is subsurface flow. Subsurface flow typically occurs along the interface between shallow organic soils and the underlying mineral soils. The mineral soils are typically frozen longer, have lower hydraulic conductivities, and are often saturated thus creating a preferential flow path along the interface (Douglas, 1961).

Regardless of the mechanisms by which water is conveyed off the hillslopes, a significant conclusion from several studies is that the ratios of runoff to precipitation in the streams is much higher in permafrost dominated basins than in non-permafrost basins (Woo and Steer, 1982, 1983, Woo, 1986; Woo et al., 1996; Sellers, 1965) due to the limited storage capacity of the active layer.

The discharge of most arctic rivers drops to nearly zero during the long winter months. Consequently, the period of active runoff is considerably shorter than for rivers in temperate or tropical regions. Water is stored in arctic basins through the winter as snow accumulates. In the water balance equation, precipitation as snow is absorbed primarily in the change in storage term. This creates a very large time lag between precipitation and runoff. During the summer, storage can occur in surface depressions and in the active layer, but the ability of the active layer to store water is limited because of the shallow depth. Hinzman et al. (1991) quantified the hydrologic role of the active layer. Typically, the underlying mineral soils are saturated year round so that transient storage only occurs in the upper organic layer. Kane et al. (1989) showed that approximately 15 mm of meltwater is required to initiate runoff during snowmelt, and approximately the same amount of precipitation is required during dry periods in the summer.

Evapotranspiration is a significant component of the basin water balance in the summer (Kane et al., 1990; Rouse et al., 1977; Ohmura, 1982, Rovansek et al., 1996), and essentially non-existent in the winter (Briazgin and Korotkevich, 1975). Evapotranspiration is typically calculated as the remainder in water and energy

balances in a watershed because direct measurement is exceedingly difficult. Kane et al. (1990) compared various techniques in a small Alaskan Arctic watershed and determined that the water balance method worked best for estimating evapotranspiration on a yearly timestep. On short time scales, the energy balance method works better. They showed that evapotranspiration is greatest immediately following snowmelt, and that the cumulative potential evaporation during a summer is greater than the cumulative precipitation.

2.1.2 Streamflow Regimes in the Arctic

Although the dominance of permafrost, snow, and ice unites all Arctic river basins, there are significant differences between rivers that have given rise to classification systems. Church (1974) developed a classification of Arctic rivers based upon the source and timing of runoff. Craig and McCart (1975) classified them according to origin of flow. Woo (1986) provided a synthesis of the different classification schemes. The following discussion is drawn from the above references.

There are generally three types of streams in the Alaskan Arctic: streams dominated by a snowmelt flood, streams dominated by glacial melt, and spring fed streams. The nival regime is dominated by spring snowmelt floods. Precipitation accumulates as snow for up to nine months during the winter and is released as runoff during a short period of about 10 days in the spring. Rainfall generated precipitation events may rival or exceed peak snowmelt floods, but the volume of flow during snowmelt dominates the annual hydrograph. The nival regime falls into the mountain stream category of Craig and McCart (1975).

The proglacial regime has large spring snowmelt floods, but also has large summer maximums from melting glaciers. Consequently, the summer runoff patterns are dictated by energy as opposed to precipitation input into the basin.

The wetland, or muskeg, regime encompasses streams in the low lying tundra areas, and belongs to the tundra stream classification of Craig and McCart (1975). These streams also have a large spring snowmelt, but not as large as nival streams. When the ground thaws, depression and active layer storage increases and runoff is initiated only after enough rain exceeds the storage capacity.

The spring fed regime has relatively stable discharges because of the moderating effect of baseflows from groundwater. These too have large spring snowmelt floods, but the baseflow remains fairly high through the summer. The springs can continue to flow through the winter and provide a minimum winter streamflow. However, it is more likely that the springs will produce large icings. If the icings are large enough, such as on the Ivishak river in Northern Alaska, they can behave hydrologically similar to glaciers in that they accumulate in the winter months, with moderated runoff from meltwater in the summer.

Aside from spring-fed streams, summer baseflow comes from the minimal storage in the active layer or from melting ice. Consequently, in the fall when the energy input is severely limited, the active layer begins to freeze, ice no longer melts, and the rivers stop flowing. Taliks, lenses of unfrozen water within the permafrost, may exist beneath streams, but they do not contribute significant flow.

Large rivers may traverse a variety of regimes, have large spring floods and relatively low baseflows, and some may have winter baseflows. The timing and magnitude of runoff is dictated by the characteristics of the various contributing sub-basins (Woo, 1986).

2.2 Scale Problems in Hydrology

Scale problems and basin hydrology gained prominent attention with the development of the geomorphologic instantaneous unit hydrograph by Rodriguez-Iturbe and Valdes (1979). Since then, the scope of scaling research has grown considerably to address a variety of hydrologic applications that includes all aspects of the hydrologic cycle. The word 'scaling' seems to appear in almost all coffee table conversation at hydrology conferences, and the National Research Council has recognized that scaling is a critical area of research (NRC, 1991). Most scale issues are focused on the problems confronted in modeling, where numerical techniques must somehow embrace the complexities of spatial and temporal variability of hydrologic processes across scales. Simply stated, scale issues in modeling are problems of distributing and aggregating information. How do we use point measurements of state variables to represent large areas, or distribute regional fluxes across points? Another aspect of scale studies involves identifying natural preferential scales that exist in landscapes, and the sources of variability on a flux of interest at different scales. For example, in drainage basins, there is a scale of transition between hillslope and channel processes (Tarboten et al., 1992), and the flow patterns and energy distributions undergo radical transformations through that transition. Both kinds of scaling, applied

and basic, have received considerable attention in hydrologic research. This prominence of the subject commands a discussion on what scaling means.

2.2.1 Definitions and Important Concepts

The term "scale" has a variety of meanings and exists as both a noun and a verb. The noun scale refers to a characteristic time or length of a process, observation, or model (Blöschl and Sivapalan, 1995). Process scale refers to natural characteristic scales that may exist, or when hydrologic processes occur at preferred time or length scales. To scale in the process sense refers to the way in which a natural process or feature varies across scales. Observation scale refers to notions such as map scale, or digital elevation model resolution. (Blöschl and Sivapalan (1995) defined observation scale as the spatial or temporal extent of a data set. Ideally, observation scale should match process scale. This, however, is nearly impossible. Modeling scale is the working scale, or the scale at which we manipulate the observed scale. Therein lies the crux of applied scale problems in hydrology. We are forced by data constraints to observe and model processes at scales other than their characteristic scale.

Scaling refers to the ways in which information is transferred across scales. Thus the verb form "to scale". Again, there is process scaling and practice scaling. Process scaling refers to the natural relationships of scale that may exist. For example, several empirical relationships have been identified that relate drainage basin characteristics to drainage area such as

$$L=CA^{b} \qquad (2.2)$$

In this example, drainage area A is the scale descriptor, and mainstream channel length L scales with A according to the scaling exponent b. Hack (1957) and Gray (1961) showed that the exponent b is fairly constant for all drainage basins and averages around 0.57. Thus there seem to be an underlying sense of regularity between basins in the manner in which channel length scales with drainage area. One objective of scaling studies is to identify such natural scale invariance and provide physical justifications for them.

Practice scaling refers to the methods used to represent natural scaling in hydrologic models. This involves either upscaling or downscaling. Blöschl and Sivapalan (1995) use the example of estimating catchment rainfall from one precipitation gauge. Upscaling involves two steps. First, the small scale information must be distributed over the entire basin. For precipitation, this is often done as a function of topography. Second, the distributed information must be aggregated into one value. Downscaling involves disaggregating and singling out information from larger scales.

Scaling problems in any sense of the term typically arise as a result of the high heterogeneity and variability of hydrologic and geomorphologic variables. The term heterogeneity is used for state variables such as soil properties (moisture, type, hydraulic conductivity) and topography. The term variability is used for fluxes such as runoff and evapotranspiration. When we upscale information, we incorporate small scale heterogeneity and variability into the larger scale representations. The problem is that we do not always know the process scaling and are forced to make assumptions

that may not be valid while deriving our analytical relationships to practice scaling. Simple averaging is often insufficient since many hydrologic processes are nonlinear with scale.

Variability can come about in two ways, either deterministic or stochastic (Seyfried and Wilcox, 1995). Deterministic variability results when the causes of variability are known. For example, there is a known topographic signature on soil moisture in most basins, where low lying areas are wetter than higher areas. Deterministic descriptions of variability result in exact values of variables or mappable trends either through empirical or theoretically derived relationships. Equation 2.2 is an example of an empirical equation of deterministic variability. Stochastic variability is essentially random. Exact values of a variable can not be predicted, but estimates of their probability distribution can be predicted.

Spatial variability is rarely entirely deterministic or stochastic, and the nature of variability changes with scale (Seyfried and Wilcox, 1995). The task of applied scaling studies for modeling purposes is to identify the nature of variability of the process to be modeled, determine if preferential scales exist, and develop analytical relationships that incorporate that variability into all scales of the model. The task of basic research into scaling involves identifying natural scales of variability in processes and patterns, and assessing physical causes.

The scope of scale problems in hydrology is much too broad to be covered in detail here. The scale problems addressed in this dissertation are basic, as opposed to applied, and are specifically restricted to the fundamental structure of drainage basins

and how that is related to hydrologic processes. Even that is a broad topic that extends beyond the scope of this work. The following review focuses on just the recent work pertinent to the scaling studies in this dissertation. For more complete reviews, readers are referred to Blöschl and Sivapalan (1995), Wood et al. (1988), and Gupta et al. (1986).

2.2.1.a Scaling and the fractal dimension

In his landmark essay "The Fractal Geometry of Nature", Mandelbrot (1982), the inventor of the term fractal, offered this definition:

> A fractal is by definition a set for which the Hausdorff-Besitovitch dimension strictly exceeds the topological dimension.

The topological dimension is the concept of dimension that we all became familiar with in elementary school. It must be an integer of 1, 2, or 3. The Hausdorff-Besitovitch dimension is more complicated. A technical definition was provided by Feder (1988). At this point, it is enough to know that the Hausdorff-Besitovitch dimension is related to the exponent in a power law function, and that it is most often a non-integer value. Mandelbrot (1986) later retracted the above definition in favor of:

> "A fractal is a shape made of parts similar to the whole in some way."

Even later, Mandelbrot (1987) stated that a concise and comprehensive characterization of the fractal dimension is still lacking. This is a frustrating reality to the neophyte fractal researcher trying to make sense of the volumes of literature regarding the various application of the fractal concept. Mandelbrot (1982) introduced several types of fractals, all of which embody the concept of similarity of objects or

distributions across scales. The discussion here encompasses only the type of fractals directly applicable to the problems at hand. For more comprehensive coverage, the reader is referred to Mandelbrot (1982) and Feder (1988).

Fractal geometry arose in part out of frustration that classical geometry is not capable of measuring or characterizing many natural forms. Classical geometry deals mainly with objects that cannot be recursively divided into self-similar components, while fractal geometry provides an approach to the analysis of self-similar and self-affine objects. Self-similarity implies that like forms are superimposed upon themselves at different scales, and self-affinity means that features at different scales appear as stretched or squashed versions of each other. The same concept can be applied to probability distributions, where the probability distribution of a self-similar random variable fixed to a scale has an identical probability distribution to that variable at another scale.

Fractal dimensions describe how the measure of some complex objects in nature changes with scale. The measure of a Euclidean object, say the length of a straight line, remains the same regardless of the scale of measurement. It is perfectly suited to be viewed and measured in one dimension. The measure of a fractal object, say the length of a self-similar line, changes with a change in scale measurement. However, there exists a dimension where the measure of that object is independent of scale, termed scale-invariant. That dimension is the fractal dimension.

To illustrate the fractal dimension, it is easiest to start with Euclidean objects with dimensions of D=1, 2, or 3. Consider a square (D=2) with a side length of L=1. Now divide the each side into b=3 units so that there are a total of

$$N=b^D = 3^2 = 9 \quad (2.3)$$

smaller squares each with sides of length r=1/b=1/3. So,

$$N=(1/r)^D \quad (2.4)$$

Taking the logarithm of both sides yields

$$\log N=D\log(1/r) \quad (2.5)$$

and

$$D=\log N/\log(1/r)=\log(9)/\log(3)=2 \quad (2.6)$$

which is the Euclidean dimension of a plane. Thus, b^D units are required to fill the space. The size of the square is calculated by multiplying the size of the division , $(1/3)^2$ by the number of divisions required to cover the square (9). $(1/3)^2*9=1$. If we divide the side of the square into 4 units, $4^2=16$ units are required to cover the square, D=log(16)/log(4)=2, and the size of the square is $(1/4)^2*16=1$. No matter how many divisions we impose on the square, the total dimension is always 2 and the size is always 1. If we had used a finite line or a cube, the dimension would have been 1 or 3 respectively. Fractal dimensions are calculated in a similar manner, except they can take on non-integer values. Fractal objects have dimensions between a line and a plane, or a plane and a volume.

A simple example of an ideal self-similar fractal is the Koch curve (Mandelbrot, 1982). Figure 2.1 illustrates the steps in the construction of a Koch curve. The straight

STEP 1: Begin with a line segment AB:

STEP 2: Replace the segment with the koch generator.

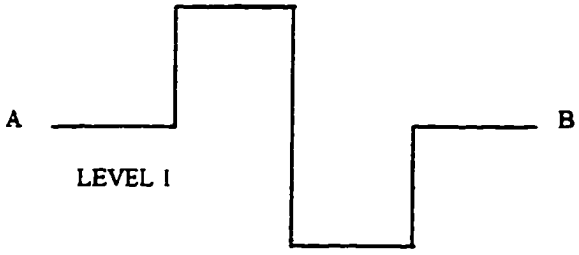

STEP 3: Now do two things with the generator. First, scale it down by 1/4:

STEP 4: Next, replace each line segment in the generator by the scaled-down version:

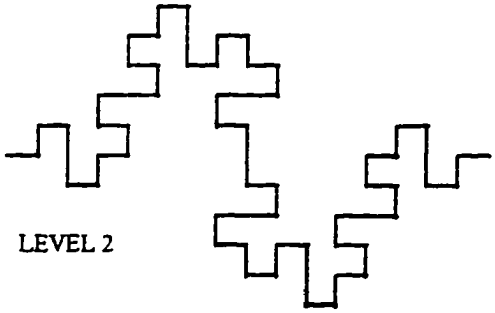

STEP 5: Scale down the generator of STEP 2 by 1/16 and replace each of the line segments of STEP 4 with the result.

STEP 6...: Repeat STEP 5 endlessly, scaling the generator by $(1/4)^n$ and replacing each of the line segments in the new figure with the scaled-down version of the generator.

Figure 2.1. Steps illustrating the construction of a Koch curve (from De Cola and Lam, 1993).

line segment is the 0^{th} generation of the Koch curve. At each successive generation, the length of the straight line segment in the generator is scaled down by ¼, then the new generator replaces each line segment from the previous generation. If this is repeated endlessly, the Koch curve is self-similar over an infinite range of scales. An important feature of the Koch curve is that it looks identical regardless of the scale of view. We can calculate the length of the curve and determine its dimension similar to the manner described for the square above.

In the 0^{th} generation, it takes one count of a ruler of a step length of one unit to cover the distance of the line. In the first generation, the curve contains 8 line segments of step length ¼, and the distance of the curve is 8*1/4=2. In the second generation, the curve contains 64 line segments of step length 1/16, and the total length of the curve is 64*1/16=4. Table 2.1 shows the continued statistics for successive generations. We see that the length of the curve changes with scale. The fractal dimension can be calculated at any one of the generations and is D= -3/2. Figure 2.2 shows a log-log plot of length versus scale. Note that the slope of the line, or the exponent of a power-law function is equal to the fractal dimension:

$$L=(1/L)^{-3/2} \qquad (2.7)$$

Thus, the fractal dimension describes how the measure of an object changes with changes in scale. D is a similarity exponent since it tells how the size changes with a change in scale. In this example, the length of the curve changes at a faster rate than the scale decreases, and the exponent is a scaling relationship that describes that

Table 2.1. Relationship between COUNT and STEP for a Koch Curve (from DeCola and Lam, 1993).

Generation	Step	Count	Distance	Log (step)	Log (count)
0	1	1	1	0	0
1	¼	8	2	-2	3
2	1/16	64	4	-4	6
3	1/64	512	8	-6	9
4	1/256	4096	16	-8	12
5	1/1024	32768	32	-10	15

transformation. The Koch curve is an ideal fractal because the self- similarity holds over all scales. Although ideal fractals rarely occur in nature, several objects exhibit fractal behavior over a finite range of scales. Consider the classic problem of measuring the length of a coastline.

"How long is the coast of Britain?" This question posed by Mandelbrot (1967) may be credited with the birth, and subsequent surge of interest in fractal concepts. It is not that the world is particularly interested in the coast of Britain, but that the question recognized a shortcoming in our Euclidean view of nature. If one measures the length of a coastline by stepping along with a ruler of length r, the length of the coastline is r times the number of steps. Mandelbrot (1967) pointed out that the total length of the coastline depends upon the length of the ruler, similar to a Koch curve.

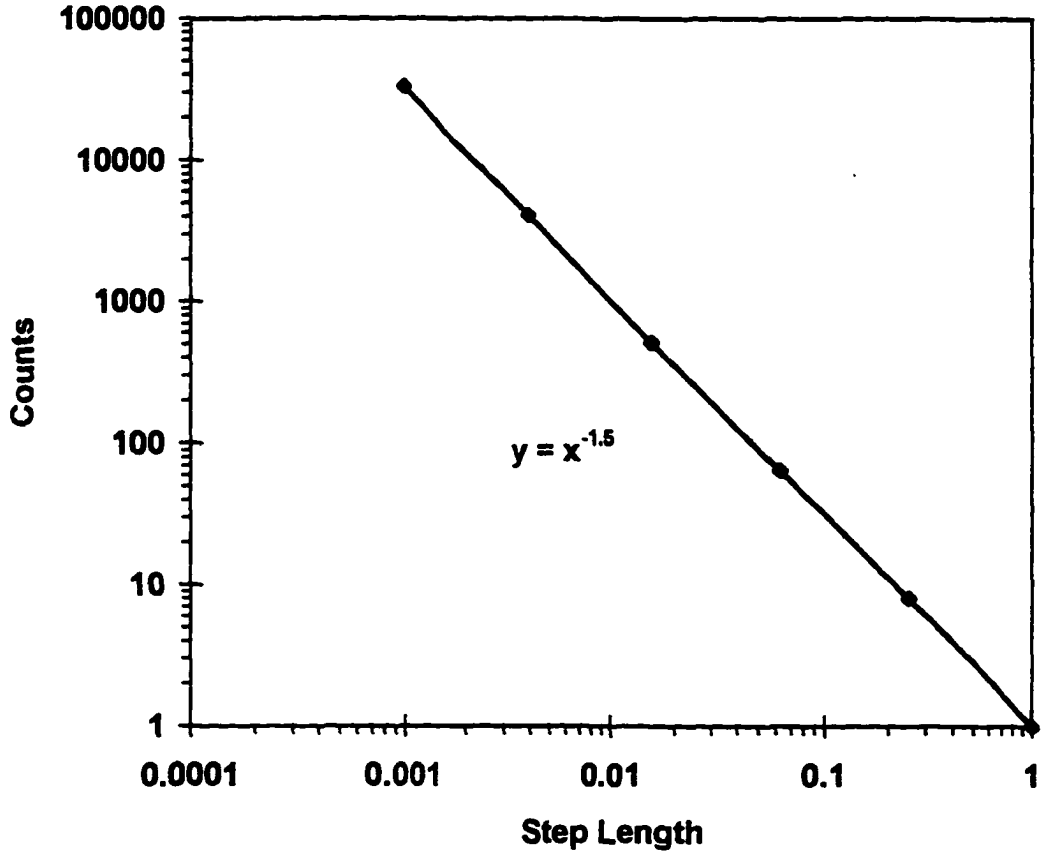

Figure 2.2. The fractal dimension of a Koch curve (Figure 2.1) is the exponent of a power law function relating the size of a ruler (step length) to the number of counts required to cover the curve.

As r decreases, each step picks up more detail of the coastline and the total length increases. The relationship between r and total length L is

$$L=Nr^{D} \qquad (2.8)$$

where N is the number of steps of length r to cover the distance L. Note that if L is a straight line, the exponent D will simply be 1 which is the Euclidean dimension of a line. Dimensional analysis confirms that indeed, the dimension should be 1 where L is a length and r is a length. However, as the line develops curves, the exponent D is somewhere between 1 and 2. Mandelbrot (1982) calculated that the coast of Britain has D~1.3. So, the length of the coastline is constant regardless of the size of the ruler in the dimension of 1.3.

Power law relationships like Equation 2.8 are the signatures of fractal objects where the product is the measure of the object in the dimension D independent of the measurement of scale. Solving for D yields

$$D \propto \log L/\log r \qquad (2.9)$$

which is identical to Equation 2.6. Thus, the fractal dimension is related to the ratio between the log of a measure and the log of the scale at which it is measured.

The review to this point has addressed only monofractals, where one dimension characterizes the entire set. This type of scaling is termed simple scaling. Geophysical fields often possess several fractal dimensions in different regions of the field. The multifractal formalism introduced by Mandelbrot (1982) offers a more robust approach. Lavalée et al. (1993) stated that geographic and geophysical fields are generally multifractal, and that problems occur when they are forced into narrow

geometric frameworks of single fractal dimensions. The monofractal approach can only deal with a few restricted forms of scaling , self-affine and self-similar objects, whereas the multifractal is much broader. Whereas the monofractal approach produces a single number, the multifractal approach produces a function describing the intensity of the measure everywhere, or the range of fractal dimensions. Whereas the monofractal describes the patterns of a geometric set of points, the multifractal formalism describes the spatial distribution of a physical quantity over a set, i.e., energy dissipation over a drainage basin, or river flows over a fractal channel network. To illustrate the difference, we return to the simple scaling (power law) example

$$L \propto r^{D(s)} \tag{2.10}$$

L is the mathematical measure of the set of points (s), say the length of a line at scale r, and D(s) is the dimension of the set of points (S). When the set is self-similar or self-affine, L and D(s) are called respectively the fractal measure and the fractal dimension. In the previous discussion we allowed D(s) to be Euclidean (1, 2, or 3), or monofractal, where the measure L is scale invariant within a single fractal dimension. If the measure is multifractal, the dimension D(s) becomes a function f(D(s), r) which allows the dimension to change with scale. Contrary to simple scaling, in multiscaling the exponent depends continuously on r. The maximum value of D in a multifractal spectrum is equal to the fractal dimension of the set over which the measure operates.

Techniques to determine fractal dimensions and multifractal spectrums of features are as varied as the interpretation of them. Klinkenberg (1994) and Lam and DeCola (1993) provide reviews of the various techniques with applications to

geographical data. The discussion below reviews some techniques directly applicable to the applications in this dissertation.

2.2.2 Scales and Scaling in Drainage Basins

The connections between drainage basin form and runoff generation have received considerable attention in recent years(Gupta and Mesa, 1988; Gupta and Waymire, 1983; Gupta and Waymire, 1996; Rinaldo et al., 1995). Since pattern and process are closely connected, perhaps hidden in the scaling of patterns are clues to how processes scale. Ultimately, it is hoped that knowledge of network morphology may lead to improved flow predictions from ungauged basins. Significant advances have been made in both the scaling of drainage basin forms, and in the scaling of runoff processes. However, sound theoretical explanations for their connections are still eluding researchers. The concepts of fractals, self-similarity, simple-scaling, and multiscaling have led to significant advances in these areas (Rodriquez-Iturbe et al., 1994). In the remaining review, the mathematical constructs of some important scaling terms are developed, then the research concerning scaling of drainage basin, river runoff, and the connections between the two are reviewed.

2.2.2.a Scaling of Drainage Basin Form

Perhaps the earliest report of scaling in hydrologic literature was Davis (1899, p. 495):

> "Although the river and hillside waste do not resemble each other at first sight, they are only extreme members of a continuous series and when this generalization is appreciated one may fairly extend the 'river' all over its basin

and up to its very divide. Ordinarily treated the river is like the veins of a leaf; broadly viewed it is the entire leaf."

This idea of continuity across scales embraces the notions of self-similarity. Classical fluvial geomorphology literature is rich with examples of power law functions (Shreve, 1966, 1967), thus illustrating the ubiquitous presence of fractal forms in river basins.

Horton (1945) introduced the first attempt at quantifying the similarity features of channel networks through his well known ordering system. Strahler (1952, 1957) revised Horton's scheme to eliminate some subjectivity. The Horton/Strahler ordering scheme is as follows. All exterior links have order one. When two upstream links of the same order join, the downstream link has order increased by one. When two upstream links of different order join, the downstream link takes higher order of the upstream links. A set of ratios called Horton's laws of network composition has arisen from the Horton/Strahler ordering scheme:

$$R_b = \frac{N_{w-1}}{N_w} \tag{2.11}$$

$$R_l = \frac{L_w}{L_{w-1}} \tag{2.12}$$

$$R_a = \frac{A_w}{A_{w-1}} \tag{2.13}$$

$$R_s = \frac{S_{w-1}}{S_w} \tag{2.14}$$

where N_w is the number of streams of order w, L_w is the mean length of streams of order w, A_w is the mean area contributing to streams of order w, and S_w is the mean

slope of streams of order w. These are called the bifurcation, length, area, and slope ratios respectively. Horton (1945) showed that these ratios were approximately constant through semi-log plots of N_w, L_w, A_w, and S_s against order. Smart (1978) pointed out that Horton's ratios really have no physical meaning regarding basin characteristics, and are not effective in discerning between basins in different regions as Horton had envisioned. However, Horton's laws are geometric scaling laws, implying that channel networks are self-similar over a range of channel orders or scales.

Since the pioneering work of Horton, there has been seemingly continual discoveries of further similarity characteristics of drainage basins. Most of them are incorporated in empirical power law functions relating some process or feature to a scale parameter such as drainage area. For many years, these observations were simply empirical with no physical explanations. Interest in these problems exploded in the 1980's with the introduction of fractal geometry as a means to characterize the complexities inherent in such relationships. The first attempt to relate early empirical observations to fractal concepts was by Mandelbrot (1982), who investigated Hack's (1957) empirical relation between catchment area and the length of the main channel in the Shenandoah Valley in Virginia

$$L=1.4A^{0.6} \qquad (2.15)$$

Dimensional analysis of Equation 2.15 shows that the exponent should be 0.5. The classical explanation for the exponent being larger than 0.5 was that basins have anisotropic shapes and tend to become narrower as they elongate. Mandelbrot (1982)

suggested that the exponent of 0.6 is due to the fractal nature of river channels. He assumed that river sinuosity is self-similar and hence can be described by a fractal dimension of $D = 2*0.6 = 1.2$. More recent research has shown that rivers tend to be self-affine, rather than self-similar (Ijjasz-Vasquez et al., 1994; Nikora and Sapozhnikov, 1993b). However, the early assumptions of self-similarity provided a base from which initial significant advances concerning the fractal nature of rivers were launched. Mandelbrot (1982) further supposed that channel networks penetrate every point in a drainage basin and thus a channel network resembles a space-filling curve with a dimension of 2. As a squiggly line inherits more and more noise, it comes closer and closer to touching every point in a plane, hence the term "space-filling", and thus assumes the dimension of a plane. Mandelbrot (1982) argued that if a person were to walk along the bank of a channel following every tributary up and around the channel heads so that a channel was always to one side, they would be walking the motion of a space filling line. Thus, according to Mandelbrot's (1982) reasoning, the channel network is a space filling object and if in Hack's law the total length of streams in the network is used instead of the main channel length, the fractal dimension should be 2. Thus, rivers can be viewed as fractals from two perspectives. One accounts for the sinuosity of river channels and is described by the sinuosity fractal dimension D_s (Mandelbrot, 1982; Hjemfelt, 1988; Snow, 1989). The other considers the branching characteristics of a channel network and is characterized by the topological dimension D_t (Tarboten et al., 1988, and 1990; La Barbera and Rosso, 1989, and 1990; Claps and Oliveto, 1996).

Since Mandelbrot's introduction, the fractal nature of individual channels and channel networks have been the subject of intense investigation. However, a consensus of what a characteristic fractal dimension should be, as well as the physical interpretation of the fractal dimension is still elusive. Self-similar or self-affine, monofractal or multifractal, the assumptions and interpretations are varied. Figure 2.3 modified from Nikora et al. (1996) summarizes the research efforts concerning the fractal nature of rivers. The variety of assumptions and results shows that this subject is still in its infancy. Never-the-less, all of this research seems to support the idea there are underlying physical principles governing the evolution of all drainage basins that produce common fractal features.

Tarboten et al. (1988, and 1990) and La Barbera and Rosso (1989, and 1990) recognized the connection between the inherent self-similarity in Horton's laws and the self-similarity captured by the fractal dimension. Both groups showed that the fractal dimension of a channel network can be obtained through Horton's Law's as

$$D = \log(R_b)/\log(R_l) \qquad (2.16)$$

Note the similarity of Equation 2.16 to Equation 2.9.

Tarboten et al. (1988) set out to test Mandelbrot's (1982) suggestion that channel networks should have fractal dimensions of 2. They used Equation 2.16, plus two additional techniques to calculate the fractal dimension of several river networks and showed that indeed they were all near 2, which is the Euclidean dimension of a plane. Hence, they concluded that Mandelbrot (1982) was right in suggesting that river networks are space-filling. However, La Barbera and Rosso (1989) used

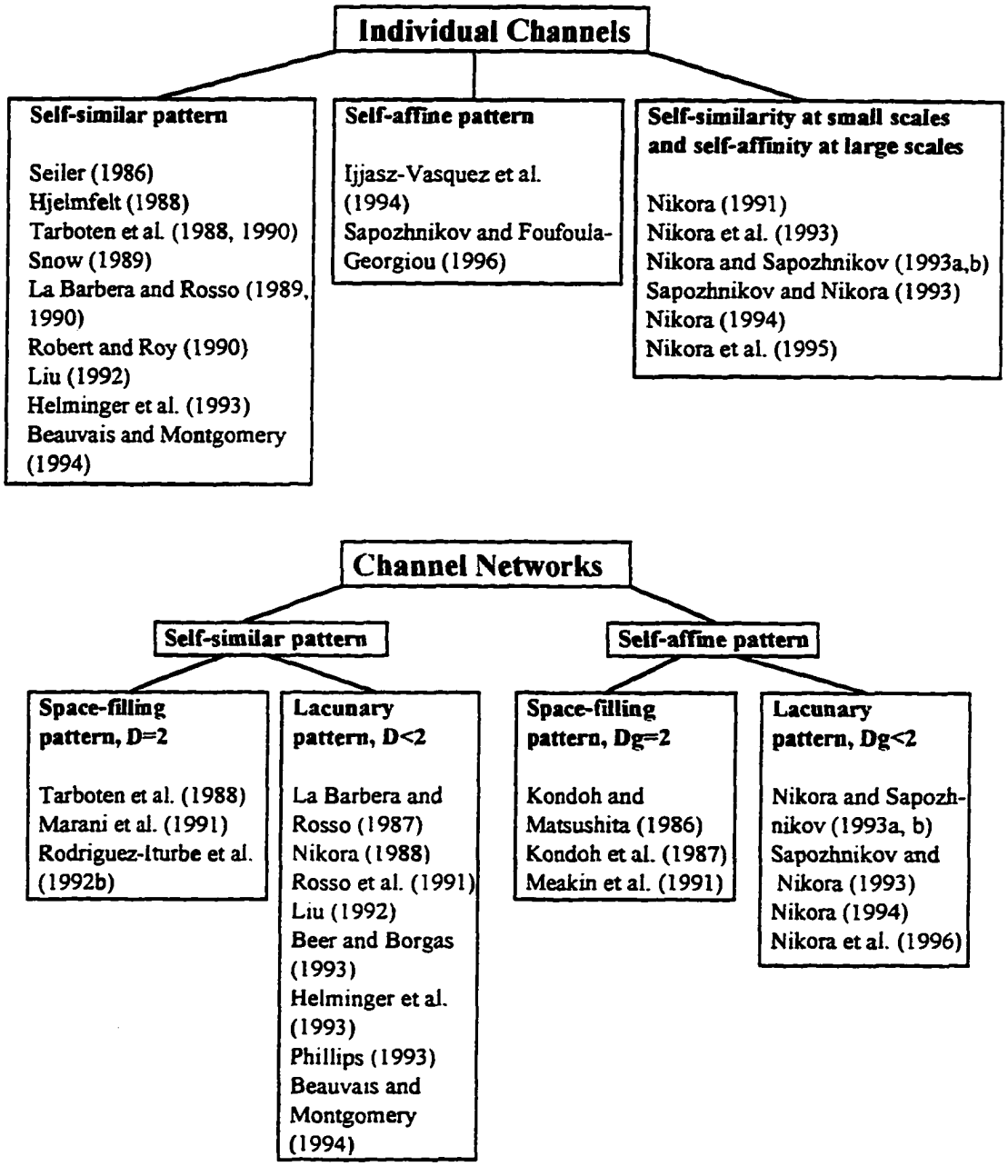

Figure 2.3. A summary of fractal models of river channels and networks (modified from Nikora et al., 1996).

Equation 2.16 and estimated the fractal dimension of river networks to range between 1.6 and 1.8.

Tarboten et al. (1990) pointed out that the methods of LaBarbera and Rosso (1989) only takes into account the fractal dimension of the network, D_t, and disregards the fractal characteristics of individual channels, D_s, recognized by Mandelbrot (1982). Tarboten et al. (1990) improved Mandelbrot's estimate of D=1.2 for individual channels by using Gray's (1961) improvement of Hack's law and showed that the fractal dimension of individual channels is generally around 1.1. They then argued that if the sinuosity fractal dimension and the topological fractal dimension are combined by $D=D_t*D_s$, the resulting dimensions should be close to 2. Indeed, if the results of La Barbera and Rosso (1989) are multiplied by 1.1, the resulting fractal dimensions are close to 2.

The debate between the two research groups motivated considerable efforts by several researchers to improve estimates of what appeared to be three fractal dimensions of rivers: the topological dimension, the sinuosity dimension, and the combined dimension. Phillips (1993) showed that estimating the fractal dimension by Horton's laws is prone to error due to the faulty assumption that Horton's laws hold true over an infinite range of scales. Peckham (1995) suggested that a better estimation of the topological fractal dimension of river networks is

$$D_t=\ln R_b/\ln R_c \qquad (2.17)$$

where R_b is the bifurcation ratio and R_c is ratio the number of stream links of order w to the number of stream links of order w-1. A stream link is a reach between

confluences. Equation 2.17 allows calculation of D_t on purely topological matters without introducing a measure such as length, which is accounted for in D_s.

Claps and Oliveto (1996) derived an equation to calculate D_t based on the distribution of links in a network:

$$D_t=\ln(M)/\ln(d) \qquad (2.18)$$

where M is the number of links in a network at a certain topological diameter d. The topological diameter is the number of links in the longest flow path in a basin. They suggested that D_t is typically near 1.508 ± 0.21. Nikora et al. (1989) used Equation 2.16 and arrived and $D_t=1.5 \pm 0.27$. Liu (1992) obtained $D_t = 1.55 \pm 0.28$.

Claps and Oliveto (1996) derived a method that combines D_s and D_t and determined that D is typically near 1.7. Moussa and Bocquillon (1993) showed similar results. These studies suggest that networks are non-plane filling, which conflicts with Tarboten et al. (1988, 1990) results.

Equation 2.16 is based on the assumption of self-similarity. Nikora (1994) suggested that because basin formation is determined by gravity which is a directional force, river networks will tend to elongate and thus self-affinity is more probable than self-similarity. He suggested that Equation 2.16 only accounts for scaling in the longitudinal directions, and that this dimension, D_l, in addition to a second fractal dimension, D_w that accounts for scaling in the transversal direction is needed:

$$D_w = \ln R_b/\ln(R_a/R_l) \qquad (2.19)$$

R_b, R_l, and R_a are from Horton's laws. If D_w and D_l are equal, then the network is self-similar. If they are not equal then the network is self-affine, and the degree of self-

affinity is characterized by the Hurst exponent, H, introduced by Mandelbrot (1986), where

$$H=D_l/D_w \tag{2.20}$$

Further, Nikora (1994) applied Mandelbrot's (1986) lacunarity dimension D_g to river basins where

$$D_g = 2D_lD_w/(D_l+D_w) \tag{2.21}$$

which characterizes the noncompactness of the dimension. Note that a self-similar, space-filling network as proposed by Tarboten et al. (1988, and 1990) will have H=1, $D_L=D_w=D_g=2$. Nikora (1994) states that river networks are typically noncompact ($D_g<2$) and self-affine (H<1).

Nikora et al. (1996) introduced yet another technique to calculate the fractal dimension which accounts for both the sinuosity of individual rivers and the channel network based on the relationships between two channel length variables and catchment area: the main channel length L, and the total length of all channels $\mathcal{L}$ where

$$L \propto A^{\beta} \tag{2.22}$$

$$\mathcal{L} \propto A^{\varepsilon} \tag{2.23}$$

From Equations 2.22 and 2.23, scaling in the longitudinal and transversal directions can be described and thus the lacunarity dimension D_g and the Hurst exponent can be obtained. Nikora et al. (1996) used this method in a case study of a river in New Zealand and showed that the basin is self-affine with H<1, but space-filling with $D_g=2$.

However, they pointed out that D_g is commonly less than 2, which conflicts with the results of Tarboten et al. (1988, and 1990).

La Barbera and Rosso (1989, and 1990) opposed the Tarboten et al. (1988, and 1990) suggestion that channel networks are space-filling by stating that the idea of a plane filling network disregards the distinctions between hillslope flow and channel flow, and that channel networks do not penetrate entire basins. They stated that a network developed under random processes without geologic constraints would tend toward dimension 2 as the network matured. But, networks rarely exist without constraints. Therefore, they reasoned that fractal dimension would be somewhat smaller than 2. Andah et al. (1987) suggested that certain techniques of channel network extraction from DEMs may bias the fractal dimension towards 2.

Phillips (1993) agreed that a space-filling network is an ideal abstraction and that the fractal dimension of channel networks should not be viewed as the degree to which a channel network is space filling, but that the proper interpretation of the fractal dimension of a channel network is that it represent the degree to which a channel network is constrained by geologic conditions. A fully unrestrained network that is allowed to develop an ideal bifurcating system will have a fractal dimension of 2. If the network is restrained by lithology, say confined to a bedrock controlled valley, the dimension will be something less than 2. He further pointed out that a flaw in the space filling concept is that it assumes that the self-similarity of Horton's laws operates at all scales ad infinum, when in fact there is a lower bound to the channel

network at the scale of the channel head. There is a break in the scaling encompassed by Horton's laws at the hillslope scale.

Tarboten et al. (1992) recognized this break in scaling, but did not view it as evidence that a network is not space filling. Instead, they recognized the break as a transition between two scaling regimes, one that exists for the channel network and one that exists for the unchanneled hillslopes. In fact, they identified this break in scaling in several channel networks and used it to determine the extent of the space filling channel networks. This break in scaling can be seen when the fractal dimension of a channel network is computed by more direct means such as functional box counting (Lovejoy et al., 1987; Tarboten et al., 1988).

Functional box counting is a two dimensional version of the ruler method discussed above, and is employed as follows:

1. Cover the channel network with a single box with sides of length L.
2. Divide the box into four quadrants with sides of length L/2, and count the number of cells N occupied by a channel.
3. Divide each quadrant into four subquadrants of size L/n, and continue doing so until the minimum box size is equal to the resolution of the data, keeping track of the number of quadrants or cells N occupied at each step.
4. Plot the number of cells N against cell size L/n on a log-log plot.

The fractal dimension is determined according to:

$$D=\log(N)/\log(L/n) \quad (2.24)$$

which is the exponent of the power law function, or the slope of the log-log plot relating N to L/n.

Tarboten et al. (1988) noted that above a certain box size, the slope of the scaling line is typically near 2 and interpreted this to be the fractal dimension of the channel network, which agrees with their estimates based on Hortonian analysis. Below that box size, the slope is typically close to one, which represents the hillslope regime. A problem with the functional box counting method is that it is only accurate if the object is self-similar (Nikora et al., 1996).

There appears to be a natural characteristic scale that exists in the structure of drainage basins that occurs at the channel head scale. Above and below this process scale are different scaling regimes. Rigon et al. (1993) showed that the threshold dividing hillslope and channel processes is related to the spatial organization of the network and is linked to energy dissipation principles. This is discussed further in chapter 7.

Simply calculating a fractal dimension is of little use unless it can be related to a physical explanation. At present it seems that it is simply a discovery that river networks evolve to a similar state. However, their utility does become significant when determining scales at which their values change, such as described for the change between hillslope and channel regimes. Goodchild and Mark (1987) suggested that most geomorphological features are not pure fractals in the sense of having a constant D, but exhibit fractal behavior over a limited range of scales. Thus, the fractal

dimension is useful for separating scales of variation that might be the result of natural processes (Burrough, 1981). These thresholds between scaling regimes signify natural preferential scales that exist in the landscape.

Fractal analysis of drainage basins has largely centered on monofractals. However, recent research has revealed that fluvial landscapes exhibit multifractal characteristics (Ijjasz-Vasquez et al., 1992; Lavalée et al., 1993; Rodriguez-Iturbe et al., 1994). It has been shown that the width function of drainage basins is multifractal (Marani et al., 1991). The width function is a shape factor that provides a measure of the proportion of drainage area located at the same distance from source to outlet (Gupta et al., 1986). Lavalée et al. (1993) observed several multifractal characteristics in real topographies, and Rodriguez-Iturbe et al. (1994) showed that the multifractal nature of river basins can be credited to the links between fractal landforms and the dynamics responsible for their growth. Indeed, the width function has been identified as one of the primary basin characteristics that controls the hydrologic response of a basin (Mesa and Mifflin, 1986) Hence, multifractal analysis provides a quantitative tool to examine the connections between drainage basin form and hydrologic response.

2.2.2.b Scaling of Hydrologic Processes

As hydrologists we are not only interested in the form of basins, but in how hydrologic fluxes vary with scale. It has long been known that discharge scales approximately linearly with drainage area. This implies self-similarity. However, self-similarity requires that all moments scale, not just the mean. In this usage, a moment refers to the average value of the nth power of all points in a set. Thus, the first

moment is the mean. Commonly used statistical moments such as standard deviation, skewness, and kurtosis are calculated by raising the difference between each point and the mean to successive powers then averaging those values. In this study, we simply raise the original values to successive powers without subtracting the mean.

If discharge Q is the random variable and drainage area A is the scale parameter, then discharge is self-similar if

$$Q(\alpha A) \stackrel{d}{=} Q(A) * \mu(\alpha) \qquad (2.25)$$

where $\stackrel{d}{=}$ denotes equality of probability distributions (Gutpa and Waymire, 1990). Here, the drainage area is changed by a factor α, and the probability distribution of Q(A) is rendered equal to the probability distribution of $Q(\alpha A)$ through the normalization function $\mu(\alpha)$. Consequently, the moments of discharge change in a systematic manner with scale. Gutpa and Waymire (1990) showed that indeed each moment of discharge scales with drainage area. However, the function relating the scaling exponents for each moment is not linear, as would be required for strict self-similarity. Each moment scales according to its own power law function, hence the term multiscaling.

The physical significance of simple and multiscaling is that simple scaling implies that the coefficient of variation remains constant across scales, whereas multiscaling does not. Gupta and Waymire (1990) found that river flows have multiscaling of the form where the coefficient of variation decreases with increasing scale, and suggested that the variability of river flow can be viewed as a consequence

of some large-scale flux cascading down to successively smaller scales. Gupta and Waymire (1996) stated that river flows inheret multiscaling features from the spatial rainfall at large scales, and from channel network geometry at small scales.

2.2.2.c Basin Morphology and Hydrologic Response

Rivers sculpt the landscape over which they flow. Conversely, river basin morphology controls the nature of the hydrologic response. There is a reciprocal relationship between the two that is far from being completely understood. Advances in understanding the connections between network morphology and hydrologic response were motivated by the pioneering work of Rodriquez-Iturbe and Valdes (1979) in which they made connections between the instantaneous unit hydrograph and network morphology. Several researchers continued this effort (Gupta et al., 1980; Rodriquez-Iturbe et al., 1982; Troutman and Karlinger, 1984; 1985). The research connecting the scaling of river flows, rainfall, and 3-D channel networks is still in its infancy. However, research by Gupta and several co-workers has provided significant advances towards an understanding of the controls on hydrologic response at the basin scale (Gupta and Dawdy, 1994, 1995; Gupta et al., 1994, 1996; Gupta and Mesa, 1988; Gupta and Waymire, 1983, 1990, 1996).

A significant advancement is this area was the proposal of a theory linking energy dissipation, runoff production, and the three-dimensional structure of river basins (Rodriguez-Iturbe et al. 1992a). The central idea is that fluvial channel networks evolve to fulfill three principles: (1) the principle of minimum energy expenditure in any link of the network; (2) the principle of equal energy expenditure

per unit area of channel anywhere in the network; and (3) the principle of minimum energy expenditure in the network as a whole. Several studies have followed up on this idea providing further evidence of those connections (Marani et al., 1991; Rigon et al., 1993, Rinaldo et al., 1992, 1995; Rodriguez-Iturbe et al., 1992b, and 1994). Rodriquez-Iturbe et al. (1992b) investigated the scaling of mean annual flow in fluvial networks by assuming that the drainage area can be used as a surrogate for mean annual flow. They showed that all rivers evolve to possess a common exponent in a power law representation of the probability distribution of cumulative area near -0.45. deVries et al. (1994) showed that this number may arise from the fractal nature of river networks. Ijjasz-Vasquez et al. (1992) studied the multifractal characteristics of several variables and found that river basins from a variety of different climates and lithologies display similar multifractal characteristics of mass and energy distribution. These observations hint to a common underlying principle governing the organization of drainage basins and their hydrologic response.

Rinaldo et al., (1992) explored these issues through the use of optimal channel network (OCNs). OCNs are developed by configuring branching structures in such a way that they provide pathways for energy flow through a system with minimal loss of energy. Rinaldo et al., (1992) found that OCNs have fractal and multifractal characteristics, and cumulative area distributions that are essentially indistinguishable from real drainage basins. Rinaldo et al., (1992) showed that the power law distribution of areas can be related to the theory of self-organized criticality (Bak et al., 1987, 1988).

Bak et al. (1987, 1988) introduced the concept of self-organized criticality (SOC) to explain the tendency for spatially extended, dissipative, dynamical systems to evolve to critical states regardless of the initial conditions. The previous sentence demands several definitions. First, "system" refers to a phenomenon that is a function of several interrelated variables. The term "dynamical" refers to phenomena that produce time-changing patterns, with the characteristics of the pattern at one time being interrelated with those at other times. "Spatially extended" refers to phenomena that produce spatially variant patterns, with the characteristics of the pattern at one location being interrelated with those at other locations. "Dissipative" refers to the property of a system to process energy from higher to lower forms. A "critical state" is when the system possesses no intrinsic time or length scales, or is spatially and temporally self-similar. "Self-organized" means that the system will reach the critical state despite the initial conditions.

The mounting evidence of spatial and temporal fractal structures in river basins suggests that rivers can be viewed as spatially extended dynamical systems. Thus, SOC provides a link between fractal landforms and the dynamics responsible for their growth. Mandelbrot (1974) showed that uniform energy input in extended dissipative systems results in power law distributions of energy dissipation. Takayasu et al. (1988) showed that aggregation systems do indeed possess power law mass distributions with an exponent of -0.465, which is remarkably close to the empirical observations on cumulative area distributions of Rodriquez-Iturbe et al. (1992b). Thus, Rinaldo et al., (1992, 1993) concluded that the apparent universality of the power law exponent for

mass distributions in river basins implies that rivers naturally evolve to a self-organized critical state, where energy expenditure is minimized and equal in all parts of the basin. The critical state is defined by the fractal and multifractal characteristics of channel networks, and the universal scaling exponents in cumulative drainage areas.

Since multifractals describe the spatial distribution of a measure over a geometric set of points, the multifractal characteristics inherent in the model of fluvial evolution based on self-organized criticality is important to understanding the connections between drainage basin form and hydrologic response. Of particular interest is the result that width function was found to be multifractal (Marani et al., 1991, Rinaldo et al., 1992). Gupta et al., (1986) originally proposed the width function as a means of connecting the hydrologic response of a basin to its geomorphologic characteristics through the geomorphologic instantaneous unit hydrograph (GIUH) (Rodriguez-Iturbe and Valdes, 1979). Thus, a link has been established between the fractal and multifractal characteristics of channel networks, the concepts of basin evolution by energy minimization, and the resulting hydrologic response.

Chapter 3

SITE DESCRIPTION

The Kuparuk River originates in the northern foothills of the Brooks Range and flows 250 kilometers northward across the Arctic Coastal Plain to the Arctic Ocean near Prudhoe Bay, Alaska (Figure 1.1). The flow season typically begins in mid-May in the headwaters and late May to early June at the mouth of the Kuparuk River. Freeze-up begins in mid-September, but the rivers and streams may not be completely frozen until October. Although neighboring watersheds have active glaciers, there are no glaciers in the Kuparuk River basin. There is a permanent field of ice, called aufeis, covering approximately 6-12 km^2 in the basin that may have a local moderating effect on streamflow, but this is insignificant at the larger basin scale and streamflow is driven entirely by precipitation and snowmelt. A small spring exists in the headwaters of the basin, but its source is believed to be from precipitation percolating through local gravel deposits (Kreit et al., 1992).

The entire region lacks trees, is underlain by continuous permafrost, and is covered with snow for 7 to 9 months. Permafrost thickness ranges from around 250 meters near the foothills to over 600 meters near the coast (Osterkamp and Payne, 1981). Hence, the region is effectively isolated from deep groundwater. Subsurface flow occurs in a shallow zone above the permafrost. This shallow layer of soil that undergoes annual freezing and thawing is called the active layer. The active layer increases in depth throughout the short summer. Soils typically thaw to maximum

depths of 25-40 cm, but can thaw to 100 cm depending on several environmental factors including soil type, slope, aspect, and soil moisture (Hinzman et al., 1991). Due to the lack of glaciers and deep flow systems, the Kuparuk River is a clear water tundra river according to the classification of Craig and McCart (1975).

The smallest scale studied is a hillslope water track that drains 0.026 km^2 on a west facing slope in a headwater basin (Imnavait Creek) (Figure 1.1). A water track is essentially a linear channel that drains an enhanced soil moisture zone that flows directly down a slope and is best detected by a change in vegetation from the surrounding hillslope (Hastings et al., 1989; Walker et al., 1989). The Imnavait Creek basin contains numerous water tracks that are generally spaced tens of meters apart, although their density varies (Walker et al., 1989). Only intermittently do incised channels exist in water tracks, but they are significant components of the hillslope hydrologic cycle. The water track ends in a peat covered valley bottom through which water travels to Imnavait Creek as diffuse subsurface flow through the active layer, or overland flow during rainfall or snowmelt events.

Imnavait Creek, the second scale of study, is a small headwater stream occupying a north-northwest trending glacial valley at an average elevation of 904 meters, which was formed during the Sagavanirktok glaciation (Middle Pleistocene) (Hamilton 1986). A gauging station with a flume was installed at a point draining 2.2 km^2 as part of a previous study (Kane et al., 1989). The dominant vegetation in the Imnavait basin is tussock sedge tundra covering the hillslopes (Walker et al., 1989).

An organic layer typically near 10 centimeters thick, but up to 50 centimeters thick in the valley bottom, overlies glacial till (Hinzman et al., 1991). The valley bottom is covered with peat overlying till. However, the depth of thaw in the valley bottom rarely gets beyond the organic peat layer. The creek is essentially a chain of small ponds, called beads, that formed where the stream has eroded and melted massive ground-ice deposits. The stream bottom rarely cuts through to mineral soil but maintains itself in the organic layer. Imnavait Creek flows another 12 kilometers beyond our station before it joins the Kuparuk River.

The third scale of study occupies 142 km^2 in the Kuparuk River headwaters, referred to here as the Upper Kuparuk River basin. At the intersection with the Dalton highway, the Kuparuk River is a fourth order stream on a USGS 1:63360 map. However, the hillslopes and tributary valleys contain a complex network of water tracks, basins similar to Imnavait Creek, and rocky headwater streams that render the actual stream order difficult to estimate. Two streams join together at the base of steep hills near the headwaters forming the main channel which occupies a North-northwest trending valley parallel to the Imnavait Creek basin. The main basin length is 16 km, with a channel length of 25 km. The average elevation of the basin is 967 meters. Vegetation in the basin consists of alpine communities at higher elevations and moist tundra communities, predominantly tussock sedge tundra, at lower elevations. Dwarf willows and birches up to 1 m in height occupy portions of the stream banks.

Beyond the Dalton Highway intersection, the Kuparuk River flows through more rolling foothills topography and eventually enters the flat coastal plain before it flows into the Arctic Ocean, draining a total area of 8140 km^2 at the U.S. Geological Survey gauging site, with a basin length of nearly 250 kilometers. The average elevation of the entire Kuparuk River basin is 304 meters. The coastal plain was never glaciated, and is characterized by abundant, wind-oriented thaw lakes (Walker et al. 1989). The dominant export of water from small basins close to the coast is by evaporation, with little overland and channel flow due to the low gradients (Rovansek et al., 1996). However, several large drainage channels originate in the foothill regions that cross the coastal plain.

Chapter 4

AN ANALYSIS OF STREAMFLOW HYDROLOGY IN THE KUPARUK RIVER BASIN, ARCTIC ALASKA: A NESTED WATERSHED APPROACH

4.1 Abstract

A hydrologic monitoring program was implemented in a nest of watersheds within the Kuparuk River basin in Northern Alaska as part of an interdisciplinary effort to quantify the flux of mass and energy from a large arctic area. Described here are characteristics of annual hydrographs and individual storm hydrographs of four basins draining areas of 0.026 km^2, 2.2 km^2, 142 km^2, and 8140 km^2. We assess the influence that permafrost has on those characteristics, and make comparisons to rivers in regions without permafrost. Snowmelt runoff was a major component of the annual runoff in each basin. A typical storm hydrograph had a fast initial response time, long time lags between the hyetograph and hydrograph centroids, an extended recession, and a high runoff/precipitation ratio due to the diminished storage capacity caused by permafrost. Seasonal trends existed in some streamflow characteristics, but it was difficult to determine if they resulted from active layer dynamics or precipitation patterns.

4.2 Introduction

The shape of a hydrograph reflects how a drainage basin transforms precipitation into runoff and embodies the integrated influence of several basin characteristics including the soils, drainage basin morphology, and vegetation. Hence, the quantitative description of hydrographs is a valuable tool for understanding the mechanisms by which the drainage basin controls hydrology, and offers a tool for

comparing hydrologic characteristics between different physiographic regions. The ubiquitous presence of permafrost is a dominant physical characteristic of all arctic basins. Several studies have shown that permafrost has significant influences on streamflow characteristics (Church, 1974; Kane et al., 1989; Newbury, 1974; Slaughter and Kane, 1979; Slaughter et al., 1983, Woo and Steer, 1982; Woo and Steer; 1983). However, the database for watersheds in regions with permafrost is still sparse.

An interdisciplinary effort called the Land-Air-Ice-Interaction (LAII) Flux Study was initiated in 1993 to estimate the flux of mass and energy between the land, atmosphere, and the Arctic Ocean in the Kuparuk River basin in Northern Alaska (Weller et al., 1995). River discharge is a major export mechanism of mass and energy out of any drainage basin. Thus, we implemented a nested watershed study to understand the nature and variability of river discharge. The analysis of simple hydrographs is a first step to meet this need.

A nested watershed study involves investigating a cascade of basins, thereby providing a framework for studying how the physics of hydrologic processes is related across scales. This study included four basins: a hillslope flow path called a water track (0.026 km^2) (see site description), Imnavait Creek (2.2 km^2), the Upper Kuparuk River (142 km^2), and entire Kuparuk River (8140 km^2). The objective of this paper is to describe the physical characteristics of streamflow hydrology at those four scales for the years 1993, 1994, and 1995 through the analysis of annual hydrographs, rainfall-runoff relationships, and nested basin interactions. An underlying theme is a

comparison of streamflow characteristics in the permafrost-dominated Kuparuk River basin with those of rivers in temperate regions.

4.3 Methods

An annual field program began with snow surveys in late April each year. An Adirondack snow sampler was used to determine the pre-melt snow water equivalent (SWEQ) in each basin. SWEQ in the Imnavait Creek basin was estimated from approximately 90 measurements in a 900 meter transect across the basin. SWEQ in the water track basin was not measured. SWEQ is highly variable due to slope, aspect, vegetation, and elevation, and is difficult to estimate over large areas. Average water equivalent in the two larger basins was estimated by traveling throughout the basins on snow machines and helicopters, and performing snow surveys in spots that were representative of landscape units, based on slope, aspect, elevation, and latitude. At least ten measurements of water equivalent and 20 snow depth measurements were performed at each station, then weighted averages based on landscape units were calculated for each basin.

Streamflow was monitored at the water track, Imnavait Creek, and the Upper Kuparuk River from the onset of snowmelt in the spring to near freeze-up in the fall using stilling wells with Stevens F-7 water level recorders mounted with variable resistance potentiometers to obtain digital data. Campbell Scientific CR10 data loggers recorded stream stage every minute, and averaged over hourly increments. The U. S. Geological Survey provided hourly stage readings and daily flow averages near the mouth of the Kuparuk River. A small weir was used at the water track, and an H-type

flume was used at Imnavait Creek. Discharge measurements were made at several different stages to produce rating curves each year from which continuous records of discharge were calculated. Several discharge measurements were taken daily during the spring snowmelt period until ice cleared from the channels and the stage-discharge relations became reliable. Seven meteorological stations recorded precipitation, wind speed and direction, air temperature, relative humidity, and various radiation terms between the foothills and the coast. Figure 1.1 shows the locations of the meteorological stations. Two stations close to each other near the coast capture the strong meteorological gradients from proximity to the ocean, and two stations within two miles of each other in the foothills capture elevation gradients. The following analyses includes the period between snowmelt and September 7th each year because that is the latest date for which consistent data are available for all three years.

4.4 Results and Discussion

4.4.1 Annual Hydrographs

Figures 4.1a-d, 4.2a-d, and 4.3a-d show the 1993, 1994, and 1995 hydrographs respectively, for each basin. Hyetographs from a rain gauge located on the eastern ridgetop of the Imnavait Creek basin are included on the plots for this drainage. Table 4.1 summarizes the hydrologic inputs and outputs for each basin and year.

Snow is a significant hydrologic input. The ratio of the amount of precipitation which comes as snow before ablation (SWEQ) to the total precipitation is P_w/P_t in Table 4.1, and it was approximately 33% in the upper basins and averaged 44% for the

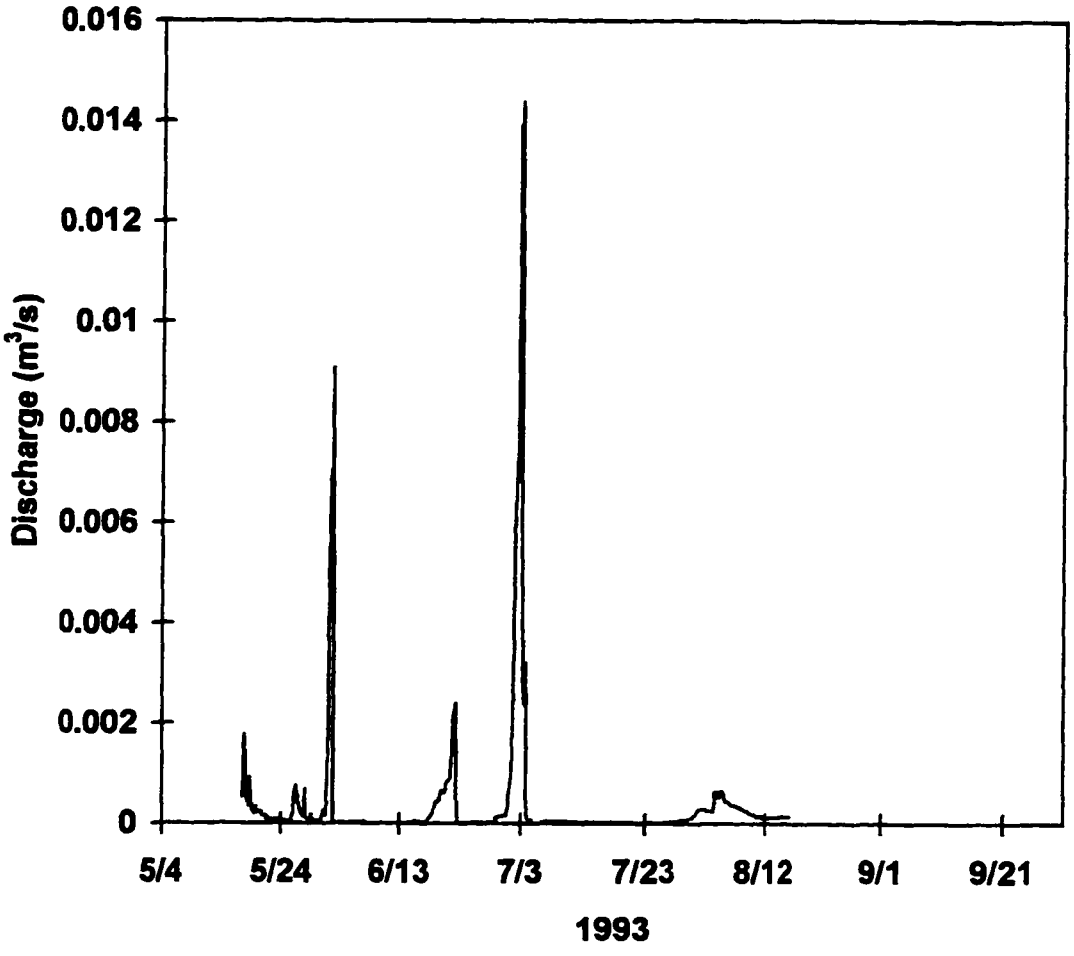

Figure 4.1a. 1993 hydrograph for Water Track 7, Imnavait Creek.

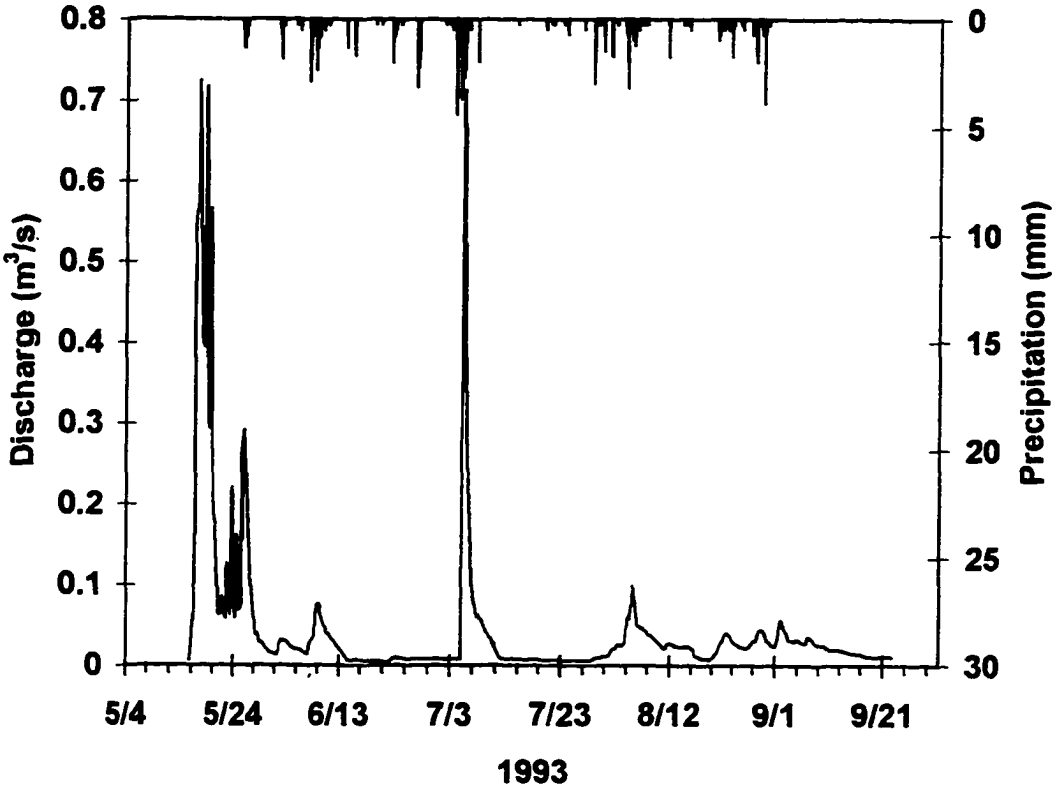

Figure 4.1b. 1993 hydrograph and hyetograph for Imnavait Creek.

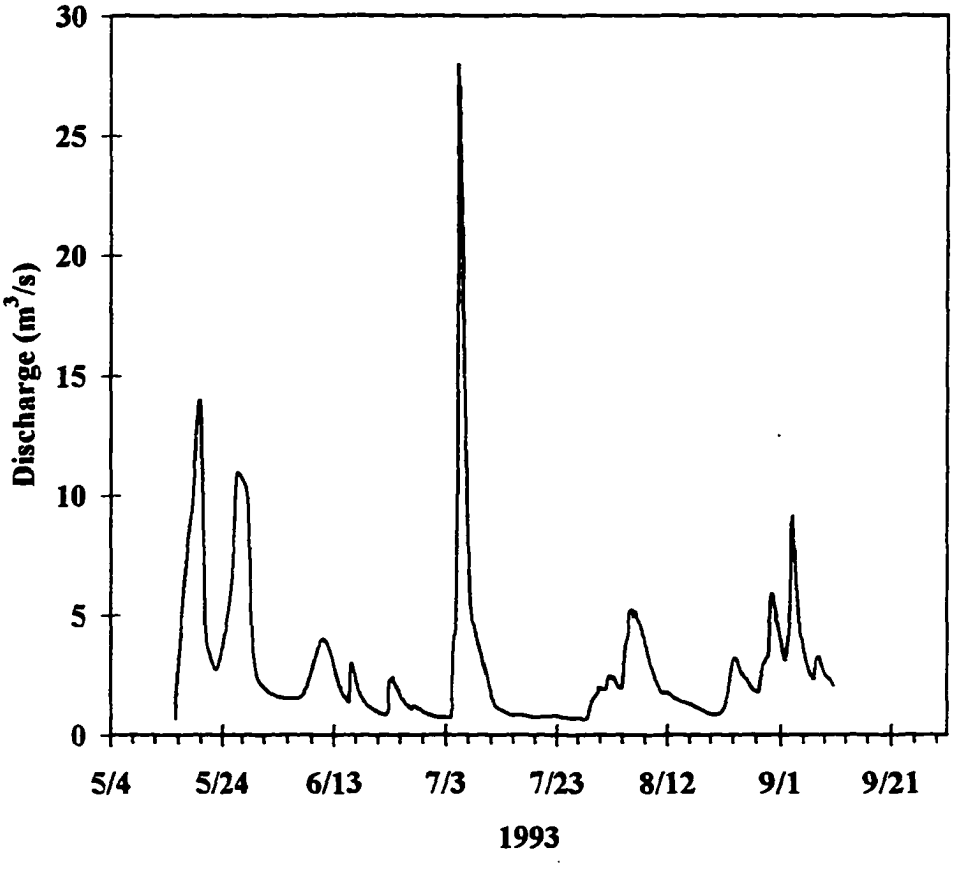

Figure 4.1c. 1993 hydrograph for the Upper Kuparuk River basin.

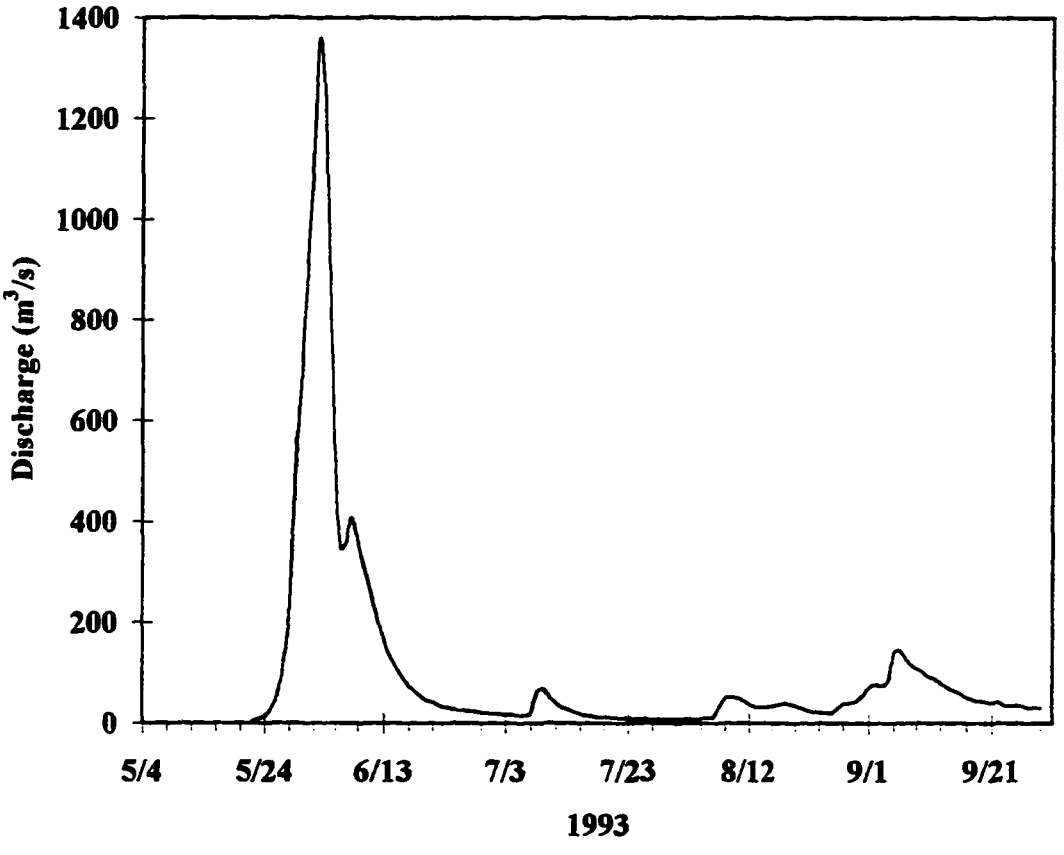

Figure 4.1d. 1993 hydrograph for the entire Kuparuk River.

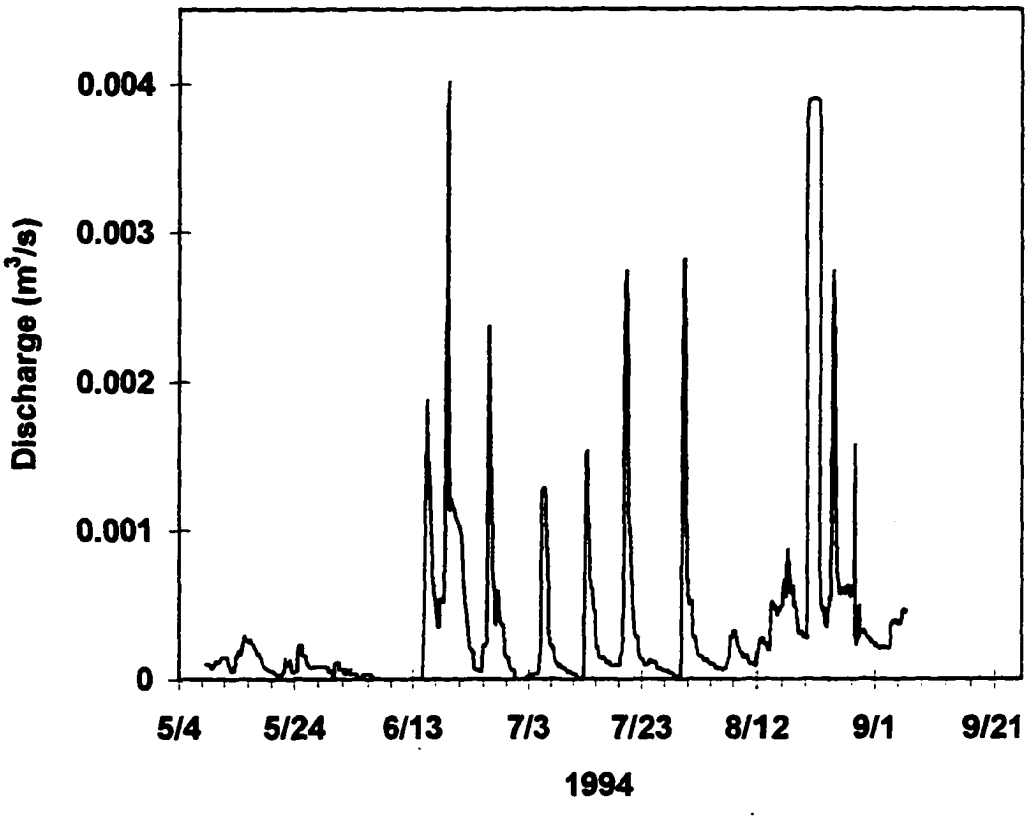

Figure 4.2a. 1994 hydrograph for Water Track 7, Imnavait Creek.

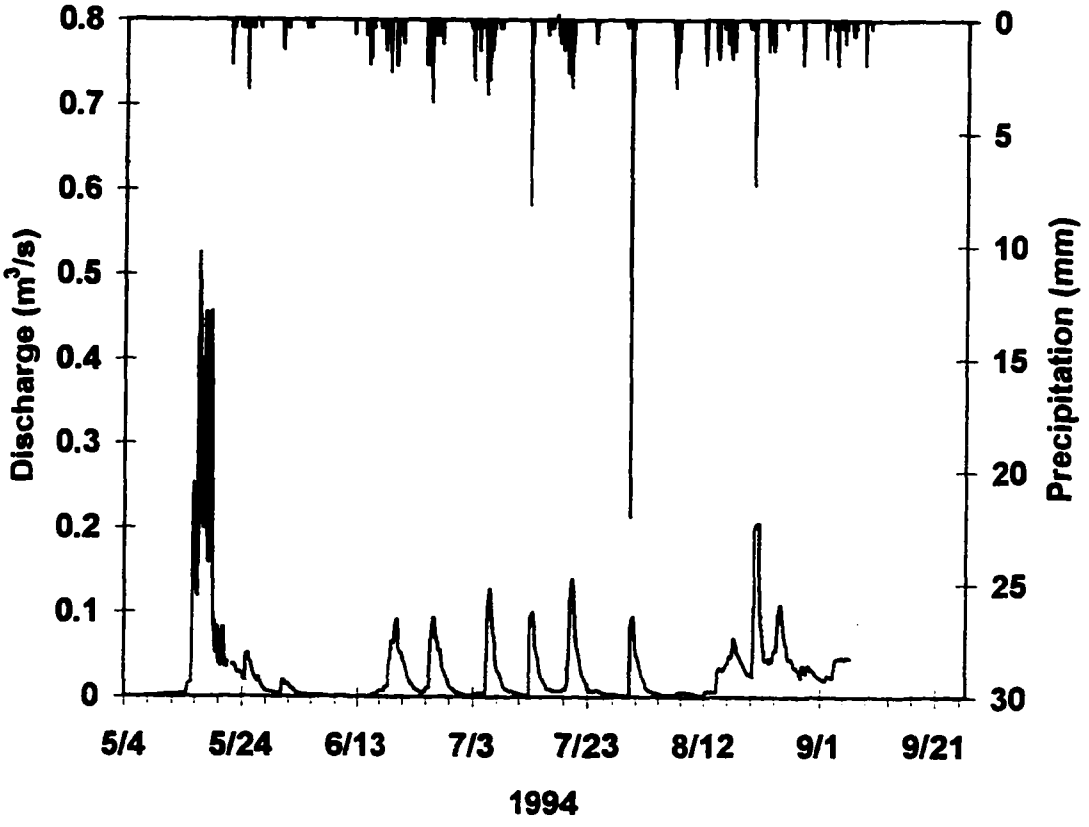

Figure 4.2b. 1994 hydrograph and hyetograph for Imnavait Creek.

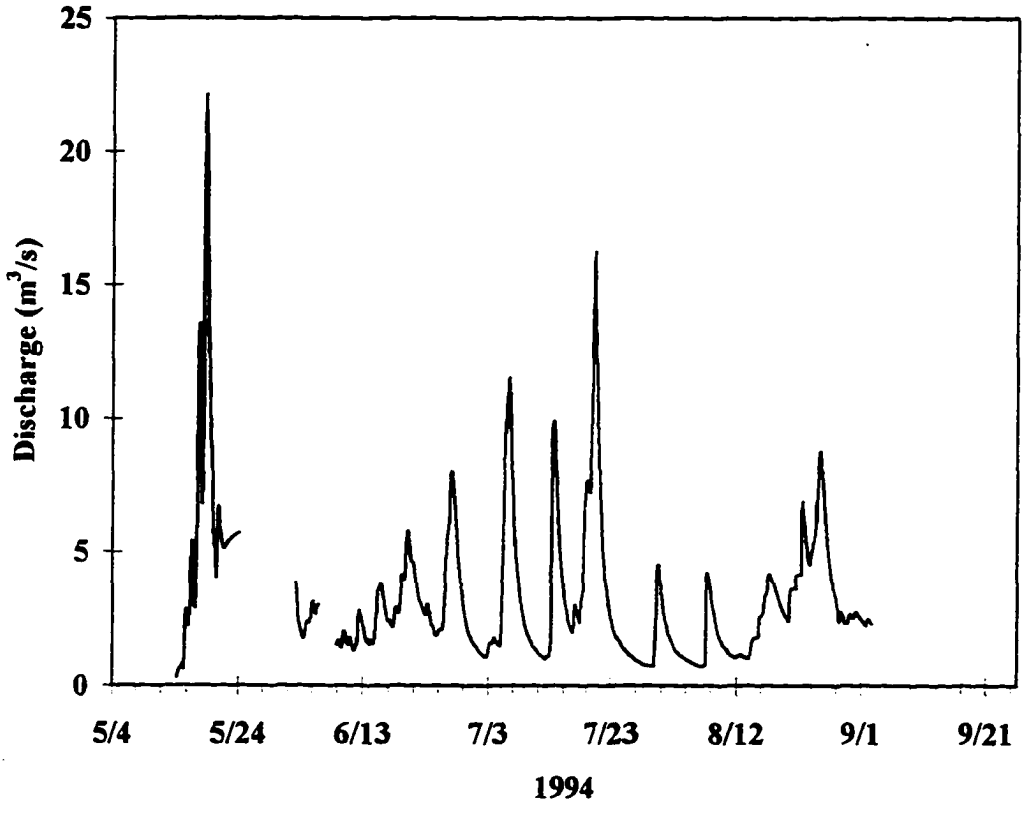

Figure 4.2c. 1994 hydrograph for the Upper Kuparuk River.

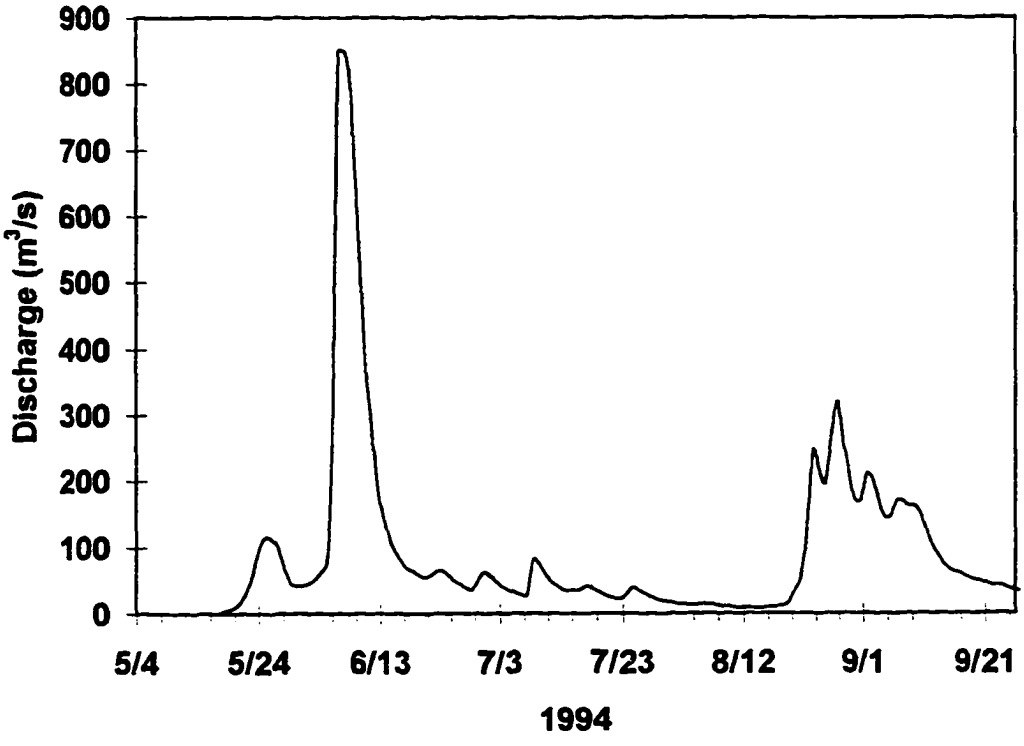

Figure 4.2d. 1994 hydrograph for the entire Kuparuk River.

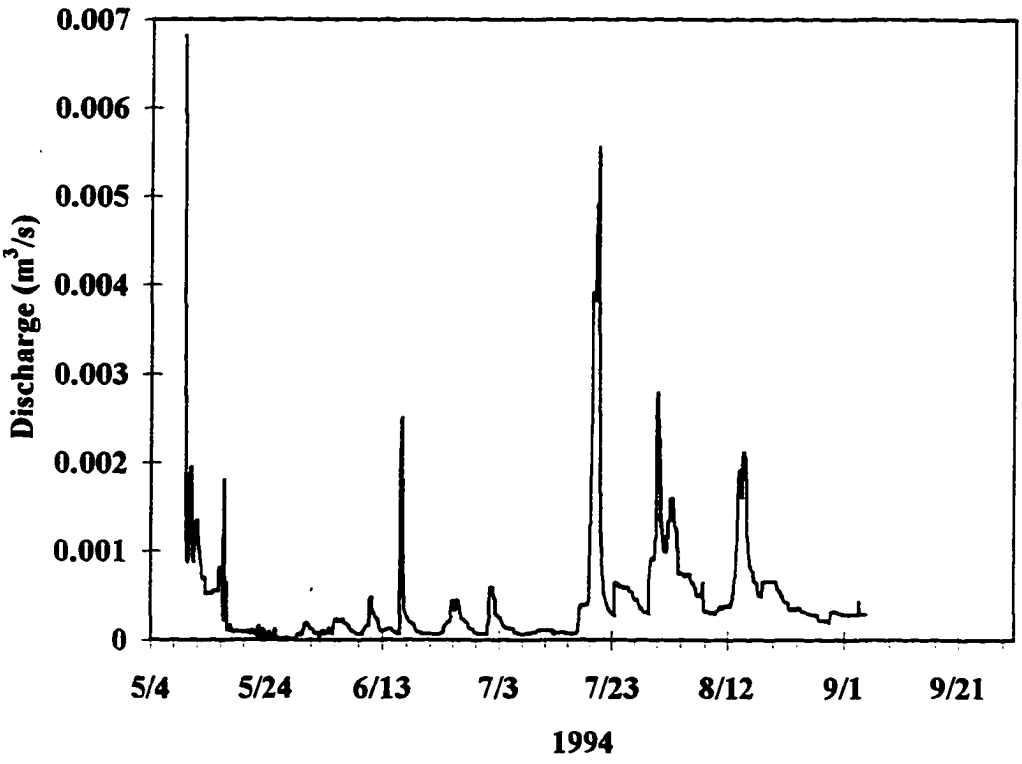

Figure 4.3a. 1995 hydrograph for Water Track 7, Imnavait Creek.

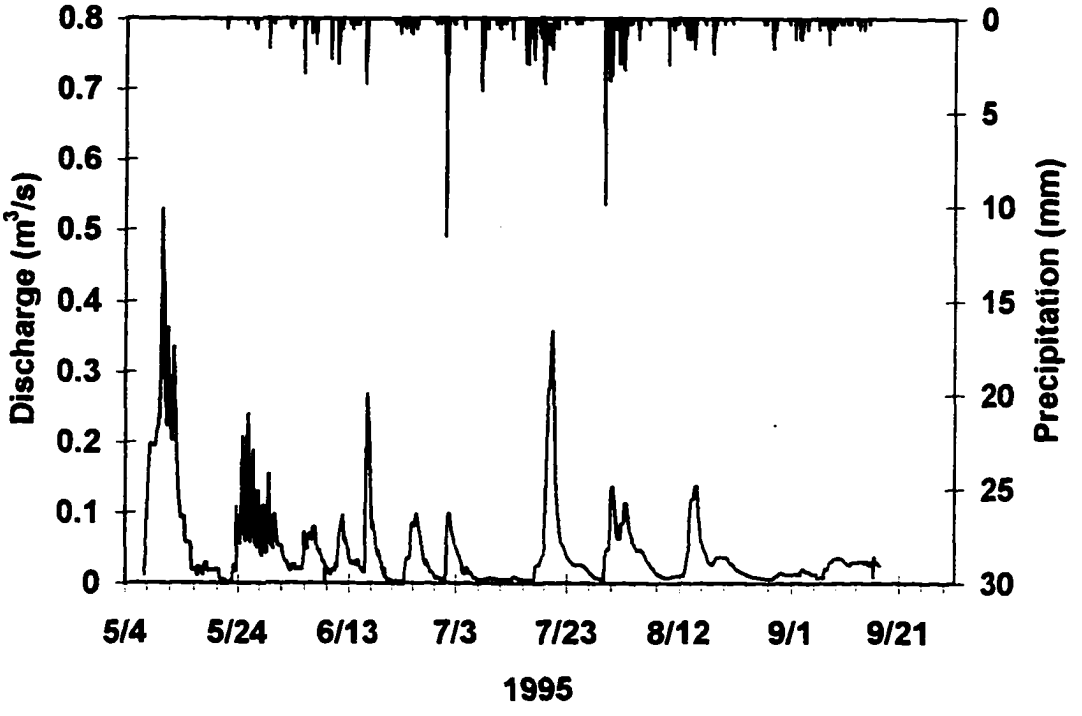

Figure 4.3b. 1995 hydrograph and hyetograph for Imnavait Creek.

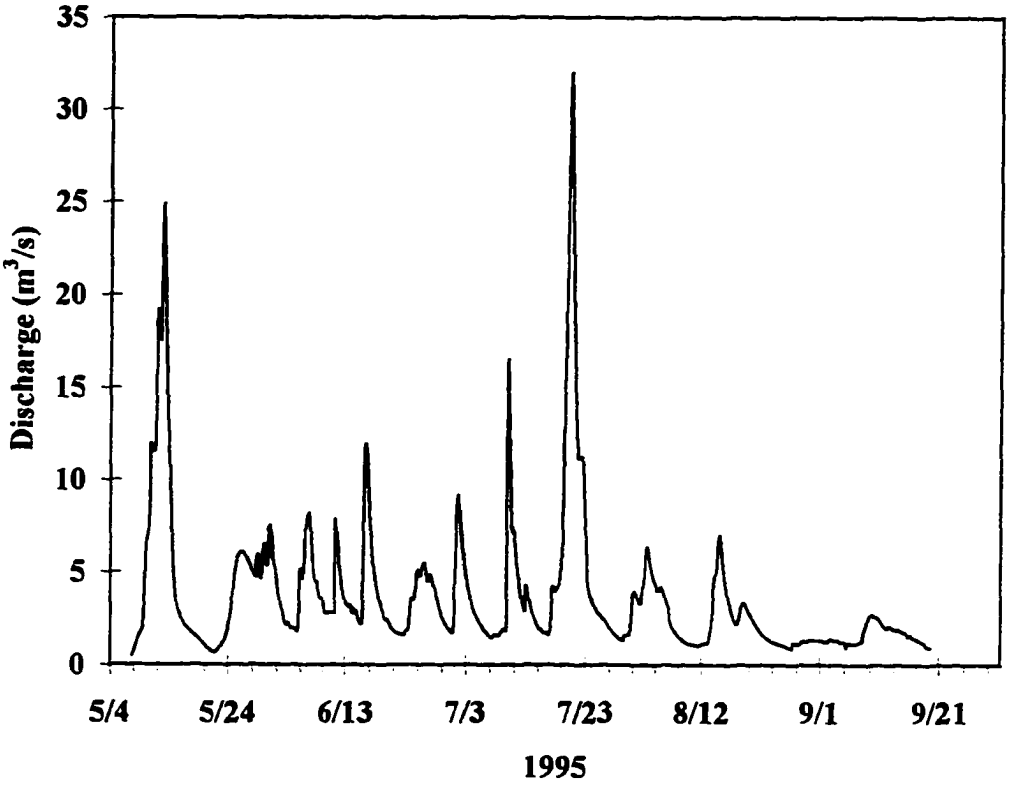

Figure 4.3c. 1995 hydrograph for the Upper Kuparuk River.

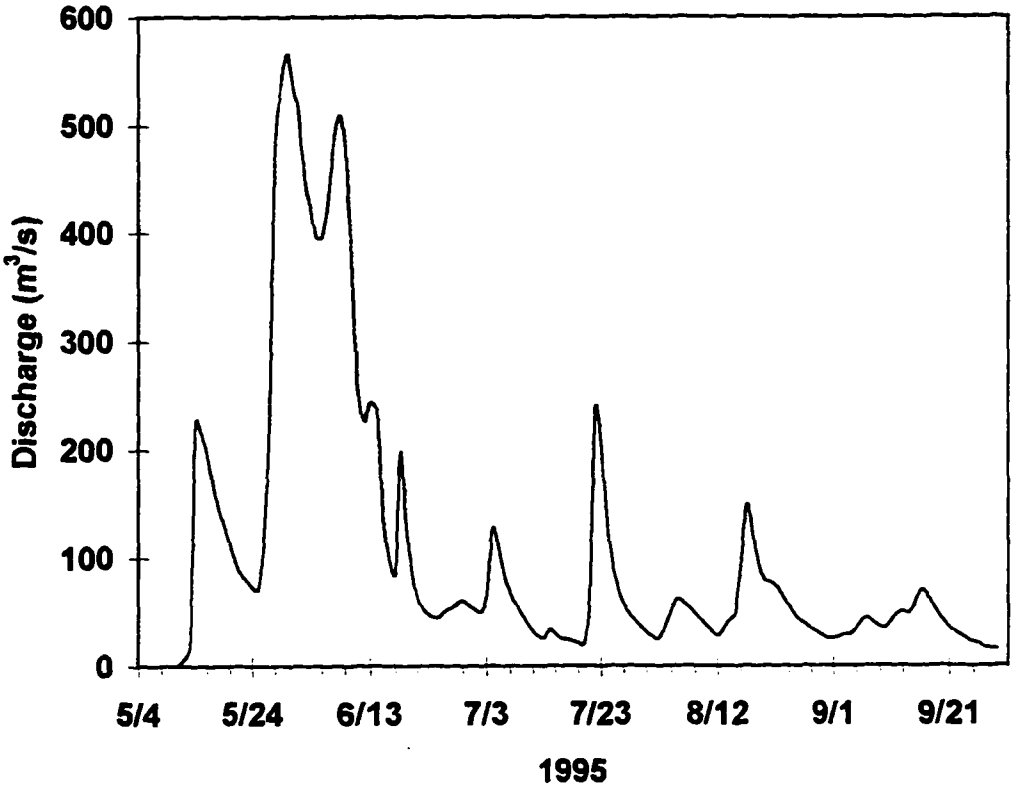

Figure 4.3d. 1995 hydrograph for the entire Kuparuk River.

Table 4.1. Annual hydrograph characteristics in the Kuparuk River basin.

	Water Track				Imnavait Creek			
	1993	1994	1995	ave.	1993	1994	1995	ave.
SWEQ P_{sn} (cm)	na	na	na	na	12.5	8.0	14.2	11.6
Summer Pcp. P_s (cm)	20.8	27.1	20.9	22.9	20.8	27.1	20.9	22.9
Total Pcp. P_t (cm)	na	na	na	na	33.3	35.1	35.1	34.5
P_{sn}/P_t	na	na	na	na	0.4	0.2	0.4	0.3
Snow Runoff R_{sn} (cm)	0.5	0.5	3.6	1.5	10.0	5.2	9.8	8.3
Summer Runoff R_s (cm)	10.5	14.2	15.2	13.3	11.7	10.0	13.9	11.9
Total Runoff* R_t (cm)	11.0	14.7	18.8	14.8	21.8	15.2	23.7	20.2
R_{sn}/R_t	na	na	0.2	na	0.5	0.3	0.4	0.4
Max Summer Storm (cm)	5.2	2.6	3.5	3.8	3.3	0.9	2.0	2.1
Runoff Ratio R_t/P_t	na	na	na	na	0.7	0.4	0.7	0.6
Snow Run. Rat. R_{sn}/P_{sn}	na	na	na	na	0.8	0.7	0.7	0.7
Summer Run. Rat. R_s/P_s	0.5	0.5	0.7	0.6	0.6	0.4	0.7	0.5

	Upper Kuparuk River				Kuparuk River			
	1993	1994	1995	ave.	1993	1994	1995	ave.
SWEQ P_{sn} (cm)	13.2	10.6	15.0	12.9	13.5	7.4	13.9	11.6
Summer Pcp. P_s (cm)	22.4	27.8	27.4	25.9	11.0	15.1	13.9	13.3
Total Pcp. P_t (cm)	35.6	38.4	42.4	38.8	24.6	25.7	28.4	26.2
P_{sn}/P_t	0.4	0.3	0.4	0.3	0.6	0.3	0.5	0.4
Snow Runoff R_{sn} (cm)	6.2	6.6	7.9	6.9	11.3	6.1	11.0	9.5
Summer Runoff R_s (cm)	14.2	17.3	21.3	17.6	2.8	5.7	4.9	4.4
Total Runoff* R_t (cm)	20.5	23.9	29.2	24.5	14.1	11.8	15.9	13.9
R_{sn}/R_t	0.3	0.3	0.2	0.3	0.8	0.5	0.7	0.7
Max Summer Storm (cm)	3.5	2.7	5.3	3.8	2.4	5.4	1.1	2.9
Runoff Ratio R_t/P_t	0.6	0.6	0.7	0.6	0.6	0.5	0.6	0.5
Snow Run. Rat. R_{sn}/P_{sn}	0.5	0.6	0.5	0.5	0.8	0.8	0.8	0.8
Summer Run. Rat. R_s/P_s	0.6	0.6	0.8	0.7	0.3	0.4	0.4	0.3

entire basin. Typically, snow depth and SWEQ decrease from the mountains to the ocean so that the upper basins have higher SWEQs than the entire basin. However, in 1993 the Upper Kuparuk River basin and the entire basin had approximately the same SWEQ.

In each year, the summer precipitation (P_s) over the entire basin was approximately half the summer precipitation in the Upper Kuparuk River basin, where "summer" is defined as the period of time between the onset of snowmelt and September 7th. Some snow may fall during this period, but most summer precipitation is rain. Table 4.2 summarizes the summer precipitation for each weather station. Nine year averages at each station were obtained from previous studies in the Kuparuk Basin (National Snow and Ice Data Center, 1994). Basin average rainfalls were estimated by kriging the station data to a one kilometer resolution then averaging the resultant points. The 1993 basin average precipitation was close to the nine year average, and both 1994 and 1995 were considerably higher than average.

Snowmelt is typically a major runoff event in all arctic watersheds as precipitation that falls over approximately an eight month period is released as potential runoff usually within a period of two weeks or less. In Table 4.1, R_m/R_t is the fraction of annual runoff due to the snowmelt period. The snowmelt period contributed between 34% to 46% of the annual runoff in Imnavait Creek, 17% to 30%, and 52% to 80% in the Upper Kuparuk River and Kuparuk River, respectively. Occasionally, a large summer rainstorm reached peak flow rates that rivaled and

Table 4.2. Summer precipitation at each station (mm) in the Kuparuk . River basin study.

Year	Prudhoe Bay	Franklin Bluffs	Sagwon Bluffs	West Kuparuk	Upper Kuparuk	Imnavait Creek	Basin Average
1993	59	72	71	na	225	208	110
1994	136	94	117	126	275	271	151
1995	79	82	147	122	274	209	140
average	91	83	112	124	258	229	134
9 year average	61	82	106	na	na	183	109

sometimes exceeded the snowmelt peaks in the upper basins. However, the volume of snowmelt runoff was always considerably greater than that of any individual summer storm in each basin. The high values of R_{sn}/R_t for the entire basin are probably due to the diminished capacity of flat coastal areas to produce runoff during the summer. The snowmelt period is the only time that significant runoff occurs from the coastal wetlands because the ground is completely frozen (Rovansek et al., 1996).

Runoff ratios were obtained by dividing runoff by precipitation for different periods: R_t/P_t, R_{sn}/P_{sn}, and R_s/P_s for total runoff ratio, snowmelt runoff ratio, and summer runoff ratio, respectively. The snowmelt runoff ratios were considerably higher than the total runoff ratios for the entire basin, which is consistent with the high R_{sn}/R_t values. Average total runoff ratios were above 0.5 for each basin. The global mean runoff ratio is 0.38 (Dingman, 1994). The high runoff ratios in the Kuparuk River basin are consistent with other studies in permafrost-dominated basins (Woo et al.,1996), and are due to two factors. First, the subsurface storage capacity is limited by permafrost in the Kuparuk River basin and essentially no precipitation enters long term storage. Second, potential evapotranspiration is reduced at high latitudes.

The ratio of snowfall to total annual precipitation (P_{sn}/P_t) was lower than the ratio of snowmelt runoff to total runoff (R_{sn}/R_t) in Imnavait Creek, with averages of 0.34 and 0.41 respectively. In the Upper Kuparuk basin the P_{sn}/P_t was higher than the R_{sn}/R_t, with averages of 0.33 and 0.25 respectively. This was likely due to delayed snowmelt in the higher elevations of the foothills that did not get incorporated into the initial snowmelt runoff peak. In the entire Kuparuk basin, P_{sn}/P_t was considerably

lower than R_{sn}/R_t with averages of 0.44 and 0.67, respectively. This could be a result of three possible contributing factors. First, rain events in the upstream regions contribute flow while snowmelt may be still occurring downstream. Hence, the snowmelt hydrograph at the mouth of the river may be a mixture of a spatial distribution of rain and snowmelt events. However, there was very little rain throughout the basin immediately after snowmelt in 1993 when 80% of the annual flow occurred during the snowmelt period. One small storm appeared in the falling limb of the lower Kuparuk River hydrograph in 1993 (Figure 4.1d), but it was insignificant in the total volume of flow during the snowmelt period. Second, snow is transported by wind and redeposited into topographic depressions such as river channels. Consequently, water that would have evaporated from flat regions is melted directly into the channel network and exported as runoff. Third, very little precipitation that falls on the low gradient coastal plain during the summer is exported as runoff; instead it is lost to evapotranspiration. This third explanation also explains the high R_{sn}/R_t for the entire basin.

Flow duration curves for each basin are shown in Figure 4.4. The slope of a flow duration curve is an indication of the temporal variability of discharge. Steep curves result when the variability is high. All of the flow duration curves have similar features. The slopes are generally flat at the high flows, which is typical of streams dominated by one large runoff event such as snowmelt (Searcy, 1959). The overall slopes up to approximately the 50th percentile remain fairly low, indicating low temporal variability of streamflow. Typically, low slopes on a flow duration curve

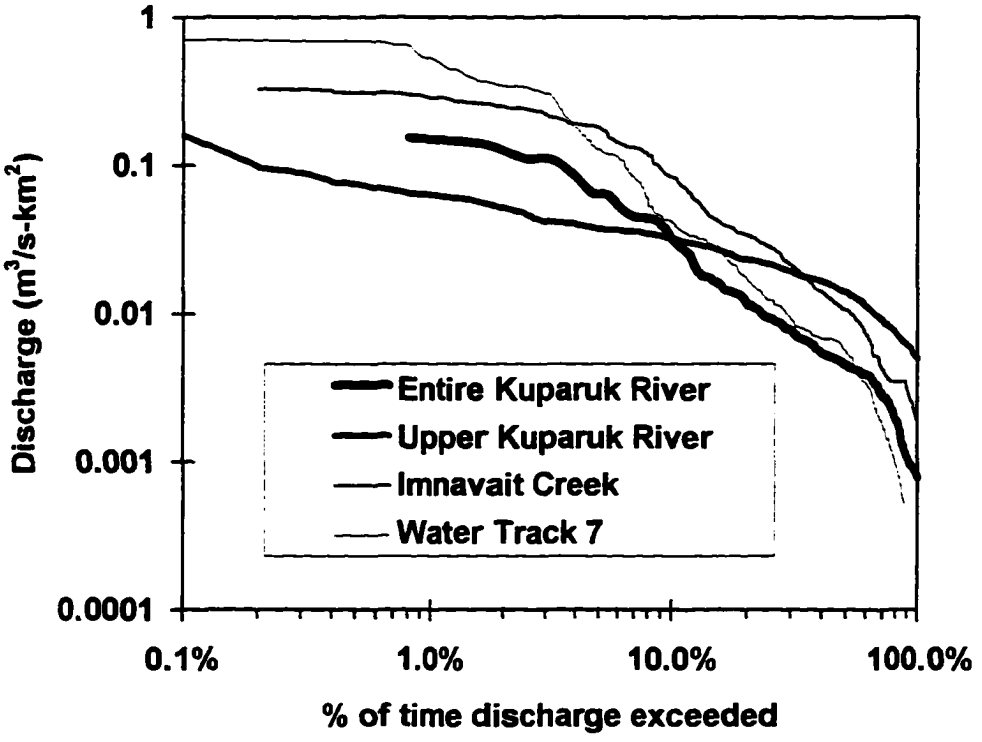

Figure 4.4a. 1993 flow duration curves for the four basins studied.

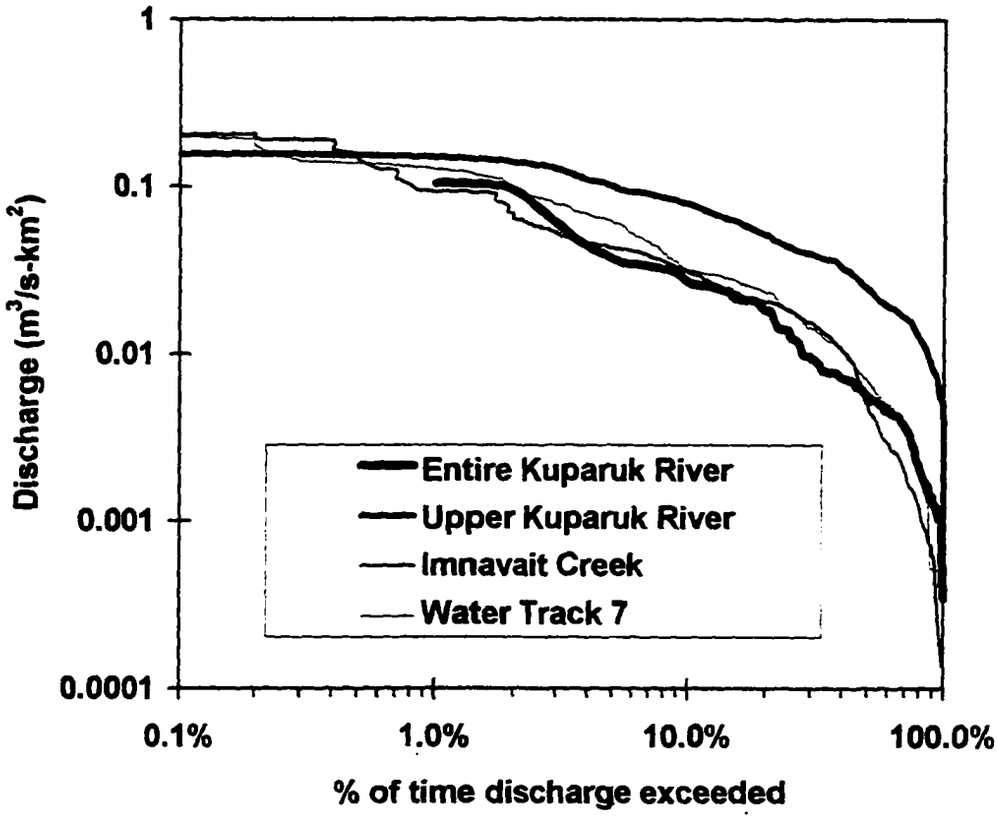

Figure 4.4b. 1994 flow duration curves for the four basins studied.

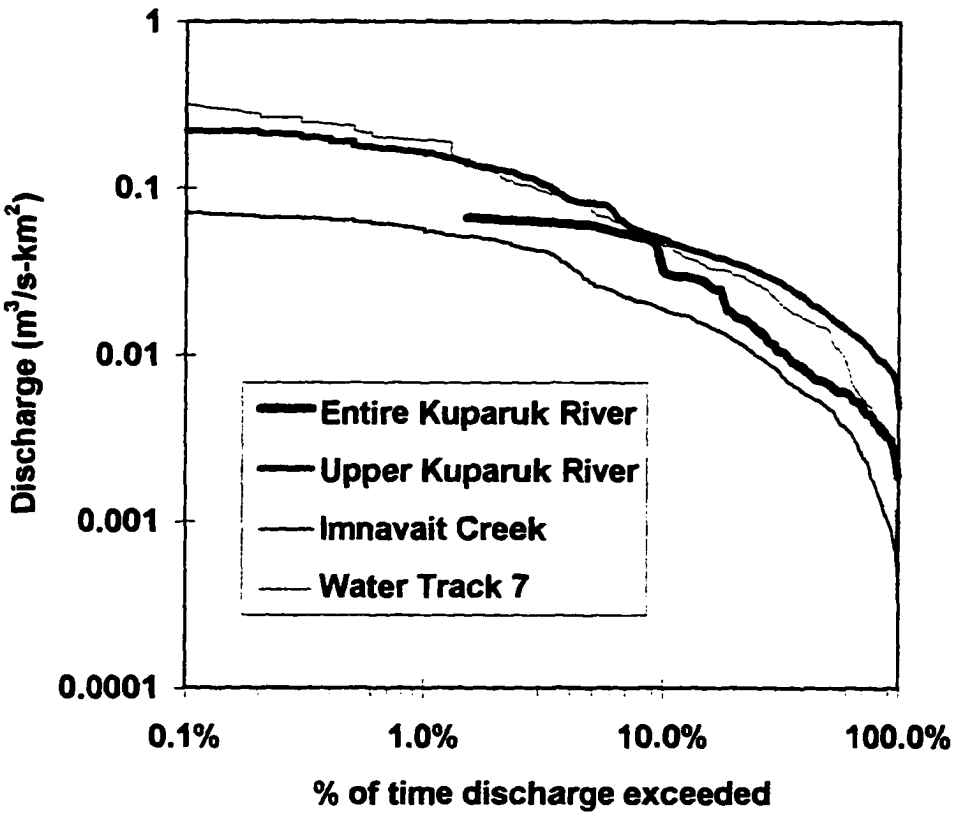

Figure 4.4c. 1995 flow duration curves for the four basins studied.

suggest that groundwater dominates the hydrograph by providing consistent baseflow. However, groundwater contributions are minimal in basins with permafrost. The steep slopes at the low flows indicate that the low flows do not settle on a consistent baseflow, but are highly variable. Searcy (1959) states that steep slopes at the low flows result from minimal basin storage. Hence, the flow duration curves for the Kuparuk River basin are unusual in that they suggest minimal basin storage while they also possess the low variability of streamflow characteristic of streams that receive consistent groundwater inputs.

That the flow duration curves have similar slopes for all four basins throughout most of the flow range suggests that the temporal variability of streamflow does not change significantly with changes in scale. This is an unusual characteristic of streamflow that has been reported thus far only in arctic basins and floods in other basins dominated by snowmelt. Scaling characteristics of arctic rivers are discussed in further detail in McNamara et al., (1997c).

4.4.2 Storm Hydrographs

Presented here are quantitative descriptions of hydrograph timing for Imnavait Creek, and cross-scale comparisons on other hydrograph characteristics including response factors, recession constants, and storm peak downstream travel times. The high spatial variability of precipitation in drainage areas greater than a few square kilometers prevents accurate rainfall-runoff timing analysis for the larger basins.

4.4.2.a Hydrograph Timing

Analysis was restricted to simple hydrographs in 1994 and 1995 with clearly defined precipitation pulses that caused the initial rises and had minimal precipitation during the recession. This resulted in seven storms in 1994 and four storms in 1995. The year 1993 had one significant rain event. However, the chart recorder in Imnavait Creek failed immediately prior to the storm and missed the beginning of the event. Table 4.3 summarizes the rainfall-runoff characteristics of those storms selected for analysis. Figure 4.5 illustrates the variables in Table 4.3.

The duration of the precipitation that contributed to the rise in the hydrograph is labeled T_{pk}. The duration of effective precipitation, T_{ep}, is T_{pk} minus the duration of the initial abstraction, P_{abst}. The initial abstraction is the precipitation that fell prior to the initial rise in the hydrograph. The total precipitation that fell during T_{pk} is labeled P_{pk}. Precipitation that did not last at least three continuous hours before the rise in the stream hydrograph was disregarded, as well as minor precipitation that occurred during the falling limb of a storm hydrograph. Significant precipitation fell during the falling limbs of some storm hydrographs. This precipitation was included in P_t, the total precipitation that fell during the time base, T_b, of the hydrograph. These two precipitation variables were separated so that the initial response of the streams and the total runoff/precipitation ratios could be analyzed separately.

Initial abstractions were quite low, ranging between 0 and 6.50 mm with an average of 1.52 mm. In many watersheds, the initial abstraction depends on watershed

Table 4.3: Rainfall-runoff analysis for Imnavait Creek.

Hyetograph Storm Date	Tp hr.	Tep hr.	P_{pk} mm	P_t mm	P_{abst} mm	$P_{5ant.}$ mm	I mm/hr	I_{max} mm/hr
6/17/94	54.0	51.0	13.5	17.1	2.3	10.5	0.2	2.3
6/24/94	37.0	42.0	16.1	19.7	0.0	8.2	0.4	3.6
7/4/94	18.0	18.0	18.4	21.3	0.0	6.6	0.9	3.3
7/12/94	10.0	9.0	21.7	21.7	0.3	0.7	2.0	8.2
7/19/94	23.0	23.0	20.3	20.3	1.6	5.6	0.5	3.0
7/29/94	7.0	6.0	34.8	36.0	1.6	0.3	4.3	22.0
8/6/94	28.7	16.0	9.5	9.5	0.7	0.7	0.6	3.0
6/10/95	19.9	19.0	5.3	7.2	0.5	5.5	0.3	1.7
6/15/95	10.1	8.1	17.8	17.8	2.4	7.2	1.8	2.7
7/1/95	16.1	10.1	15.7	18.0	6.5	3.6	0.9	3.1
7/18/95	89.0	87.1	39.8	45.8	0.7	12.5	0.5	2.7
Average	28.4	26.3	19.3	21.3	1.5	5.6	1.1	5.0

Hydrograph Storm Date	Tr_1 hr.	Tr_2 hr.	Tr hr.	Tlp hr.	Tlc hr.	Tb days	q_0 $m^3/s*10^3$	q_{pk} $m^3/s*10^3$	R mm
6/17/94	3.0	2.0	53.0	14.0	24.8	4.0	6.6	92.3	6.1
6/24/94	-5.0	1.0	43.0	24.4	41.6	4.1	4.5	94.2	5.8
7/4/94	0.0	3.0	21.0	13.6	34.2	5.4	3.1	121.7	6.3
7/12/94	1.0	12.0	21.0	17.0	33.3	4.3	1.8	100.7	5.5
7/19/94	0.0	1.0	24.0	11.6	25.0	2.9	9.5	95.0	6.8
7/29/94	1.0	10.0	16.0	12.1	35.1	7.0	1.4	9.5	5.3
8/6/94	12.7	15.2	31.2	25.8	49.3	3.8	1.5	5.6	0.5
6/10/95	1.0	7.0	26.0	22.8	20.8	1.5	14.0	96.8	3.8
6/15/95	2.0	3.9	12.0	9.1	22.8	3.3	16.4	219.2	10.8
7/1/95	6.0	4.9	15.0	11.8	51.7	8.6	5.6	99.3	6.1
7/18/95	2.0	-1.1	86.0	33.8	44.6	3.2	22.0	351.8	21.1
Average	2.9	5.4	31.7	17.8	34.8	4.4			

Tp = Duration of precipitation.
Tep = Duration of effective precipitation.
P_{pk} = Precipitation prior to hydrograph peak.
P_t = Total precipitation during storm.
P_{abst} = Precipitation prior to initial rise in hydrograph.
$P_{5ant.}$ = Precipitation during 5 days prior to storm.
I = Rainfall intensity averaged over storm.
I_{max} = Maximum hourly intensity.
Tr_1 = Time from first rainfall to first rise in hydrograph.
Tr_2 = Time from end of rainfall to hydrograph peak
Tr = Duration of hydrograph rise.
Tlp = Time from hyetograph centroid to hydrograph peak.
Tlc = Time from hyetograph centroid to hydrograph centroid.
Tb = Time from initial rise to antecedent discharge.
q_0 = Antecedent discharge.
q_{pk} = Peak discharge.
R = Total runoff volume.

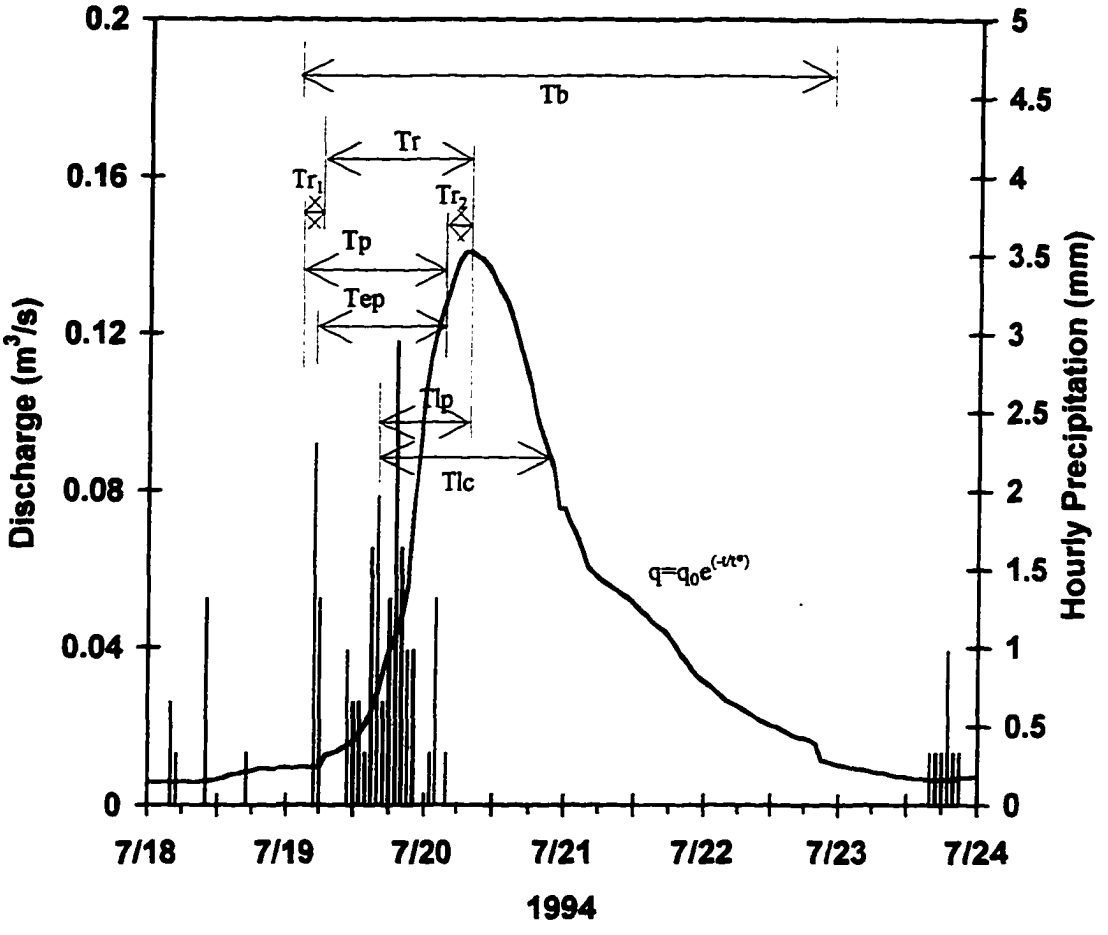

Figure 4.5. Storm hydrograph and hyetograph from Imnavait Creek in mid-July, 1994 illustrating the variables used in table 4.3.

wetness, with high soil moisture leading to low initial abstractions. However, no significant correlations existed at a 95% confidence level between the initial abstraction and various indices of watershed wetness, including the 5 day antecedent precipitation ($P_{5\ day}$) and the antecedent discharge (q_{ant}). The low initial abstractions and lack of correlation with watershed wetness were most likely results of the diminished subsurface storage capacity due to the presence of permafrost. Essentially, the watershed appears wet with very little precipitation. However, Kane et al. (1989) reported that an average of 15 mm of precipitation were required to initiate runoff in Imnavait Creek during dry antecedent conditions in surface organic soils. They found a similar value for storage in the active layer prior to ablation. Thus, surface storage in the tundra vegetation and organic soils can be significant, and the relations between hydrologic response and the indices of watershed wetness can be quite different between dry and wet periods.

The initial response time in Imnavait Creek was fast, and ranged between 0 and 6 hours with an average of 2.15 hours. This is largely determined by the time required to fill the soil water deficit and depression storage (Dingman, 1994). Church (1974) compiled response times from permafrost basins and also concluded that rapid response times are characteristic of northern rivers. The storm of June 25th, 1994 had a negative initial response time, which is impossible and is likely the result of the spatial variability of rainfall. This value was not included in the average response time. The Imnavait Creek basin is small enough that precipitation is generally uniform over the basin. However, small convective storms can occur over portions of the basin remote

from the precipitation gauge. The rapid response can be credited to the network of water tracks that exist on the slopes (Kane et al. 1989). The water tracks remain saturated for much of the summer except during extreme dry times. Thus, the tracks respond immediately to precipitation and a relatively constant saturated area exists to convey saturation overland flow to the creek.

The time from the initial rise in the hydrograph to the hydrograph peak, T_r, is plotted against the duration of precipitation (T_p) on Figure 4.6. A linear regression between the two variables gave the relation

$$T_p=0.89T_r+6.64. \quad (4.1)$$

At the 95% confidence level, the slope and intercept from Equation 4.1 are not significantly different from 1 and 0, respectively. Hence, the duration of precipitation was essentially equal to the time of the hydrograph rise, which further attests to the fast response of Imnavait Creek.

Recession began soon after the cessation of rainfall for all storms. Tr_2 ranged between -1.08 and 115.2 hours with an average of 5.36 hours. The negative value was included in the average for Tr_2 because during a storm of diminishing rainfall intensity it is possible for a hydrograph to peak before the end of the rainfall.

The lag to peak (Tlp) and the lag to centroid (Tlc) were surprisingly long. Holton and Overton (1963) reported an average Tlc of 19.5 hours in a study of 40 streams in the conterminous United States ranging in drainage area between 76 km^2 and 4200 km^2. The drainage area of Imnavait Creek is over an order of magnitude smaller than the smallest basin in Holton and Overton's study, yet the mean Tlc was

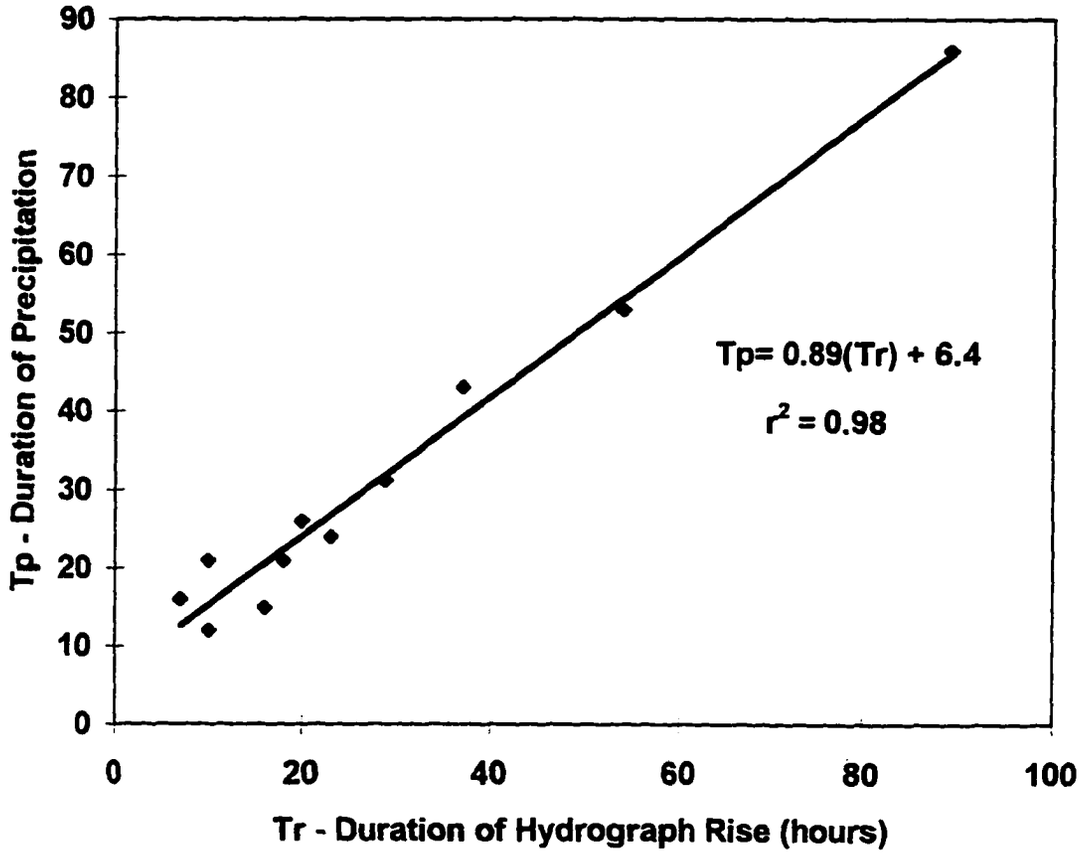

Figure 4.6. Relationship between duration of precipitation (T_p) and the time of hydrograph rise (T_r).

nearly twice as long. Holton and Overton's data show a slight positive relationship between Tlc and drainage area with an r^2 of 0.34 (Figure 4.7a). A Tlc similar to those in Imnavait Creek would come from a basin draining approximately 3400 km^2 in the Holton and Overton data. Dunne and Leopold (1978) summarized data from rural, temperate regions and produced much better correlations between both lag variables and drainage area. Imnavait Creek produced a mean Tlc and Tlp approximately twice as high as their data for its basin size. A much better correlation in the Holton and Overton (1963) data exists between Tlc and the recession constant of the falling limb of the hydrograph, t* (Figure 4.7b). The relationship between mean Tlc and mean t* from Imnavait Creek fits nicely on the trendline in Figure 4.7b. Essentially, long recessions induce later hydrograph centroids, which creates higher time lags.

4.4.2.b Recession Analysis

The falling limbs of storm hydrographs typically follow exponential decays according to

$$q=q_0 e^{(-t/t^*)} \qquad (4.2)$$

where q is the streamflow rate at t hours after the beginning of the recession, q_0 is the streamflow rate at the beginning of recession, and t* is the recession constant in hours. In this representation, t* is the time lapse between the occurrence of a given flow rate, q_0, and the occurrence of 1/e times that rate. To determine t*, a correlation of ln(q) vs t was performed for points on the falling limb of each storm hydrograph; with the regression coefficient taken as 1/t*. Recession constants are given in Table 4.4 for several storms in each basin. Holton and Overton (1963) compared the recession

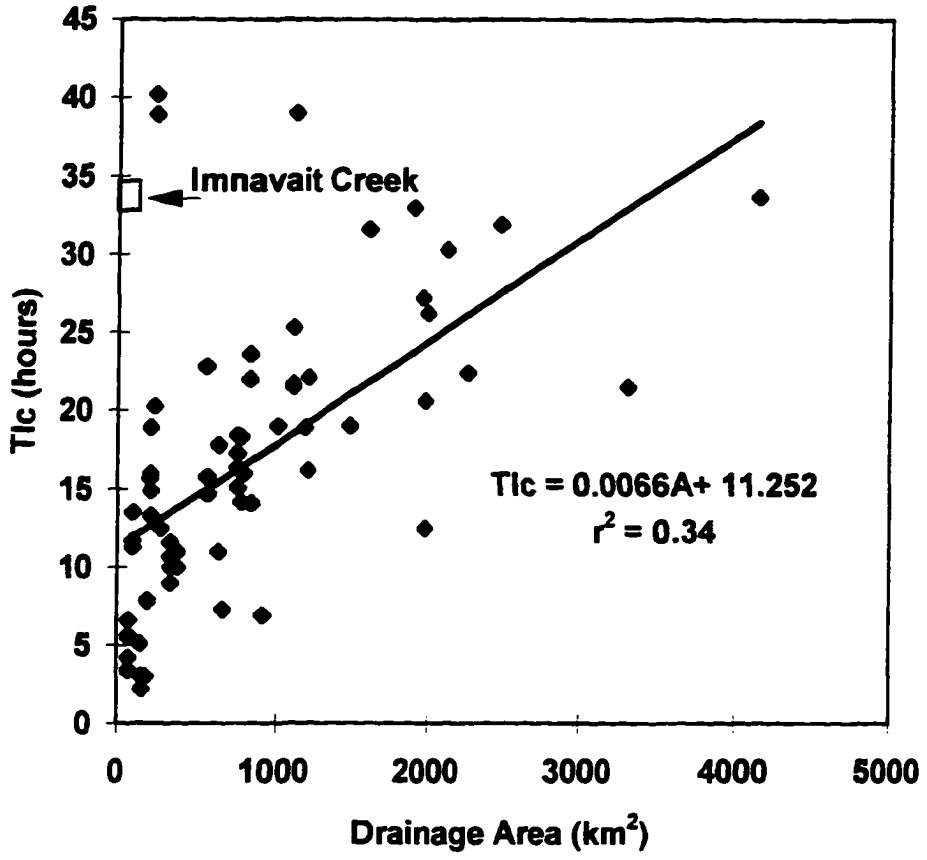

Figure 4.7a. Relationship between centroid lag (Tlc) and drainage area (A) from a study of 40 streams in the conterminous United States by Holton and Overton (1963). The mean value from Imnavait Creek is shown as an open square.

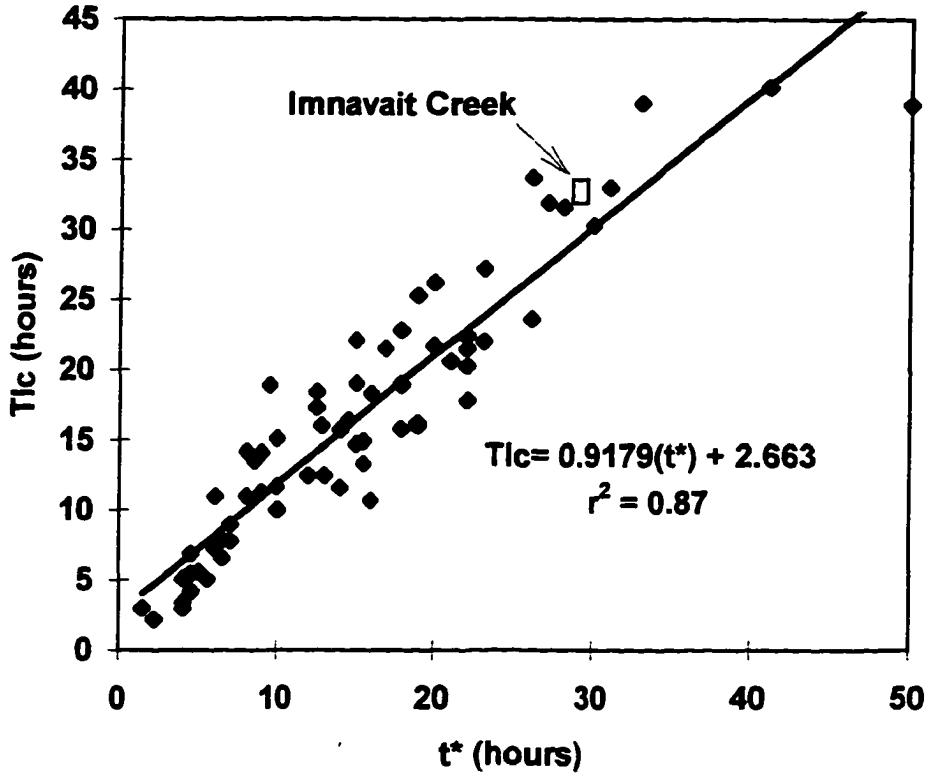

Figure 4.7b. Relationship between centroid lag (Tlc) and hydrograph recession (t*) from a study of 40 streams in the conterminous United States by Holton and Overton (1963). The mean value from Imnavait Creek is shown as an open square.

Table 4.4. Response factors (R/P) and recession constants (t^*) for several storms in each basin.

Location	Storm Date	R/P	t^* (hours)
Water Track	6/24/94	0.47	29.28
	7/4/94	0.29	17.04
	7/12/94	0.36	25.92
	7/18/94	0.49	23.76
	7/29/94	0.29	20.64
	8/6/94	0.30	6.96
	Average	0.37	20.60
Imnavait Creek	6/17/94	0.35	28.56
	6/24/94	0.29	25.68
	7/4/94	0.30	27.36
	7/12/94	0.25	24.72
	7/19/94	0.29	27.12
	7/29/94	0.15	
	8/6/94	0.05	
	6/10/95	0.53	32.16
	6/15/95	0.61	32.13
	7/1/95	0.34	44.16
	7/18/95	0.46	
	Average	0.33	30.24
Upper Kuparuk River	6/17/94		61.44
	6/25/94	0.38	136.56
	7/4/94	0.37	76.08
	7/12/94	0.33	63.84
	7/29/94	0.11	84.96
	8/7/94	0.23	40.56
	6/11/95	0.36	42.00
	6/15/95	0.43	69.60
	7/1/95	0.20	95.04
	7/17/95	0.61	
	Average	0.33	74.45
Kuparuk River	6/20/94		213.60
	6/28/94		176.16
	7/7/94		159.36
	7/18/94		185.52
	7/22/94		202.32
	6/16/95		95.04
	7/2/95		131.04
	7/20/95		99.60
	8/2/95		194.64
	8/12/95		214.56
	Average		167.18

constants of 40 streams (Figure 4.8). Their data follow the power law

$$t^*=1.14A^{0.38}. \quad (4.3)$$

where t* is the recession constant in hours and A is the drainage are in km^2. Recession constants in the Kuparuk basin (Figure 4.8 and Table 4.4) follow

$$t^*=33.5A^{1.66} \quad (4.4)$$

Equation 4.4 plots much higher than Equation 4.3 indicating that for similar drainage areas the recession constants in the Kuparuk River basin are higher than those reported by Holton and Overton (1963).

Other studies have also documented extended recessions in basins with permafrost. Dingman (1973) reported an average t* of 39 hours for a 1.8 km^2 basin near Fairbanks, Alaska. Likes (1966) reported a t* of 35 hours for a 98 km^2 basin in the Cape Thompson region of Alaska. Brown et al. (1968) reported recessions constants up to 160 hours for a small basin in Barrow, Alaska. Likes (1966) explained the high recession as a result of infiltration of water into a highly absorptive surface layer and subsequent slow release. Dingman (1973) showed that recession constants decrease as evapotranspiration increases, and suggested that low evapotranspiration rates in arctic and sub-arctic regions are responsible for long hydrograph recessions. An alternative explanation may be that essentially zero precipitation goes into long-term storage in basins with permafrost, and a greater proportion of the input precipitation makes it to the stream during the response hydrograph. All event water is exported either as runoff or as evapotranspiration. Slaughter and Kane (1979) showed that basins with permafrost have higher peak flows and lower baseflows than basins

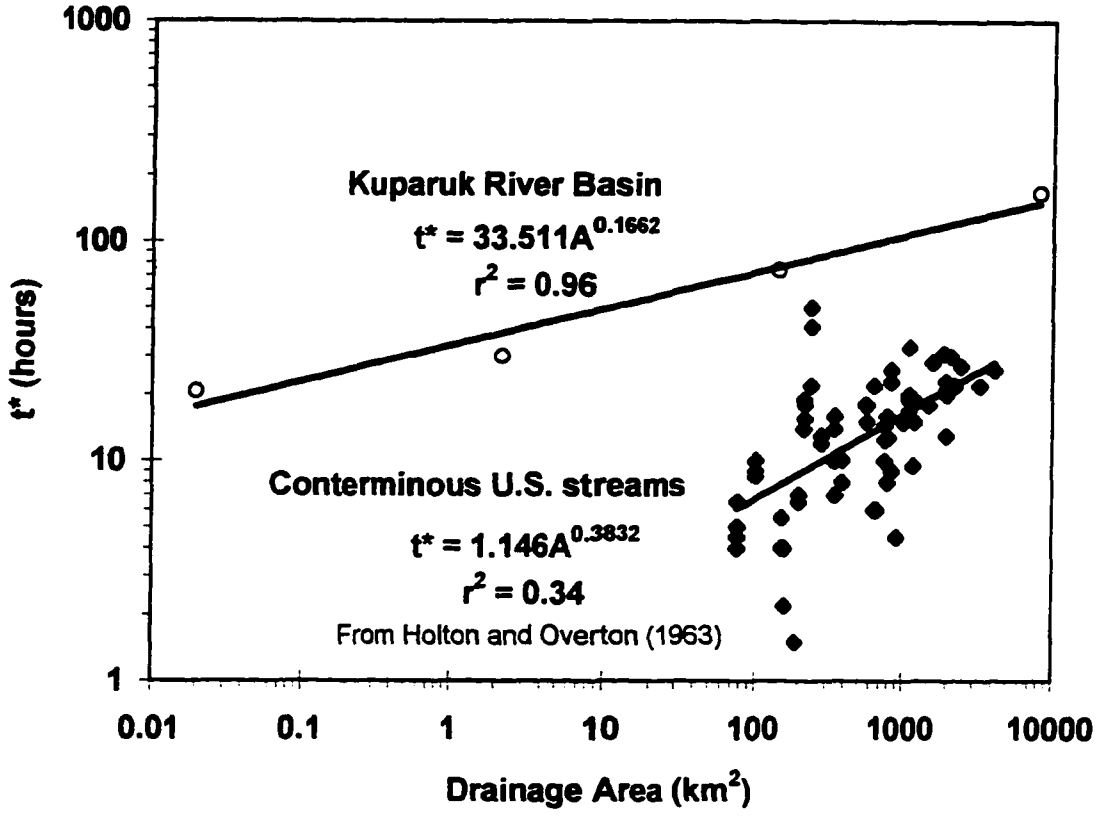

Figure 4.8. Relationship between hydrograph recession (t*) and drainage area (A) for the Kuparuk River basin and 40 streams studied by Holton and Overton (1963).

without permafrost. Consequently, the falling limbs of hydrographs have greater distances to fall and the recessions are extended. In basins without permafrost, some precipitation infiltrates into the soil and enters into long term storage as groundwater. This water may ultimately reach the stream, but not during the storm from which it originated. This is essentially a difference in accounting. The entire recession is visible in hydrographs from basins with permafrost, while the tail end of recessions in basins without permafrost are masked by baseflow.

Hinzman et al. (1991) calculated recession constants for small runoff plots on a hillslope in Imnavait Creek. Their data showed that the runoff plots produced lower recession constants than Imnavait Creek. However, as the season progressed, the plot recession constants increased and approached that of the Creek. They explained this seasonal trend as a result of increasing active layer thickness. As the season progresses, the storage capacity of the basin increases and more of the soil profile contributes to runoff. We did not observe seasonal trends in recession constants at the scales in this study. However, that the thawing active layer imposes seasonal trends in hydrologic response at the hillslope scale suggests that active layer dynamics will influence other factors such as the timing and magnitude of the delivery of water from the hillslopes to the streams. This is discussed further in the section on response factors.

It is the long recessions in permafrost basins that produce the extended time lags discussed above. It follows then that the ratio of storm runoff to precipitation should be higher in permafrost basins than in non-permafrost basins.

4.4.2.c Response Factors

Hewlett and Hibbert (1967) called the ratio of direct runoff to precipitation the response factor (R/P), where direct runoff is the total runoff minus the baseflow. Note that the response factors are different from the runoff ratios reported in Table 4.1, as those included total streamflow. Several graphical techniques exist to separate baseflow from direct runoff, none of which is more physically justifiable than the others. Hewlett and Hibbert (1967) projected a line from the initial hydrograph rise across to the falling limb at a slope of 0.05 $ft^3/s\text{-}mi^2\text{-}hr$ (0.000547 $m^3/s\text{-}km^2\text{-}hr$) and called the volume of water above that line direct runoff. Baseflow is minimal in the Kuparuk River basin, and streams drop to very low levels between storms. The method of Hewlett and Hibbert (1967) overestimates baseflow contributions in regions with minimal baseflow. In such regions, it is reasonable to simply project a straight line across the hydrograph from the point of initial rise to the point where the discharge returns to its antecedent value. However, to avoid possible overestimation of direct runoff and to allow more favorable comparisons to the extensive data of Hewlett and Hibbert (1967) and Woodruff and Hewlett (1970), a method closer to theirs was used. A line was projected from the initial rise in the hydrograph to the point on the falling limb where a break in slope occurred on a semi-logarithmic plot (Linsley et al., 1982). The volume of water above that line is the direct runoff. The method is subjective, but most likely underestimates direct runoff and consequent response factors.

The average response factors for all storms in the water track, Imnavait Creek, and the Upper Kuparuk River were 0.37, 0.33, and 0.33, respectively (Table 4.4).

Dingman (1994) stated that response factors are often less than 0.10. Woodruff and Hewlett (1970) studied long term averages of response factors for basins in the southeastern United States and reported values around 0.08, and Colonell and Higgins (1973) reported similar results for basins in New England. Hewlett and Hibbert (1967) found response factors ranging between 0.02 to 0.34, with an average of 0.10, in several small watersheds in the eastern United States. Although the ranges overlap slightly, response factors in the Kuparuk River basin are clearly higher than those reported in the studies above. Newbury (1974) compared runoff ratios between permafrost and non-permafrost basins and also found that permafrost basins produce higher runoff ratios. Dingman (1973) reported an average value of 0.18 for the Glenn Creek basin near Fairbanks, Alaska. It is interesting to note that 60% of the Glenn Creek basin is underlain by permafrost, and the response factors are intermediate between those reported in the permafrost free temperate basins and the 100% permafrost Kuparuk basins. However, more case studies are required to document such a trend. Slaughter et al. (1983) compared three basins in interior Alaska with differing percentages of their areas underlain by permafrost, and showed that the basins with more permafrost generated higher flows per unit area, regardless of the moisture conditions of the basins.

The low response factors in temperate basins imply that large portions of precipitation do not enter the streams during the storm in which it falls, but presumably enter into long term storage as groundwater (Dingman, 1994). This water may appear in the streams in later storms. In basins with permafrost such as the

Kuparuk, higher portions of the volume of storm precipitation reach the streams during the storm in which it falls due to the lack of storage. Although, most of the water that reaches the streams is old water (McNamara et al., 1997b). Hewlett and Hibbert (1967) determined that foremost among variables controlling response factors was soil mantle depth where shallow-soiled basins produced the highest response factors. Dingman (1970) found a positive correlation between response factors and antecedent discharge, an indicator of watershed wetness. Both watershed wetness and soil depth influence the storage capacity of a basin. Storage capacity controlled by soil depth dictates the spatial variability between basins, while storage capacity controlled by moisture dictates temporal variability within a basin.

Permafrost basins essentially mimic shallow-soiled, wet basins and produce high response factors due to their limited storage capacity. The variability of storage capacity in permafrost-dominated basins is subject to the same controls as in non-permafrost basins. However, in basins with permafrost the soil depth varies temporally as well as spatially. Whereas soil moisture is a stochastic variable dependent upon precipitation patterns, active layer depth is deterministic and directional, increasing as the ground thaws through the summer. Woo and Steer (1983) showed that thawing of the active layer has significant control on basin storage capacity, which in turn influences slope runoff processes. They showed that surface runoff decreased through the summer as a result of thawing of the active layer. It follows that in the absence of soil moisture controls, increases in active layer thickness through the season may impose decreases in response factors.

Figure 4.9 shows that response factors did have decreasing trends in Imnavait Creek and the Upper Kuparuk River in 1994. These trends were not observed in 1995; they may have been masked by soil moisture conditions. Antecedent discharges (q_{ant}) for the storms analyzed in Imnavait Creek were typically greater for storms in 1995 than in 1994. However, it is difficult to isolate the influence of individual variables in such a dynamic system. Table 4.5 gives a correlation matrix of the potential influences on response factors at a 5% level of significance. Our analysis was restricted to one basin and one season so that storm date (a surrogate for active layer thickness) could be included as a variable. The sample size is small (n=7). However, the correlation matrix of these data at least provides a means to question potential relationships between controlling variables.

As suspected, R/P was highly correlated to storm date and the indicators of antecedent moisture conditions (q_{ant} and P_{5ant}). However, P_{5ant} was also highly correlated with storm date. Also, although the correlation between q_{ant} and R/P is low, the reader can confirm from Table 4.3 that just one high value, due to an incomplete recession of the previous storm, disrupted an otherwise smooth decrease in q_{ant} through the 1994 season. This suggests that storm date may not represent active layer depth, but may represent the seasonal soil moisture pattern as dictated by precipitation. With only four storms to work with in 1995, it was difficult to decipher trends. Neither R/P or q_{ant} in Imnavait Creek showed a seasonal decrease in 1995 while the active layer thickened as it always does. This suggests that the trends observed in 1994 were most likely caused by trends in antecedent moisture conditions

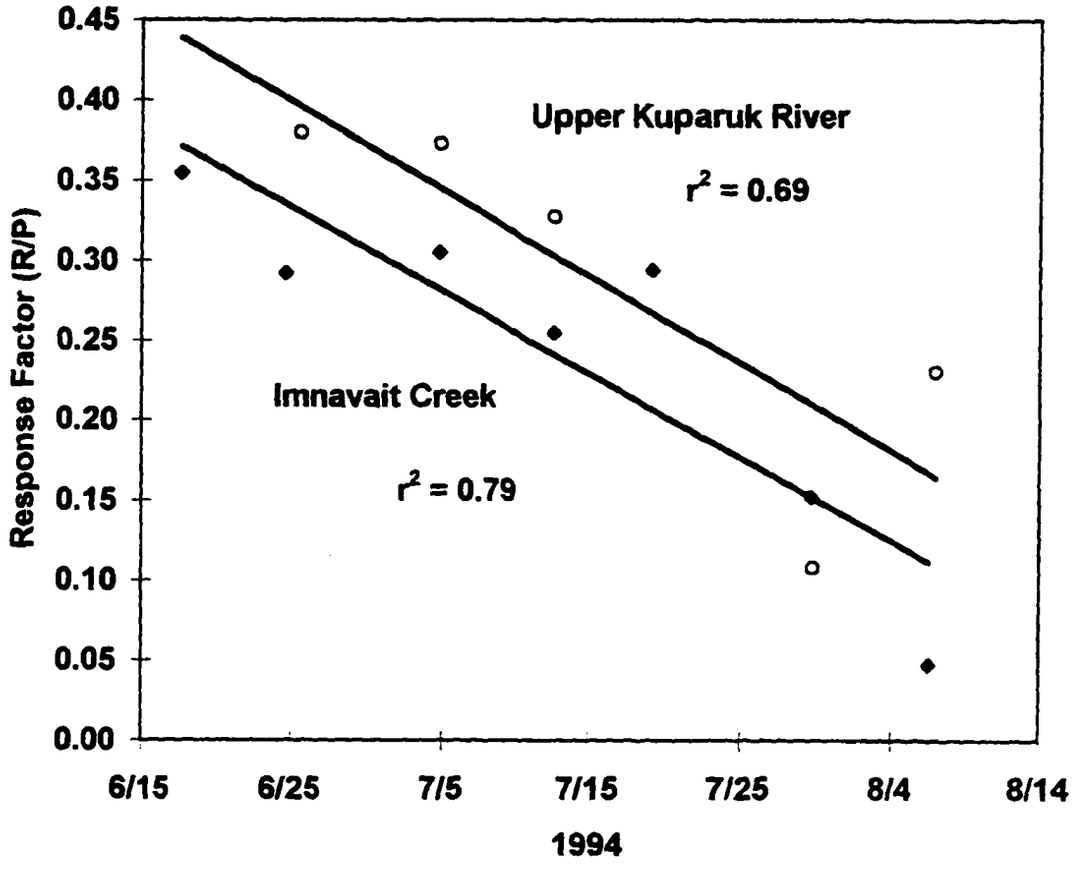

Figure 4.9. The ratio of storm runoff to precipitation (R/P) decreased through the summer of 1994 for both Imnavait Creek and the Upper Kuparuk River.

Table 4.5. Correlation matrix of potential controls on response factors (R/P) in Imnavait Creek, 1994. Correlations between +0.61 and -0.61 are not significant at the 5% significance level.

	R/P	q_0	$P_{5ant.}$	date	P_t	I	I_{max}
R/P	1.00						
q_0	0.64	1.00					
$P_{5ant.}$	0.81	0.67	1.00				
date	-0.89	-0.42	-0.88	1.00			
P_t	0.39	0.49	0.79	-0.63	1.00		
I	-0.38	-0.55	-0.65	0.46	-0.73	1.00	
I_{max}	-0.38	-0.49	-0.59	0.43	-0.64	0.99	1.00

as opposed to active layer dynamics. The seasonal influence of the thawing active layer on response factors may exist , but is easily dominated by precipitation patterns. McNamara et al. (1997b) suggested that early in the season the increases in active layer thickness greatly influence storm flow composition, but precipitation patterns become more significant as the summer progresses.

To summarize the features of storm hydrographs, the streams initially respond to precipitation very quickly because there is a limited reservoir to store new water in the basin. Consequently, large proportions of precipitation reach the streams as runoff, as opposed to entering long term storage, resulting in high response factors. Baseflows are typically low since there are minimal groundwater contributions. Consequently, the falling limbs must drop from relatively high peaks to low bases and thus have high recession constants. The high recession constants result in long time lags between the centroids of hyetographs and the centroids of hydrographs.

4.4.3 Basin Interactions

The portion of stormflow coming from the contributing basin (PSCB) is obtained by dividing the volume of a storm hydrograph from one basin by the volume of the same storm from the next downstream basin. PSCBs are reported in Table 4.6. The Upper Kuparuk River basin drains less than 2% of the total Kuparuk River basin area. That PCSBs between these two basins are considerably higher than 2% suggests that storm-generated flow in the upper basin was more significant than ones in the coastal regions in contributing flow to the mouth of the river. This may have been the result of greater precipitation in the headwater regions, but may also have resulted

Table 4.6. Basin interactions in the Kuparuk River drainage.

Storm Date*	Water Track - Imnavait Creek Travel Days	Upper Kuparuk - Kuparuk Mouth Travel Days	PSCB** Water track to Imnavait Creek	PSCB Upper Kuparuk to Kuparuk Mouth
6/17/94	0.75	3.46	3.28	4.93
6/25/94	0.33	3.46	1.42	5.86
7/4/94	0.42	2.33	1.01	7.12
7/12/94	0.29	3.71	1.34	6.75
7/17/94	0.13	4.13	1.42	14.52
7/29/94	0.13	5.50	1.91	19.13
8/7/94	0.50	6.29	4.62	21.13
8/17/94	0.08	6.33		
Mean	0.33	4.40	2.14	11.35
6/4/95		2.92		
6/11/95		1.67		
6/15/95	0.04	1.63	0.52	
6/22/95		3.00		
7/1/95	0.04	2.29	0.58	
7/8/95		4.79		
7/17/95	1.63	4.63	1.45	6.86
7/29/95		4.75		
8/12/95		2.08		2.15
Mean	0.57	3.08	0.85	4.51

* Dates are associated with the beginning of the hydrograph rise in the Upper Kuparuk River

** PSCB is the percent of the volume of the storm coming from the contributing basin.

from differences in topography and the potential to produce runoff between foothills and coastal regions (high gradient versus low gradient). Rovansek et al. (1996) studied an essentially flat coastal plain wetland near Prudhoe Bay and observed that negligible surface runoff occurs from summer storms. Similar storms in regions with more relief would potentially produce runoff. Consequently, after the snowmelt period, a large portion of the basin contributes little to streamflow, and the higher foothills regions contribute to basin-scale streamflow disproportionate to their drainage areas. This effect will be enhanced through the thawing season. As the active layer increases in thickness, more slopes continue to lose the ability to produce runoff and the steepest headwater basins will continue to produce runoff increasingly disproportionate to their drainage areas. Indeed, in 1994 the PSCB between the Upper Kuparuk River and the mouth of the Kuparuk River increased through the season (Table 4.6). The same mechanism may be responsible for the increase in the storm peak travel time between the Upper Kuparuk River and the Kuparuk River mouth through the 1994 season (Table 4.6).

The PSCB between Imnavait Creek and the Upper Kuparuk River averaged 0.8% in 1994 and 1.1% in 1995; the Imnavait Creek basin is 1.5% of the size of the upper Kuparuk Basin. The PSCB between the water track and Imnavait Creek averaged 2.1% in 1994 and 0.9% in 1995; the water track drains 0.9% of the Imnavait Creek basin.

4.4.4 Runoff, Permafrost, and Drainage Basin Structure

The above results raise an interesting problem: streams respond quickly to precipitation, but have extended recessions. If a basin responds quickly, why cannot it get rid of the water quickly after the storm? A few explanations were given above to account for the extended recessions including highly absorptive surface layers, low evapotranspiration, and the absence of significant baseflow. The important question is why the storage effect that extends the recession is bypassed in the initial response. Consider the structure of drainage basin in light of this problem.

The hillslopes in the Upper Kuparuk River and Imnavait Creek basins contain numerous water tracks, which exist as linear zones of enhanced soil moisture with wetland soils and vegetation that drain directly downslope. The water track network and the valley bottom wetlands provide a large saturated area from which rapid saturation overland flow can occur. Walker et al. (1996) showed that 56% of the Imnavait Creek basin is covered by some form of water track or valley bottom wetland. McNamara (1997b) separated storm hydrographs into source components and showed that all of the storm flow derived from new water can be accounted for by precipitation directly onto the water tracks and valley bottom wetlands. Thus, the saturated water track network provides a partial source area effect for rapid response. When runoff in the water tracks declines after a storm, surface storage in mosses, peat, or depressions on parts of the hillslopes without water tracks may continue to release water and produce an extended recession.

Chapter 7 suggested that water tracks may comprise a rudimentary channel network that was never allowed to fully develop due to the erosional resistance of permafrost soils. Geomorphologic analysis suggest that the heads of the water tracks are positioned on the hillslopes where current models of channel formation suggest that channels should occur, but they rarely contain incised channels. Further, as a network they do not possess aggregation patterns that are characteristic of mature channel networks. Instead, they remain as direct downslope flow paths with no bifurcation, which is characteristic of immature channel networks. Numerous water tracks remain that may have converged if permafrost had not restricted erosion. Instead of forming fully incised channels, erosion was limited enough to allow wetland soils to develop in the water tracks, which creates the large saturated area for runoff production.

4.5 Summary and Conclusions

The streamflow hydrology in the Kuparuk River basin is dominated by two dominant features: snow and permafrost. Approximately one third to one half of the annual precipitation over the entire basin fell as snow, and approximately 70% of the annual runoff at the mouth was due to snowmelt. No summer storm in any year of the study approached the significance of snowmelt in the annual water budget at the mouth of the river. At the smaller scales there was at least one summer storm that had peak flow rates that rivaled or exceeded the snowmelt flood. However, the volume of snowmelt runoff was always greater than that of any individual summer storm in any basin.

A typical storm hydrograph in the Kuparuk River basin shows a fast initial response time, long time lags between the hyetograph and hydrograph, an extended recession, and a high runoff/precipitation ratio. We credit these characteristics to the presence of permafrost. A network of water tracks exist on the hillslopes that provide a large saturated area which allows rapid response to precipitation. Much higher amounts of precipitation are forced into the streams than would occur in non-permafrost basins due to diminished subsurface storage capacity. Thus, the runoff/precipitation ratios (response factors) are high. The falling limbs of storm hydrographs must then drop from relatively high peaks to the typically low base flows that result from the lack of subsurface contributions. This in addition to the slow release of water from the tundra vegetation can account for the extended recessions. The extended recessions result in long lag times between the precipitation centroids and hydrograph peaks, and between the precipitation centroids and hydrograph centroids.

The hydrologic response in the Kuparuk River basin is adjusted to the presence of permafrost. This implies that changes in the permafrost may induce changes in the hydrologic response. On a seasonal time scale, this may occur as streamflow characteristics such as response factors and basin interactions change systematically through the season coincident with the thawing active layer. However, it is difficult to separate the influence of the active layer from the overriding precipitation patterns. On a longer time scale, the sensitivity of streamflow hydrology on the presence of permafrost has strong implications that arctic ecosystems may experience significant

changes in a changing global climate. At any time scale, the relationship between permafrost and hydrologic response may have resounding ecological impacts on processes such as the timing and magnitude of the delivery of nutrients to the aquatic system.

Chapter 5

HYDROGAPH SEPARATIONS IN AN ARCTIC WATERSHED USING MIXING MODEL AND GRAPHICAL TECHNIQUES

5.1 Abstract

Several storm hydrographs in the Upper Kuparuk River basin (142 km^2) in Arctic Alaska were separated into source components using a two-member mixing model and by recession analysis. In non-Arctic regions, old water previously existing in a basin commonly dominates storm hydrographs. We suspected that the presence of permafrost would alter this common observation, and that the increase in thaw depth through the summer would impose seasonal trends in storm flow composition. However, summer storm flow was indeed primarily composed of old water, despite the diminished old water reservoir. Snowmelt was almost entirely composed of new water. New water contributing areas were over an order of magnitude higher in the Kuparuk River basin than in some non-permafrost basins. There were significant increases in old water contributions from snowmelt to the first summer storm in both years. This increase continued moderately through the summer in 1994, but not in 1995.

5.2 Introduction

Permafrost is a ubiquitous presence in the Arctic that influences nearly all physical and biological ecosystem processes. Several studies have shown that permafrost has significant hydrological consequences which result primarily from the minimal subsurface storage capacity due to frozen ground (Hinzman et al., 1993;

Dingman, 1970; McNamara et al., 1997a, b, and c; Roulet and Woo, 1988; Woo and Steer, 1983). This is of particular concern to the National Science Foundation Land-Air-Ice-Interaction (LAII) Arctic Flux Study operating in the Kuparuk River basin in Northern Alaska. The goal of the Arctic Flux study is to estimate the regional fluxes of mass and energy in the Kuparuk River basin between the land, atmosphere, and the Arctic Ocean (Weller et al., 1995) This requires a comprehensive understanding of the mechanisms and pathways by which water travels through the system. Hence, we investigated the composition of storm flow in the Kuparuk River basin by asking the following questions: Is storm flow primarily composed of precipitation, called new water, or sub-surface water previously existing in the basin, called old water, and what influence does permafrost have on storm flow composition? An understanding of both the partitioning of hydrographs and the mechanisms responsible for the partitioning is a pre-requisite to understanding the relationships that exist between terrestrial and aquatic systems.

Several case studies in various non-permafrost regions have shown that old water typically dominates storm hydrographs, including snowmelt events (Buttle and Sami, 1992; Bottomley et al., 1986; Dincer et al., 1970; Eshleman et al., 1993; Kennedy et al., 1986; Kobayashi et al., 1993; McDonnel et al., 1991; Rodhe, 1981; Peters et al., 1995). This may have significant influences on the transport of nutrients from the terrestrial to the aquatic system - a primary area of research in the Kuparuk River study. The old water reservoir in a basin with permafrost is severely restricted due to the frozen ground. Essentially all subsurface flow occurs in a shallow zone

called the active layer that undergoes annual freezing and thawing cycles. Consequently, we suspected that storm flow may not be dominated by old water, as is commonly observed.

An analog for permafrost basins may be watersheds on the southern Canadian Shield, where impermeable bedrock underlies shallow soils. However, several workers have shown that storm flow is indeed composed primarily of old water in Canadian Shield watersheds, even with their diminished old water reservoirs (Peters et al., 1995; Bottomley, et al., 1986; Wels et al., 1991; and Hinton et al., 1994). An important distinction between Canadian Shield watersheds and the Kuparuk River basin is that the subsurface reservoir and consequent basin storage capacity in the Kuparuk River basin increases as the ground thaws during the summer months from essentially zero depth in the spring to depths approaching those in the Canadian Shield watersheds late in the summer. Other studies have shown that certain hydrologic processes undergo coincident changes with the thawing active layer. Hinzman et al.(1991) showed that the portion of the soil profile that contributes to hillslope runoff increases through the summer. Further, McNamara et al. (1997a) suggested that runoff/precipitation ratios may decrease as the active layer thickness increases. Thus, we suspected that the systematic increase in active layer thickness would produce consequent changes in storm hydrograph compositions through the summer.

The specific objectives of this paper are (1) determine the proportions of old and new water in storm flow in the Kuparuk River basin during 1994 and 1995, (2) investigate the potential influences, particularly of permafrost, on storm flow

composition. Storm flow compositions were determined from hydrograph separations using mixing model and graphical techniques. The influences on storm flow composition were investigated by constructing correlation matrices with variables including old water composition, precipitation characteristics, and storm date as a surrogate for active layer thickness. Runoff generating mechanisms were qualitatively evaluated using a technique developed by Eshleman et al. (1993) to compute contributing areas based on hydrograph separations. We focused on summer storms in the Upper Kuparuk River basin (Figure 1.1), with a limited analysis of snowmelt processes. Additional analyses were performed in the much smaller neighboring Imnavait Creek (2.2 km^2).

5.3 Hydrograph Separation

Early techniques to separate storm hydrographs into source components involved graphical separation, or recession analysis, to determine the portion of storm flow that originates from groundwater or baseflow. The shape of the hydrograph recession curve is used to decipher the timing and magnitude of surface and subsurface runoff. Newer, more physically based, techniques involve separating hydrographs into source components using naturally occurring tracers. Simple two-component mixing models are used to partition storm flow into old and new water assuming flow sources have distinct chemical or isotopic signatures, where old water is water that existed in the basin prior to a storm, (i.e. soil moisture and groundwater), and new water is the rain or snowmelt contributed by a storm or snowmelt event. Commonly used tracers include oxygen isotopes, chloride, and specific conductivity. Advances in hydrograph

separation techniques have expanded the two-component mixing model to include soil water and deep groundwater as separate components in a three-component model (DeWalle et al., 1988). The two-component mixing model is acceptable in this study due to the absence of a deep groundwater system.

We used specific conductivity as the primary tracer and compared those results to recession analysis of the same hydrographs. We used ^{18}O as the tracer for one of the hydrographs as a check on the specific conductivity approach, and to evaluate flow sources during the snowmelt period. We used recession analysis when possible, but several storms contained multiple peaks, which made recession analysis impossible. Conductivity signals of new water and old water in Imnavait Creek were often too close to allow hydrograph separation by the mixing model. Consequently, we were only able to use recession analysis in Imnavait Creek.

5.3.1 Mixing Model

The mixing model is based on the steady state form of the mass balance equations for water and a conservative tracer,

$$Q_s(t)=Q_o(t)+Q_n(t) \qquad (5.1)$$

$$Q_s(t)\, C_s(t)=Q_o(t)C_o(t)+Q_n(t)C_n(t) \qquad (5.2)$$

where Q is the flow rate, C is the tracer concentration, t is time, and the subscripts s, n, and o refer to the total streamflow, new component of the flow, and old component of the flow, respectively. The streamflow attributed to old water at any time (t) is

$$Q_o(t)=Q_s(t)\,(C_s(t)-C_n(t))/(C_o(t)-C_n(t)) \qquad (5.3)$$

and the new water flow is

$$Q_n(t)=Q_S(t)-Q_O(t) \qquad (5.4)$$

Instantaneous proportions of total streamflow arising from either new or old water are $Q_n(t)/Q_S(t)$ and $Q_O(t)/Q_S(t)$, respectively. By summing Equations 5.3 and 5.4 over the duration of the storm, Q_n, Q_O, Q_O/Q_S and Q_n/Q_S are obtained.

This natural tracer technique requires that the tracer signatures be conservative, that is, they do not change through a storm, or the changes can be corrected for in calculations. The signatures of old and new water must also be distinct. Specific conductivity is not entirely conservative because rain water dissolves solutes as it passes through the soil. However, we believe our technique corrected for changes in specific conductivity due to soil contact, and produced results reliable enough to gain insight into runoff processes.

5.3.1.a Definition of End Members

Given the potential for spatial heterogeneity of soil water chemistry, it is difficult to obtain an accurate chemical signature of the old water component. For this reason, a common method for estimating the old water component is to assume that the stream water during the low flow periods between storms represents an integrated sample of the old water in the basin. A continuous record of specific conductivity during low flow periods then provides a simple estimation of the old water component. Following Hooper and Shoemaker (1986), we used a linear regression between the pre-storm specific conductivity and the post-storm specific conductivity to estimate

the instantaneous old water signature through a storm. This method considers the seasonal trend in the specific conductivity of old water. In cases where the post-storm conductivity was lower than the pre-storm conductivity due to dilution from the next storm, we used a constant conductivity through the storm equal to the pre-storm conductivity. For the ^{18}O old water signature on storm 7, we used a constant value through the storm equal to the stream ^{18}O content immediately prior to the storm.

The new water specific conductivity was more difficult to estimate. Typically, the specific conductivity of precipitation for the event is used as the new water end member. However, Pilgrim et al. (1979) showed that the specific conductivity of dilute water changes with soil contact time and is not a reliable end member. They developed laboratory relationships for the changes in specific conductivity and found that the conductivity changed dramatically during the early stages, then approached equilibrium and increased more slowly. They then used these relationships to correct for the changing new water signature, successfully separating storm hydrographs using corrected specific conductivity.

We estimated the changing new water signature by measuring the specific conductivity of runoff in a small hillslope water track which drains an area of 0.026 km^2 on the west facing slope of the Imnavait Creek basin. We assumed that the conductivity in the water track during the falling limb of the hydrograph was not significantly influenced by old water, but was the result of rain water dissolving solutes from the soil. Therefore, the increase in specific conductivity of the water track during the falling limb of the hydrograph represented the slow increase in specific

conductivity as the water approaches equilibrium. Hence, for each storm in the Upper Kuparuk River basin, the conductivity of the corresponding storm on the water track at peak flow was used as the new water end-member. A potential error in this method is that the water track runoff may indeed have been influenced by old water. If so, our estimates of new water conductivity may be too high. This would result in erroneously low computations of old water contributions. However, the specific conductivity in the water track ranged between 6 and 9 μmhos/cm, which is close to that of local precipitation. Therefore, underestimation of old water contributions will not be significant. The specific conductivity of the water track was distinctly lower than the Kuparuk River for all summer storms, which allowed us to use the two member mixing model for all storms. For the ^{18}O content of new water on storm 7, we used the ^{18}O content of a bulk precipitation sample collected through the duration of the storm.

5.3.2 Recession Analysis

Graphical hydrograph separation has received considerable criticism as there is no physical basis for its assumptions. Freeze (1972) called the technique "convenient fiction". However, when tracer techniques can not be used, recession analysis can provide a qualitative way to evaluate runoff mechanisms. The technique becomes difficult to use on complex hydrographs such as those from overlapping storms, or from a rain on snow event. Hydrograph recessions typically follow an exponential function. If plotted on a semi-logarithmic graph with discharge on the logarithmic scale, the recession should be a straight line (Linsley et al., 1982). However, the actual recession typically occurs in separate log-linear segments with different slopes for the

different sources of runoff. In a two member system, surface flow and subsurface flow, the break in slope is assumed to be the point where surface runoff ceases. The remaining recession is due to subsurface baseflow. By projecting the line representing baseflow recession backward in time to the corresponding peak of the hydrograph, the old flow recession curve is obtained. A linear fit from the initial storm response to the old flow peak completes the old flow hydrograph. The proportion of old flow contributing to the storm is calculated by dividing the area under the old flow hydrograph by the area under the total hydrograph.

5.4 Field Methods

Streamflow was monitored at the Upper Kuparuk River basin and Imnavait Creek outlets using stilling wells with Stevens F-1 water level recorders mounted with variable resistance potentiometers to obtain digital data. Campbell Scientific CR10 data loggers recorded stream stage every minute, and averaged over hourly increments. An H-type flume was used at Imnavait Creek to aid discharge measurements. Discharge measurements were made following USGS standards at several different stages to produce rating curves from which continuous records of discharge were calculated. Two complete meteorological stations recorded precipitation, wind speed and direction, air temperature, relative humidity, and various radiation terms. Hydrographs were produced for both basins from the initiation of snowmelt in early May, to just prior to freeze-up in mid-September. To monitor active layer thickness, thaw depth on a ridge top and on the west facing slope in the Imnavait

Creek basin were estimated by tracking the 0° isotherm using thermistors at various depths between 0 and 150 centimeters.

Specific conductivity was logged hourly at the Upper Kuparuk River, Imnavait Creek, and the water track using Campbell Scientific conductivity probes. Water samples for oxygen isotope analysis were collected every three hours during several storms using an ISCO automatic sampler, and by hand during snowmelt and between storms in the summer. Snowpack meltwater was collected by digging a snow pit and inserting a high density polyethylene tray at the base of the snowpack before the initiation of melt. The pit was then covered with foam board to reduce melting of the pit wall. All of the meltwater in the tray at the end of each day was collected using a plastic syringe. Water samples for oxygen isotope analysis were collected with no head space in glass scintillation vials and stored in a cool, dark room until they were analyzed. Isotopic analysis of rain was completed only on samples collected for storms in August, 1994. Only bulk precipitation samples were collected through the storms. Consequently, we are unable to address the isotopic variability of rain. Oxygen isotope measurement was performed at the University of Alaska Fairbanks Water and Environmental Research Center by extracting CO_2 from the water samples using a vacuum extraction line, then analyzing the gas for ^{18}O content on a VG Isogas series 2 mass spectrometer.

5.5 Results

5.5.1 Summer Storms

Both 1994 and 1995 were unusually wet summers with frequent storms. In 1994, 275 mm of rain fell at our gauge in the Upper Kuparuk River basin, and 274 mm fell in 1995. The nine year average recorded at a nearby gauge in Imnavait Creek was 183 mm. Figures 5.1a and 5.1b shows the resulting hydrographs for the Upper Kuparuk River basin and identifies the storms used in this study. Storms 1, 2, 3, 4, 6, and 7 from 1994 and storms 2, 3, 4, 6, 7, 8, and 10 from 1995 were separated into source flow components using the mixing model with specific conductivity as the tracer. Storms 2, 3, 4, 6, and 7 from 1994 storms and storms 3, 4, 6, and 7 from 1995 were separated using recession analysis. Storm 7 from 1994 was also separated using ^{18}O as the tracer in the mixing model.

Figures 5.2a-c show the results for storm 7 of 1994 as an example of each technique. The old water contribution for this storm calculated by the conductivity mixing model, ^{18}O mixing model, and recession analysis were 79%, 81%,and 81%, respectively. These favorable comparisons confirm that hydrograph separation using specific conductivity as a tracer is acceptable. The old water and new water conductivity values used in the calculations are shown on the plots. The calculated old water contributions for each storm using chemical and recession separation are shown in Table 5.1. The old water contributions from the mixing model ranged from 65% to 81% in 1994 and 53% to 83% in 1995 with averages of 72% and 68%, respectively. These results indicate that old water dominated storm hydrographs in the Upper

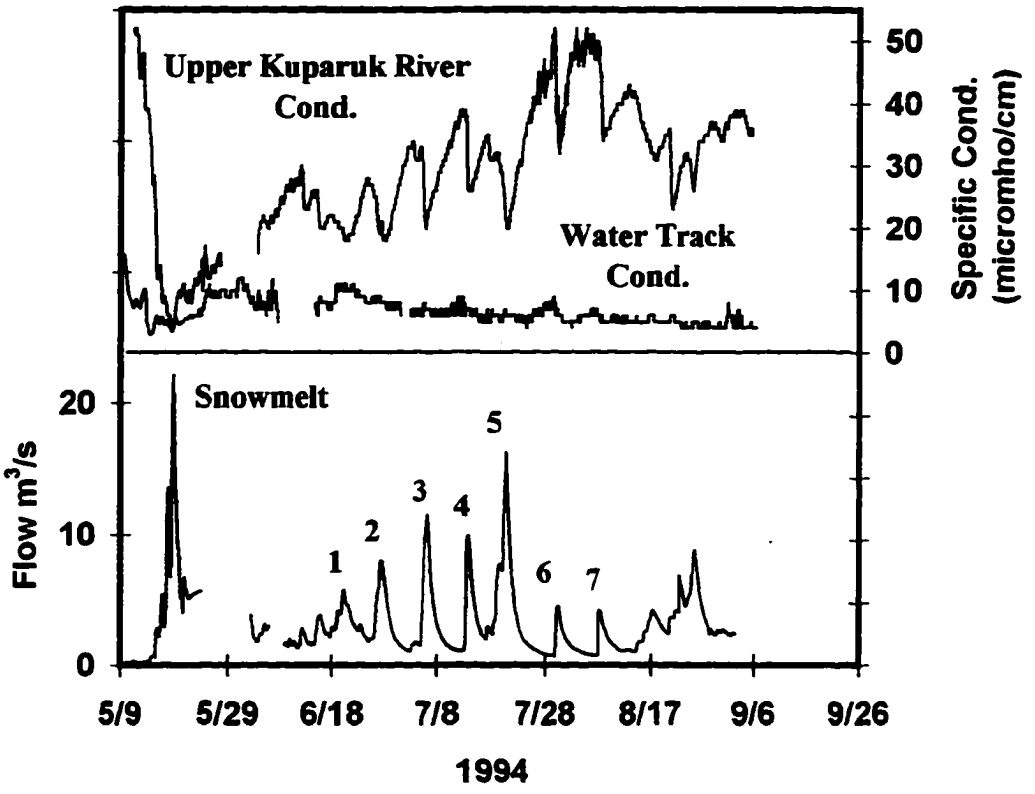

Figure 5.1a. 1994 hydrograph and specific conductivity records for the Upper Kuparuk River. The storms analyzed in this study are numbered chronologically.

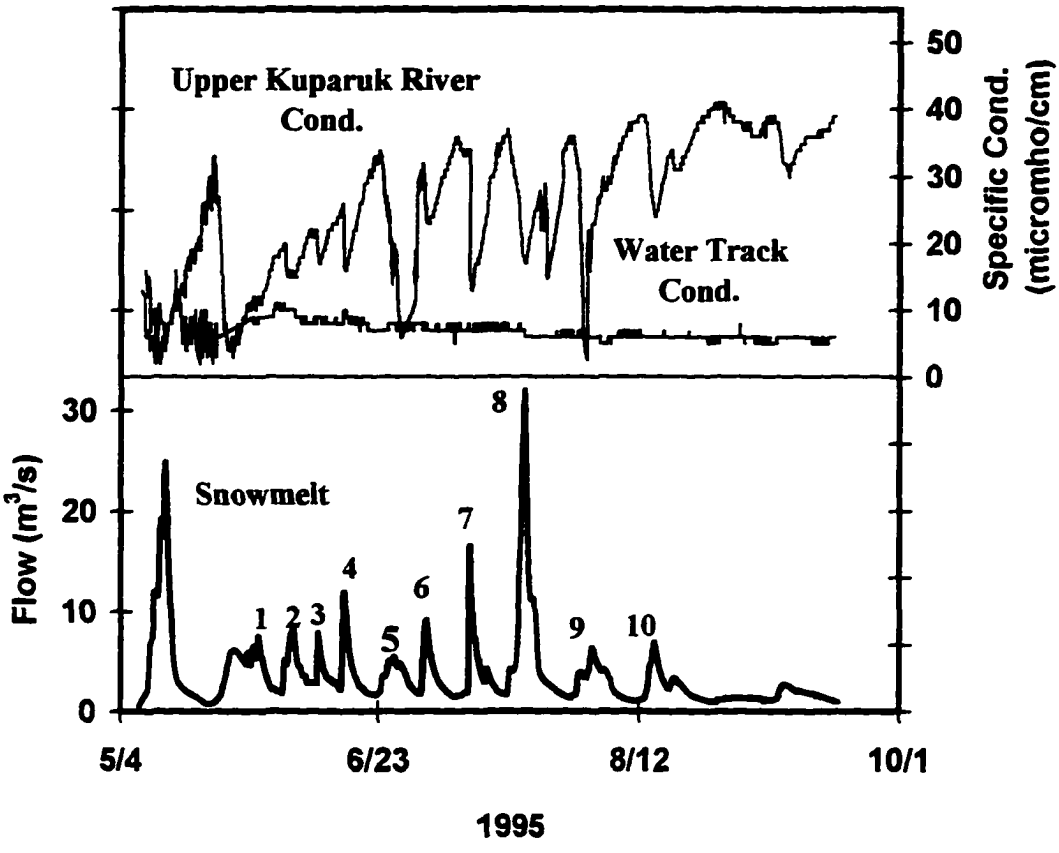

Figure 5.1b. 1995 hydrograph and conductivity records for the Upper Kuparuk River. The storms analyzed in this study are numbered chronologically.

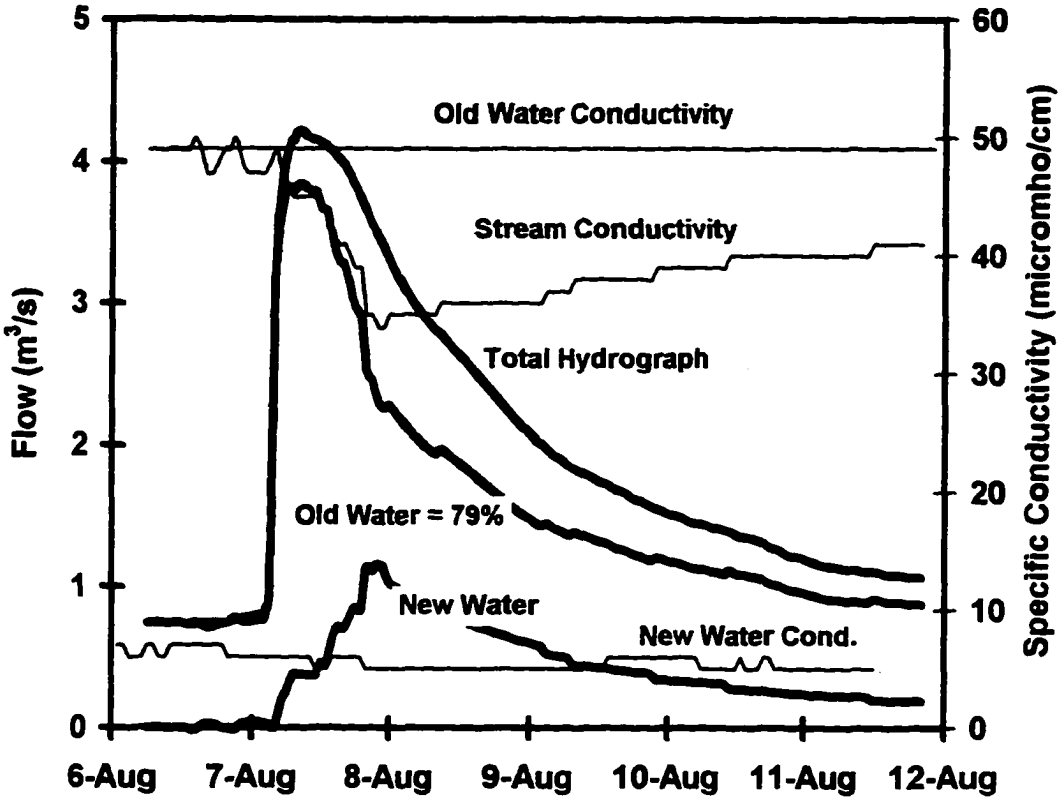

Figure 5.2a. Upper Kuparuk River storm 7, 1994 hydrograph separation using specific conductivity as a tracer resulted in an old water contribution of 79%.

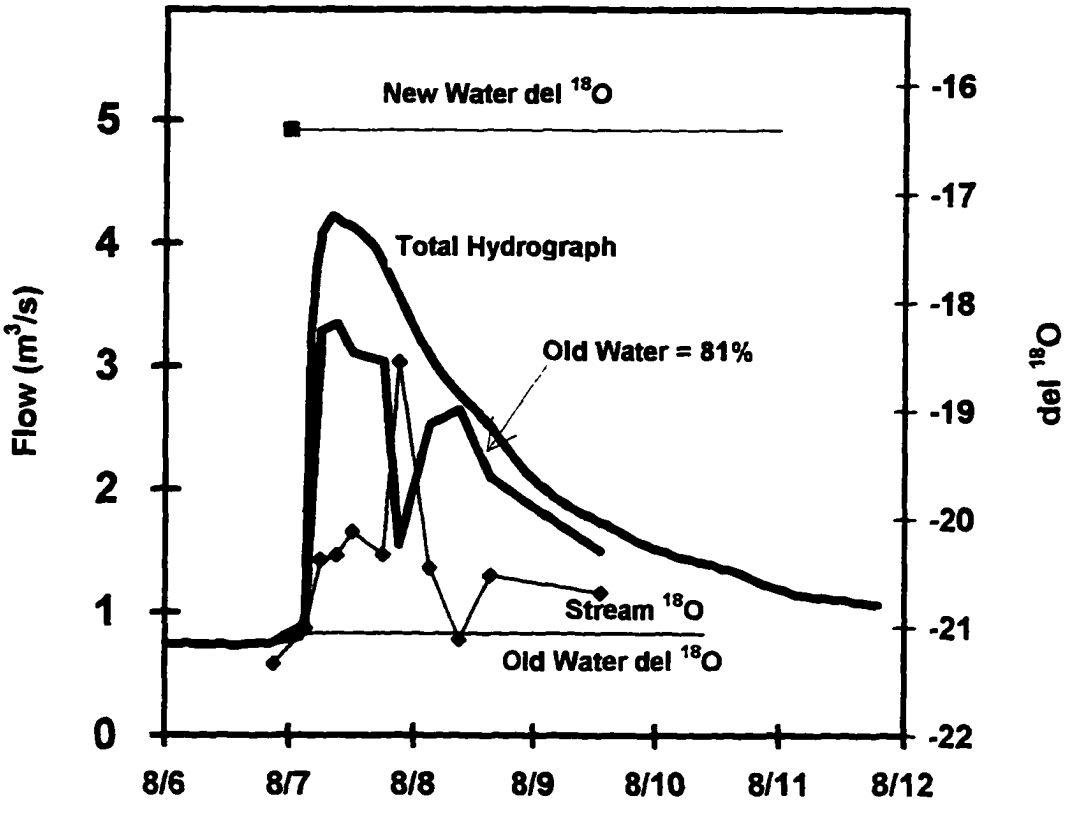

Figure 5.2b. Upper Kuparuk River storm 7, 1994 hydrograph separation using ^{18}O as a tracer resulted in an old water contribution of 81%.

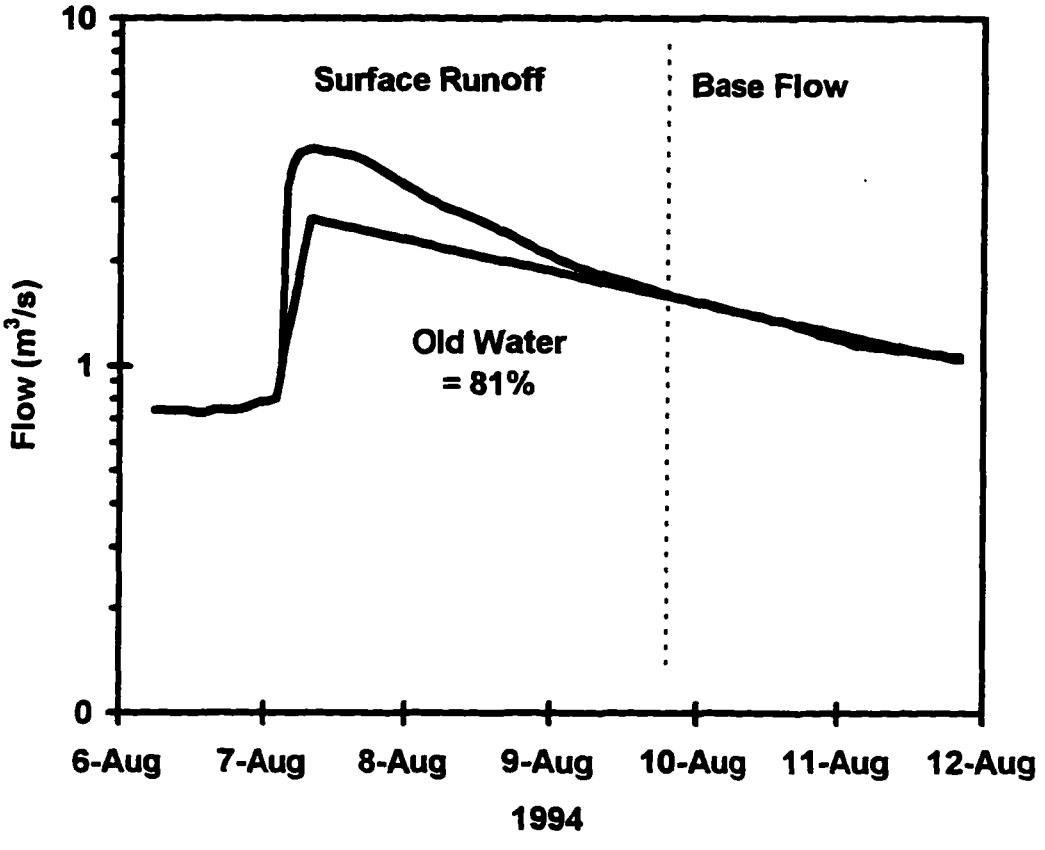

Figure 5.2c. Upper Kuparuk River storm 7, 1994 hydrograph separation using recession analysis resulted in an old water contribution of 81%.

Table 5.1. Hydrograph separation results for the Upper Kuparuk River.

Storm	Date	Total Discharge m^3	Total Rainfall * mm	Rainfall Intensity mm/hour	New Water Discharge m^3	New Water mix. mod. %	Old Water mix. mod. %	Old Water recession %	NWCA** km^2	NWCP*** %
94 1	6/17	2049238	19.8	0.25	837964	35	65	na	42	29.7
2	6/25	2007369	17.2	0.43	841169	33	67	66	49	34.4
3	7/4	2505238	33.9	1.02	1000386	30	70	65	29	20.8
4	7/12	1543135	19.6	1.97	450912	31	69	63	23	16.2
6	7/29	1115632	28.2	4.97	216286	19	81	75	8	5.4
7	8/7	873229	12.3	0.56	192928	22	79	81	16	11.1
average						28	72	70	28	20
95 2	6/4	2035175	6.7	0.13	691960	34	66	na	104	73.2
3	6/11	1150804	5.2	0.26	195637	17	83	88	38	26.5
4	6/15	2380086	17.8	1.77	809229	34	66	67	45	31.9
6	7/1	2106950	18.1	1.12	505668	24	76	77	28	19.7
7	7/9	2627313	20.0	0.06	1234837	47	53	47	62	43.5
8	7/17	7499286	39.8	0.45	3299686	44	56	na	83	58.4
10	8/12	2917276	28.7	0.24	758492	26	74	na	26	18.6
average						32	68	70	47	33

* Measured near Kuparuk Headwaters stream gauge

** New Water Contributing Area = new water flow volume / precipitation volume

*** New Water Contributing Portion = NWCA / basin area

Kuparuk River basin. Recession analysis yielded similar results. Points would fall on the diagonal line on Figure 5.3 if the two techniques produced identical results. Although there is some scatter and clustering, there is fairly good agreement between the two techniques, which lends credence to the widely used but physically unjustified graphical method of hydrograph separation. Kobayashi et al. (1993) also found that tracer techniques and recession analysis produced similar results.

Eshleman et al. (1993) found a negative correlation between precipitation intensity and old water contribution to storm flow. Table 5.2 shows that no such correlation existed in the Kuparuk River basin at the 5% significance level (α=0.05). Table 5.1 contains the supporting precipitation data. Other potential influences on old water contribution include total runoff, total rainfall, rainfall duration, and active layer depth. We used storm date as a surrogate for depth of thaw to test for seasonal trends as a result of active layer thawing. Table 5.2 shows that the only significant correlation to old water contribution was storm date in 1994. There were no significant correlations to old water contribution in 1995.

Additional results based on the tracer separations following the format of Eshleman et al. (1993) are included in Table 5.1. The new water contributing area (NWCA) is an estimate of the area of the basin that produces direct runoff during a storm, and is computed by dividing the new water flow volume by the corresponding total rainfall for the event. The new water contributing portion (NWCP) is the NWCA divided by the total watershed area and is an estimate of the percentage of the watershed that produces direct runoff during a storm. In 1994, NWCP in the Upper

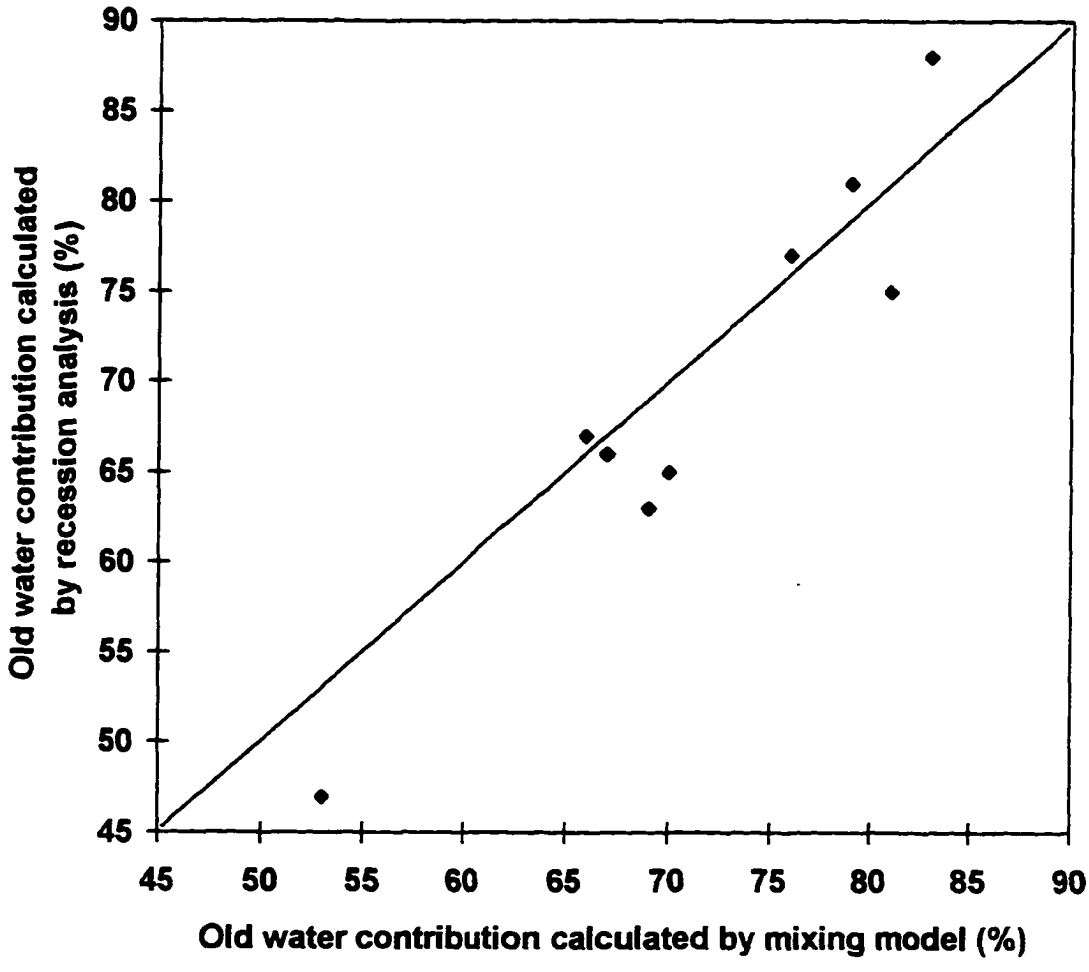

Figure 5.3. Plot showing the relationship between results obtained from the mixing model and recession analysis. The diagonal line indicates where the points would plot with a perfect relationship.

Table 5.2. Correlation matrices of potential influences on old water contributions to storm flow. a) 1994. Correlations between + 0.62 and - 0.62 are not significant at the 5% significance level. b) 1995. Correlations between +0.61 and - 0.61 are not significant at the 5% significance level.

a.

1994	Storm Date	Total Flow	Total Rainfall	Rainfall Duration	Rainfall Intensity	Old Water
Storm Date	1					
Total Flow	-0.85	1				
Total Rainfall	-0.07	0.37	1			
Rainfall Duration	-0.69	0.43	-0.47	1		
Rainfall Intensity	0.48	-0.36	0.71	-0.79	1	
Old Water	0.93	-0.77	0.17	-0.64	0.62	1

b.

1995	Storm Date	Total Flow	Total Rainfall	Rainfall Duration	Rainfall Intensity	Old Water
Storm Date	1					
Total Flow	0.46	1				
Total Rainfall	0.52	0.90	1			
Rainfall Duration	0.43	0.93	0.75	1		
Rainfall Intensity	-0.11	-0.22	0.16	-0.50	1	
Old Water	-0.14	-0.59	-0.46	-0.42	0.01	1

Kuparuk River basin ranged from a high of 34% early in the season with a decreasing trend to a low of 5% later in the season. In 1995, NWCP ranged between 73% early in the season to 18% at summers end, although there was no seasonal trend between the two extremes.

The specific conductivities for Imnavait Creek were too close to those for the water track to use the mixing model technique for separating Imnavait Creek hydrographs. This could mean that storm flow in Imnavait Creek is primarily composed of new water, or that old water in the basin has undergone very few chemical transformations during its residence in the basin. Thus, we used recession analysis to calculate storm flow compositions in Imnavait Creek. Most of the storm hydrographs in Imnavait Creek were complicated by multiple peaks, which made recession analysis unreliable. Hence, we were only able to perform recession analysis on storms 3 and 6 in 1994 (Figure 5.4a and b). Both storms in 1994 had old water contributions of 41%, indicating that new water dominated the storm hydrographs in Imnavait Creek. The lack of usable storms prohibited determination of whether or not a seasonal trend existed. However, storm 6 is late in the season and still has a relatively low old water contribution compared to the 75% for the recession analysis of the Upper Kuparuk River on the same date. NWCP's for storms 3 and 6 in Imnavait Creek were 14% and 13%, respectively.

5.5.2 Snowmelt

We were unable to perform accurate hydrograph separations during snowmelt due to the difficulties in obtaining representative end-member samples. However, the

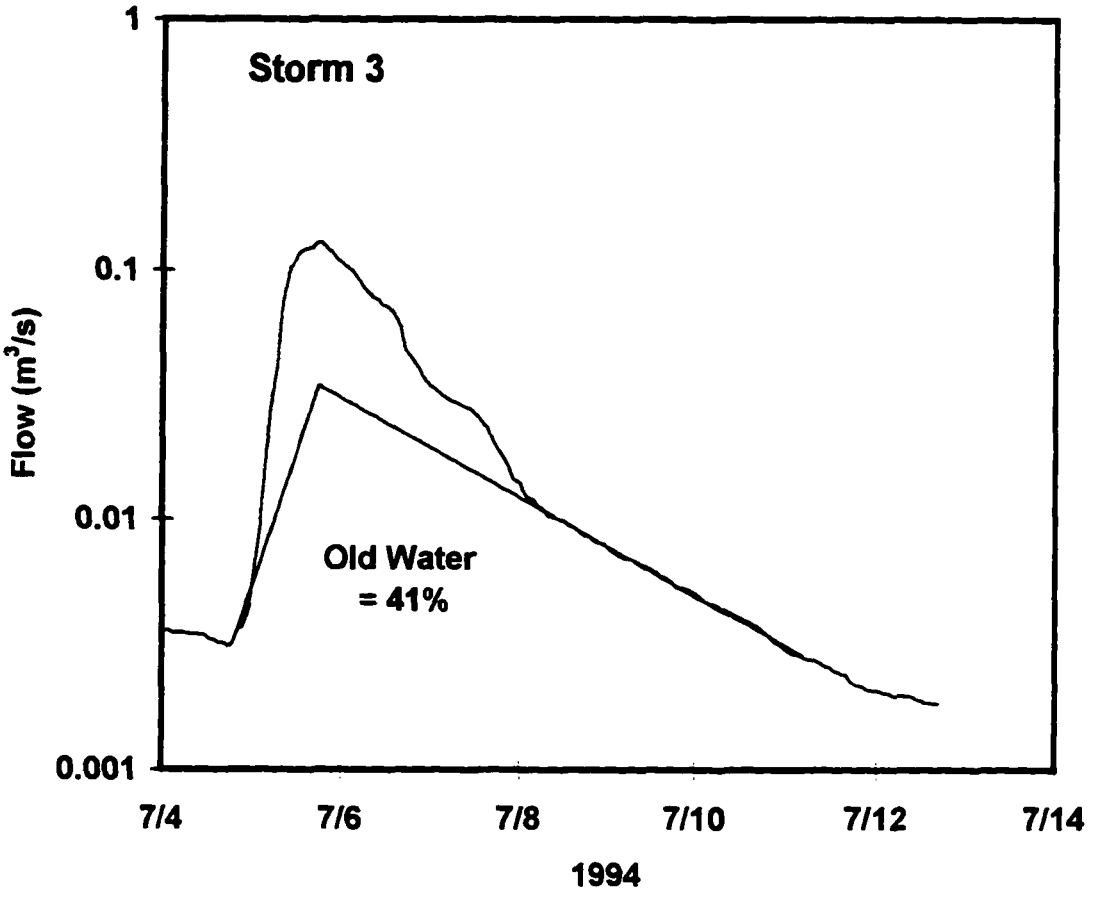

Figure 5.4a. Imnavait Creek storm 3, 1994 hydrograph separation using recession analysis.

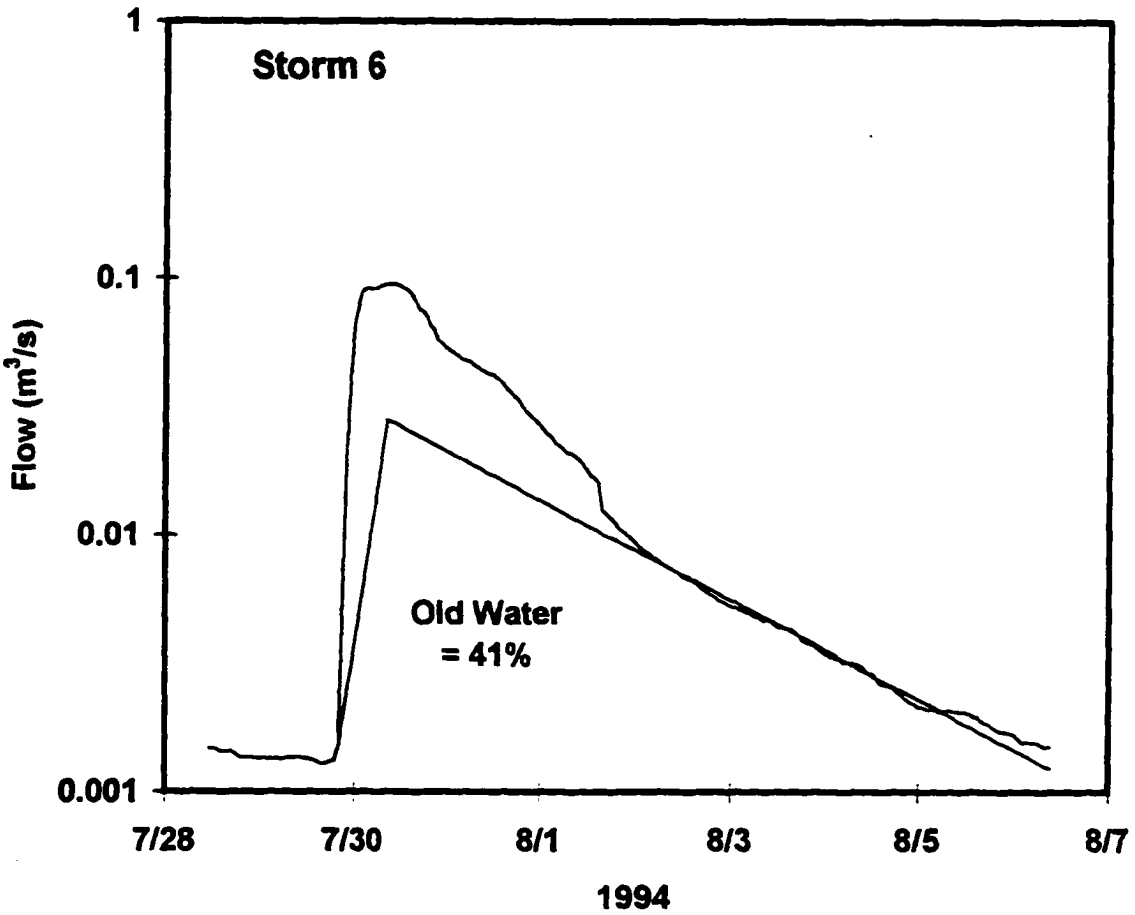

Figure 5.4b. Imnavait Creek storm 6, 1994 hydrograph separation using recession analysis.

trends in ^{18}O content and conductivity in the streams during snowmelt enable reasonable approximations. The ^{18}O content in the Upper Kuparuk River, Imnavait Creek, and the water track increased dramatically throughout snowmelt in remarkably similar patterns (Figure 5.5). Cooper et al. (1993) reported similar data in Imnavait Creek. This initially appears to represent mixing of waters with distinct isotopic signatures. However, meltwater collected immediately under the snowpack that had not reached the soil had a similar trend. This suggests that enrichment of ^{18}O in streamwater during snowmelt is due to isotopic fractionation, as opposed to mixing of different source waters. Cooper et al. (1993) suggested this explanation to explain heavy isotope enrichment in their data, but did not have the meltwater data to confirm their explanation.

Thawed soil moisture that originated from the previous fall precipitation is the potential old water source during snowmelt. Cooper et al. (1991, 1993) reported soil moisture ^{18}O contents around -20 ppt in two different years in the Imnavait Creek basin, and reported that the variability around the basin was minimal. Further, the isotopic content of the water track through most of the summer of the Cooper et al. (1993) study was close to their estimation of soil moisture isotopic content. In 1994, the isotope content of the water track rose to a plateau around -20.5 ppt. These favorable comparisons suggest that this value can be used to approximate the potential old water source during snowmelt. That the ^{18}O contents in the Kuparuk River and Imnavait Creek remain distinctly lower than the estimated soil water value further suggests that these waters are almost entirely derived from melting snow.

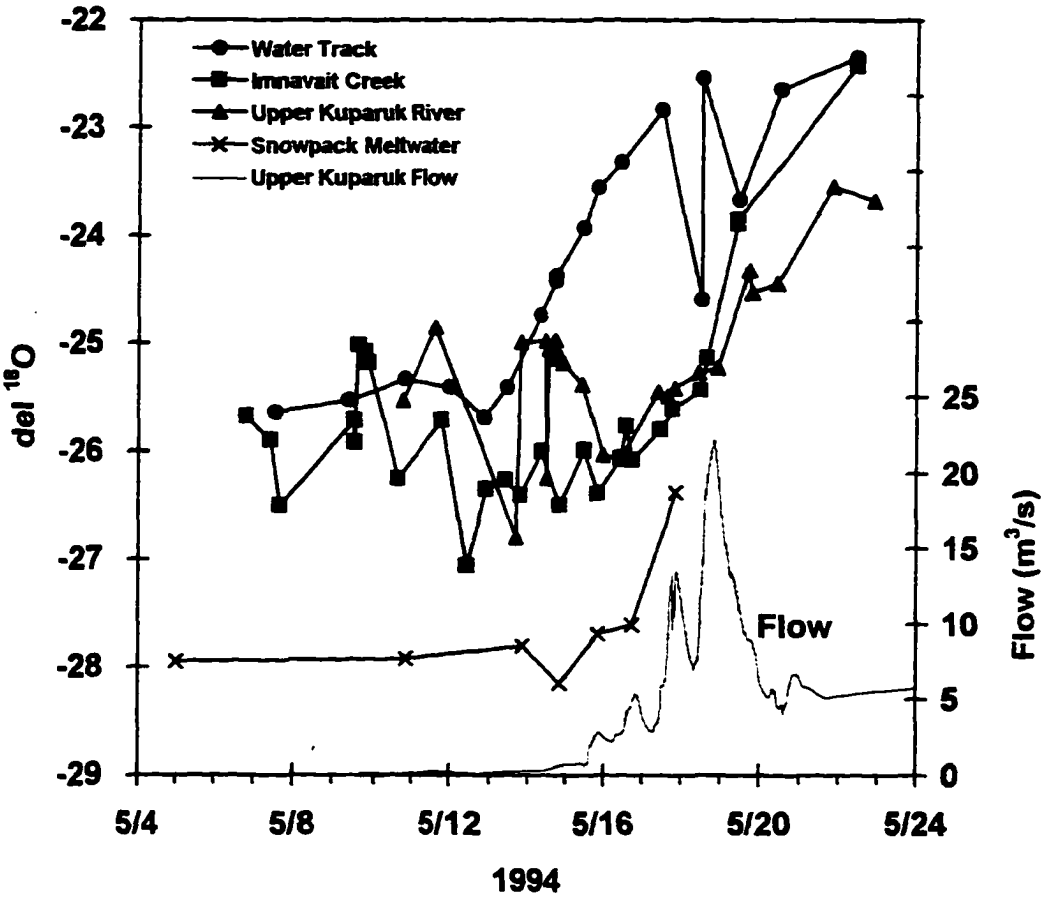

Figure 5.5. ^{18}O contents for the Upper Kuparuk River, Imnavait Creek, the water track, and snowpack meltwater during the 1994 snowmelt period, with flow for the Upper Kuparuk River shown in the lower right.

Cooper et al. (1993) reported that the lightest snow (lowest ^{18}O content) in the Imnavait Creek basin occurred in the valley bottom. This may explain why the ^{18}O values of the water track were distinctly higher than in Imnavait Creek and the Upper Kuparuk River, but followed a similar pattern through the snowmelt period. The meltwater sampling location was in the valley bottom, while the weir on the water track where the samples were collected integrated the areas higher on the slope. If the runoff in the water track during the snowmelt period was entirely from meltwater heavier than meltwater in the valley bottom, then Imnavait Creek should be a mixture between the light meltwater collected in the valley bottom and the heavier meltwater from the water track. Figure 5.5 shows that the ^{18}O content of Imnavait Creek was indeed between the water track and the valley bottom meltwater. The Upper Kuparuk River had an almost identical pattern in ^{18}O content to Imnavait Creek. These patterns suggest that the isotopic contents of streamwater can be explained entirely by the mixing of fractionating meltwater sources without interaction with subsurface waters.

Without continuous data, we could not partition the hydrographs for the snowmelt period. However, we calculated the old water contributions at one time instant, the latest time for which we have meltwater isotopic data. At that time, the meltwater had an ^{18}O content of -26.4 ppt, and the Kuparuk River had an ^{18}O content of -26.0 ppt. Using these values in the two-component mixing model (Equation 5.3) resulted in an old water contribution of 7%. If the valley bottom meltwater data was indeed lighter than the basin average, then the old water contribution would be even lower. It is possible that -20.5 ppt is a heavy estimate of the soil moisture and that

fractionation occurs as soil moisture thaws, as well. If we subtract 2 ppt from the estimate of soil moisture ^{18}O content, which was the approximate range of fractionation in the snow meltwater data, then the old water contribution to snowmelt increases to 10%. This was on the rising limb of the hydrograph, where old water contributions are typically highest. Cooper et al. (1991) reported an old water contribution to snowmelt storm flow of 14% at peak flow in Imnavait Creek.

The patterns in conductivity during the snowmelt period for the water track and the Upper Kuparuk River (Figure 5.1) confirm the above results. The high conductivity at the onset of snowmelt runoff results from solute exclusion in the snowpack. Ions migrate to the points of snowflake crystals during the freezing process. Initial meltwaters flush these ions and result in meltwater concentrations much higher than the bulk snowpack. The remaining snowpack is depleted of ions and further meltwater therefore has low conductivity. After this process occurred early in the snowmelt period, the water track and the Upper Kuparuk River had nearly equal conductivities, which were similar to the conductivity of snowpack meltwater collected before it had contact with the soil. This further suggests that streamflow during the snowmelt period was almost entirely due to melting snow with little contributions from subsurface waters.

Hydrologic budget studies in Imnavait Creek confirm that there can be essentially no mixing of meltwater with underlying soils (Kane et al., 1989, 1991; Hinzman et al., 1991). Approximately 1.5 cm of meltwater infiltrates the desiccated surface soils before runoff ensues (Kane et al., 1989), but this meltwater re-freezes

when it contacts the colder soil and essentially eliminates infiltration (Hinzman et al., 1991; Kane and Stein, 1983).

5.6 Discussion

5.6.1 Influences on Storm Flow Composition

Summer storm flow in the Upper Kuparuk River basin is dominated by old water, as is commonly observed in other regions, despite the presence of permafrost. However, whereas streamflow during the snowmelt period in other regions is dominated by old water, streamflow during the snowmelt period in the Upper Kuparuk River is almost entirely composed of new water. Hence, there is a dramatic shift in storm flow composition from the snowmelt period to the earliest summer storms. This change can be credited to active layer thickness. Immediately following snowmelt, storage capacity of the soil is restricted to a thin layer in the surface organic soils. The fastest rate of increase in active layer thickness occurs early in the summer. Thus, soon after snowmelt, rainfall is able to infiltrate the mineral soils, which was not possible during snowmelt, and displace old water into the streams. The basin storage capacity and the potential old water reservoir continue to increase as the active layer increases through the summer. In the summer of 1994, a high correlation between storm date and old water confirmed that old water contributions increased through the summer (Table 5.2), although at a moderate rate. Figure 5.6a illustrates the seasonal trends in thaw depth and old water contributions in 1994. The lack of continued increase in old water contributions in the summer of 1995 suggests that other factors influenced storm flow compositions.

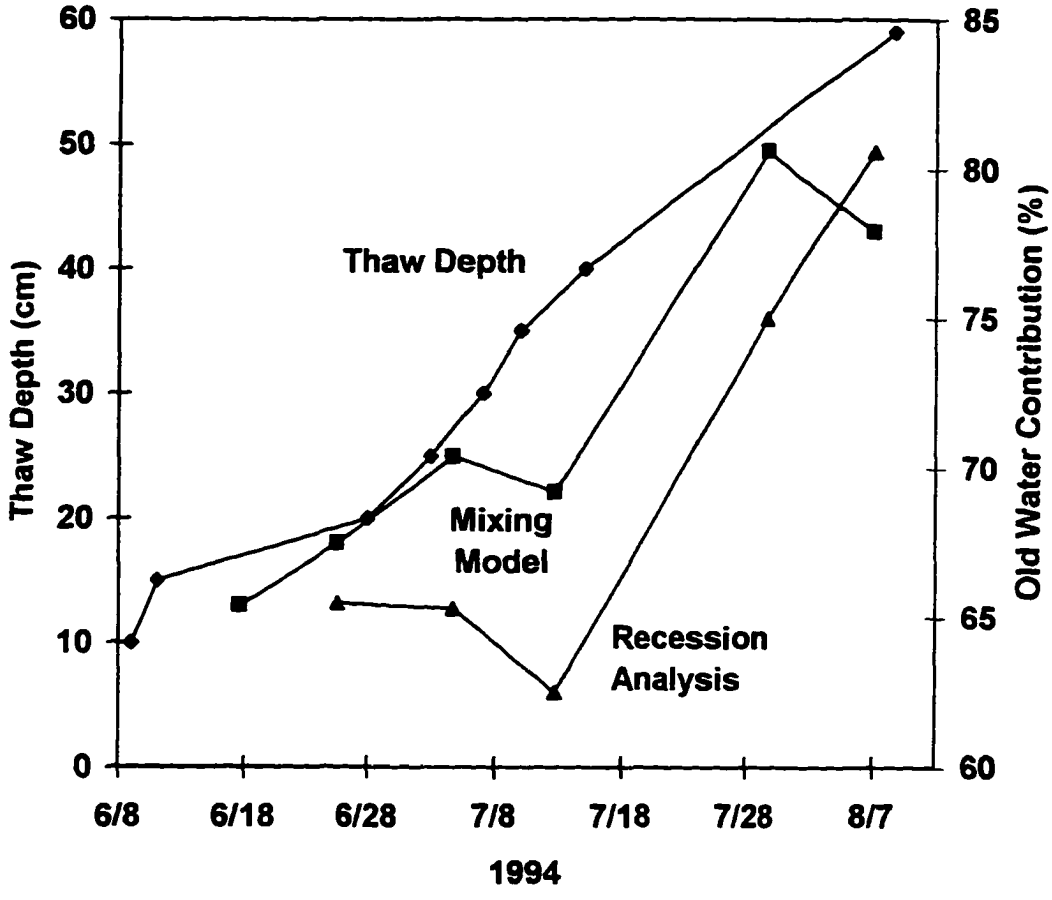

Figure 5.6a. The contribution of old water to storm flow in the Upper Kuparuk River in 1994 increased through the season. Depth of thaw is plotted on the primary axis to illustrate the correlation to old water contributions.

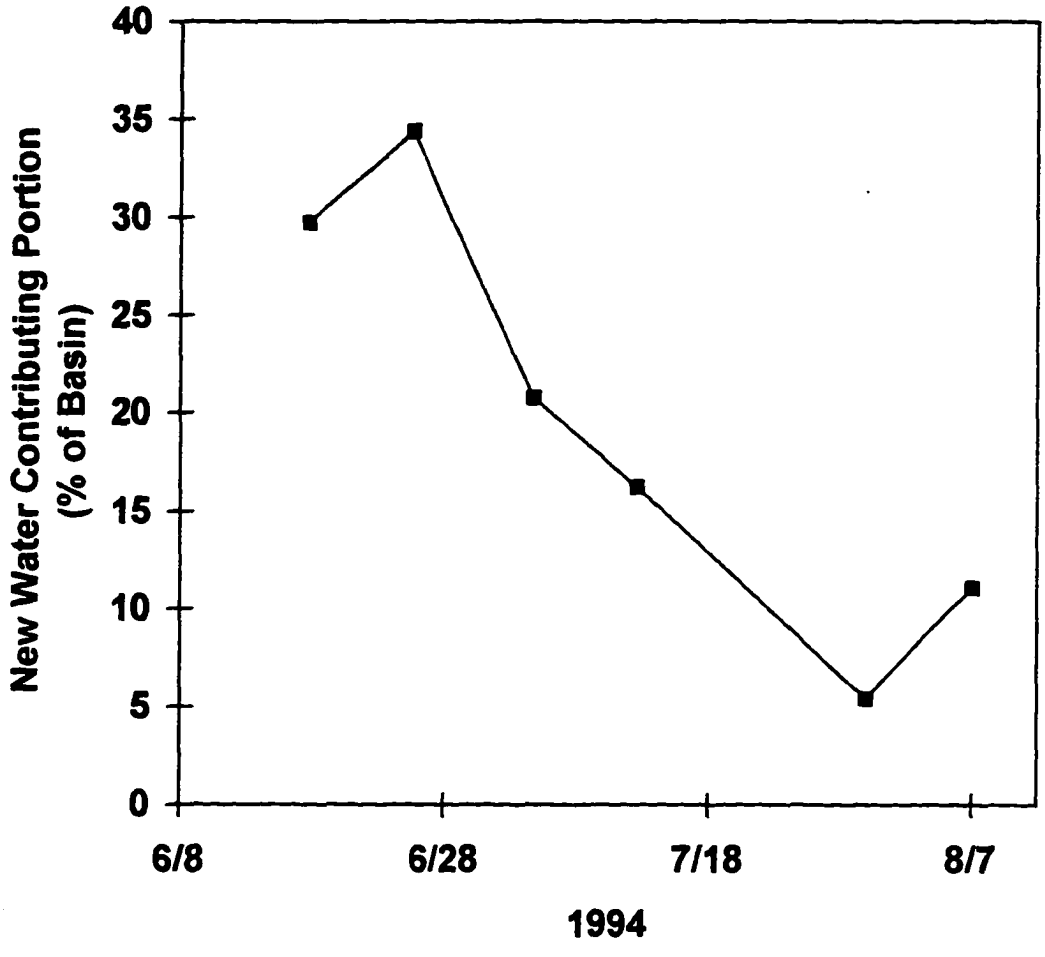

Figure 5.6b. The new water contributing portion (NWCP) in 1994 decreased through the season.

Eshleman et al. (1993) demonstrated that old water contribution to stormflow decreases as precipitation intensity increases. However, Hinzman et al. (1993) showed that vertical hydraulic conductivities in the Imnavait Creek near surface organic soils are so great that precipitation intensity rarely exceeds infiltration capacity, and that runoff occurs more commonly as a result of saturation of the active layer. Roulet and Woo (1988) arrived at a similar conclusion in the Canadian Low Arctic. They stated that in wetland soils, minimal runoff occurs until the soil saturates and the water table rises above the surface, effectively initiating a simultaneous response over the whole wetland area. This is a threshold response of runoff initiation, and it suggests that total precipitation combined with basin storage capacity should be more significant than precipitation intensity in determining hillslope response to precipitation events.

Basin storage capacity is dictated by the active layer thickness and soil moisture conditions. Thus, the depth of active layer thaw, in conjunction with precipitation patterns, influences old water contributions to stormflow. Hinzman et al. (1991) showed that the soil moisture in the surface organic soil layer in Imnavait Creek is highly sensitive to recent precipitation patterns, while the soil moisture in the underlying mineral soil remains fairly constant. Therefore, the influence of active layer depth on basin storage capacity is diminished once the thaw depth reaches the mineral soil. Thus, in the period immediately following snowmelt, increases in active layer thickness have dramatic influences on storm flow compositions. However, later in the summer, any influence of the active layer can be easily masked by soil moisture conditions as dictated by precipitation patterns.

New water contributing portion (NWCP) results showed similar patterns to old water contribution with a seasonal trend in 1994 (Figure 5.6b), but not in 1995. NWCP may be influenced by changes in the active layer thickness in the same manner as is old water contribution. However, a more significant result of the NWCP calculations is the difference between permafrost and non-permafrost basins. Eshleman et al. (1993) reported NWCP values between 0.1% and 3% for the Reedy Creek watershed in the Virginia coastal plain which has a humid subtropical climate. Although these values range by a factor of 30, they are considerably lower than those we report from the Upper Kuparuk River (Table 5.1). This suggests much more interaction with the subsurface in non-permafrost environments.

5.6.2 Flow Sources and Hillslope Response

Walker et al. (1996) constructed a hierarchic GIS of the Upper Kuparuk River basin which showed that open water, including streams, lakes, and ponds comprise 0.5% of the basin. The computed NWCP's are significantly higher indicating that the new water storm flow response can not be accounted for just by precipitation onto the channel network, and that there is indeed interaction with the surrounding hillslopes. However, by adding the riparian wetland areas (1.4%), the well developed hillslope water tracks (10.9%), and the poorly developed water tracks (21.9%), the total area of the extended channel network is 34.7% of the total basin area. This is remarkably close to the 34% early season NWCP in 1994 indicating that all of the early season new water storm flow can be accounted for by precipitation onto the extended channel network. The hillslope contributions to storm flow are likely coming from only the

water tracks with very little interaction with the unchanneled hillslopes. Thus, the water track network may act as the maximum potential saturated area during storms. The storage capacity in the water tracks increases as the season progresses which could account for the decrease in NWCP and the increase in old water contributions through the summer of 1994. By the end of the season, the new water contributing area is probably restricted to narrow margins around the streams. The early season NWCP in 1995 was 73%, which is considerably higher than the area of the extended channel network. However, this storm was fairly close to the end of the snowmelt period when large snowdrifts persisted on the east facing slopes and at the higher elevations. Consequently, the runoff during this storm was likely a mixture of precipitation and meltwater, which would alter the contributing area of runoff generation. The mean 1995 NWCP was 33%, indicating that throughout the season new water storm flow can be accounted for by precipitation onto the extended channel network. These results suggest that the mechanisms that are occurring on the unchanneled hillslopes are overwhelmed by the water tracks, and are not significant in the basin response except in extreme events.

A good agreement between NWCP and the extended channel network was also found by Eshleman et al. (1993) in Reedy Creek, where runoff generation is dominated by saturation overland flow. So perhaps a common mechanism of runoff generation exists among watersheds in these different regions, despite radically different hydroclimatological conditions.

The commonly accepted groundwater ridging hypothesis proposed by Sklash

and Farvolden (1979) states that old water originates in narrow margins around the streams. In the Kuparuk River basin, the water tracks are ephemeral streams that exist as zones of enhanced soil moisture during dry periods. It is likely then that old water contributions come directly from moisture existing in the water tracks that are replenished during storms. We have suggested that the unchanneled hillslopes are not significant components of new water runoff, and it is likely that they are not significant as old water sources as well. We must clarify our above explanations relating hillslope thaw depth to storm flow response by stating that those processes described are occurring within the hillslope water tracks as well. It is important to note that water tracks are distinct geomorphologic features of drainage basins in the Arctic, not simply zones of preferential saturation during storms. Essentially, water tracks function as both hillslopes and channels. Early in the season, the thaw depths in both the unchanneled hillslopes and the water tracks are near zero. In the following summer months, the water tracks thaw deeper than the adjacent tundra regions. Hence, the old water reservoir per unit of surface area is greater in the water tracks, thereby enhancing the relationships between thaw depth and runoff described above, and lending further support to our statement that old water storm contributions come primarily from water existing in the water tracks and saturated valley bottoms.

The distinct differences in specific conductivity between Imnavait Creek and the Upper Kuparuk River suggests that there is a source of solutes present in the Kuparuk basin that is not present in Imnavait Creek. The specific conductivity of Imnavait Creek is rarely greater than local precipitation, suggesting that there is no

significant interaction with underlying mineral soil, and that the old water source exists in the organic soil horizon. A spring located in the Kuparuk River headwaters 8 kilometers upstream of our gauging station was sampled periodically through the summer, and the specific conductivities closely followed the low flow stream concentrations. Kreit et al. (1992) suggested that this spring water originates from precipitation within the basin that percolates through coarse glacial sediments. Also, many of the small streams and water tracks in the headwaters of the Upper Kuparuk River have specific conductivities similar to those of the spring. The water discharging from the spring and in the upper streams is likely from the same source as the old water contributions to storm flow.

Small streams and water tracks may have differing chemical signatures depending on the bed material. Water tracks that exist only in the upper organic soil layer have very low specific conductivities, and will retain signatures close to new water throughout a storm, as in Imnavait Creek. Water tracks and streams that cut through to mineral soil pick up more solutes and develop an old water signature similar to what we see in the Upper Kuparuk River. The consequence is that we may overestimate the new water contributions in peaty channels. The Upper Kuparuk River basin contains both peaty and stony channels. However, that our recession analysis and mixing model results are similar for the Upper Kuparuk River suggests that our storm flow separations are not significantly influenced by this potential error. Further, this supports our explanation that the source of old water is from soil moisture within the

water tracks and ephemeral streams, and that the differing old water signatures between basins does not require different explanations of storm response.

The above discussion raises the question why Imnavait Creek storm flow is not dominated by old water. This may be due simply to the density of hillslope water tracks, and the presence of a large wetland in the valley bottom of Imnavait Creek. GIS mapping of the Imnavait Creek basin indicates that 56% of the basin is either part of the channel network, riparian wetland, or water track providing a very large potential saturated area for quick flow of new water compared to 35% in the Upper Kuparuk River basin (Walker et al., 1996). The NWCP's for Imnavait Creek (14% and 13% for storms 3 and 6 in 1994) are considerably less than the potential saturated area, even though new water dominates the storm runoff. This suggests that a relatively small portion of the basin contributes a majority of the runoff during storms. That contributing portion may be the broad wetland in the valley bottom which occupies 12% of the basin and remains saturated most of the summer. A likely scenario is that the water tracks provide a mixture of old and new water to the wetland valley bottom, which produces a saturated surface in the valley bottom from which continued precipitation runs off. A lower portion of the Upper Kuparuk basin is valley bottom wetland (1.4%), thus more of the water tracks connect directly with the streams without passing through a wetland.

5.7 Summary

We suspected that permafrost may alter the composition of storm flow in the Kuparuk River basin from the common observation in other regions that old water

dominates storm hydrographs. Further, we suspected that the gradual increase in subsurface storage capacity due to thawing of the active layer would impose seasonal trends on storm flow characteristics. Using both a chemical mixing model and graphical recession analysis, we found that storm flow in the Upper Kuparuk River basin in 1994 and 1995 was indeed dominated by old water contributions. However, Imnavait Creek storm flow was dominated by new water contributions. The difference between the two basins may be a result of the differences in the potential saturated portions of each basin. Favorable comparisons between the specific conductivity mixing model, ^{18}O mixing model, and recession hydrograph separation techniques support our use of specific conductivity as a tracer and lend credence to the physically unjustified recession analysis technique.

In 1994, old water contributions to storm flow in the Upper Kuparuk River increased moderately through the summer. Those seasonal trends were not apparent in 1995, and no seasonal trends were observed in the storm flow dynamics of Imnavait Creek in either year. However, there were large differences in the compositions of storm flow between the snowmelt period and the first summer storms each year. Thus, in the period immediately following snowmelt, increases in active layer thickness have dramatic influences on storm flow compositions. Later in the summer, the influence of the depth of the active layer can be masked by soil moisture conditions as dictated by precipitation patterns.

New water contributing portion (NWCP) was much greater in the Upper Kuparuk River basin than in the basin without permafrost studied by Eshleman et al.

(1993), which suggests that more interaction occurs between the surface and subsurface in basins without permafrost. Further, NWCP decreased through the summer of 1994, which agrees with the increase in old water contributions. As the storage capacity of the basin increases through the thawing season, more new water enters the soil, as opposed to going directly to runoff, and mixes with old water to produce runoff.

We credit both new water and old water sources to hillslope water tracks, and suggest that very little interaction occurs between unchanneled hillslopes and streams. The small amount of interaction between the two zones is diminished even more with the increasing storage capacity in the unchanneled hillslopes as the season progresses. That storm flow composition has even moderate dependence on active layer thickness has implications that a warming climate may impose significant changes in the hydrology of watersheds in the Arctic, which may then influence the timing and magnitude of the delivery of nutrients to the aquatic system.

Chapter 6

SCALING OF STREAMFLOW IN THE ALASKAN ARCTIC

6.1 Abstract

A demand has been placed on hydrologists in recent years to quantify hydrologic fluxes at scales larger than those for which data are typically available. Hence, a critical area of research is the scaling and spatial variability of hydrologic processes. We examined the scaling of streamflow in the Kuparuk River basin in Arctic Alaska using streamflow data from 4 basins ranging in drainage areas from 0.026 km^2 to 8140 km^2. Further, we examined the differences in scaling of annual flood peaks for several Arctic and Appalachian rivers. We show that rainfall-generated streamflow in the Kuparuk River basin exhibits simple scaling, whereas other researchers have shown that rainfall-generated streamflow in temperate basins generally exhibit multiscaling. A possible explanation for this regional difference lies in the different controls on hydrograph characteristics at the headwater scale that exist for permafrost and non-permafrost basins.

6.2 Introduction

The linking of atmospheric and terrestrial models to produce holistic earth system models is receiving extensive effort in global climate change research. The hydrologic cycle is the communicating link between terrestrial, oceanic, and atmospheric processes. Consequently, there is a need for large scale, physically based hydrologic models to provide that necessary link. Researchers are developing one such model for Kuparuk River basin in Arctic Alaska, a critical region in global climate

dynamics (Weller et al., 1995). A problem at the heart of large scale modeling is that past hydrologic process studies have typically focused on headwater basins or plot studies. Hence, hydrologic information is required at scales much larger than what is typically available. One approach to solve this scale disparity is to develop analytical relationships that bridge the data from the understandable smaller scales to the larger scales of interest. Consequently, scaling of hydrologic processes has emerged as a critical area of research (NRC, 1991).

One goal of a scaling study is to identify the patterns of spatial variability of a variable across a range of observation scales. Another is to develop techniques to "scale up" or "scale down" information. Scaling up means to generate information at a large scale from an aggregate of heterogeneous small scale information, whereas scaling down means to break down large scale information into smaller components. Ideally, these techniques are based on the ways in which variables scale in nature. Simple averaging may suffice in some instances. However, many non-linearities exist in the ways in which hydrologic processes vary across scales. It is imperative to determine the natural scaling characteristics for all components of the hydrologic cycle to develop large scale hydrologic models. Here, we address the natural scaling of streamflow in the Kuparuk River basin to support the regional modeling effort taking place in that basin.

Gupta and Waymire (1990) investigated the spatial variability of streamflow in Brandywine Creek, PA. Using drainage area as a scale parameter, they concluded that streamflow can be represented by a multiplicative cascade model in which the spatial

variability of flow is a result of the cascading down of a large scale flux to successively smaller scales. They documented how changes in scale are accompanied by systematic changes in the probability distribution of discharges that are best described by a multiscaling formalism, as opposed to simple scaling. Generally, simple scaling implies a constant coefficient of variation (CV) across all scales, and multiscaling does not. A question is whether their model is universal. They suggested that similar studies be implemented in differing geologic settings and climates. Smith (1992) found that multiscaling exists in Appalachian flood data. Gupta and Dawdy (1995) showed that floods generated by snowmelt display simple scaling while floods generated by rainfall display multiscaling for drainage areas above a certain threshold.

The Kuparuk River basin is entirely underlain by permafrost. Consequently, the runoff generating mechanisms and streamflow patterns are considerably different than in temperate regions where most other scaling studies have been performed. We suspected that the small scale differences in runoff generating mechanisms between arctic and temperate basins might produce differences in the scaling of streamflow. The objective of this study was to identify the nature of the scaling of streamflow in the Kuparuk River basin. We summarize the current research on scaling of streamflow to explain the basis of our tests, and present the results of a scaling analysis on flows across 4 scales in the Kuparuk River basin. Further, we examine the differences in scaling of annual flood peaks of several Arctic and Appalachian rivers, and suggest a potential explanation for the significant differences in the scaling behavior between the two regions.

6.3 Scaling Concepts

Scale relationships have long been a part of quantitative hydrology, and several power law type equations exist that relate physical features of a basin to discharge. One example is the relationship between drainage area and discharge:

$$Q \propto A^b \tag{6.1}$$

Here, discharge Q scales with drainage area A according to the scaling exponent b. This and several similar relationships found in hydrology imply a systemic variability and interdependence between hydrologic processes and fluvial landforms. These relationships are based entirely on empiricism, and until recently few attempts have been made to provide theoretical justifications. Significant advances have been made using the concepts of self-similarity, fractal distributions, and simple and multiscaling to identify the nature of the systematic variability in fluvial systems and provide theoretical justifications for those empiricisms (examples include Beer and Borgas, 1993; Rodriguez-Iturbe, et al., 1992b; Tarboton et al., 1988).

A spatially distributed random variable scales if the distribution of that variable exhibits systematic and predictable variations with changes in scale that can be described mathematically. That change of scale may come about in two ways, which we call apparent scaling and true scaling. Apparent scaling is concerned with map scale. At any given map resolution, a mapped feature is manifested with a certain amount of detail. Consider a fluvial channel network. More channels are evident as the map scale increases. At some unknown scale is the true channel network. In this case,

scaling analysis involves varying the apparent scale to identify patterns of variability as functions of map resolution. True scaling is concerned with the actual physical changes of a spatially distributed variable over physical changes in landscape scale, as opposed to map scale. This is the type of scaling embodied in the empiricisms described above. Hydrologic variables change in a predictable manner in the downstream direction. It is true that the measurements of drainage basin features such as drainage area are dependent on map scale, indicating that the two concepts of scaling are intricately connected. In this study, we were interested in the dependence of discharge on drainage area. We measured drainage area at several physical scales from a common map scale, the apparent scaling, and thus focused on true scaling.

A random variable possesses self-similarity or scale invariance if the distribution of that variable remains identical under scale transformations (Gupta and Waymire, 1989). If discharge Q is the random variable and drainage area A is the scale parameter, then discharge is self-similar if

$$Q(\alpha A) \stackrel{d}{=} Q(A)\mu(\alpha) \qquad (6.2)$$

where $\stackrel{d}{=}$ denotes equality of probability distributions. Here, the drainage area is changed by a factor α, and the probability distribution of Q(A) is rendered equal to the probability distribution of $Q(\alpha A)$ through the normalization function $\mu(\alpha)$. Consequently, the statistical moments of discharge change in a systematic manner with scale.

If we establish a reference scale Q(1), and all other scales are related to that scale through the generalized normalization, or scaling, function $\mu(\cdot)$, then Equation 6.2 can be alternately stated as

$$\frac{Q(A)}{\mu(A)} \stackrel{d}{=} Q(1) \tag{6.3}$$

The discharge at some reference scale, say unity, is identically distributed to the discharge at any other scale normalized by some function of the drainage area. This is the definition of self-similarity given by Gupta and Waymire (1989). We refer to this definition as moment based scaling. An alternate approach uses quantiles (Gupta and Dawdy et al., 1994). We explain both approaches below.

6.3.1 Moment Based Scaling

Gupta and Waymire (1989) and Smith (1992) showed that the scaling function, or normalization function, has the form

$$\mu(A) = A^{\theta} \tag{6.4}$$

where θ is called the scaling exponent. Equation 6.3 can then be written as

$$Q(A) \stackrel{d}{=} A^{\theta} Q(1) \tag{6.5}$$

There is a clear resemblance between the self-similarity model in Equation 6.5 and the empirical relationship in Equation 6.1. It follows then that if the physical causes of self-similarity in discharge can be determined, a physical explanation for the long established empirical equations exists.

Equation 6.5 can further be transformed into equations for each moment order n. If the nth moment of Q(A) is $E[Q_A^n]$, where E[] represents the expected value of a random variable, Equation 6.5 becomes

$$E[Q_A^n] = A^{\theta_1 n} E[Q_1^n] \quad \text{for } n = 1,2,3,... \tag{6.6}$$

where θ_1 is the exponent when n=1.

Taking the logarithm of both sides, Equation 6.6 becomes

$$\log E[Q_A^n] = \theta_1 n \log A + \log E[Q_1^n] \tag{6.7}$$

Q_1^n is independent of A and is therefore constant for each n. So,

$$\log E[Q_A^n] = \theta_1 n \log A + C_n. \tag{6.8}$$

Or,

$$\log E[Q_A^n] = m_n \log A + b. \tag{6.9}$$

Embodied in Equation 6.8 are the two requirements of simple scaling as defined by Gupta and Waymire (1990): 1) Log-log linearity in the plot of each statistical moment versus the scale of measurement, or a linear relationship between $\log Q_n$ versus logA for any moment order n, and 2) linearity between the moment order, n, and the slope of the log-log relationships from Equation 6.9, i.e., $m_n = \theta_1 n$. This is referred to herein as a linear growth of slopes. The physical interpretation of this second requirement is very significant, and is the primary focus of this paper.

We illustrate the application of these requirements using two synthetic data sets. For set A, consider 6 basins with drainage areas $A_1,\ldots,A_6$ increasing successively

by 1 order of magnitude. Each basin has 10 discharge measurements $Q_1,\ldots,Q_{10}$ which also increase with drainage area by an order of magnitude. Hence, there is a linear relationship between discharge and drainage area. Figure 6.1a shows each moment of Q plotted against drainage area for set A. log-log linearity for each moment is maintained and the first test of simple scaling is passed. Taking the slope of each line from Figure 6.1a and plotting it against moment order produces Table 6.1a. The column labeled "Empirical Slope" in Table 6.1 contains the slopes of the log-log plots for the moment of Q versus drainage area from Figure 6.1a, and the r^2 values refer to those plots as well. The theoretical slopes that Figure 6.1a should have if the data are subject to simple scaling are calculated by multiplying the first empirical slope by the successive moment orders. For set A, the two slopes are the same for each moment order. Consequently, m_{th}/m_1 equals the moment order and the set A is simple scaling, where m_{th} is the theoretical slope for each moment divided by the empirical slope for moment 1,. The last column in Table 6.1 contains the power law function that describes the empirical growth of slopes and is explained below.

The linear function M(n) that describes the empirical growth of slopes for data set A on Figure 6.2 is

$$M(n) = (1)n+0. \qquad (6.10)$$

Since $\theta_1=1$, $m_n=\theta_1 n$ in Equation 6.9 and the second test of simple scaling is passed. An important feature of this data set, and the fundamental definition of simple

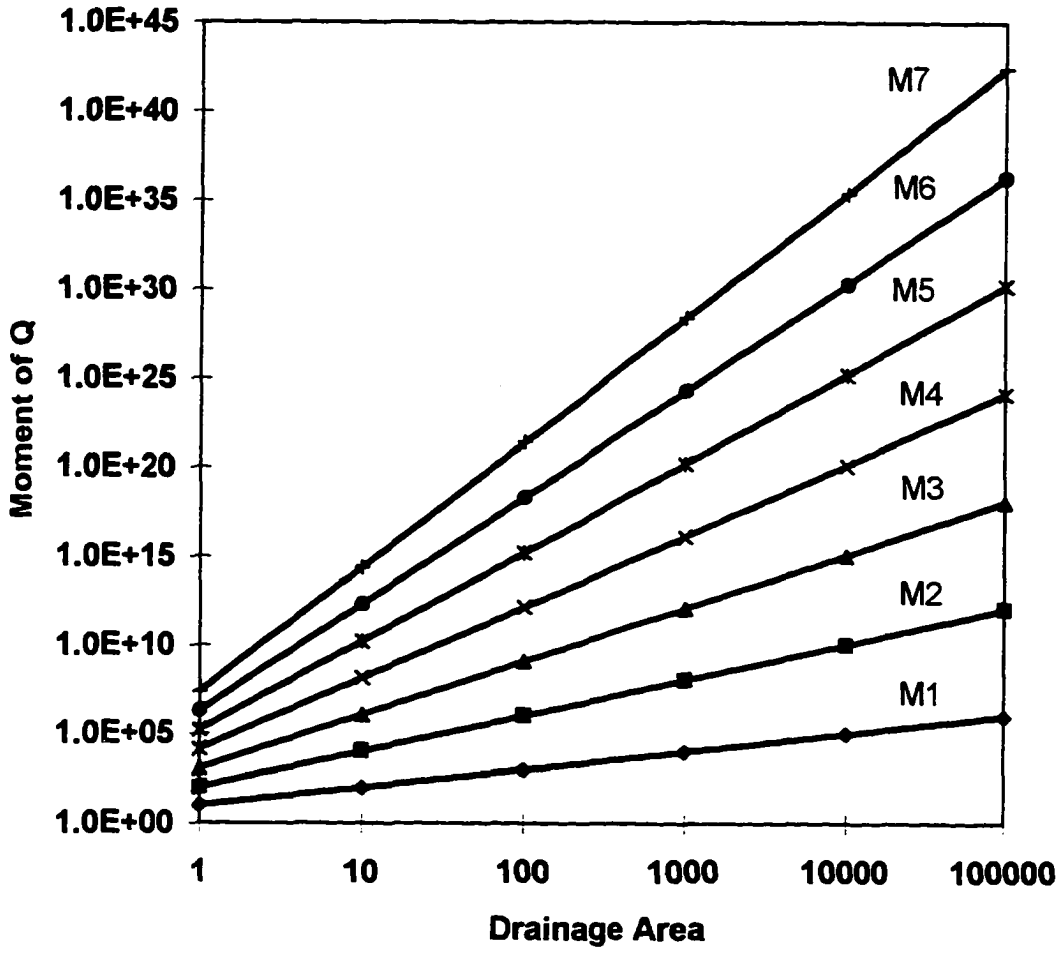

Figure 6.1a. Moment of discharge, Q, versus drainage area for synthetic data set A. Linearity of each relationship comfirms that set A passes the first test of simple scaling.

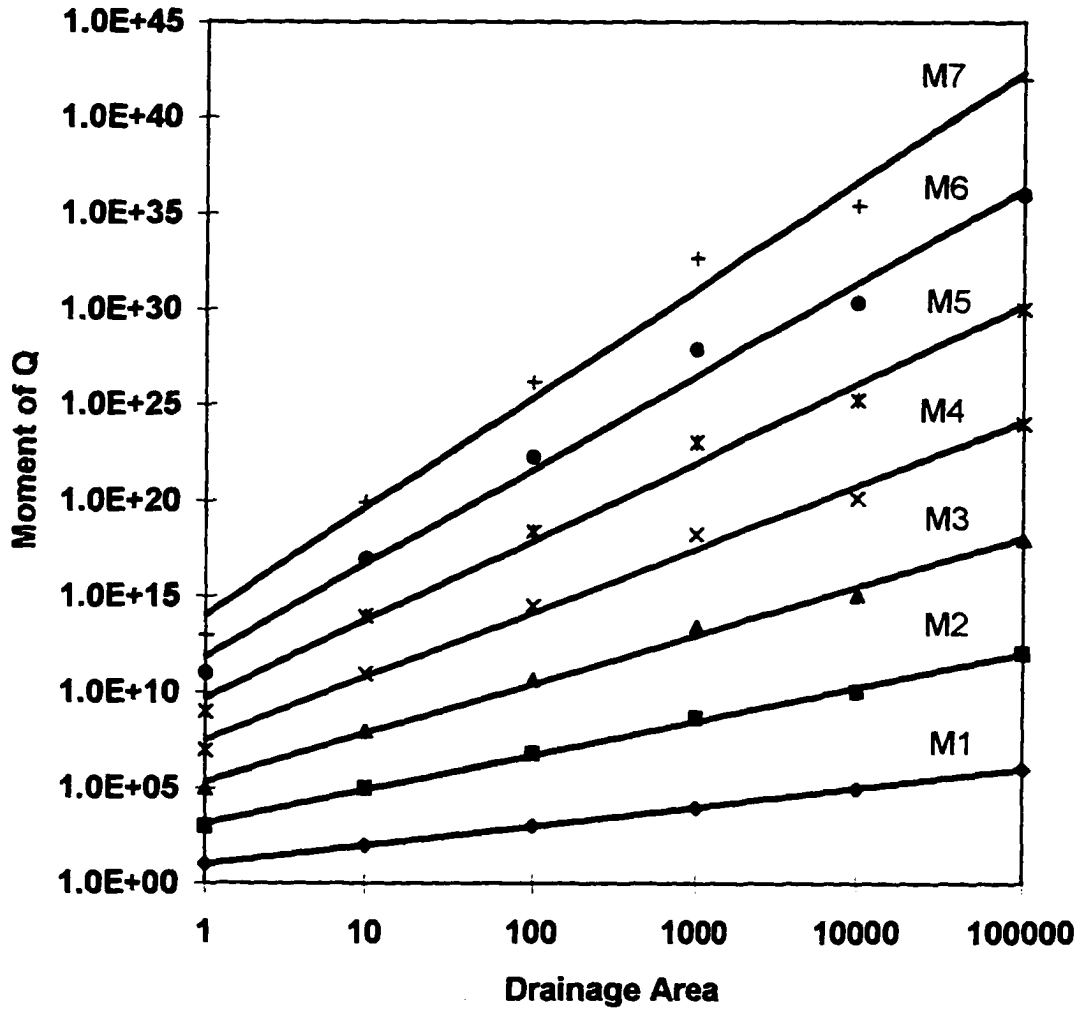

Figure 6.1b. Moment of discharge, Q, versus drainage area, A, for synthetic data set B. Linearity of each relationship comfirms that set B passes the first test of simple scaling.

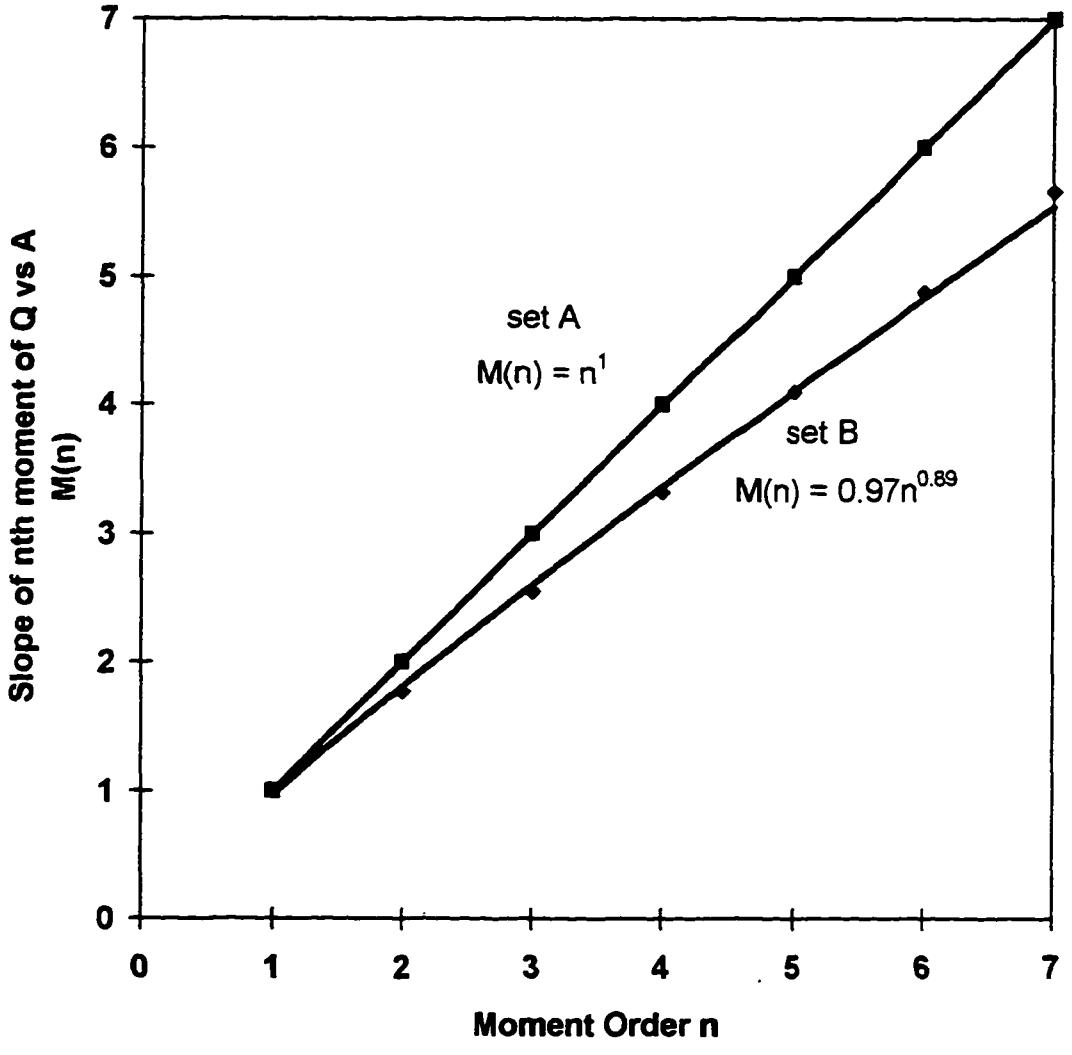

Figure 6.2. The growth of slopes for both the synthetic data sets A and B. Set A has an exponent of 1 in a power function indicating linearity and passes the second test of simple scaling. Set B has an exponent of 0.89 and therefore does not pass the second test of simple scaling.

Table 6.1. Results of scaling analysis on two synthetic data sets illustrating a) simple scaling, and b) multiscaling.

	Variable	Moment Order n	Empirical Slope m_n	r^2	Theoretical Slope m_{th}	m_n/m_1	M(n)
a)	Set A						$M(n)=n^{1.00}$
		1	1.00	1.00	1.00	1.00	
		2	2.00	1.00	2.00	2.00	
		3	3.00	1.00	3.00	3.00	
		4	4.00	1.00	4.00	4.00	
		5	5.00	1.00	5.00	5.00	
		6	6.00	1.00	6.00	6.00	
		7	7.00	1.00	7.00	7.00	
b)	Set B						$M(n)=0.97n^{0.89}$
		1	1.00	1.00	1.00	1.00	
		2	1.77	1.00	2.00	1.77	
		3	2.55	1.00	3.00	2.55	
		4	3.32	1.00	4.00	3.32	
		5	4.10	0.99	5.00	4.10	
		6	4.88	0.99	6.00	4.88	
		7	5.66	0.99	7.00	5.66	

scaling, is that the coefficient of variation (CV) remains constant across all scales. Equation 6.10 illustrates two features of the second requirement of simple scaling. Specifically, the slope of the line also must match the slope of the relationship between the first moment of discharge and drainage area, and the y intercept must be 0.

Next consider the same basins and the same mean discharges, but the variability around the mean, or the coefficient of variation, decreases with increasing

drainage area. Again, there is log-log linearity between discharge and area for each moment (Figure 6.1b and Table 6.1b). A linear function can be fit to the growth of slopes for set B quite successfully:

$$M(n)=0.78n+0.22 \qquad (6.11)$$

However, the parameters a and b from Equation 6.10 must equal θ_1 and 0 to be simple scaling. Hence, although Equation 6.11 represents a linear growth of slopes, it does not meet the specific restrictions and fails the second test of simple scaling. This does not suggest that the data set does not scale, for we know from Figure 6.1b that each moment of Q possesses its own functional scaling relationship with A. Gupta and Waymire (1990) call this phenomenon multiscaling. The linear Equation 6.11 tells us that the process is not simple scaling. However, it tells us nothing about the nature of its multiscaling properties. A more appropriate function that can represent both simple and multiscaling is a power law function.

A power law representation of the growth of slopes for the synthetic data set B on Figure 6.2 is

$$M(n) = (0.97)n^{0.89} \qquad (6.12)$$

The departure from the linear simple scaling line is contained in the exponent 0.89. Note that a power law representation of the linear relationship that embodies the slope and intercept restrictions imposed by the second requirement of simple scaling (Equation 6.10) is

$$M(n)= \theta_1 n^1 \qquad (6.13)$$

If M(n) can be represented by a linear function but the slope is not equal to θ_1, then the exponent in Equation 6.13 will deviate from 1 as happens in Equation 6.12. Further, M(n) can be strictly non-linear and be represented well by a power law function. Thus a power law representation of the growth of slopes can represent both multi- and simple scaling processes and has the form

$$M(n)=\alpha n^{\eta} \qquad (6.14)$$

Here, η and α are called the structural parameters as they determine the structure of the scaling of a random process, either simple or multiscaling. Using the structural parameters we rewrite the second requirement of simple scaling as: 2) The growth of slopes represented by a power law function must have structural parameters $\alpha=\theta_1$ and $\eta=1$.

The fundamental differences between the two synthetic data sets is the change from a constant to an area-dependent CV, and this is the primary difference between the simple scaling and multiscaling formalisms. The power law function M(n) describing the growth of slopes contains important information regarding the spatial variability of streamflow. The next section explains how M(n) reflects the spatial variability of a data set.

6.3.1.a Spatial Variability and the Function M(n)

Consider that the function M(n) is describing the change in $\log E[Q_A^{n}]$ with respect to the change in the log of the drainage area, or

$$M(n) = \frac{d \log E[Q_A^n]}{d \log(A)} \qquad \text{(Gupta and Waymire, 1990)} \quad (6.15)$$

Further, consider the relationship between $\log E[Q_A^n]$ and moment order, n, for any given drainage area, A. Suppose that all discharge values for a given A are equal; i.e. there is no variability in the data. Then a plot of $\log E[Q_A^n]$ versus n will be linear. A power law representation of this relationship has an exponent of 1

$$\log E[Q_A^n] = cn^1 \qquad (6.16)$$

Note that the second derivative ($[]^{''}$) with respect to n of Equation 6.16 is $\left[\log E[Q_A^n]\right]^{''} = 0$. With increasing variability, the exponent in Equation 6.16 becomes greater than or less than 1 and $\left[\log E[Q_A^n]\right]^{''}$ becomes a positive or negative real number. Hence, $\left[\log E[Q_A^n]\right]^{''}$ is a measure of the variability of the data at any given scale. From Equation 6.15,

$$M(n)^{'} = \frac{d \log E[Q_A^n]^{'}}{d \log A} \qquad (6.17)$$

It follows from above then that $M(n)^{'}$ is a measure of the change in variability with respect to a change in scale. From Equations 6.14 and 6.15 we can write

$$M(n) = \frac{d \log E[Q_A^n]}{d \log(A)} = cn^{\eta} \qquad (6.18)$$

and

$$M(n)^{\cdot} = \frac{d\log E\left[Q_A^n\right]^{\cdot}}{d\log A} = (\eta - 1)(\eta)\alpha n^{(\eta-1)(\eta-2)} \qquad (6.19)$$

Recall that for simple scaling

$$M(n) = \theta_1 n^1 \qquad (6.20)$$

If η=1, then $M(n)^{\cdot} = 0$. This implies that there is no change in variability with a change in scale, or the coefficient of variation remains constant across all scales. This is the meaning of statistical self-similarity, which forms the basis of the definition of simple scaling.

In a multiscaling process the exponent η is either greater than or less than 1. In the synthetic multiscaling data set B discussed above, η=0.89 which produces a concave curve, and M"(n) is negative. This implies a decrease in the spatial variability with an increase in scale, or variability of streamflow decreases downstream. The reverse is true for a convex M(n).

To summarize, if a function $M(n)= \alpha n^{\eta}$ exists that satisfies

$$\log E[Q_A^n] = \alpha n^{\eta} \log A + C_n, \qquad (6.21)$$

then Equation 6.21 is a testable model to determine the nature of the scaling of streamflow with drainage area.

6.3.2 Quantile Based Scaling

Gupta et al. (1994) developed the quantile approach from the inherent multiscaling assumptions built into the USGS quantile regression method of flood frequency analysis. Similarly, simple scaling assumptions are analogous to the index

flood method of flood frequency analysis (Smith, 1992; Gupta and Dawdy, 1995). The index flood assumption implies that the CV of flood peaks for a given region does not vary with drainage area. Recall that this is a characteristic of simple scaling. In terms of quantiles, the simple scaling assumption states that the pth quantile of peak floods $q_p(A)$ varies with drainage area as

$$q_p(A)=c(p)A^{\theta} \tag{6.22}$$

where a quantile is a probability of exceedence defined as

$$P[Q(A)>q_p(A)]=p \tag{6.23}$$

The coefficient c(p) in Equation 6.22 depends on the probability of exceedence p, but the scaling exponent θ does not (Gupta and Dawdy, 1995). It is apparent that there are two requirements for quantile based simple scaling: 1) the quantile-drainage area relationship is log-linear for each quantile, and 2) the slope, θ, is the same for every p. Dawdy (1961) observed that the exponent θ does indeed vary with p for annual peak floods. Essentially, flood peaks are multiscaling in that the scaling exponent relating flow to drainage area changes with the probability of exceedence. A multiscaling representation of Equation 6.22 is then

$$q_p(A)=c(p)A^{\theta(p)} \tag{6.24}$$

where both the coefficient c(p) and the scaling exponent $\theta(p)$ are functions of the probability of exceedence. The physical implications of Equations 6.22 and 6.24 are similar to those explained in the moment based approach. If θ is independent of p, then the CV is constant. If θ is a function of p, then the CV changes with drainage area (see

Gupta et al., 1994 for details) This approach was developed for annual peak flows, but the same concepts can be applied to random instantaneous discharges.

6.4 Empirical Tests and Results

We used the moment based approach to analyze the scaling of streamflow using 3 variables of discharge in 1994 across 4 scales in the Kuparuk River basin:

1) random instantaneous flows

2) intra-storm minimum flows

3) storm peak flows

For comparison, we repeated test 1 using the quantile based approach.

To summarize; the moment based procedure to test for simple scaling of river discharge is as follows: 1) Calculate the statistical moments of discharge for each basin. 2) Generate a log-log plot of moment vs. drainage area for each moment order. 3) Determine the slopes of each line using least squares regression. 4) Fit a power law function to the growth of slopes with moment order and determine the structural parameters α and η according to Equation 6.14. 5) Compare the growth of slopes with order against the slopes predicted by simple scaling. Taking the slope for the first empirical moments as θ_1, successive theoretical slopes are calculated by

$$m_n = \theta_1(n) \quad \text{for } n=1,2,3,... \tag{6.25}$$

For comparison, we review the results of Gupta and Waymire (1990) and Cadavid (1988). Using discharge data from Wolman (1955) at 7 gauging stations in Brandywine Creek ranging in drainage area from 25 to 260 mi^2, they found that the

statistical moments of discharge exhibit log-log linearity with respect to drainage area. Thus, the data passed the first test of self-similarity. However, the function M(n) that describes the growth of slopes was found to be non-linear (Figure 6.3) with the function

$$M(n) = 0.77n^{0.85} \qquad (6.26)$$

Since η=0.85<1, $M(n)^{\cdot} < 0$ and the variability of streamflow in Brandywine Creek decreases downstream. Gupta and Waymire (1990) identified several other data sets that exhibit multiscaling in the sense that the function M(n) is non-linear and concave, and they used this common empirical observation to formulate a multiplicative cascade model of the spatial variability of regional hydrologic processes. We applied the same techniques to quantify the spatial variability of streamflow in the Kuparuk River, and to test the universality of their conclusions. Figure 6.4 shows hydrographs for the summer of 1994 at 4 scales within the Kuparuk River basin.

Figures 6.5 a, b, and c show log-log plots of the moments of discharge versus drainage area for each test. Table 6.2 summarizes the results. There is log-log linearity between the statistical moments of discharge and drainage area for each test as indicated by the high r^2 values for the log-log fits. Thus, the first test of simple scaling is passed in all cases. The theoretical slopes in Column 5 are close to the empirical slopes in Column 3, and the values in Column 6 are close to the moment orders. Both favorable comparisons suggest that all tests pass the second requirement of simple scaling.

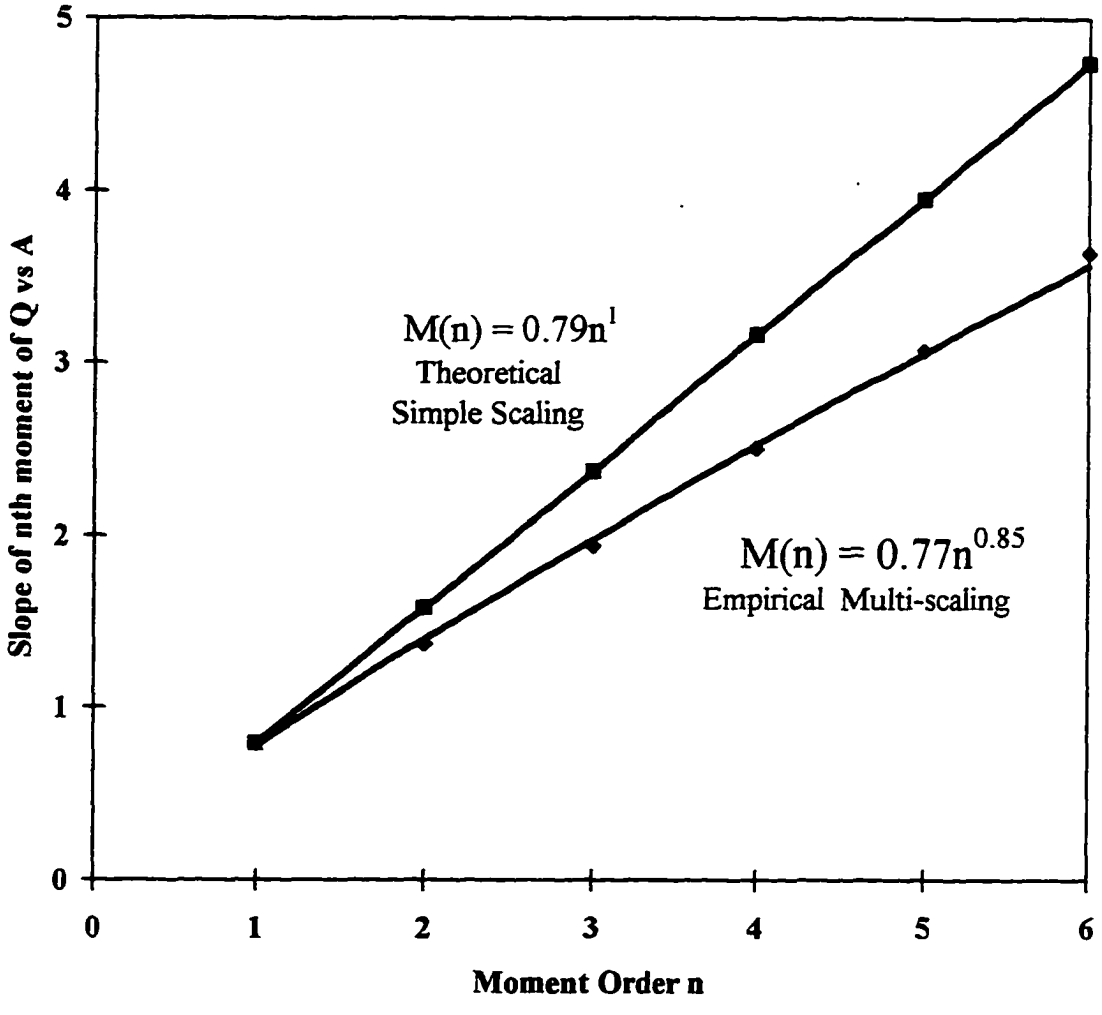

Figure 6.3. The growth of slopes for discharges in Brandywine Creek, PA. The empirical growth of slopes deviates significantly from the theoretical simple scaling line. Gupta and Waymire (1990) used this result to show that the data is multiscaling.

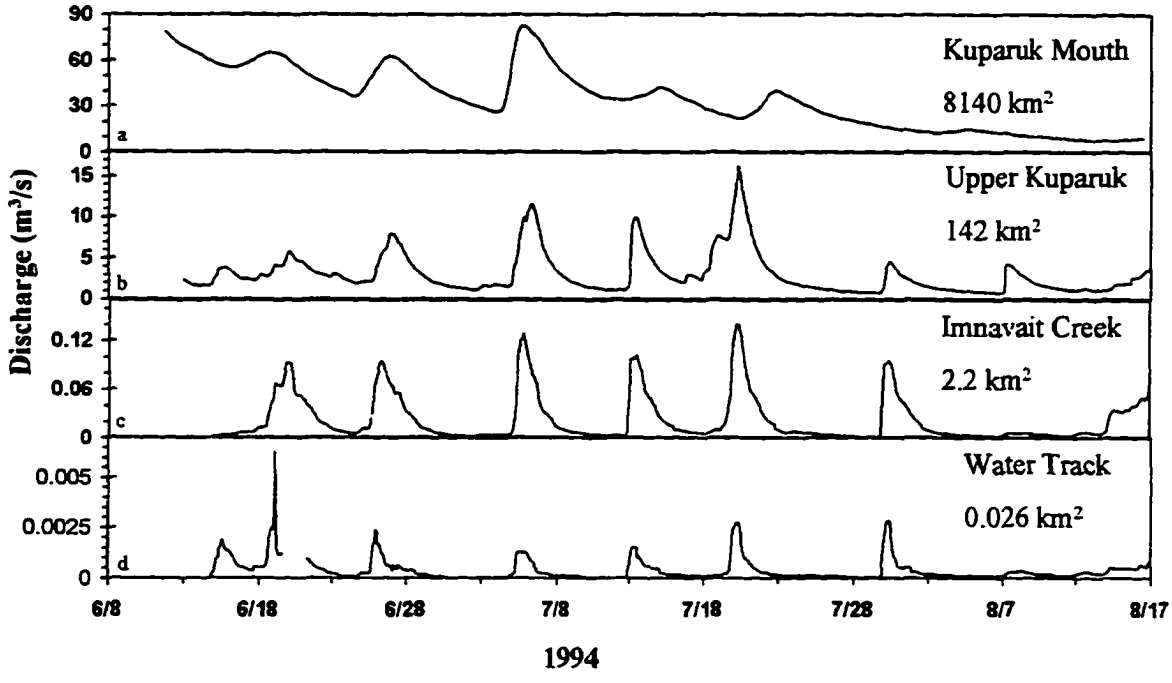

Figure 6.4. Summer hydrographs of a) the Kuparuk river near its mouth (8140 km²), b) the Upper Kuparuk River (142 km²), c) Imnavait Creek (2.2 km²), and d) the water track (0.026 km²).

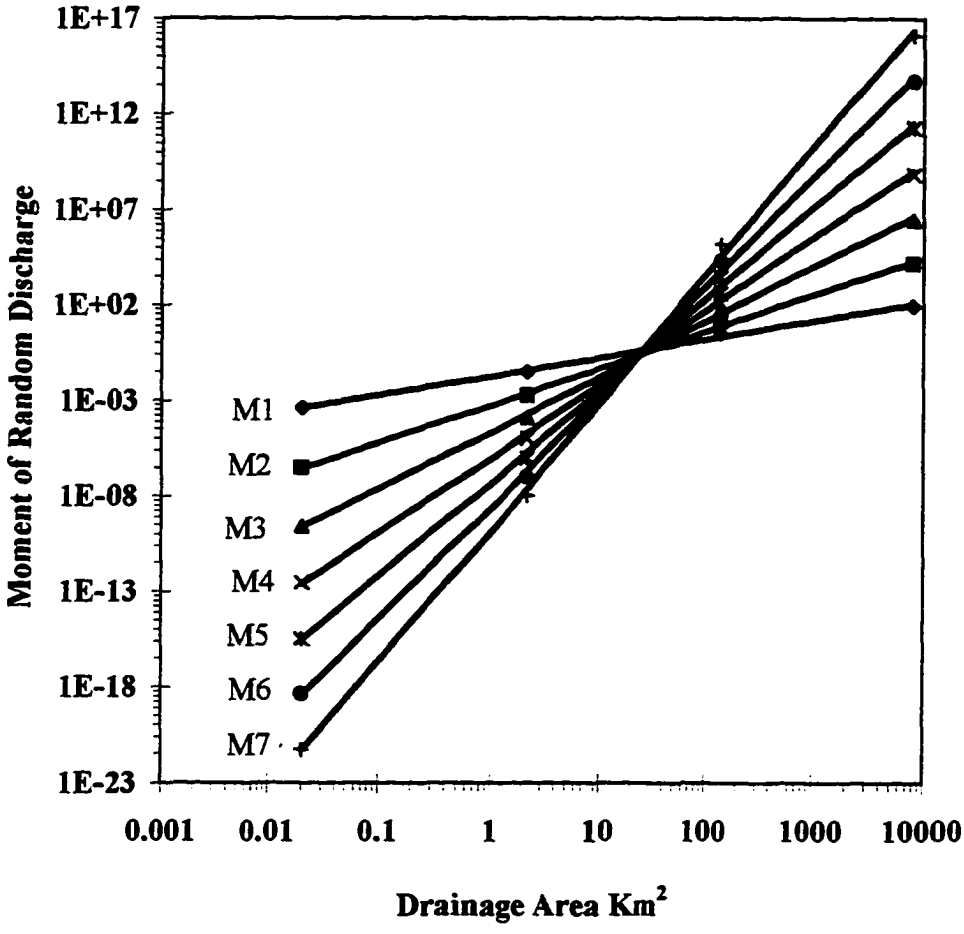

Figure 6.5a. Plot of moments of Q versus drainage area for random flows from the 1994 Kuparuk River hydrographs. Log-log linearity confirms that the first requirement of simple scaling is passed. The r^2 values are given in Table 6.2.

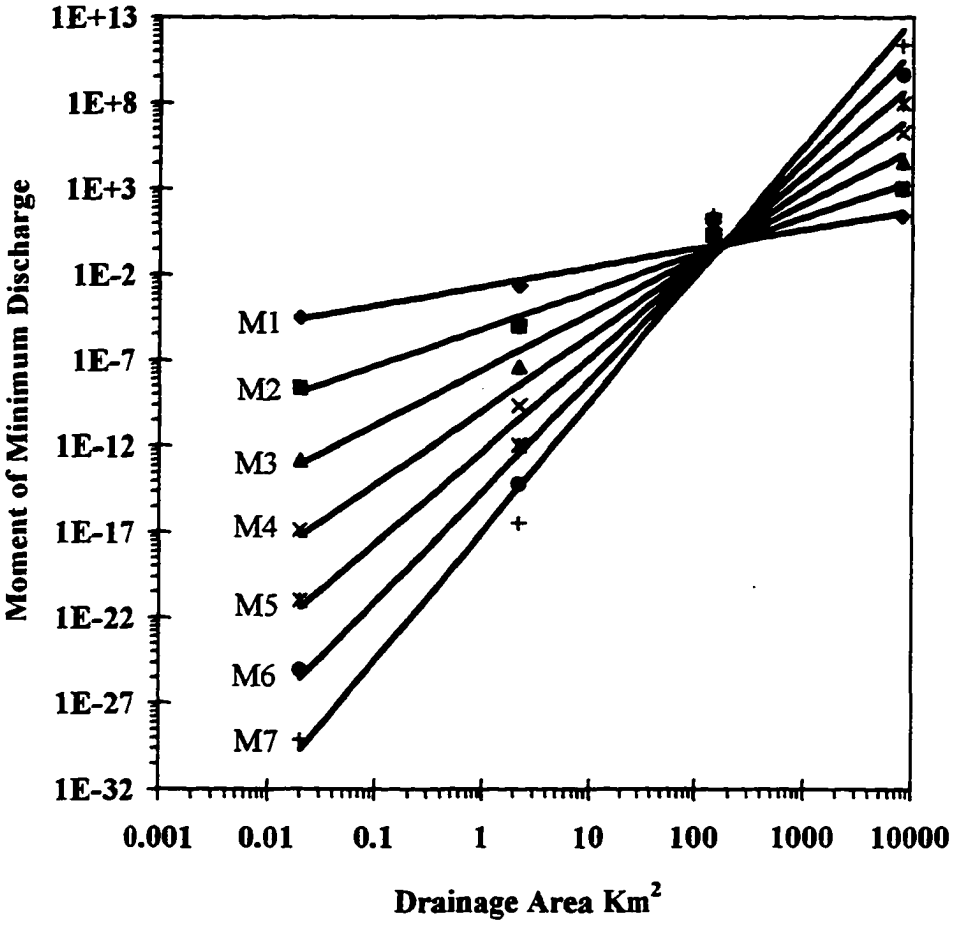

Figure 6.5b. Plot of moments of Q versus drainage area for minimum intra-storm discharges from the 1994 Kuparuk River hydrographs. Log-log linearity confirms that the first test of simple scaling is passed. The r^2 values are given in Table 6.2.

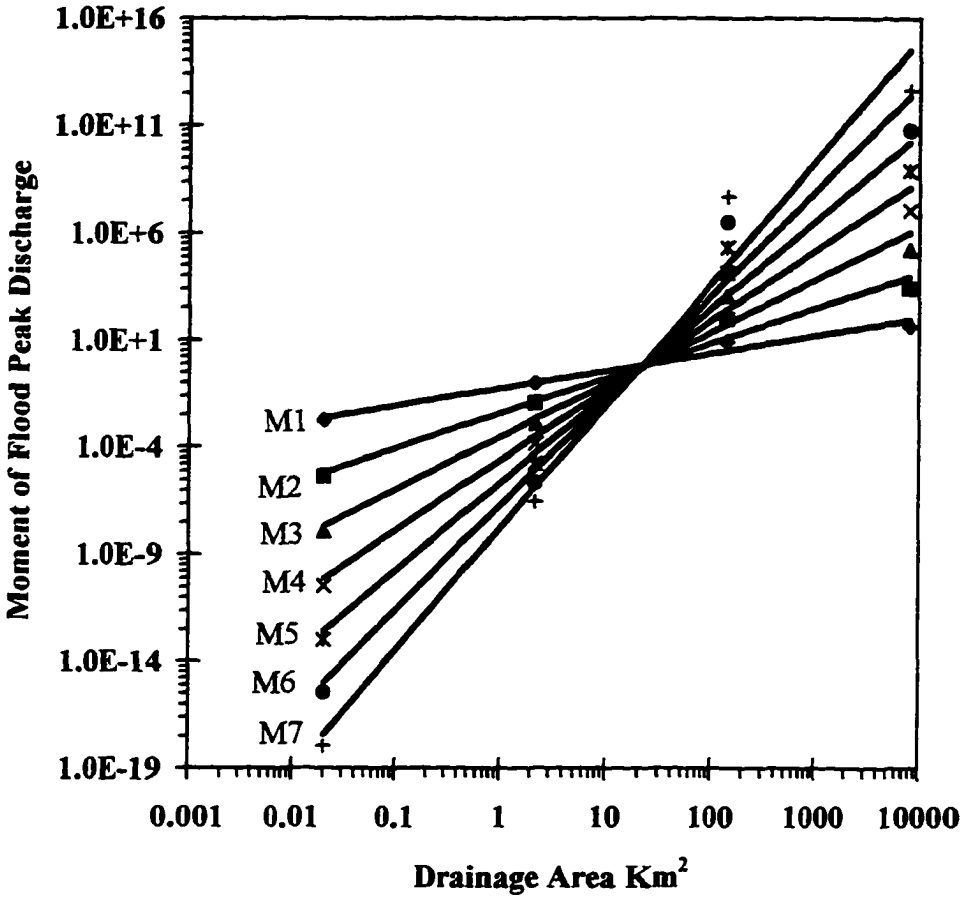

Figure 6.5c. Plot of moments of Q versus drainage area for flood peaks from the 1994 Kuparuk River hydrographs. Log-log linearity confirms that the first requirement of simple scaling is passed. The r^2 values are given in Table 6.2.

Table 6.2. a) Results of a moment based scaling analysis on three variables of flow from the 1994 Kuparuk River summer hydrograph. b) Results of a quantile based scaling analysis of random flows from the Kuparuk River 1994 summer hydrograph.

a)

variable	moment order n	empirical slope m_n	r^2	theoretical slope m_{th}	m_n/m_1	M(n)
Random Flows						$M(n)=0.97n^{1.00}$
	1	0.96	1.00	0.96	1.00	
	2	1.93	1.00	1.93	2.00	
	3	2.89	1.00	2.89	3.00	
	4	3.85	1.00	3.86	4.00	
	5	4.81	1.00	4.82	4.99	
	6	5.77	1.00	5.79	5.98	
	7	6.73	1.00	6.75	6.97	
Flood Peaks						$M(n)=0.82n^{1.00}$
	1	0.82	0.98	0.82	1.00	
	2	1.63	0.98	1.63	2.00	
	3	2.44	0.98	2.45	2.99	
	4	3.26	0.98	3.27	3.99	
	5	4.07	0.98	4.08	4.99	
	6	4.89	0.98	4.90	5.99	
	7	5.70	0.98	5.71	6.99	
Minimum Flows						$M(n)=1.10n^{0.98}$
	1	1.11	0.99	1.11	1.00	
	2	2.17	0.99	2.21	1.96	
	3	3.23	0.99	3.32	2.92	
	4	4.29	0.99	4.42	3.88	
	5	5.36	0.99	5.53	4.85	
	6	6.43	0.99	6.63	5.82	
	7	7.50	0.99	7.74	6.78	

b)

Quantile	θ
0.02	1.003
0.1	1.01
0.25	1.011
0.5	1.006
0.75	1.008
0.99	0.992

Figures 6.6 a, b, and c shows the empirical growth of slopes and the theoretical growth of slopes for simple scaling. For each test, the structural exponent η is remarkably close to 1, which further suggests that all tests pass the second requirement of simple scaling. At present, it is a subjective determination whether η is "close enough" to 1 to pass the test for simple scaling. More rigorous statistical tests must be developed in the future to distinguish between simple scaling and multiscaling exponents.

The exponents, θ, for the quantile based test on random instantaneous flows are given in Table 6.2. The approximate constancy of the exponents indicates again that simple scaling holds.

There are two significant conclusions inherent in the above results. First, streamflow across the 4 scales in the Kuparuk River is simple scaling. Second, there is a significant difference in the arrangement of spatial variability between this arctic river and the Appalachian drainage, Brandywine Creek. More fundamental is the physical interpretation of the differences in that there is a systematic decrease in variability of discharge downstream in the Appalachian basin, while the variability remains constant in the Arctic watershed.

To further explore the regional differences we performed a similar scaling analysis on annual flood peaks from rivers in the Alaskan Arctic and compared the results to Appalachian data. There is a problem of course in the paucity of data in the Arctic. We used 5 USGS gauging stations from Alaskan rivers. The Appalachian

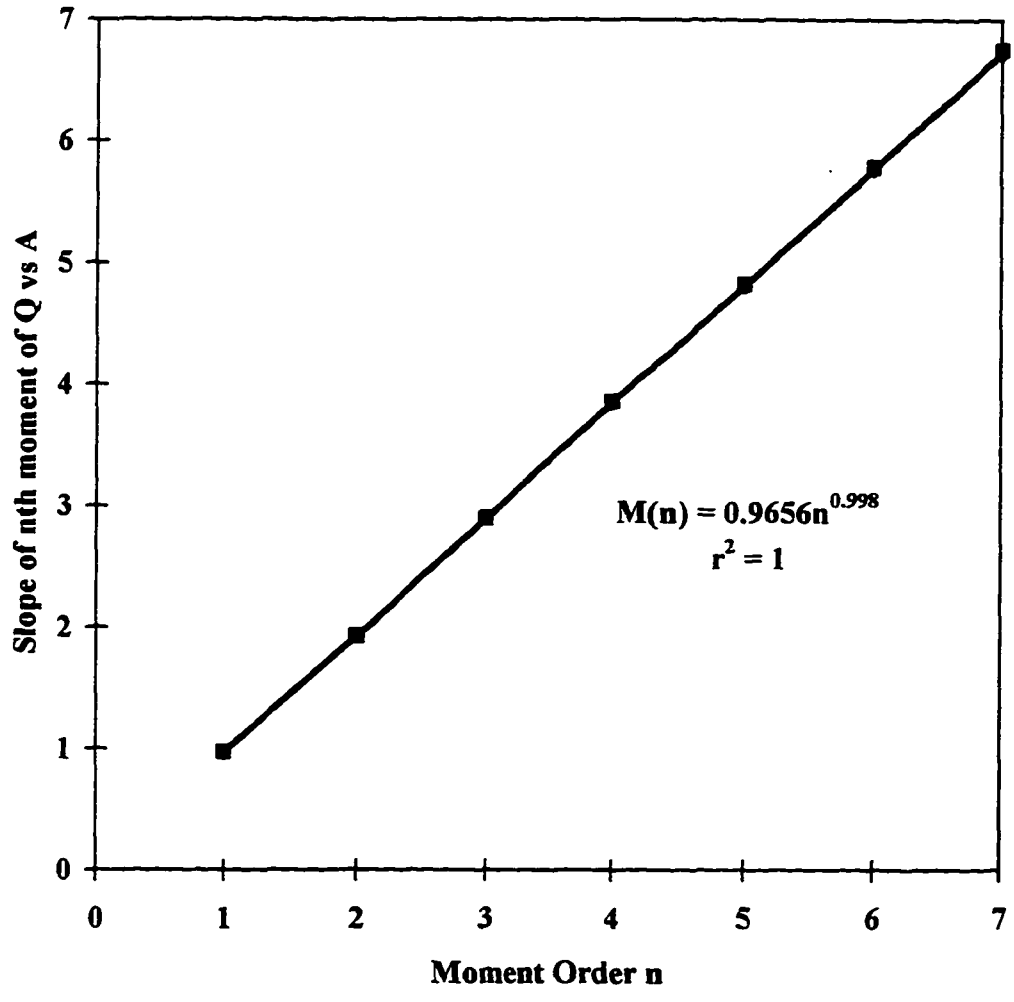

Figure 6.6a. Growth of slopes for random flows from the 1994 Kuparuk River hydrographs. The exponent is close to 1, suggesting the second requirement of simple scaling is passed.

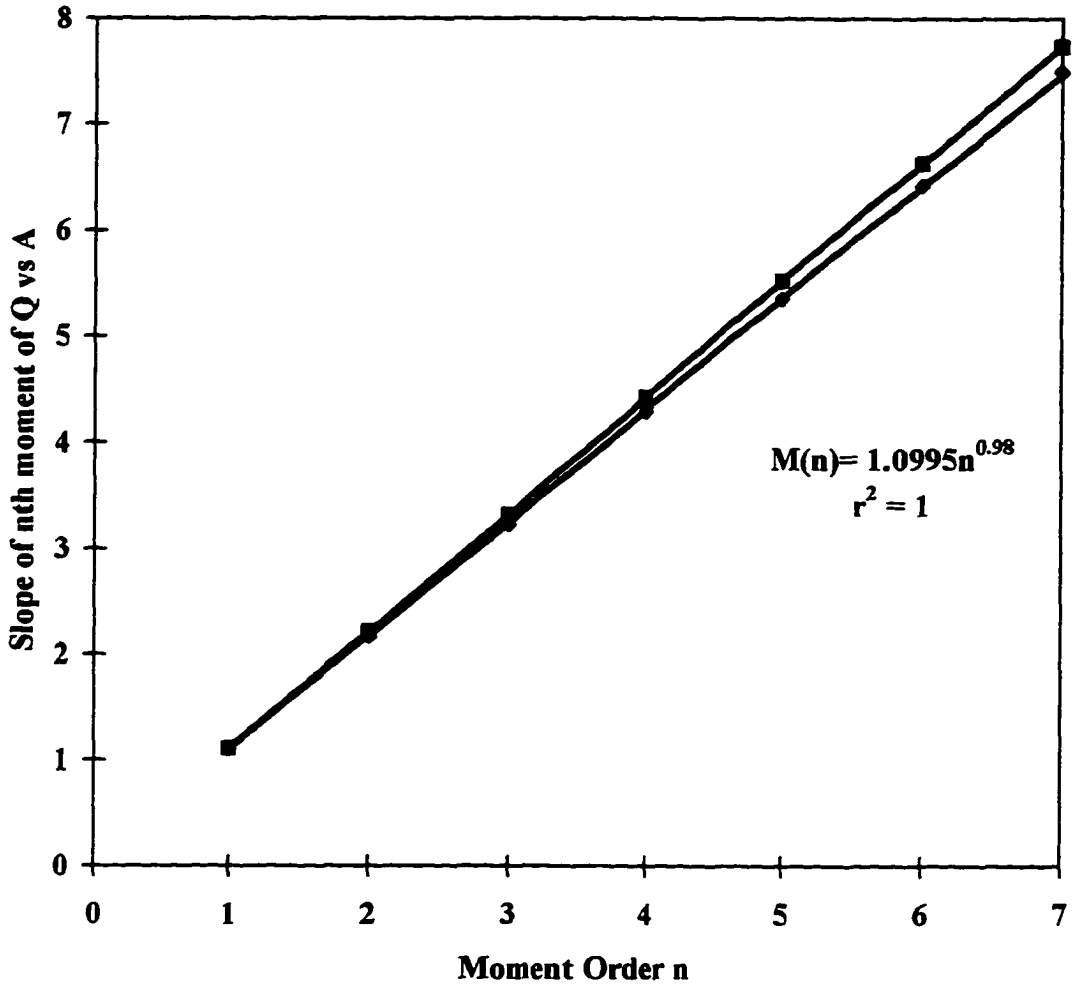

Figure 6.6b. Growth of slopes for minimum intra-storm discharges from the 1994 Kuparuk River hydrographs. The exponent is close to 1, suggesting that the second test of simple scaling is passed.

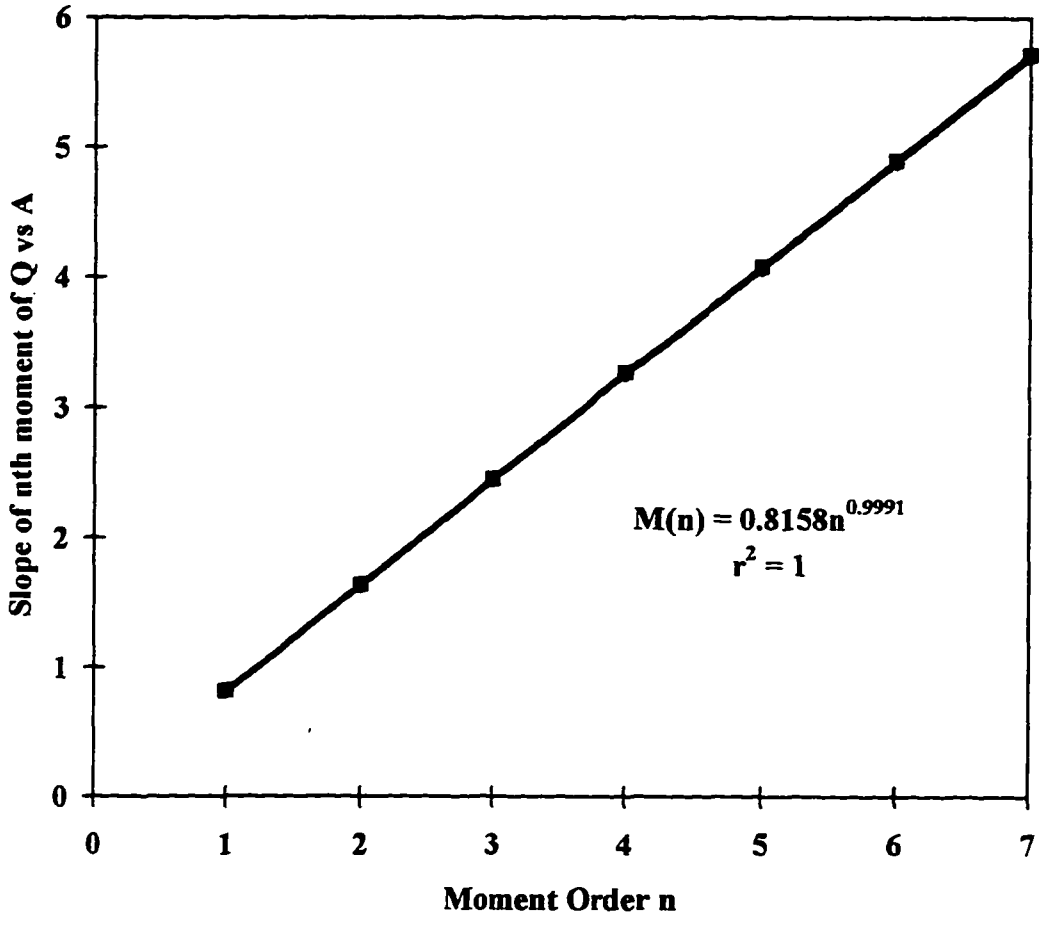

Figure 6.6c. Growth of slopes for flood peaks from the 1994 Kuparuk River hydrographs. The exponent is close to 1, suggesting that the second requirement of simple scaling is passed.

results are taken from Cadavid (1988) based on 28 stations. Table 6.3 gives the results of the moment based scaling analysis. The r^2 values for the log-log fits suggest that both tests passed the first requirement of simple scaling. For the arctic rivers the structural parameters from the function M(n) are $\alpha=0.93=\theta_1$, and $\eta=0.98$. α is the appropriate value, and η is close to 1, indicating simple scaling. For the Appalachian rivers the structural parameters are $\alpha=0.75$, and $\eta=0.86$; α is close to the required 0.74, but η is quite different from 1. Again, it is a qualitative judgment as to what is close enough to 1 to pass the second test of simple scaling. Cadavid (1988) used these results to suggest that Appalachian flood peaks are not simple scaling. Smith (1992) developed a maximum likelihood procedure to distinguish between simple and multiscaling of flood peaks and showed that Appalachian floods are multiscaling above a threshold drainage area. We conclude that rainfall generated flows in arctic rivers obey simple scaling, while flows in Appalachian rivers obey multiscaling.

6.5 Discussion

Our results suggest that differences exist in the organization of variability of streamflow between arctic and Appalachian basins. This opens the problem of why basins respond differently. We suggest some possible explanations based on known differences on the controls of streamflow patterns between permafrost and non-permafrost basins (McNamara et al., 1997a and b).

The controls on streamflow characteristics in all regions can be lumped into two groups: precipitation characteristics, and drainage basin characteristics. Robinson

Table 6.3. Results of a moment based scaling analysis for flood peaks from a) Arctic basins, and b) Appalachian basins.

Variable	Moment order n	Empirical Slope m_n	r^2	Theoretical Slope m_{th}	m_n/m_1	M(n)
a) Arctic Annual						$M(n)=0.93n^{0.98}$
Flood Peaks	1	0.93	0.98	0.93	1.00	
	2	1.83	0.98	1.86	1.96	
	3	2.71	0.98	2.79	2.91	
	4	3.59	0.98	3.73	3.85	
	5	4.48	0.98	4.66	4.81	
	6	5.38	0.98	5.59	5.77	
	7	6.27	0.98	6.52	6.74	
b) Appalachain						
Annual	1	0.74	0.97	0.74	1	$M(n)=7.45n^{0.86}$
Flood Peaks	2	1.36	0.98	1.49	1.83	
	3	1.91	0.98	2.23	2.57	
	4	2.46	0.98	2.98	3.31	

et al. (1995) argued that above a threshold drainage area, rainfall controls the scaling of streamflow and below that threshold, basin geomorphologic characteristics control the scaling of streamflow. Gupta and Dawdy (1995) credited the multiscaling of streamflow to the inherent multiscaling characteristics of precipitation where the patterns of spatial variability of rainfall are simply translated through the system to streamflow. In relatively small basins, precipitation may uniformly cover the entire basin and response hydrographs will closely follow the timing of precipitation events. In larger basins, hydrographs may be smoothed by baseflows from contributing basins

not receiving rain. This implies that if large basins received uniform precipitation inputs, then flows would reflect simple scaling. Indeed, Gupta and Dawdy (1995) reasoned that since snowmelt occurs more uniformly over large basins than does precipitation, then perhaps snowmelt generated floods would show simple scaling. They showed this to be true, whereas rainfall generated floods in the same basins obeyed multiscaling (Gupta and Dawdy, 1995). There is no reason to suspect that precipitation in the Arctic is not subject to the same patterns of variability as in temperate regions. Consequently, we must investigate the physical characteristics of drainage basins to explain differences in scaling behavior.

Downstream streamflow variability is essentially the product of the timing of upstream hydrographs. Hence, the controls on the shape of headwater hydrographs must have some influence on streamflow variability downstream. Gupta and Waymire (1996) suggested that the shape of the initial headwater hydrograph, as dictated by hillslope runoff processes, is insignificant downstream compared to the influence that the channel network has on a hydrograph as it travels downstream. There are indeed differences in the channel networks of arctic and temperate basins that may contribute to differences in scaling of streamflows. However, a more fundamental difference is the runoff generating mechanisms and resultant headwater basin hydrograph characteristics caused by the presence or absence of permafrost. Given similar precipitation events and other properties, some permafrost and non-permafrost basins will produce significantly different hydrographs. As these hydrographs are translated

downstream, we would then expect that differences would exist in the scaling of streamflow between permafrost and non-permafrost basins.

Due to the diminished storage capacity caused by permafrost, hydrographs from permafrost dominated basins typically have fast initial response times, prolonged falling limb recessions, high runoff/precipitation ratios, high peak flows, and low baseflows (McNamara, 1997a). The higher runoff/precipitation ratios in permafrost basins indicate that higher proportions of rainfall leave the basins via the channel networks during the storms in which it fell and appear as direct runoff in the initial response hydrographs. In non-permafrost basins, less precipitation reaches the streams during the initial response hydrographs and large proportions of rainfall may enter long-term storage as groundwater. This water may appear in the streams later as baseflow. Consequently, regardless of the respective time bases of the response hydrographs, the influence of storms in non-permafrost basins last longer due to their contributions to baseflow. Consequently, a key difference in annual hydrographs between the two basin types is that given similar precipitation regimes, non-permafrost basins have higher ratios of baseflow to stormflow than permafrost basins. Hence, in non-permafrost basins it is primarily baseflow that is translated downstream, whereas in permafrost basins it is primarily stormflow that is translated downstream.

Baseflow has a moderating effect on the variability of hydrographs. Hence, as baseflows are accumulated downstream, the moderating effect will be enhanced and the variability of streamflow will decrease. Due to the high peaks and low baseflows characteristic of permafrost basins, a higher range of flows is translated downstream

for a given storm with the absence of moderating baseflows. Hence, the variability of headwater storm hydrographs will be maintained downstream.

We acknowledge that the preceding explanation lacks justification in its present state. However, we offer it as an impetus to launch further investigations into the regional differences in the scaling of streamflow.

6.6 Summary

We have shown that rainfall generated streamflow in the permafrost dominated Kuparuk River basin and flood peaks in other arctic rivers obey simple scaling. This is a significant deviation from other studies that have shown that in other regions, rainfall generated flows are multiscaling. Essentially, significant differences exist in the nature of spatial variability of streamflow between arctic and temperate basins. The nature of downstream discharge variability is the product of the controls on the characteristics of upstream hydrographs. We have suggested that the regional scaling differences may result from the differences in the characteristics of headwater response hydrographs due to the presence or absence of permafrost. For example, in permafrost basins, stormflow hydrographs are translated downstream without the moderating effect of baseflows from other contributing basins. Hence, the variability is maintained downstream. In non-permafrost basins, stormflow hydrographs are smoothed by baseflows from other contributing basins as they accumulate downstream. Hence, the variability decreases downstream. More studies in different regions are needed to further our understanding of the connections between rainfall, landscapes, and scaling of streamflow.

Chapter 7

A Geomorphologic Analysis of an Arctic Drainage Basin using Digital Elevation Models

7.1 Abstract

Fundamental differences exist between basins with and without permafrost in the nature and scaling of hydrologic processes. Since hydrologic response is sensitively adjusted to drainage basin form, we suspected that further differences may exist in the spatial organization of drainage basins with permafrost. Using digital elevation models (DEMs), we explored the hillslope/channel scaling regimes, the spatial distribution of mass, and the fractal characteristics of channel networks in the Kuparuk River basin in Northern Alaska. Fractal analysis and field mapping show that the imprint of a rudimentary channel network was initially laid down as water tracks on the hillslopes. However, flow path aggregation patterns in the water track networks do not possess certain universal characteristics common to channel networks in other regions. We suggest that permafrost has prevented the erosional development of mature channel networks, and the drainage basins have been frozen in an immature state.

7.2 Introduction

The form and function of the fluvial environment reflects a landscape's response to the prevailing climate. Since pattern and process are closely connected, perhaps hidden in the scaling of landscape patterns are clues to how hydrologic processes vary across scales. Hence, a quantitative description of drainage basin form, and the scaling properties therein, provides essential information to the understanding

and prediction of hydrologic fluxes from the plot to the basin scale. The purpose of this paper is to provide a quantitative description of the Kuparuk River basin in Northern Alaska using digital elevation models (DEMs) to improve our understanding of basin controls on the hydrologic response in arctic regions.

The advent of DEMs has allowed an unprecedented capability to explore the spatial organization of landscape patterns and the controlling processes over a broad range of scales. Consequently, a surge of research concerning the scaling of landscape form has produced a new suite of descriptive parameters that relate patterns and processes across scales. Foremost among these is the fractal dimension (Mandelbrot, 1982). The use of DEMs fostered the first observations that fluvial channel networks possess fractal characteristics (Tarboten et al., 1988; La Barbera and Rosso, 1989). The term "fractal" implies that an object or pattern has self-similar or self-affine properties. Self-similar means that parts of an object are identical to the whole, and self-affine means that parts of an object resemble systematically squashed or stretched versions of the whole. This implies that channel networks possess a deep sense of similarity that transcends geologic controls. Rodriguez-Iturbe et al. (1992b) analyzed the distribution of discharge using DEMs and discovered that all rivers share a common distribution function. deVries et al. (1994) showed that this commonality is related to the fractal nature of channel networks. Ideal fractals display similarity across an infinite range of scales, which is rarely seen in nature. Instead, fractality commonly has scale boundaries, and the ranges of fractality can be used to decipher characteristic scales and thresholds at which physical processes operate.

Perhaps the most significant result from this surge in research concerning the scaling of drainage basins has been the quantitative affirmation of the commonality of drainage basins from all geologic and environmental conditions. Indeed, these concepts have contributed to the development of a new theory of drainage basin evolution wherein chance and the rules of optimum energy expenditure control the structure of drainage networks (Rodriguez-Iturbe et al., 1992a, 1994). Optimal channel networks (OCNs) developed under such principles exhibit fractal characteristics identical to natural channel networks (Marani et al., 1991; Rigon et al., 1993; Rinaldo et al., 1992; Rodriguez-Iturbe et al., 1992a). Rinaldo et al. (1993) suggested that this arises from the idea that channel networks evolve to a state of self-organized criticality (SOC). SOC means that dissipative, spatially extended, dynamical systems (rivers) naturally evolve to critical states (states that lack intrinsic spatial or temporal scales) despite the initial conditions (self-organized) (Bak et al., 1987 and 1988). Rinaldo et al. (1992) and Rigon et al. (1993) suggested that this SOC in river basins is maintained by the interplay of hydrologic processes operating at different scales. Thus, it appears that the scaling of hydrologic response is somehow linked to the fractal characteristics of drainage basins. These are significant advances towards establishing long needed theoretical connections between the spatial variability of hydrologic processes and landscape form for which hydrologists often work with unjustified empiricisms.

We are seeking such connections in the Kuparuk River basin in Northern Alaska. The presence of permafrost imposes significant influences on the form and hydrologic response of drainage basins in the Arctic. For example, McNamara et al.

(1997a) showed that the shallow, hydrologically active soil layer in permafrost basins, called the active layer, exerts important controls on the response of streams to precipitation inputs. Further, McNamara et al. (1997c) showed that there are significant differences between arctic and temperate regions in the scaling of rainfall generated streamflow, which can be attributed to the influence that permafrost has on runoff generation.

Since fundamental differences exist in hydrologic response between basins with and without, we suspected that further differences are manifested in the spatial organization of drainage basin form. For example, the erosional development of fluvial channel networks may be altered by the presence of permafrost, which would affect the organization and scaling of mass and energy distribution in the basin. One physical consequence of permafrost is the presence of water tracks that convey water off hillslopes (Hastings et al., 1989). Water tracks are essentially zones of enhanced soil moisture where flow is directly downslope. They typically do not have incised channels, but are integral components of the basin hydrology. Hillslope flowpaths transport mass and energy differently than do fluvial channel networks. An interesting geomorphologic problem, and a practical modeling problem, is whether water tracks belong to the hillslope or channel regime. By examining distributions of mass and energy through DEMs, we can infer the function of water tracks in the drainage basin.

The objectives of this paper are to provide a quantitative geomorphologic description of the Kuparuk River basin using DEMs, to investigate the role of hillslope water tracks in the structure of drainage basins, and to determine if this permafrost-

dominated basin possesses the same organizational characteristics common to basins without permafrost. We evaluate the transition in scaling regimes between hillslope and fluvial processes by examining the relationships between local slope and drainage area (Tarboten et al., 1992; Montgomery and Foufoulo-Georgiou, 1993), the spatial distribution of mass and energy dissipation in the basin (Rodriguez-Iturbe et al, 1992a), and the structure of the channel networks using fractal analysis (Claps and Oliveto, 1996; La Barbera and Rosso, 1989, 1990; Tarboten et al., 1988, 1990).

7.3 Study Area

Chapter two contains a detailed site description. Additional information is necessary to support this chapter. Two basins in the headwaters of the Kuparuk River in Northern Alaska were used in this study, the Upper Kuparuk River (drainage area = 142 km^2), and Imnavait Creek (drainage area = 2.2 km^2). Figure 7.1 shows a topographic map of the Upper Kuparuk River basin. The main basin length is 16 km, with a channel length of 25 km that occupies a valley bottom approximately 1.5 km wide. Expansive, relatively undissected valley walls with fairly consistent slopes extend the length of the basin, with ridgelines that are approximately 9 km apart. The expansive valley walls on Figure 7.1 show very few crenulations which would indicate the presence of streams. However, Figure 7.2 is a photograph that shows an abundance of hillslope water tracks. At the intersection with the Dalton highway, the Upper Kuparuk River is a fourth order stream on a USGS 1:63360 map, but the hillslopes and tributary valleys contain a complex network of water tracks and rocky headwater streams that do not appear on maps at that scale.

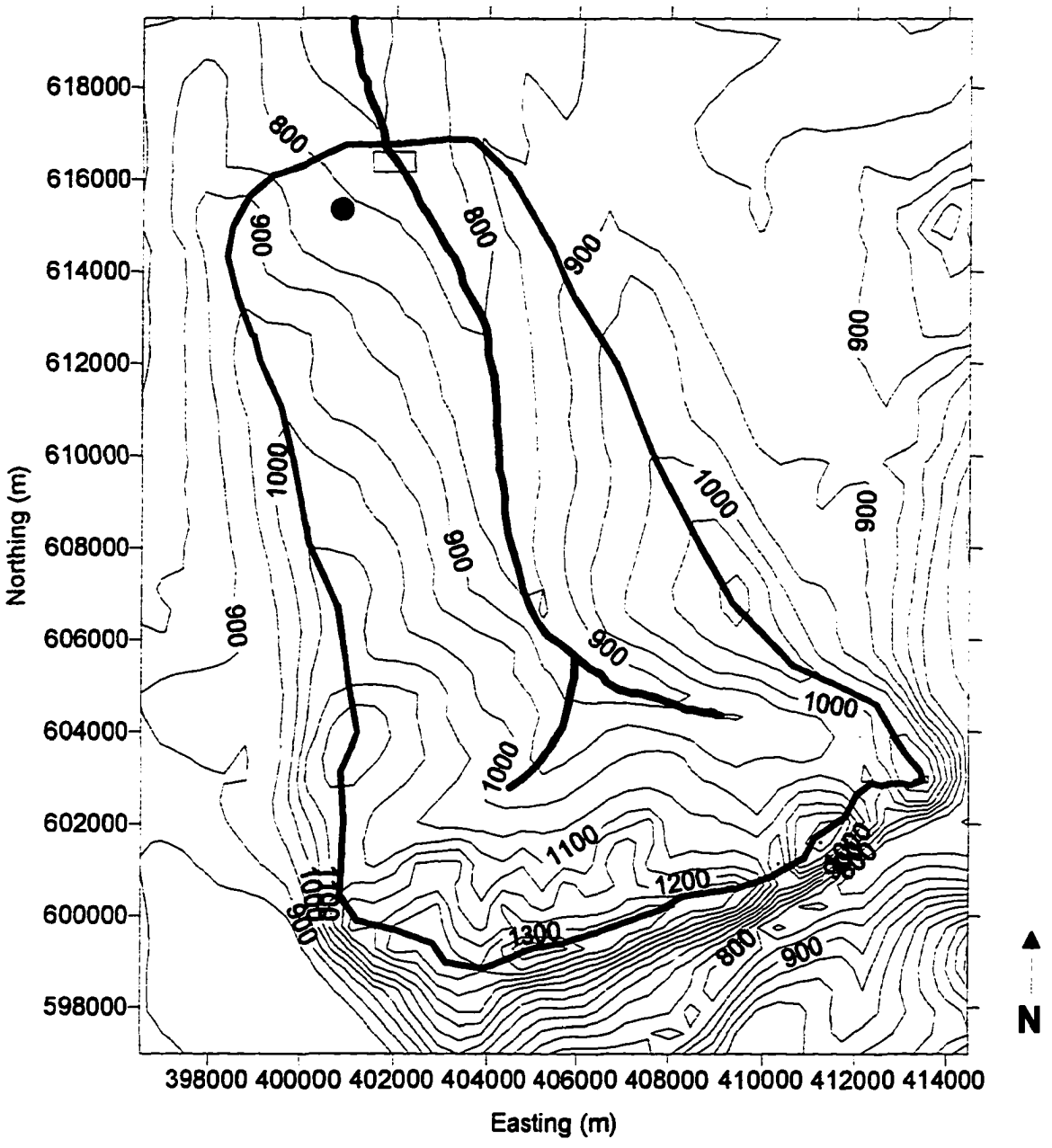

Figure 7.1. Topographic map of the Upper Kuparuk River Basin at a 50 m contour interval.

= Gauging station = meteorological station

= main stream channel = watershed boundary

Imnavait Creek is a small beaded stream occupying a north-northwest trending glacial valley adjacent to the Upper Kuparuk River. Figure 7.3 shows a topographic map of the Imnavait Creek basin at a 5 m contour. Again, notice the lack of crenulations on the hillslopes indicating very little incision, despite the dense network of water tracks.

7.4 Review

7.4.1 Slope-Area Scaling

Slope-area scaling of the form

$$S \sim A^{-\theta} \qquad (7.1)$$

has long been recognized in fluvial geomorphology where S is channel slope, A is drainage area, and θ is a scaling exponent typically between 0.2 and 0.6 for stream channels (Flint, 1974). Recent studies have investigated this relationship in terms of the scaling characteristics and aggregation patterns of drainage networks (Tarboten, 1991, 1992; Willgoose et al., 1991; Gupta and Waymire, 1989). Equation 7.1 can not hold ad infinum as it implies an infinite slope as the drainage area approaches zero. There is a lower bound to Equation 7.1 where the channel network gives way to the hillslopes, and hence a change in the scaling regime exists. Flow on the hillslopes is diffusive, and erosive powers act to smooth irregularities. Flow in the channels is advective, and erosion further incises channels. Consequently, the channel head (furthest upslope extent of the boundary between hillslope and stream) represents an important threshold in the manner in which mass and energy are exported.

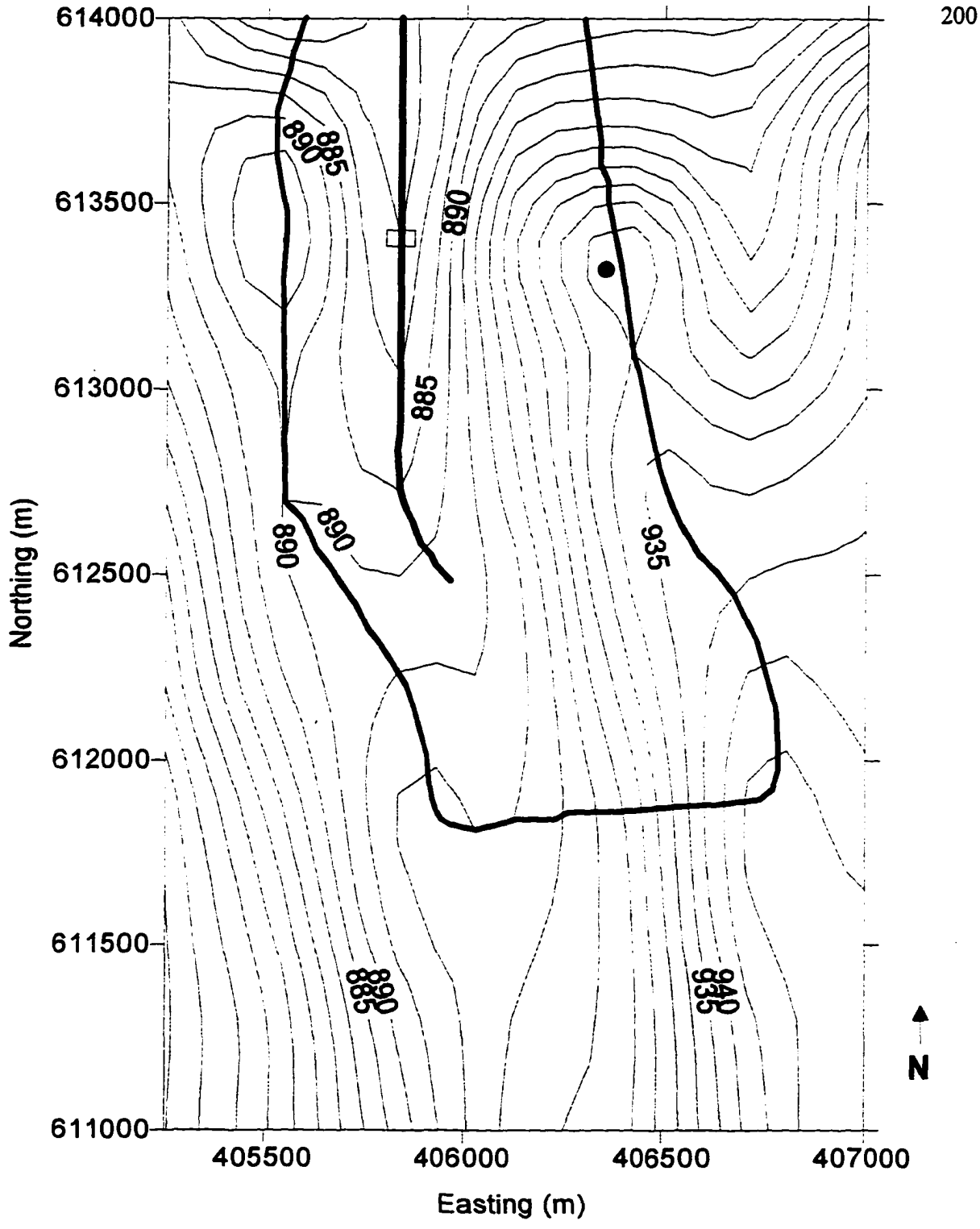

Figure 7.3. Topographic map of the Imnavait Creek basin at a 5 m contour interval.

= Gauging Station. = Meteorological station.

= main stream channel = watershed boundary

The most commonly used method to represent channel heads in a channel network model is to select a threshold drainage area below which channels will not occur, called the channel support area. The channel support area can be estimated from the relationship between local slope and drainage area. Tarboten et al. (1992) used the hillslope stability criterion proposed by Smith and Bretherton (1972) to show that diffusive sediment transport occurs when dS/dA is positive, and advective transport occurs when dS/dA is negative. According to Tarboten et al. (1992) the erosive power of runoff is related to a hillslope's resistance to erosion by

$$A\frac{\partial F}{\partial S}\frac{dS}{dA} = A\frac{\partial F}{\partial A} \qquad (7.2)$$

where F is the sediment flux, A is the upstream drainage area, and S is the local slope. If the right side of Equation 7.2 is negative, small perturbations grow into channels. If the right side of Equation 7.2 is positive, small perturbations do not grow and the landscape remains unchanneled. The only way for the left side of Equation 7.2 to be negative is in the dS/dA term. Therefore, a slope reversal in a plot of local slope against drainage area should occur at the transition from unchanneled to channeled regions. The drainage area at that slope reversal should equal the minimum drainage area required before channels can form.

However, Montgomery and Dietrich (1992) showed that channel support areas are not constant within a basin, but depend on local slope. They reported empirical relationships between slope (S) and threshold area (A_{th}) of the form $A_{th} = CS^{-\beta}$, where C and β are constants empirically determined from field data. Consequently,

Montgomery and Foufoulo-Georgiou (1993) argued that it is not appropriate to assign one drainage area to represent the initiation threshold for all channels in a basin. They suggested that the slope reversals on slope-area plots described by Tarboten et al. (1992) do not represent where channels will occur, but represent the transition from convex to concave landscapes, or the transition from hillslopes to unchanneled valleys, and that channels will initiate in the valleys somewhere downslope depending on the slope.

Ijjasz-Vasquez and Bras (1995) proposed a method to derive slope-dependent channel support areas entirely from slope-area plots. They showed that four distinct scaling regimes, as opposed to two identified by Tarboten et al. (1992), exist on slope-area plots. In the first region, dS/dA is positive. In the second, dS/dA is negative. This reversal is the channel support area described by Tarboten et al. (1992). In region three, dS/dA is still negative, although much less. In region four, dS/dA returns to a large negative value. According to Ijjasz-Vasquez and Bras (1995), region four represents the regime where channels can exist. Region three represents the transition where channel heads occur between unchanneled valleys and the channel network. They suggested a technique for separating channeled and unchanneled locations by constructing a quadrilateral around region 3. The line connecting the upper left and lower right corners of the quadrilateral is the slope dependent drainage area threshold for channel initiation. The threshold line has the form $S=KA^{-\theta}$. Channels occur at locations above the threshold line, or when $S> KA^{-\theta}$.

7.4.2 The Fractal Nature of Channel Networks

Several studies have shown that channel networks possess fractal characteristics (Beer and Borgas, 1993; Claps and Oliveto, 1996; LaBarbera and Rosso, 1989, 1990; Nikora, 1994; Tarboten et al., 1988, 1990). The fractal dimension (D) describes how a measure, say length L, changes with a scale transformation, say ruler size r:

$$L \sim r^D \tag{7.3}$$

Solving for D yields

$$D \sim \log(L)/\log(r) \tag{7.4}$$

Thus, the fractal dimension represents the ratio between the log-value of a measure and the scale at which it was measured. It is said that L scales with r by the scaling exponent D.

In conventional geometry, D is either one, two, or three. For example, the measured length of a finite straight line, D=1, is independent of the actual size of the ruler, and is simply the number of steps the ruler must take times the measure of the ruler. As the ruler decreases in size, the number of steps increase linearly and the measured length remains the same. However, some objects, constructed and natural, can not be classified by the conventional dimensions. The measured length of a self-similar curve depends upon the size of the ruler. As the size of the ruler decreases, L increases non-linearly with r. The exponent D then takes on non-integer values, hence the term "fractal". Conceptually, the fractal dimension can be viewed as the dimension

in which the measure is independent of the size of the ruler. Its deviation from the conventional dimension is an indicator of complexity (DeCola and Lam, 1993).

Several empirical relationships in fluvial geomorphology have the form of Equation 7.3. Perhaps the most famous, due to the attentions of Mandelbrot (1982), is the relationship between mainstream length (L) and drainage basin area (A):

$$L=aA^m \qquad (7.5)$$

where a and m are empirical parameters. Hack (1957) reported a value of m=0.6 in the Shenandoah Valley. Gray (1961) compiled the measures of 47 rivers and determined that m is approximately 0.568. Dimensional analysis of Equation 7.5 suggests that m should equal 0.5. Mandelbrot (1982) suggested that the anomalous value of m is due to the fractal nature of rivers, and thus launched a flurry of research concerning the fractality of rivers. He suggested that the fractal dimension of a river channel is D = 2 * m = 1.1 to 1.2, and further suggested that the branching channel network is space-filling and takes on the dimension of a plane, D = 2.

Several direct and indirect methods have emerged to calculate the fractal dimension of channel networks. A computationally simple technique is functional box counting, a two dimensional version of the ruler method discussed above (Feder, 1988; Mandelbrot, 1982; Rosso et al., 1991; Tarboten et al., 1988). A grid is imposed on the channel network with four quadrants of size r. The number of boxes N required to cover the network is calculated. Then each quadrant is itself divided into quadrants and again the number of boxes required to cover the network is computed. This

continues down to the resolution of the grid, and the fractal dimension is the slope of the plot of log N against log r, or

$$D=\log(N)/\log(r) \tag{7.6}$$

which is identical to Equation 7.4.

Horton (1933, 1945) recognized the self-similar nature of river networks decades before fractal concepts were introduced to the scientific community, and formulated a set of similarity numbers that collectively became known as Horton's laws of drainage network composition. When a channel network is ordered according to Horton (1945) or Strahler (1952), the following ratios can be calculated:

$$R_b = \frac{N_{w-1}}{N_w} \tag{7.7}$$

$$R_l = \frac{L_w}{L_{w-1}} \tag{7.8}$$

$$R_a = \frac{A_w}{A_{w-1}} \tag{7.9}$$

where R_b, R_l, and R_a are the bifurcation ratio, length ratio, and area ratio respectively, N_w, L_w, and A_w are the number of streams, the mean length of streams, and the drainage area of order w. When Horton's laws hold true, R_b, R_l, and R_a plotted against stream order produce straight lines. Hence, Horton's numbers are geometric scaling laws. Tarboten et al. (1988) and La Barbera and Rosso (1989) recognized the connection between Horton's numbers and the self-similarity embodied in Equation 7.4, and independently derived the fractal dimension in terms of Horton's numbers as

$$D = \log(R_B)/\log(R_L), \text{ if } R_B > R_L \qquad (7.10)$$

However, Phillips (1993) suggested that calculating the fractal dimension by Horton's laws may be prone to error due to the faulty assumption that Horton's laws hold true at all scales.

Tarboten et al. (1988) used several methods including functional box counting and Hortonian analysis, and determined that the fractal dimension of mature networks should be 2, as Mandelbrot (1982) suggested. Mandelbrot's logic was that if a river is to completely drain a basin, it must penetrate everywhere. By walking the banks of a river keeping the river always to one side, one performs a plane-filling motion. Hence, the dimension should be 2. However, La Barbera and Rosso (1989) used Equation 7.10 and estimated D values around 1.6 to 1.7. Tarboten et al. (1990) reasoned that this was because Equation 7.10 does not account for the fractal nature of individual stream reaches, which is most commonly around 1.1, and suggested by combining the two fractal dimensions, the true fractal dimension of 2 is revealed. La Barbera and Rosso (1990) countered that 2 is a limiting case, and that the fractal dimension of channel networks varies between 2 and unity, depending on the landscape. Claps and Oliveto (1996) determined that D is typically around 1.7, similar to the results of La Barbera and Rosso (1989, 1990).

Phillips (1993) stated that Horton's laws only apply if they hold true for all scales, which is rare, and suggested that using Horton's laws to calculate the fractal dimension of a channel network is prone to error. He used Equation 7.10 to calculate the fractal dimension of 50 third order drainage basins and over a third had D values

greater than 2, which is impossible. In addition, Philips (1993) argued that a fractal dimension of 2 for channel networks is unrealistic in nature. If the network does indeed drain the entire basin, then the fractal dimension should be 2. However, this would require that self-similarity of the channel network holds at all scales, or that closer and closer inspection a fractal channel network should show more and more channels yielding an infinite length of streams. However, we know that there is a finite lower limit to channel networks (Montgomery and Dietrich, 1988, 1992). This lower limit of the channel network is called the drainage density, which is the total length of streams divided by the drainage area. The suggestion by Mandelbrot (1982) that a channel network must penetrate everywhere in order to drain a basin does not distinguish between hillslope flow paths and incised channels. The drainage density represents a lower boundary to the range of scales for which channel networks can exhibit fractal characteristics, and the fractal dimension of a channel network should be somewhat less than 2. Tarboten et al. (1992) proposed that this lower boundary corresponds to the shift in scaling regimes on slope-area plots discussed above.

If D = 2 is a theoretical upper limit representing an ideal space filling channel network, what is the meaning of a fractal dimension less than 2? La Barbera and Rosso (1989) and Phillips (1993) contend that the fractal dimension reflects the degree to which the network is constrained by geologic factors, where D = 2 implies an unrestrained basin. Thus, we can infer the controls that a landscape imparts on the evolution of a channel network.

7.4.3 Spatial Distribution of Mass and Energy

Rodriguez-Iturbe et al. (1992a, 1992b) suggested that a river network is an open, dissipative system with constant injection of mass that evolves to a state of self-organized criticality, and that adjusts its three dimensional structure so that the average energy dissipation per unit area within a basin is constant everywhere. Their evidence was that there are apparent universalities in the spatial distributions of mass (discharge) and energy expenditure for all basins. They showed that the cumulative probability of any point in a fluvial channel network having a mass M larger than m scales according to

$$P[M>m] \propto m^{-\beta} \tag{7.11}$$

where the exponent, β, is consistently near 0.45. Similarly, the distribution of energy has an exponent consistently near 0.9. Equation 7.11 is a cumulative area distribution and measures the degree to which flow paths converge (Moglen and Bras, 1994). Hence the universal exponents observed by Rodriguez-Iturbe et al. (1992b) likely result from a common underlying principle governing the aggregation patterns of fluvial networks. Moglen and Bras (1994) showed that cumulative area distributions can also be applied to hillslopes, and that a distinct change in the value of the exponent occurs between the channel and hillslope regimes, which indicates a change in the patterns of flow aggregation between hillslopes and channel networks.

Rinaldo et al. (1992) developed optimal channel networks (OCNs) under the principles that channel networks arrange themselves to minimize energy expenditure, and showed that they possess the same exponents in Equation 7.11 as the real

networks reported by Rodriguez-Iturbe et al. (1992a). OCNs also display fractal characteristics identical to real networks. Thus, Rodriguez-Iturbe et al. (1992a) suggested that the universal values of β may arise from the fractal nature of channel networks. deVries et al. (1994) derived a relation between the exponent β and the topological fractal dimension D_t of ideal channel networks. They showed that $\beta = 1-(1/D_t)$. Assuming that $D_t = 1.8$ (Tarboten et al., 1988), results in $\beta = 0.44$, which is remarkably close to the empirical values reported by Rodriguez-Iturbe et al. (1992a). The apparent universality of β, its relation to fractality of the drainage basin, and the favorable comparison to OCNs suggests that fluvial channel networks evolve to a common state of self-organizing criticality.

7.5 Data Structure and Analysis

North Pacific Arial Surveys from Anchorage, Alaska provided digitized elevation contours at 5 m contour intervals from aerial photographs of the Imnavait Creek basin. We then kriged the contour data to produce a 10 m resolution DEM. We produced a 100 m resolution DEM of the Upper Kuparuk River basin by kriging a U.S.G.S 90 m resolution DEM of the Philips Smith Mountains topographic map.

Several methods exist for extracting drainage basin features from DEMs (see for example, Band, 1986; Chorowitz et al., 1992; Fairfield and Leymarie, 1991; Freeman, 1991; Jenson and Domingue, 1988; Mark, 1984; Martz and deJong, 1988; Meisels et al., 1995; Morris and Heerdegen, 1988; and O'Callaghan and Mark, 1984). A commonly used method for drainage network extraction is the D8 method in which

flow paths are identified from each node by comparing the elevation of the node to the elevations of the surrounding nodes (O'Callaghan and Mark, 1984). One flow path originates from each node directed toward its steepest neighbor so that a flow path network connects every point in the basin at the resolution of the DEM data. Recently, multiple flow direction algorithms have been developed that assign flow paths from a node to each of its downslope neighbors weighted according to slope (Freeman, 1991; Quinn et al. 1991). In both techniques, drainage areas at each node are calculated by summing the total number of nodes that contribute flow to that node. Wolock and McCabe (1995) compared single flow direction and multiple flow direction algorithms and showed that multiple flow direction algorithms are superior for capturing the spatial variability of geomorphologic features.

Both single flow direction and multiple flow direction algorithms produce a network with flow originating from every node in the source file. Somewhere in this network is a transition from hillslope flow paths to fluvial channels. The most common method of extracting the true channel network from a DEM is to specify a minimum upstream drainage area, called a channel support area, that is required to initiate a channel. Various methods have been devised to determine the threshold drainage area for channel initiation (Morris and Heerdegen, 1988; Jenson and Domingue, 1988; Tarboten et al., 1991, Chorowitz et al., 1992, 1993; Montgomery and Foufoulo-Georgiou, 1993). Flow paths with drainage areas less than the threshold area are designated as hillslope flow paths and the remainder are channels. Recently, new methods have been developed to recognize channel heads strictly from the DEM

contours without inferring the physical processes involved in channel head formation (Meisels et al, 1995; Tribe, 1992) These methods offer the advantage of removing the subjectivity in determining channel support areas.

In this study, we used a collection of FORTRAN codes called DRCHAN, written by the author, to extract information from DEMs. DRCHAN uses a multiple flow direction D8 algorithm similar to Quinn et al. (1991). After the initial identification of flow paths, DRCHAN fills artificial depressions by a flooding routine until flow spills to the lowest surrounding point completing all flow paths to basin outlets at the domain boundaries. Each flow path from one node to another forms a flow segment, and the top coordinates, bottom coordinates, drainage area, and slope of each flow segment are written to a file. A second algorithm arranges the flow segments into a flow path network by matching the bottom coordinates of a segment to the top coordinates of its downslope continuation until all nodes drain to an outlet at the edge of the DEM file. Each outlet is assigned a number, and every flow segment is coded according to their outlet so individual basins can be isolated for analysis. The channel networks are then distinguished from hillslope flow paths by assigning a channel support area below which channels can not occur (Tarboten et al., 1992). After the channel network is identified, the network is characterized by the Horton/Strahler stream order scheme (Strahler 1952, 1957). Individual streams, defined as the reach between changes in Strahler order, are identified and their coordinates, slopes, lengths, stream orders, and stream magnitudes are stored. Similar details are recorded for stream links, defined as the reach between any two stream

junctions. From this information, Horton's numbers can be determined. Additional algorithms calculate the probability distributions of slope, area, and energy dissipation, and the fractal dimension of channel networks by functional box counting.

7.6 Results and Discussion

Local slopes and drainage areas were calculated for every point in the Imnavait Creek and Upper Kuparuk River basins at 10 m and 100 m resolution respectively. To reduce scatter on slope-area plots, local slopes were sorted by drainage area. Each point on Figures 7.4a and 7.5a represents the average of every 50 sorted slopes. The slope-area plot for Imnavait Creek (Figure 7.4a) appears similar to those described by Ijjasz-Vasqez and Bras (1995). However, there appears to be a fifth region at the high drainage areas. In region 1, ds/da is positive and is therefore the unchanneled hillslope regime. At 0.0032 km^2, ds/da becomes negative. This transition is clearly the reversal in slope that Tarboten et al. (1992) credited as the transition between diffusive and advective sediment transport, and the average drainage area required to form channels. Field surveys using a GPS accurate to 1 m showed that the heads of the eight largest water tracks in Imnavait Creek had an average contributing area of 0.0028 km^2 , which is reasonably close to the drainage area at the slope reversal in Figure 7.4a. Thus, water tracks are positioned in the basin where channels should occur, according to the logic of Tarboten et al. (1992). However, recall that Montgomery and Foufoulo-Georgiou (1993) argued that the slope reversal in a slope-area plot represents only the valley network, and that incised channels begin somewhere downslope in the valleys dependent upon local slope.

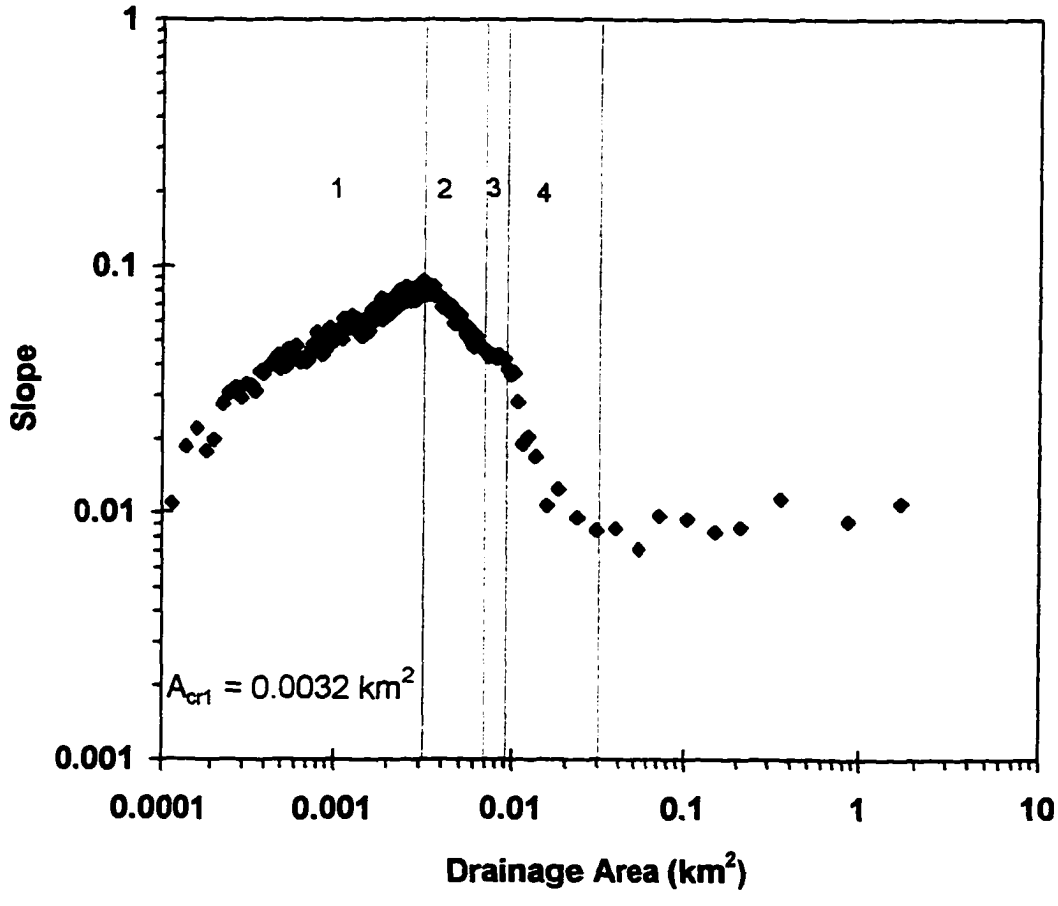

Figure 7.4a. Slope-area plot for Imnavait Creek, 10 m resolution DEM. The numbered regions correspond to the regions described by Ijjasz-Vasquez and Bras (1995),

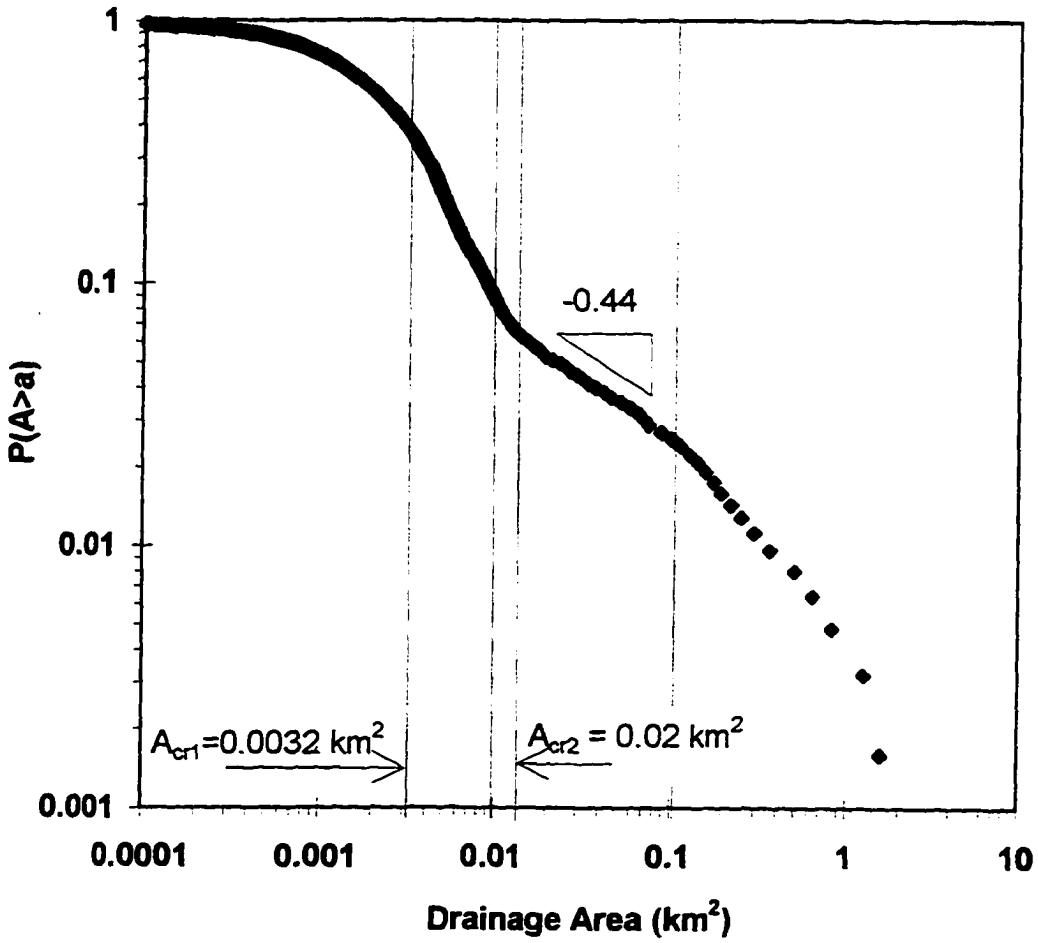

Figure 7.4b. Cumulative probability distribution of drainage areas in the Imnavait Creek basin from a 10 m resolution DEM. Critical drainage areas occur at 0.0032 km^2 and 0.02 km^2.

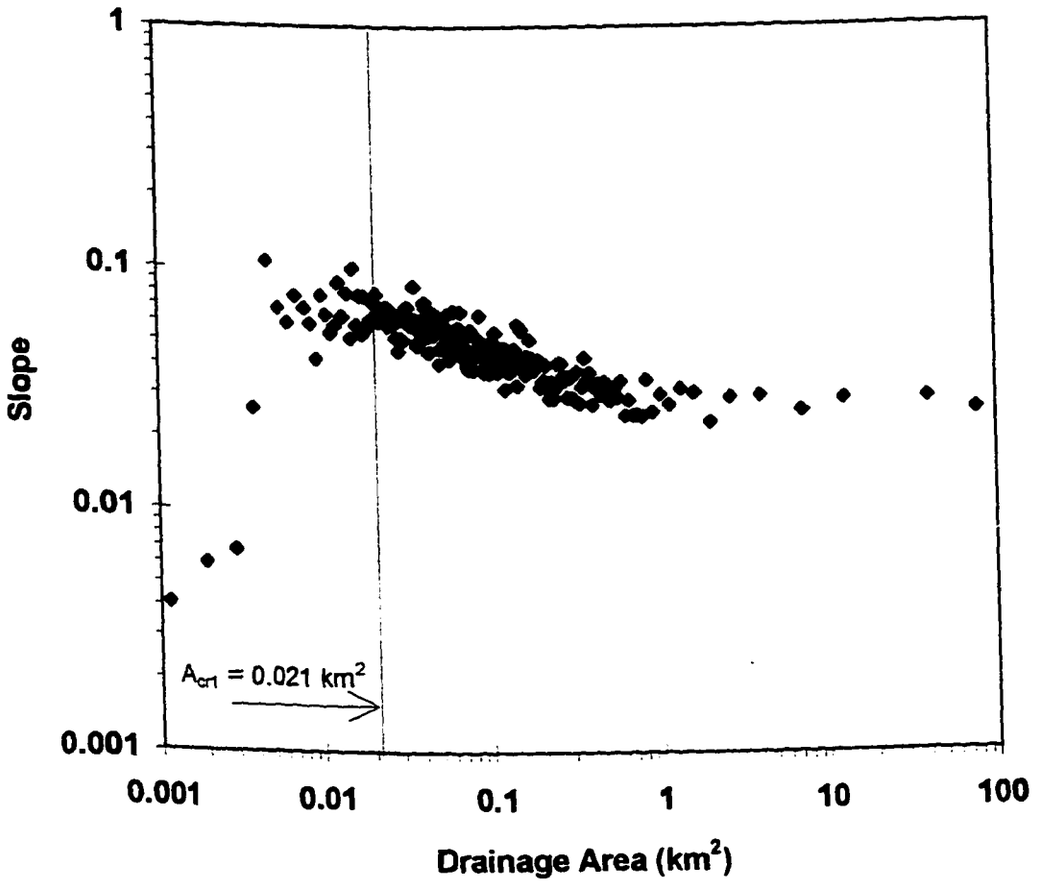

Figure 7.5a. Slope-area plot for the Upper Kuparuk River basin 100 m resolution DEM. A critical drainage area occurs at 0.021 km^2.

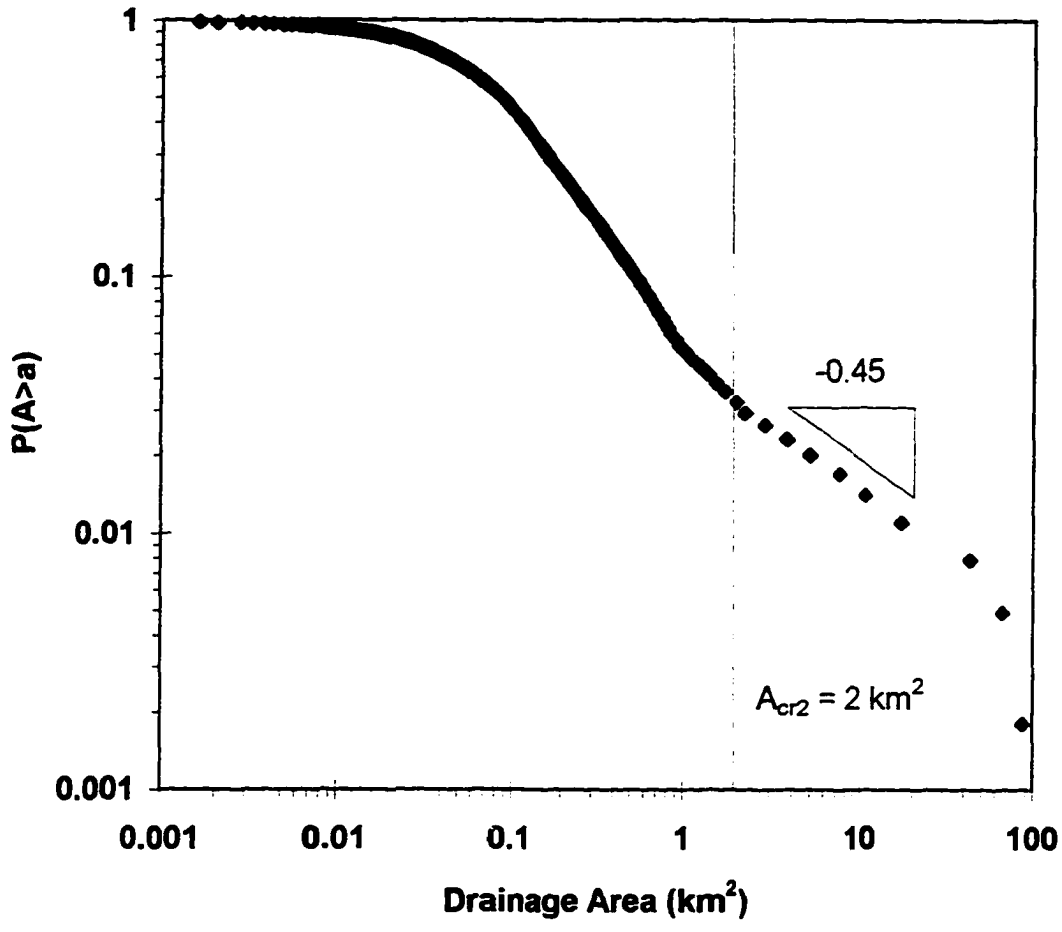

Figure 7.5b. Cumulative probability distribution of drainage areas in the Upper Kuparuk River basin from a 100 m resolution DEM. A scaling transition occurs at 2 km^2.

According to the technique of Ijjasz-Vasquez and Bras (1995), the transition between the hillslope and channel regimes begins in region three, and is completed at the beginning of region four. Region four begins at approximately 0.009 km^2 in the Imnavait Creek basin, and a final change in slope that was not identified by Ijjasz-Vasquez and Bras (1995) begins at approximately 0.03 km^2. However, Figure 7.4b shows a significant transition occurs in the aggregation pattern of flow paths within this final region. At approximately 0.02 km^2, the exponent in the power law function of the cumulative area probability distribution becomes -0.44. Recall that Rodriguez-Iturbe et al. (1992b) reported that a slope on a log-log plot of -0.45 appears to be universal for well developed fluvial channel networks. Therefore, the organization of flow paths at drainage areas to the right of the break in slope on Figure 7.4b possess aggregation patterns common to other fluvial channel networks, and the drainage areas to the left represent the unchanneled hillslope regime. Figures 7.4a and 7.4b suggest that the fluvial channel network in the Imnavait Creek basin begins at a minimum drainage area between 0.01 km^2 and 0.03 km^2. This range in drainage areas approximately brackets the drainage areas at the bottom of the hillslope water tracks, or the transition from the valley walls to the valley bottom. This coincidence suggests that the minimum scale of the fluvial channel network occurs in the main valley bottom, and excludes the hillslope water tracks.

There is a change in the cumulative area distribution on Figure 7.4b at a drainage area coincident with the slope reversal on Figure 7.4a at 0.0032 km^2. That the field mapped drainage areas at the tops of water tracks closely matches this critical

area suggests that there is indeed a change in the organization of flow at the water track scale, but it does not resemble fluvial channel networks. The slope reversal at 0.0032 km^2 likely represents the transition from divergent to convergent topography and is the extent of the unchanneled valley network as suggested by Montgomery and Foufoulo-Georgiou (1993). Thus, there appears to be three different scaling regimes in the flow paths in the Imnavait Creek basin with each exhibiting different aggregation patterns: 1) the hillslope regime at drainage areas less than 0.0032 km^2, 2) the water track regime between 0.0032 and 0.02 km^2, and 3) the fluvial channel regime at drainage areas greater than 0.02 km^2.

Figure 7.5a shows the slope-area plot for the Upper Kuparuk River at 100 m resolution. The slope reversal between regions 1 and 2 discussed above occurs at approximately 0.02 km^2. The distinctions between regions 2, 3, and 4 as discussed by Ijjasz-Vasquez and Bras (1995) are not apparent on Figure 7.5a. This may be a result of data resolution.

The cumulative area plot for the Kuparuk River (Figure 7.5b) shows a similar trend to Figure 7.4b, although shifted to higher drainage areas. Again, there are three distinct regimes, each corresponding to a change in the slope on the slope-area plot (Figure 7.4a). Again, the slope of the cumulative area distribution in the final regime, -0.45, is similar to what Rodriguez-Iturbe et al. (1992b) reported to be universal for fluvial channel networks. However, the transition to that regime begins at approximately 1 km^2, and is not completed until approximately 2 km^2. On Figure 7.5a, a break in slope occurs near that region as well. Thus the flow patterns in the Upper

Kuparuk River basin exhibit features similar to fluvial channel networks beginning at drainage areas between 1 and 2 km^2. Above 2 km^2, very little change occurs in slope with increases in drainage area. This range of drainage areas is approximately coincident with the drainage areas at the transition from the valley walls to the main valley bottom. Thus, the patterns of flow aggregation common to fluvial channel networks excludes the hillslope water tracks, as was observed in Imnavait Creek.

The above results show that two potential channel support areas exist, one from slope-area scaling and one from cumulative area distribution. If we use the channel support area that occurs at the first slope reversal on slope-area plots (Figures 7.4a and 7.5a) as suggested by Tarboten et al. (1992), the resulting channel networks are shown in Figures 7.6a and 7.6b. The main valley bottom channels show up nicely. However, notice that the hillslopes have downslope flowpaths spaced at the resolution of the data flowing directly down the slopes. Essentially, there is very little convergence of flow paths or valley dissection on the hillslopes. The fractal dimension of the Imnavait Creek network is 1.69 by functional box counting (Figure 7.7a). Tarboten et al. (1990) stated that the true fractal dimension is obtained by multiplying by 1.1 to take into account the sinuosity of the individual stream channels. This would result in a fractal dimension of 1.86. Notice that the log-linear fit breaks down at box sizes smaller than approximately 50 m, or 2500 m^2, which is reasonably close to the channel support areas predicted by Figures 7.4a and 7.4b. For the Upper Kuparuk River, the fractal dimension is 1.82 using functional box counting (Figure 7.7b). The functional box counting result multiplied by 1.1 results in D=2.0, precisely the value

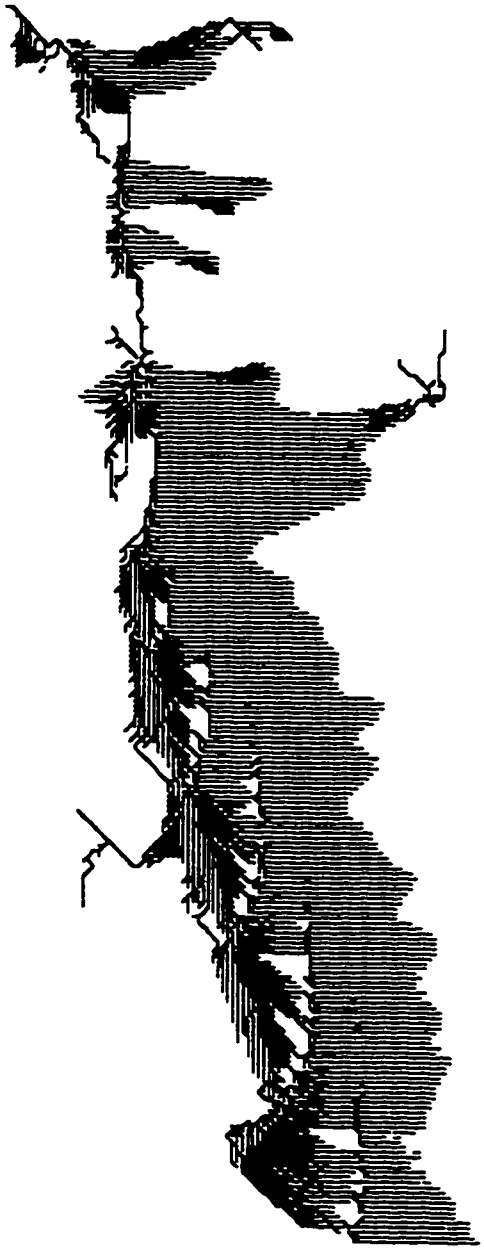

Figure 7.6a. Flow path network of Innavait Creek using a channel support area of 0.0032 sq-km.

Figure 7.6b. Flow path network of the Upper Kuparuk River basin using a channel support area of 0.02 sq-km.

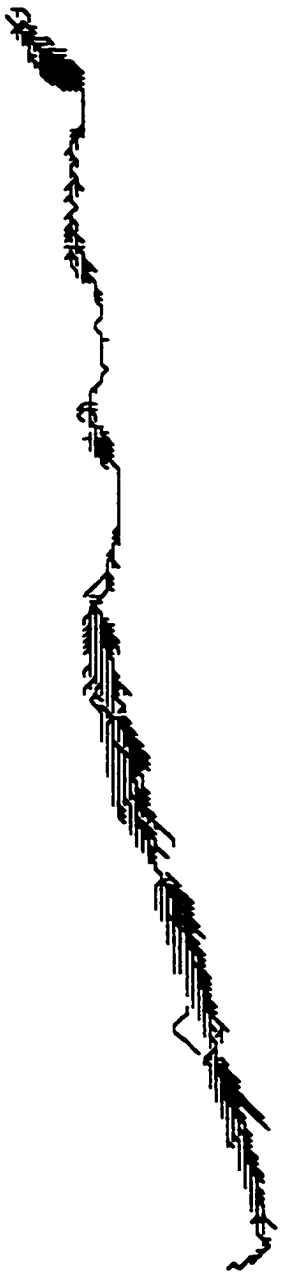

Figure 7.6c. Flow path network of Imnavait Creek using a channel support area of 0.02 sq-km.

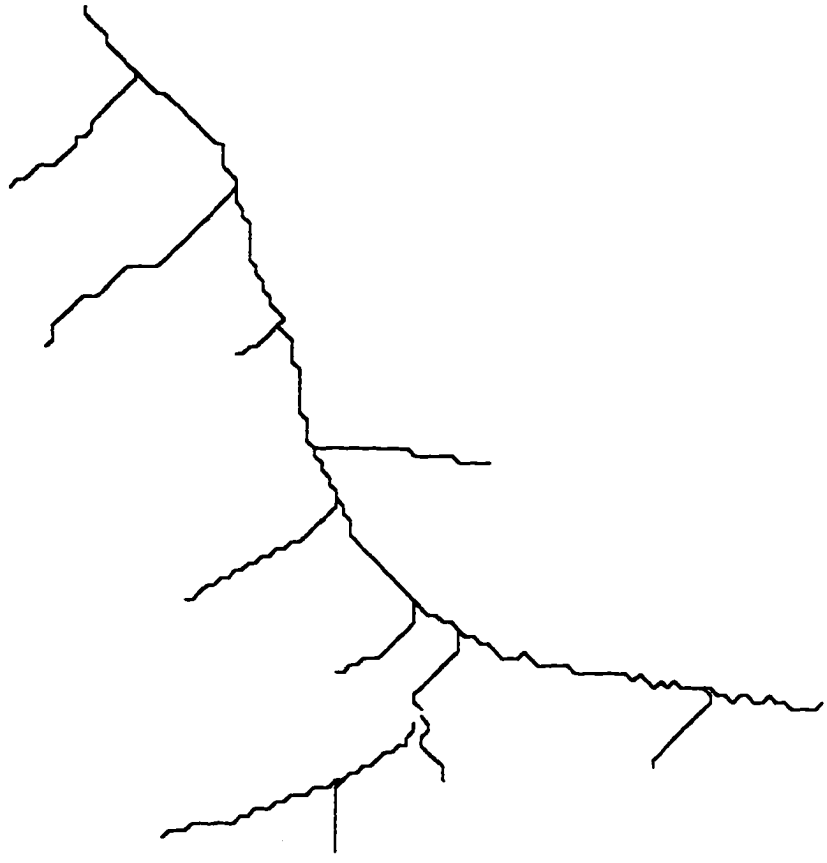

Figure 7.6d. Flow path network of the Upper Kuparuk River basin using a channel support area of 2 sq-km.

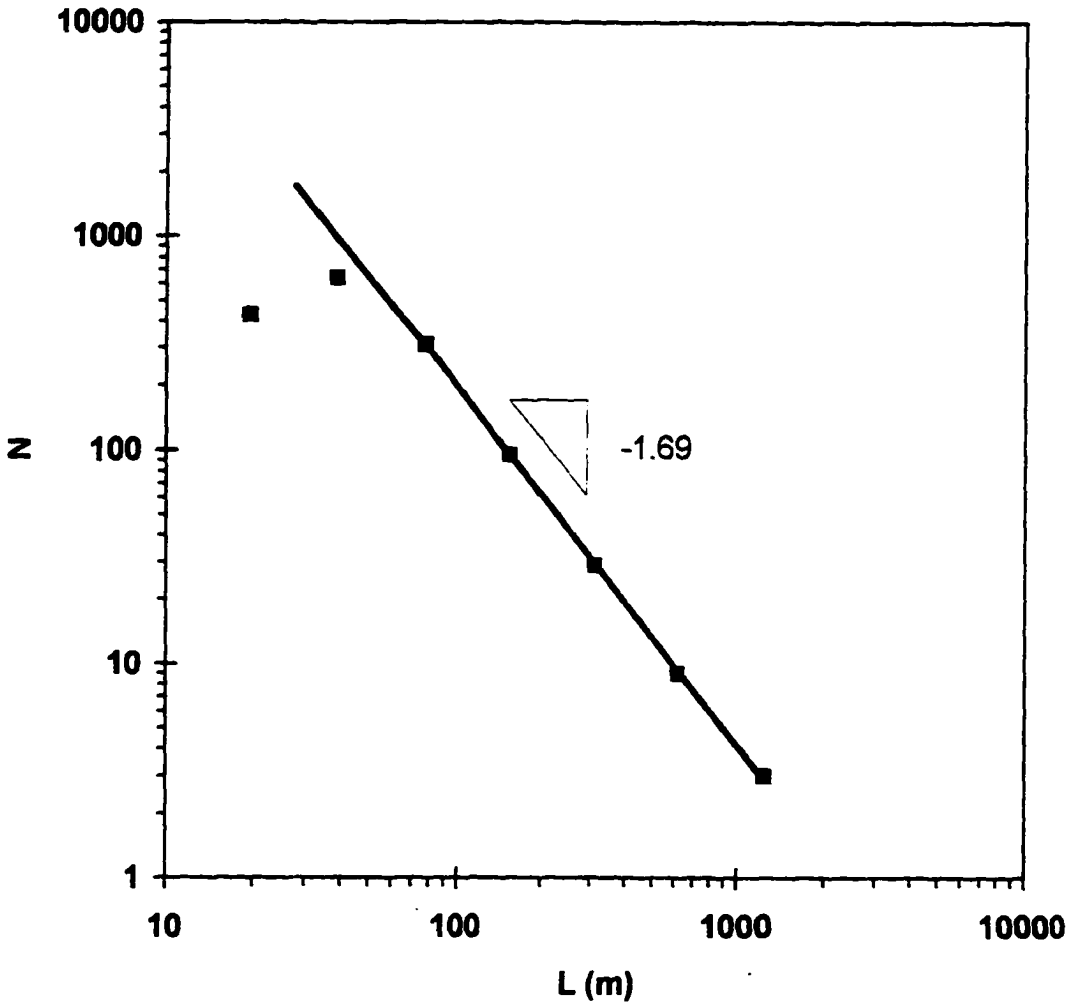

Figure 7.7a. Fractal dimension by functional box counting of Imnavait Creek using a channel support area of 0.0032 km^2. N is the number of boxes of side length L required to cover the channel network.

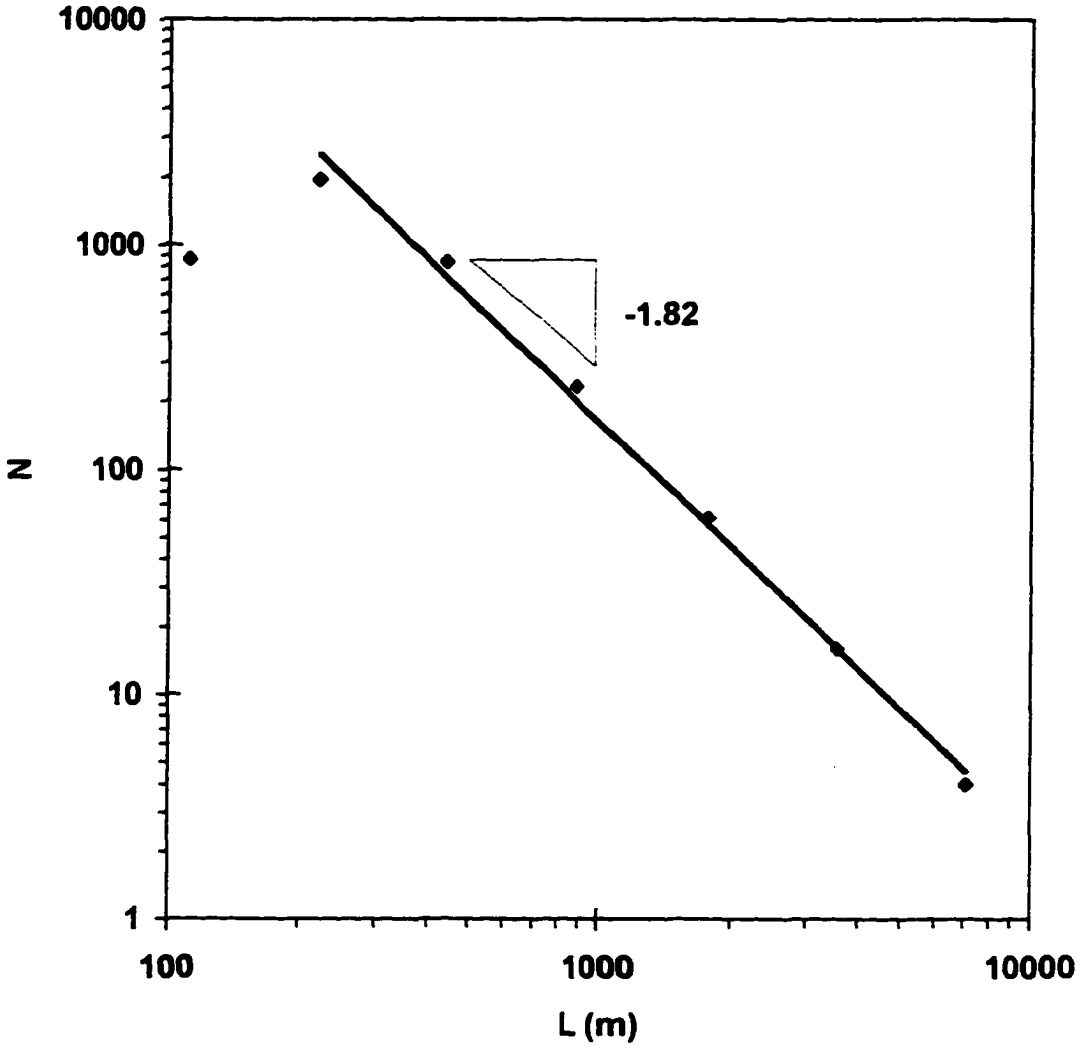

Figure 7.7b. Fractal dimension by functional box counting of the Upper Kuparuk River using a channel support area of 0.021 km^2. N is the number of boxes of side length L required to cover the channel network.

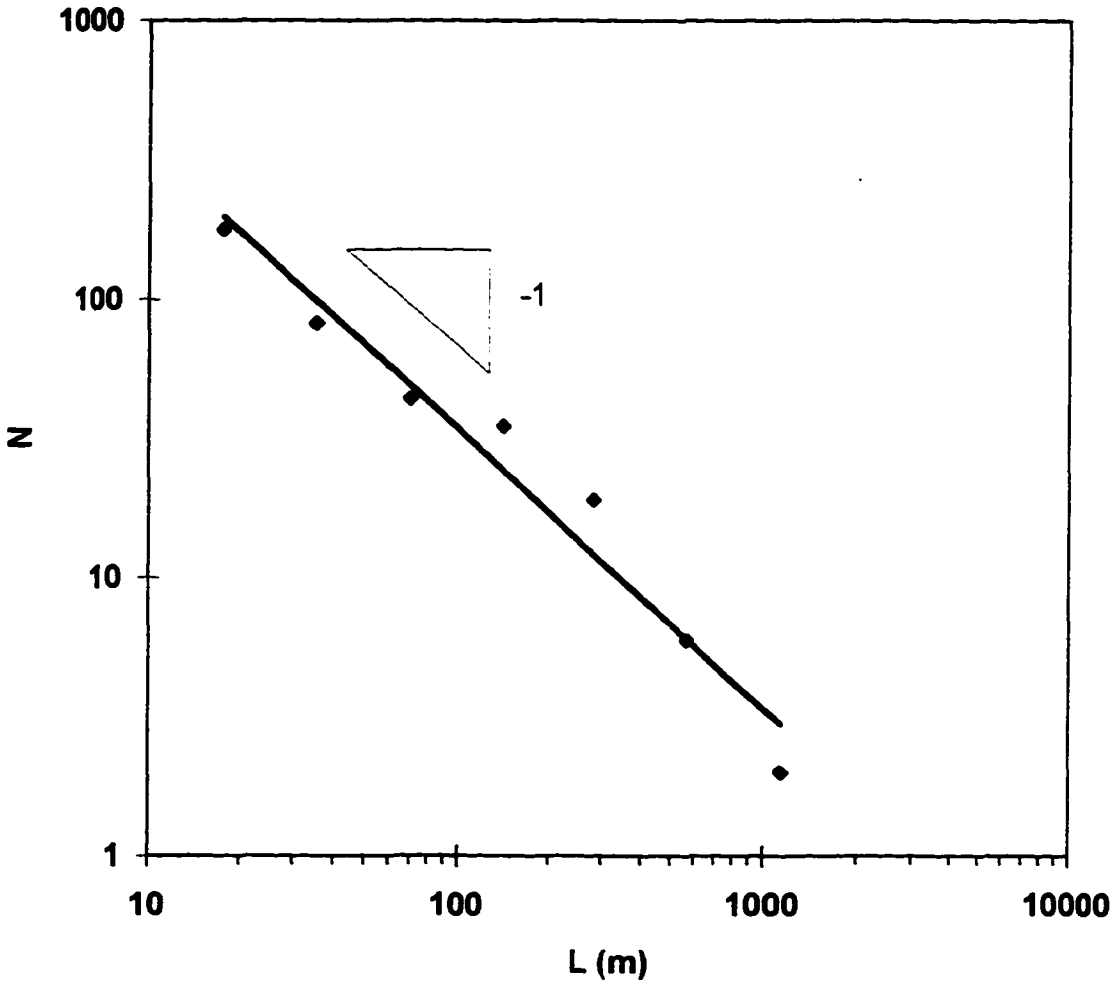

Figure 7.7c. Fractal dimension by functional box counting of Imnavait Creek using a channel support area of 0.03 km^2. N is the number of boxes of side length L required to cover the channel network.

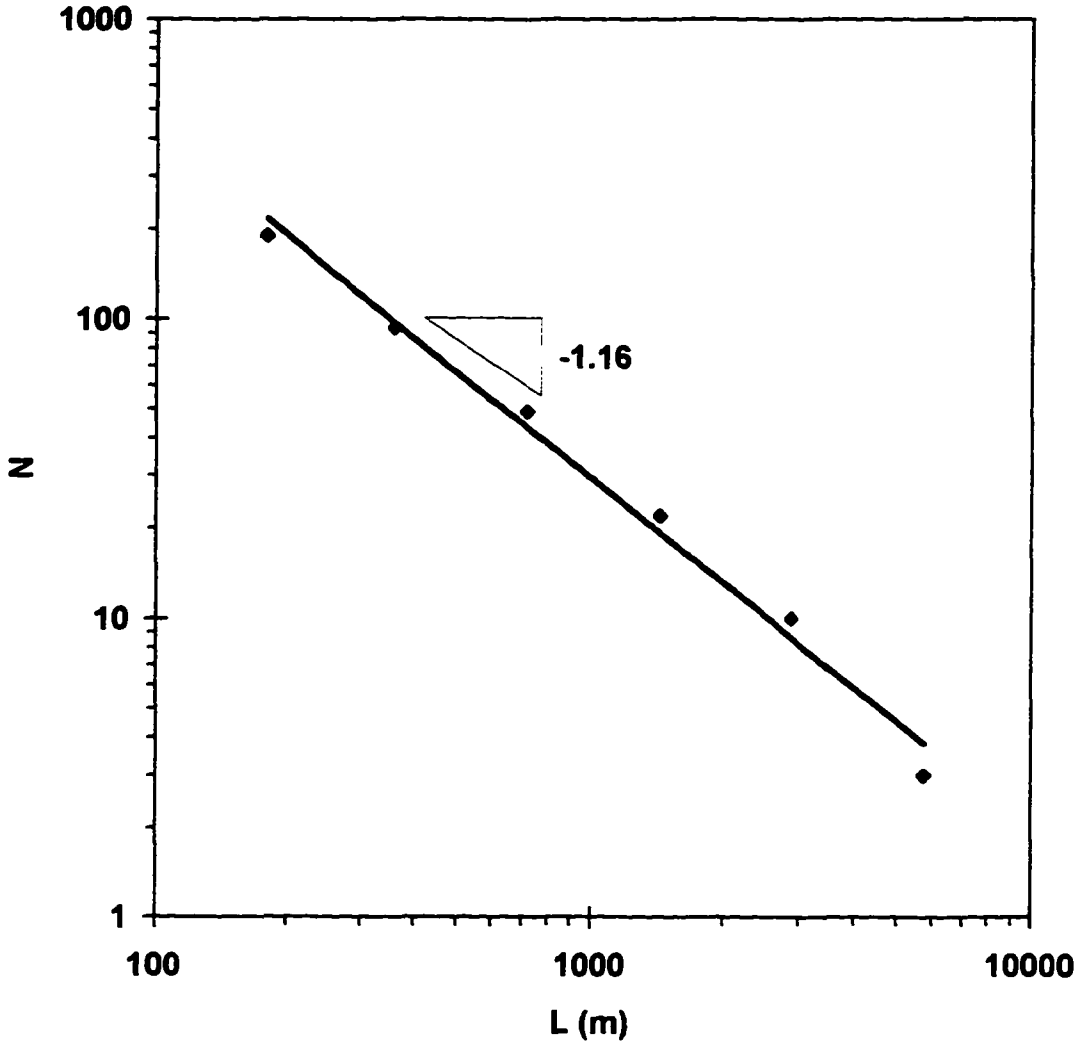

Figure 7.7d. Fractal dimension by functional box counting of the Upper Kuparuk River using a channel support area of 2 km^2. N is the number of boxes of side length L required to cover the channel network.

for a space filling network.

The above fractal dimensions include the entire networks of water tracks and channels, and are close to what other researchers have reported as typical values for mature channel networks (LaBarbera and Rosso, 1989; Claps and Oliveto, 1996). This alone might suggest that the water tracks operate as part of the fluvial channel network. However, evidence from slope-area scaling and the cumulative area distributions suggest that the water tracks do not belong to the same class of aggregation patterns as fluvial channels. If we change the channel support areas to those at the second critical drainage areas discussed above, the fractal dimensions of Imnavait Creek and the Upper Kuparuk River (Figure 7.6c and 7.6d) become 1.00 and 1.16 respectively (Figures 7.7c and 7.7d). The dimension of 1.00 is the dimension of a straight, unbifurcated line lacking the even the slightest sinuosity. This is a reasonable description of the main channel of Imnavait Creek. The dimension of 1.16 is reasonably close to what Mandelbrot (1982) and Tarboten et al. (1990) suggested is the typical dimension of a single sinuous channel. Note that the channel networks in Figures 7.6c and 7.6d are essentially restricted to the dominant valley bottom channels as suggested in previous discussions. Thus, the fractal dimensions of Imnavait Creek and the Upper Kuparuk River using the second threshold channel support areas support the suggestion that only the main valley bottom channels act as "normal" fluvial systems.

There are two seemingly conflicting lines of evidence here. Fractal analysis suggests that the channel networks begin at the channel support areas coincident with

the first slope reversals of Figures 7.4a and 7.5a. However, flow aggregation patterns do not possess universalities until much greater drainage areas which yield very low fractal dimensions. According to Phillips (1993), these low fractal dimensions imply that the channel networks are severely constrained by the geology of the basins. Essentially, the channel networks are underdeveloped and constrained to single valley bottom channels with essentially no encroachment onto the surrounding slopes. Underdeveloped networks can exist for two reasons. They may not have had time to fully develop into mature networks, or they may be constrained by geologic conditions such as bedrock controls. The Imnavait Creek basin has been exposed for nearly one million years and can be considered an old basin, thus ruling out the first explanation. However, there are no bedrock controls in the basin, and there is very little in the main valley of the Upper Kuparuk River basin. Further, the dominant composition of the soils and underlying lithology in the region is organic soil overlying silt and glacial till; material that typically does not constrain the erosive development of channel networks. The constraining variable may be permafrost.

The water track network may be the imprint of a fully unconstrained channel network that was initially laid down soon after deglaciation, but permafrost may have limited erosion in the basin and inhibited the water tracks from incising the hillslopes. Indeed, Howard (1990) suggested that an initial rudimentary drainage network is rapidly created on a new surface before a more regular, process controlled network is formed. We suggest that the water tracks form networks of flow paths that efficiently drain the basins, yielding fractal dimensions close to those of fluvial channel networks,

but were "frozen" in immaturity and were never allowed to develop mature aggregation patterns. The consequence is large valleys with extensive, relatively undissected hillslopes.

7.7 Summary

The fractal dimensions of the combined networks of hillslope water tracks and valley bottom channels are similar to those reported in other regions for fully developed fluvial channel networks. This evidence alone suggests that hillslope water tracks function as part of the fluvial channel network. However, fully developed channel networks evolve to self-organized states of criticality and possess certain universal characteristics (attractors) in their aggregation. The channel networks studied here possess those commonalities only above the hillslope water track scale, or when the drainage areas reach the main valley bottom channels. However, field mapped drainage areas at the tops of water tracks coincide with predicted channel support areas from slope-area plots, and there is a change in the aggregation patterns at the water track scale.

Our interpretation of these results is that a rudimentary channel network was set on the hillslopes, but was never allowed to develop into a mature channel network. Consequently, the undissected hillslopes are extensive. The low fractal dimensions of the fluvial channel networks further suggest that the channel network is being constrained from complete development. Since the lithology in the basin is not restrictive, we suggest that the presence of permafrost has restricted the channel

network development. Thus, a warming climate may have resounding impacts on the erosional development of channel networks in the Arctic.

Chapter 8

SUMMARY

Permafrost is a dominant feature that has overwhelming influence on nearly all physical and biological processes in the Arctic. The central hypothesis of this dissertation is that permafrost influences the form, function, and scaling of hydrologic and geomorphologic characteristics in the Kuparuk River basin in Northern Alaska. This issue was addressed in four independent studies that addressed the streamflow hydrology and geomorphology of the basin. Drainage basin form and hydrologic response are intimately related. Thus, the results of each study are closely connected. An encompassing conclusion is that indeed, the Kuparuk River basin is adjusted to arctic conditions in both form and function. It is most straightforward to begin with a summary of drainage basin form (Chapter seven), then discuss how it influences hydrologic response (Chapters four through six).

Chapter seven addressed the drainage basin form using digital elevation models, and explored the function of hillslope water tracks in the organization of drainage basins. Water tracks are linear drainage features that rapidly convey water off slopes, but do not typically have incised channels. Instead, they exist as zones of enhanced soil moisture. An interesting question is whether water tracks belong in the hillslope or channel regime. The fractal dimensions of the combined networks of hillslope water tracks and fluvial channels are similar to those reported in other regions for fully developed fluvial channel networks. This evidence alone suggests that hillslope water tracks function as part of the fluvial channel network. However, fully

developed channel networks evolve to self-organized states of criticality and possess certain universal characteristics in their aggregation patterns. The channel networks studied in the Kuparuk River basin possess those universalities only when the hillslope water tracks are excluded from the channel networks and only the main valley bottom channels are included. However, field mapped drainage areas at the tops of water tracks coincide with predicted channel support areas from slope-area plots, and there is a change in the aggregation patterns at the water track scale. It may be that a rudimentary channel network was set on the hillslopes, but was never allowed to develop into a mature channel network. Low fractal dimensions of the fluvial channel networks further suggest that the channel network is being constrained from complete development. The constraining variable may be permafrost, which inhibits erosion. Instead of a few well-developed incised channels, the hillslopes contain numerous water tracks. These water tracks in conjunction with the active layer have tremendous hydrologic significance, which is apparent in the results of Chapters four through six.

Chapters four and five address the physical characteristics of streamflow in the Kuparuk River basin, with the general hypothesis that streamflow characteristics would be influenced by permafrost in two ways: First, by the limited water storage capacity, and second, by the changing storage capacity as the active layer increased through a thawing season. This hypothesis was tested simply by comparing streamflow characteristics in the Kuparuk River basin to those in temperate basins. The results were that indeed, the hydrologic response in the Kuparuk River differs from the hydrologic response in temperate basins, and the differences can be explained

by the presence of permafrost. Surface and depression storage in the Kuparuk River basin fills quickly, and the watershed appears wet after very little precipitation. Therefore, runoff/precipitation ratios (response factors) in the Kuparuk River basin are high. The falling limbs of storm hydrographs must then drop from relatively high peaks to the typically low base flows that result from the lack of subsurface contributions. Consequently, the recession constants are high. This produces long lag times between the precipitation centroids and hydrograph peaks, and between the precipitation centroids hydrograph centroids.

The composition of stormflow in the Upper Kuparuk River is dominated by water previously existing in the basin, called old water, as is commonly observed in all regions. However, Imnavait Creek storm flow was dominated by new water contributions. The difference between the two basins may be a result of the density of water tracks on the hillslopes. The portion of the basin that contributes new water to storm flow (NWCP) was significantly greater in the Upper Kuparuk River basin than in the non-permafrost basins, which suggests that more interaction occurs between the surface and subsurface in non-permafrost basins. Water tracks play an important role in the composition of storm flow as they provide a large saturated area from which runoff can be generated.

The suspected seasonal trends due to the thawing active layer were not as apparent as anticipated. Response factors decreased through the thawing season in 1994, but not in 1995. Also, old water contributions to storm flow in the Upper Kuparuk River increased moderately through the 1994 summer season with an

associated decrease in new water contributing portion (NWCP). Again, those seasonal trends were not apparent in 1995, and no seasonal trends were observed in the storm flow dynamics of Imnavait Creek in either year. However, there were large differences in storm flow compositions between snowmelt and the first summer storms each year. Thus, in the period immediately following snowmelt, increases in active layer thickness have dramatic influences on storm flow compositions. However, later in the summer, any influence of the active layer can be easily masked by soil moisture conditions as dictated by precipitation patterns.

Chapter six showed that significant differences exist in the spatial variability of streamflow between arctic and temperate basins. Rainfall generated streamflow in the permafrost-dominated Kuparuk River basin, and flood peaks in other arctic rivers, obey simple scaling, whereas rainfall generated flows in some other regions studied obey multiscaling. The nature of downstream discharge variability is the product of the controls on the characteristics of upstream hydrographs. Thus, the regional scaling differences may result from the differences in the characteristics of headwater response hydrographs due to the presence or absence of permafrost. For example, in permafrost basins, stormflow hydrographs are translated downstream without the moderating effect of baseflows from other contributing basins. Hence, the variability is maintained downstream. In non-permafrost basins, stormflow hydrographs are smoothed by baseflows from other contributing basins as they accumulate downstream. Hence, the variability decreases downstream.

That the form and function of the Kuparuk River basin are influence by arctic conditions implies that changes in the permafrost may induce changes in the erosional development of channel networks and the consequent hydrologic response. On a seasonal time scale, this may occur as streamflow characteristics change systematically through the season coincident with the thawing active layer. For example, response factors may decrease as more water is able to enter long-term storage. On a longer time scale, the sensitivity of streamflow hydrology on the presence of permafrost has strong implications that arctic ecosystems may experience significant changes in a changing global climate. For example, water tracks may develop into incised channels. This would alter the hillslope water delivery system and influence the timing and magnitude of runoff. Further, the large saturated area occupied by water tracks would be eliminated, which would alter the composition of stormflow. At any time scale, the relationship between permafrost and hydrologic response may have resounding ecological impacts on processes such as the timing and magnitude of the delivery of nutrients to the aquatic system.

REFERENCES

Andah, K., F. Siccardi, and P. La Barbera. 1987. Is a drainage network from a digital terrain model a model for the real network? EOS Trans. AGU, 68(44): 1272.

Anderson, J. C. 1974. Permafrost - hydrology studies at Boot Creek and Peter Lake watersheds, N.W.T. Proc. of Workshop Seminar on Permafrost Hydrology, Calgary, Alberta, Canada, February 26-28, 1974. Canadian National Committee, p. 39-44.

Anderson, E. A., and P. J. Neuman. 1984. Inclusion of frozen ground effects in a flood forecasting model. Proc. of the Fifth Northern Research Basins Symposium, Vierumāki, Finland. March 19-23, 1984. p. 5.1-5.15.

Bak, P., C. Tang, and K. Wiesenfeld. 1987. Self-organized criticality: An explanation of 1/f noise. Phys. Rev. Lett., 59: 381-385.

Bak, P., C. Tang, and K. Wiesenfeld. 1988. Self-organized criticality. Phys. Rev. A, 38(1): 364-374.

Band, L. E.1986. Topographic partition of watersheds with digital elevation models. Water Resour. Res., 22(1): 15-24.

Beauvais, A., and D. R. Montgomery. 1994. Planform scaling properties of rivers and channel networks. EOS Trans. AGU, 75(44), Fall Meet. Suppl., 303.

Beer, T., and M. Borgas. 1993. Horton's laws and the fractal nature of streams. Water Resour. Res., 25(5): 1475-1487.

Benson, C. S. 1982. Reassessment of winter precipitation on Alaska's arctic slope and measurements on the flux of wind blown snow. Research Report UAG R-288. Geophysical Institute, University of Alaska Fairbanks.

Betson, R. P. 1964. What is watershed runoff? Journal of Geophysical Research, 69: 1541-1552.

Black, R. F. 1954. Precipitation at Barrow, Alaska, greater than recorded. American Geophysical Union Transactions, 35: 203-206.

Blöschl, G., and M. Sivapalan. 1995. Scale issues in hydrological modeling: A review. In: Scale Issues in Hydrological Modelling, eds: J. D. Kalma and M. Sivapalan, John Wiley and Sons, England. p. 9-48.

Bottomley, .J., D. Craig, and L. M. Johnson. 1986. Oxygen-18 studies of snowmelt runoff in a small Precambrian shield watershed: Implications for streamwater acidification in acid-sensitive terrain. J. Hydrol., 88: 213-234.

Briazgin, N. N., and E. S. Korotkevich. 1975. The Arctic and Antarctic. U. S. Army CRREL, Translation 474.

Brown, J., S. L. Dingman, and R. J. Lewellen. 1968. Hydrology of a drainage basin on the Alaskan Coastal Plain. U.S. Army Cold Regions Research and Engineering Laboratory, Hanover, NH, Research Report 240.

Burrough, P. A. 1981. Fractal dimensions of landscapes and other environmental data. Nature, 294(19): 240-242.

Buttle, J.M., and K. Sami. 1992. Testing the groundwater ridging hypothesis of streamflow generation during snowmelt. J. Hydrol., 135: 53-72.

Cadavid, E. E. 1988. Hydraulic geometry of channel networks: Tests of scaling invariance, M.S. thesis, Dept. of Civ. Engr., Univ. of Miss.

Carlson, R. F., W. Norton, and J. McDougall. 1974. Modeling snowmelt runoff in an Arctic coastal plain. Institute of Water Resources, University of Alaska Fairbanks. Report No. IWR-43.

Childers, J. M., D. R. Kernodle, and R. M. Loeffler. 1979. Hydrologic reconnaissance of Western Arctic Alaska, 1976 and 1977, United States Geological; Survey Open File Report 79-699.

Chorley, R. J. 1978. The hillslope hydrologic cycle. In Kirkby, M. J. 1978. Hillslope Hydrology. New York, NY: John Wiley and Sons. p. 1-42.

Chorowitz, J., C. Ichoku, S. Riazanoff, Y. J. Kim, and B. Cervelle. 1992. A combined algorithm for automated drainage network extraction. Water Resour. Res., 28(5): 1293-1302.

Chorowitz J., C. Ichoku, S. Riazanoff, Y. J. Kim, and B. Cervelle. 1993. Reply to comment on "A combined algorithm for automated drainage network extraction," by J. Garbrecht and L. W. Martz. Water Resour. Res., 29(5): 537-539.

Church, M. 1974. Hydrology and permafrost with reference to northern North America. Proc. Workshop Seminar on Permafrost Hydrology, Can. Nat. Comm., IHD, Ottawa, p. 7-20.

Clagget, G. P. 1988. The Wyoming windshield - and evaluation after 12 years of use in Alaska. Proc. of Western Snow Conference, p. 113-123.

Claps, P., and G. Oliveto, 1996. Reexamining the determination of the fractal dimension of river networks. Water Resour. Res., 32(10): 3123-3135.

Colonell, J. M., and G. R. Higgins. 1973. Hydrologic response of Massachusetts watersheds. Water Resour. Bull., 9:793-800.

Cooper, L. W., C. R. Olsen, D. K. Solomon, I. L. Larsen, R. B. Cook, and J. M. Grebmeier. 1991. Stable isotopes of oxygen and natural and fallout radionuclides used for tracing runoff during snowmelt in an Arctic watershed. Water Resour. Res, 27(9): 2171-2179.

Cooper, L. W., C. S. Solis, D. L. Kane, and L. D. Hinzman. 1993. Application of oxygen-18 tracer techniques to arctic hydrological processes. Arctic and Alpine Research, 25: 247-255.

Craig, P. C., and P. J. McCart.1975. Classification of stream types in Beaufort Sea drainages between Prudhoe Bay, Alaska and the Mackenzie Delta, N.W.T., Canada. Arctic and Alpine Research, 7: 183-198.

Davis, W. M. 1899. The geographical cycle, Geogr. J., 14: 481-504 (reproduced in Geographical Essays, edited by W. M. Davis, Ginn, Boston, MA, 1909.)

Dawdy, D.R. 1961. Variation of flood ratios with size of drainage area, U.S. Geological Survey Research, 424-C, Paper C36, Reston, VA..

De Cola, L., and N. S. Lam. 1993. Introduction to fractals in geography. In: Fractals in Geography, edited by N. S. Lam and L. De Cola, Prentice Hall, New Jersey, p. 3-22.

deVries, H., T. Becker, and B. Eckardt. 1994. Power law distribution of discharge in ideal networks. Water Resour. Res., 30(12): 3541-3543.

DeWalle, D. R., B. R. Swistock, and W. E. Sharpe. 1988. Three component tracer model for storm flow on a small Appalachian forest catchment. J. Hydrol., 104: 301-110.

Dincer, T., B.R. Payne, T. Florkowski, J. Martinec, and E. Tongiorgi. 1970. Snowmelt runoff from measurements of tritium and oxygen 18. *Water Resour. Res.*, 6: 110-124.

Dingman, S. L. 1970. Hydrology of the Glenn Creek watershed, Tanana River basin, central Alaska. Research Report 297. U.S. Army Cold Regions Research and Engineering Laboratory, Hanover, New Hampshire.

Dingman, S. L. 1973. Effects of permafrost on stream characteristics in the discontinuous permafrost zone of central Alaska. In Permafrost: North American Contribution to the Second International Conference. Washington, DC: National Academy of Sciences, p. 447-453.

Dingman, S. L. 1994. Physical Hydrology. MacMillan Publishing Company, New York.

Douglas, L. A. 1961. A pedological study of tundra soils from northern Alaska. Ph.D. thesis, Rutgers University.

Dunne, T., and R. D. Black. 1970. Partial area contributions to storm runoff in a small New England watershed. Water Resour. Res., 6:1296-1311.

Dunne, T., and L. B. Leopold. 1978. Water in Environmental Planning. W. H. Freeman and Company, San Francisco.

Eshleman, K.N., J.S. Pollard, and A.K. O'Brien. 1993. Determination of contributing areas for saturation overland flow from chemical hydrograph separations. Water Resour. Res., 28: 3577-3587.

Fairfield, J., and P. Leymarie. 1991. Drainage networks from grid digital elevation models, Water Resour. Res. 27(5): 709-717. (Correction, Water Resour. Res., 27(10): 2809, 1991.)

Feder, J.1988. Fractals, Plenum, New York.

Flint, J. J. 1974. Stream gradient as a function of order, magnitude and discharge. Water Resour. Res., 10(5): 969-973.

Freeman, T. G. 1991. Calculating catchment area with divergent flow based on a regular grid. Comput. Geosci., 17(3): 413-422.

Freeze, R.A. 1972. Role of subsurface flow in generating surface runoff: 1. Baseflow contributions to channel flow. Water Resour. Res., 8: 609-623.

Goodchild, M. F., and D. M. Mark. 1987. The fractal nature of geographic phenomena. Annals Assoc. Amer. Geog., 77(2): 265-278.

Gray, D. M. 1961. Interrelationships of watershed characteristics. J. Geophys. Res., 66(4): 1215-1233.

Gupta, V. K., S. L. Castro, and T. M. Over. 1996. Scaling exponents of peak flows from spatial rainfall and channel networks. J. Hydrol., 187(1/2): 81-104.

Gupta, V.K., and D.R. Dawdy. 1994. Regional analysis of flood peaks: Multiscaling theory and its physical basis In: Advances in Distributed Hydrology, edited by R. Rosso, A. Peano, I. Becchi, and G. A. Bemporad, Water Resources Publications, Highlands Ranch, CO, p. 149-166

Gupta, V.K., and D.R. Dawdy. 1995. Physical interpretation of regional variations in the scaling exponents of flood quantiles. Hydrol. Proc., 9: 347-361.

Gupta, V. K. and O. Mesa. 1988. Runoff generation and hydrologic response via channel network geomorphology - recent progress and open problems. J. Hydrol., 102: 3-28.

Gupta, V. K., O. Mesa, and D.R. Dawdy. 1994. Multiscaling theory of flood peaks: regional quantile analysis. Wat. Resour. Res., 30(12): 3405-3421.

Gupta, V. K., I. Rodriguez-Iturbe, and E. F. Wood, (ed) 1986. Scale Problems in Hydrology, Reidel, Dorchert.

Gupta, V.K., and E. Waymire. 1983. On the formulation of an analytical approach to hydrologic response and similarity at the basin scale. J. Hydrol., 65: 95-123.

Gupta, V.K., and E. Waymire. 1989. Statistical self-similarity in river networks parameterized by elevation. Water Resour. Res., 25: 463-476.

Gupta, V.K., and E. Waymire. 1990. Multiscaling properties of rainfall and river flow distributions. Journal of Geophysical Research, 95(D3): 1999-2009.

Gupta, V.K., and E. Waymire. 1996. Multiplicative cascades and spatial variability in rainfall, river networks, and floods. In: Reduction and Predictability of Natural

Disasters, Eds. Rundle, Turcotte, and Klein, Sfi Studies in the Sciences of Complexity, Vol. XXV, Addison-Wesley.

Gupta, V. K., E. Waymire, and C. T. Wang. 1980. A representation of an instantaneous unit hydrograph from geomorphology. Water Resour. Res., 16(5): 855-862.

Hack, J. T. 1957. Studies of longitudinal profiles in Virginia and Maryland, U.S. Geol. Surv. Prof. Pap., 294-B, 1.

Hamilton, T. D. 1986. Late Cenozoic glaciation of the Central Brooks Range. in Glaciation in Alaska: the Geologic Record, edited by T. D. Hamilton, K. M. Reed, and R. M. Thorson, Alaska Geological Society, p. 9-49.

Hastings, S. J., S. A. Luchessa, W. C. Oechel, and J. D. Tenhunen. 1989. Standing biomass and production in water drainages of the foothills of the Phillip Smith Mountains. Holarctic Ecology, 12(3): 304-311.

Haugen, R. K. 1980. Regional climate, in Environmental Engineering and Ecological Baseline Investigations Along the Yukon River - Prudhoe Bay Haul Road. U.S. Army CRREL Report 80-19, p. 9-19.

Helminger, K., P. Kumar, and E. Foufoula-Georgiou. 1993. On the use of digital elevation model data for Hortonian and fractal analyses of channel networks. Water Resour. Res., 29(8), 2599-2613.

Hewlett, J. D., and A. R. Hibbert. 1967. Factors affecting the response of small watershed to precipitation in humid areas. In: International Symposium of Forest Hydrology, Permagon, Oxford, p. 275-290

Hinton, M.J., S.L. Schiff, and M.C. English. 1994. Examining the contributions of glacial till water to storm runoff using two- and three- component hydrograph separations. Wat. Resour. Res., 30: 983-993.

Hinzman, L, D., D. L. Kane, and K. R. Everett. 1993. Hillslope hydrology in an Arctic setting. In: Proceedings of the Sixth International Conference on Permafrost, Beijing, China, July 5-9, p. 267-271.

Hinzman, L. D., D. L. Kane, R. E. Gieck, and K. R. Everett. 1991. Hydrologic and thermal properties of the active layer in the Alaskan Arctic. Cold Reg. Sci. and Tech., 19: 95-110.

Hjemfelt, A. T., Jr. 1988. Fractals and the river-length catchment-area ratio. Water Resour. Bull., 24(2): 455-459.

Holton, H. N., and D. E. Overton. 1963. Analyses and application of simple hydrographs. J. Hydrol., 2:309-323.

Hooper, R.P., and C.A. Shoemaker. 1986. A comparison of chemical and isotopic hydrograph separation. Water Resour. Res., 22: 1444-1454.

Horton, R. E. 1933. The role of infiltration in the hydrologic cycle. American Geophysical Union Transactions, 14: 446-460.

Horton, R. E. 1945. Erosional development of streams and their drainage basins: Hydrophysical approach to quantitative morphology. Geol. Soc. Am. Bull., 56, 275-370.

Howard, A. D. 1990. Theoretical model of optimal drainage networks. Water Resour. Res., 26(9): 2107-2117.

Ijjasz-Vasquez, E. J., R. L. Bras, and I. Rodriguez-Iturbe. 1994. Self-affine scaling of fractal river courses and basin boundaries. Phys. A, 209: 288-300.

Ijjasz-Vasquez, E., and R. L. Bras. 1995. Scaling regimes of local slope versus contributing area in digital elevation models. Geomorphology, 12: 299-311.

Ijjasz-Vasquez, E. J., I. Rodriguez-Iturbe, and R. L. Bras. 1992. On the multifractal characterization of river basins. Geomorphology, 5: 297-310.

Jenson, S. K., and J. O. Domingue.1988. Extracting topographic structure from digital elevation data for geographic information system analysis. Photogramm, Eng. Remote Sens., 54(11): 1593-1600,.

Kane, D. L., and R. F. Carlson, 1973. Hydrology of the central arctic river basins of Alaska. Institute of Water Resources, University of Alaska, Fairbanks. Report No. IWR-41.

Kane, D. L., R. E. Gieck, and L. D. Hinzman. 1990. Evapotranspiration from a small Alaskan Arctic watershed. Nordic Hydrology, 21(4/5): 253-272.

Kane, D. L., and L. D. Hinzman. 1988. Permafrost hydrology of a small arctic watershed. In: Proc. Fifth Int. Conf. Permafrost, edited by K. Senneset, The Norwegian Committee on Permafrost, p. 590-595.

Kane, D. L., L.D. Hinzman, C. S. Benson, and G. E. Liston. 1991. Snow hydrology of a headwater Arctic basin. 1: Physical measurements and process studies. Water Resour. Res., 27(6): 1099-1109.

Kane, D. L., Hinzman, L. D., Everett, K. R., and Benson, C. S. 1989. Hydrology of Imnavait Creek, an arctic watershed. Holarctic Ecology, 12: 262-269.

Kane, D. l., L. D. Hinzman, M. K. Woo, and K. R. Everett. 1992. Arctic hydrology and climate change. In: Arctic Ecosystems in a Changing Climate, an Ecophysiological Perspective, eds. Chapin, F. S., III, R. L. Jeffries, J. F. Reynolds, G. R. Shaver, and J. Svoboda. New York: Academic Press Inc.

Kane, D. L., and J. Stein. 1983. Water movement into seasonally frozen soils. Water Resour. Res., 19(6): 1547-1557.

Kennedy, V.C., C. Kendall, G.W. Zellweger, T.A. Wyerman, and R.J. Avanzino. 1986. Determination of the components of storm flow using water chemistry and environmental isotopes, Mattole River basin, California. J. Hydrol., 84: 107-140.

Kirkby, M. J. 1978. Hillslope Hydrology. New York, NY: John Wiley and Sons.

Klinkenberg, B. 1994. A review of methods used to determine the fractal dimension of linear features. Mathematical Geology, 26(1): 23-46.

Kobayashi, D. Y. Komama, M. Nomura, and Y. Ishii. 1993. Comparison of snowmelt hydrograph separation by recession analysis and by stream temperature and conductance. In: Tracers in Hydrology, Proceedings of the Yokohama Symposium, July 1993, IAHS publ. no. 215.

Kondoh, H., and M. Matsushitu. 1986. Diffusion-limited aggregation with anisotropic sticking probability: A tentative model for river networks. J. Phys. Soc. Jpn., 55(10): 3289-3292.

Kondoh, H., M. Matsushitu, and Y. Fukuda. 1987. Self-affinity of Sheidegger's river patterns. J. Phys. Soc. Jpn., 56(6): 1913-1915.

Kreit, K., B. J Peterson, and T. L. Corliss. 1992. Water and sediment export of the upper Kuparuk River drainage of the North Slope of Alaska. Hydrobiologica, 240: 71-81.

La Barbera, P., and R. Rosso. 1987. Fractal geometry of river networks (abstract). Eos Trans. AGU, 68(44): 1276.

La Barbera, P., and R. Rosso. 1989. On the fractal dimension of stream networks. Water Resour. Res., 25(4): 735-741.

La Barbera, P., and R. Rosso. 1990. Reply to comment on "On the fractal dimension of stream networks," by D. G. Tarboten, R. L. Bras, and I. Rodriguez-Iturbe. Water Resour. Res., 26(9): 2245-2248.

Lam, N. S., and L. DeCola. 1993. Fractal measurement. In: Fractals in Geography, edited by N. S. Lam and L. De Cola, Prentice Hall, New Jersey, p. 23-55.

Lamke, R. D. 1979. Flood characteristics of Alaska streams, U.S. Geological Survey, Water Resources Investigations 78-129.

Lavalée, D., S. Lovejoy, D. Schertzer, P. Ladoy. 1993. Nonlinear variability of landscape topography: Multifractal analysis and simulation. In: Fractals in Geography, Prentice Hall, New Jersey, p. 23-55.

Lewkowicz, A.G. and H.M. French. 1982. The hydrology of small runoff plots in an area of continuous permafrost, Banks Island, N.W.T. Proc. Fourth Canadian Permafrost Conference, March 2-6, 1981. Calgary, Alberta, Canada. p. 151-161

Likes, E. H. 1966. Surface-water discharge of Ogoturuk Creek. In: Environment of the Cape Thompson Region, Alaska. U.S. Atomic Energy Commission, Oak Ridge, Tennessee, p. 125-131

Linsley, R. K., M. A. Kohler, and J. L. H. Paulhus. 1982. Hydrology for Engineers, McGraw-Hill.

Lovejoy, S., D. Schertzer, and A. Tsonis.1987. Functional box counting and multiple elliptical dimensions in rain. Science, 235: 1036-1038..

Liu, T. 1992. Fractal structure and properties of stream networks. *Water Resour. Res.*, 28(11): 2981-2989.

Mandelbrot, B. B. 1967. How long is the coast of Britain? Statistical self-similarity and fractional dimension. Science, 156: 636-638.

Mandelbrot, B. B. 1974. Intermittent turbulence in self-similar cascades: Divergence of high moments and dimension of the carrier. J. Fluid Mech. 62: 331-358.

Mandelbrot, B. B. 1982. The Fractal Geometry of Nature. W. H. Freeman, New York.

Mandelbrot, B. B. 1986. Self-affine fractal sets. In: Fractals and Physics, North-Holland, New York,. p. 3-28

Mandelbrot, B. B. 1987. Fractals. Encyclopedia of Physical Science and Technology, 5: 579-593.

Marani, A., R. Rigon, and A. Rinaldo. 1991. A note on fractal channel networks. Water Resour. Res., 27(12): 3041-3049.

Mark, D. M. 1984. Automated detection of drainage networks from digital elevation models. Cartographica, 21: 168-178.

Martz, L. W., and E. de Jong. 1988. CATCH: A FORTRAN program for measuring catchment area from digital elevation models. Comput. Geosci., 14(5): 627-640.

McDonnell, J. J, M. K. Stewart, and I. F. Owens. 1991. Effect of catchment-scale subsurface mixing on stream isotopic response. Water Resour. Res., 27: 3065-3073.

McNamara, J. P., D. L. Kane, and L. D. Hinzman. 1997a. An analysis of streamflow hydrology in the Kuparuk River basin: a nested watershed approach. J. Hydrol., in press.

McNamara, J. P., D. L. Kane, and L. D. Hinzman. 1997b. Hydrograph separations in an Arctic watershed using mixing model and graphical techniques, Water Resour. Res., in press.

McNamara, J. P., D. L. Kane, and L. D. Hinzman. 1997c. Scaling of river flows in the Alaskan Arctic, submitted to *Water Resour, Res.*, in review.

Meakin, P., J. Feder, and T. Jossang. Simple statistical models for river networks. Physica A, 176(3): 409-429.

Meisels, A., S. Raizman, and A. Karnieli. 1995. Skeletizing a DEM into a drainage network. Comput. Geosci., 21(1): 187-196.

Mesa, O. J., and E. R. Mifflin. 1986. On the relative roles of hillslope and network geometry in hydrologic response. In: Scale Problems in Hydrology, Reidel Publishing Company, p. 1-17.

Moglen, G. E., and R. L. Bras. 1994. The importance of spatially heterogeneous erosivity and the cumulative area distribution within a basin evolution model. Geomorphology, 12: 173-185.

Montgomery, D. R., and W. E. Dietrich. 1988. Where do channels begin? Nature, 336: 232-234.

Montgomery, D. R., and W. E. Dietrich. 1992. Channel initiation and the problem of landscape scale. Science, 255: 826-830.

Montgomery, D. R., and E. Foufoulo-Georgiou. 1993. Channel network representation using digital elevation models. Water Resour. Res., 29(12): 3925-3934.

Morris, D. G., and R. G. Heerdegen. 1988. Automatically derived catchment boundaries and channel networks and their hydrological applications. Geomorphology, 1: 131-141.

Moussa, R., and C. Bocquillon. 1993. Morphologie fractale du réseau hydrographique (in French). Hydrol. Sci. J., 38(3): 187-201.

Mueller, S. W. 1943. Permafrost or permanently frozen ground and related engineering problems. U.S. Army Office Chief of Engineers, Military Intelligence Division Strategic Engineering Study 62, 231 p.

National Snow and Ice Data Center. 1994. ARCSS/LAII Data Series Volume 1: Alaska North Slope Data Sampler.

Newbury, R.W. 1974. River hydrology in permafrost areas. Proc. Workshop Seminar on Permafrost Hydrology, Can. Nat. Comm., IHD, Ottawa, Ont., p. 31-37.

Nikora, N. F., E. D. Gopchenko, and V. I. Nikora. 1989. Models of river systems (in Russian), Prof Pap. 944 GM-89, VNIIGMIMCD, Obninsk, Russia, p. 1-72

Nikora, V. I. 1988. Fractal properties of some hydrological objects (in Russian), Acad. of Sci. of the Moldavian Sov. Soc. Repub., Kishinev.

Nikora, V. I. 1991. Fractal structures of river plan forms, Water Resour. Res., 27(6): 1327-1333.

Nikora, V. I. 1994. On self-similarity and self-affinity of drainage basins. Water Resour. Res., 30(1): 133-137.

Nikora, V. I., D. M. Hicks, G. M. Smart, and D. A. Noever. 1995. Some fractal properties of braided rivers, paper presented at 2nd International Symposium: Fractals and Dynamic Systems in Geoscience, Dtsch. Forsch., Frankfurt am Main, Germany, April 4-7, 1995.

Nikora, V., R. Ibbit, and U. Shankar. 1996. On channel network fractal properties: A case of study of the Hutt River Basin, New Zealand. Water Resour. Res., 32(11): 3375-3384.

Nikora, V. I., and V. B. Sapozhnikov. 1993a. River network fractal geometry and its computer simulation. Water Resour. Res., 29(10): 3569-3575.

Nikora, V. I., and V. B. Sapozhnikov. 1993b. On fractal properties of the river network and individual watercourses. Ann. Geophys. Suppl. II, 11(2): 304.

Nikora, V. I., V. B. Sapozhnikov, and D. A. Noever. 1993. Fractal geometry of individual river channel and its computer simulation. Water Resour. Res., 29(10): 3561-3568.

NRC, National Research Council, 1991. Opportunities in Hydrologic Sciences. National Academy Press, Washington, DC.

O'Callaghan, J. F., and D. M. Mark. 1984. The extraction of drainage networks from digital elevation data. Comput, Vision Graphics Image Process., 28: 323-344.

Ohmura, A. 1982. Evaporation from the surface of the arctic tundra on Axel Heiberg Island. Water Resour. Res., 18(2): 291-300.

Osterkamp, T. E., and M. W. Payne.1981. Estimates of permafrost thickness from well logs in northern Alaska. Cold Reg. Sci. and Technol., 5(1): 13-27.

Peckham, S. D. 1995. New results for self-similar trees with applications to river networks. Water Resour. Res., 31(4): 1023-1029.

Peters, D.L., J.M. Buttle, C.H. Taylor, and B.D. LaZerte. 1995. Runoff production in a forested, shallow soil, Canadian Shield basin. Water Resour. Res., 31: 1291-1304.

Phillips, J. D. 1993. Interpreting the fractal dimension of river networks, In: Fractals and Geography, edited by N. S. Lam and L. De Cola, Prentice Hall, New York, p. 142-157.

Pilgrim, D. H., D. D. Huff, and T. D. Steele. 1979. Use of specific conductance and contact time relations for separating flow components in storm runoff. Water Resour. Res., 15: 329-339.

Quinn, P., K. Beven, P. Chevallier, and O. Planchon. 1991. The prediction of hillslope flow paths for distributed hydrological modelling using digital terrain models. Hydrol. Processes, 5: 59-79.

Rigon, R, A. Rinaldo, I. Rodriguez-Iturbe, R. L. Bras, and E. Ijjasz-Vasquez. 1993. Optimal channel networks: a framework for the study of river basin morphology. Water. Resour. Res., 29(6): 1635-1646.

Rinaldo, A., I. Rodriguez-Iturbe, R. Rigon, R. L. Bras, E. Ijjasz-Vasquez, and A. Marani. 1992. Minimum energy and fractal structures of drainage networks. Water Resour. Res., 28(9): 2183-2195.

Rinaldo, A., I. Rodriguez-Iturbe, R. Rigon, E. Ijjasz-Vasquez, and R. L. Bras. 1993. Self-organized fractal river networks. Physical Review Letters, 70(6): 822-825.

Rinaldo, A., G. K. Vogel, R. Rigon, and I. Rodriguez-Iturbe. 1995. Can one gauge the shape of a basin? Water Resour. Res., 31(4): 119-1127.

Robinson, J.S., M. Sivapalan, and J. Snell. 1995. On the relative roles of hillslope processes, channel routing, and network geomorphology in the hydrologic response of natural catchments. Water Resour. Res., 31(12): 3089-3101.

Rodhe, A. 1982. Spring flood - melt water or groundwater? Nord. Hydrol., 12: 21-30.

Rodriguez-Iturbe, I., M. González-Sanabria, and G. Caamaño. 1982. On the climatic dependence of the IUH: A rainfall-runoff analysis of the Nash model and the geomorphoclimatic theory. Water Resour. Res., 18(4): 887-903.

Rodriguez-Iturbe, E. Ijjasz-Vasquez, and R. L. Bras.1992b. Power law distributions of mass and energy in river basins. Water Resour. Res., 28(4): 1089-1093.

Rodriguez-Iturbe, I., M. Marani, R. Rigon, and A. Rinaldo. 1994. Self-organized river basin landscapes: Fractal and multifractal characteristics. Water Resour. Res., 30(12): 3531-3539.

Rodriguez-Iturbe, I., A. Rinaldo, R. Rigon, R. L. Bras, A. Marani, and E. Ijjasz-Vasquez. 1992a. Energy dissipation, runoff, and the three-dimensional structure of river basins. Water Resour. Res., 28(4), 1095-1103.

Rodriguez-Iturbe, I., and J. B. Valdes. 1979. The geomorphic structure of hydrologic response. Water Resour. Res., 15(6):1409-1420.

Rosso, R., B. Bacchi, and P. La Barbera. 1991. Fractal relation of mainstream length to catchment area in river networks. Water Resour. Res., 27(3):381-387.

Roulet, N.T., and M.K. Woo. 1988. Runoff generation in a low Arctic drainage basin. J. Hydrol., 101: 213-226.

Rouse, W. R., P. F. Mills, and R. B. Stewart. 1977. Evaporation in high latitudes. Water Resour. Res., 13(6): 909-914.

Rovansek, R. J., L. D. Hinzman, and D. L. Kane. 1996. Hydrology of a tundra wetland complex on the Alaskan Arctic Coastal Plain. Arctic and Alpine Research. 28(3): 311-317.

Sapozhnikov, V. B., and E. Foufoulo-Georgiou. 1996. Self-affinity in braided rivers. Water Resour. Res., 32(5): 1429-1439.

Sapozhnikov, V. B, and V. I. Nikora. 1993. Simple computer model of a fractal river network with fractal individual watercourses. J. Phys. A Math. *Gen.*, 26: L623-L627.

Scott, K. M. 1978. Effects of permafrost on stream channel behavior in arctic Alaska. U. S. Geological Survey Professional Paper 1068. Washington D.C.

Seagel, G. C., and R. P. Parish. 1974. Permafrost-runoff: the consulting engineer's experience. Proc. Of Workshop Seminar on Permafrost Hydrology, February 26-28, 1974. Calgary, Alberta, Canada, Canadian National Committee. p. 59-61.

Searcy, J. K.1959. Flow duration curves - Manual of hydrology, Part 2. Low flow techniques. U.S.G.S Water Supply Paper 1542-A.

Seiler, F. A. 1986. Use of fractals to estimate environmental dilution factors in river basin. Risk Anal., 6: 15-25.

Sellers, W. D. 1965. Physical Climatology. University of Chicago Press, Chicago.

Seyfried, M. S., and B. P. Wilcox. 1995. Scale and the nature of spatial variability: field examples having implications for hydrologic modeling. Water Resour. Res., 31(1), 173-184.

Shreve, R. L.1966. Statistical law of stream numbers. J. Geol., 74: 17-37.

Shreve, R. L. 1967. Infinite topologically random channel networks. J. Geol., 75(2): 178-86.

Sklash, M. G., and R. N. Farvolden. 1979. The role of groundwater in storm runoff. J. Hydrol., 43: 45-65.

Slaughter, C. W., and Kane, D. L. 1979. Hydrologic role of shallow organic soils in cold climate. Proc. Canadian Hydrology Symposium: 79 Cold Climate Hydrology, Vancouver, B. C., p. 380-389.

Slaughter, C. W., J. W. Hilgert, and E. H. Culp, E. H. 1983 Summer streamflow and sediment yield from discontinuous-permafrost headwaters catchments. Proc.

Fourth International Conference on Permafrost, Fairbanks, Alaska, p. 1172-1177.

Sloane, C. E., C. Zenone, and L. R. Mayo. 1975. Icings along the Trans-Alaska pipeline route. U.S. Geological Survey Open File report 75-87.

Smart, J. S. 1978. The analysis of drainage network composition. Earth Surface Processes, 3:129-170.

Smith, J.A. 1992. Representation of basin scale flood peak distributions. Water Resour. Res., 28: 2993-2999.

Smith, T. R., and F. P. Bretherton. 1972. Stability and the conservation of mass in drainage basin evolution. Water Resour. Res., 8(6): 1506-1529.

Snow, R. S. 1989. Fractal sinuosity of stream channels. Pure Appl. Geophys., 131: 99-109.

Strahler, A. N. 1952. Hypsometric (area-altitude) analysis of erosional topography. Geol. Soc. Am. Bull., 63: 1117-1142.

Strahler, A. N. 1957. Quantitative analysis of watershed geomorphology. Transactions of the American Geophysical Union, 38: 913-920.

Takayasu, H., I. Nishikawa, and H. Tasaki. 1988. Power-law mass distribution of aggregation systems with injection. Phys. Rev. A, 37: 3110-3117.

Tarboten, D. G., R. L. Bras, and I. Rodriguez-Iturbe. 1988. The fractal nature of river networks. Water Res. Resour., 24 (8): 1317-1322.

Tarboten, D. G., R. L. Bras, and I. Rodriguez-Iturbe. 1990. Comment on "On the fractal dimension of stream networks" by Paolo La Barbera and Renzo Rosso. Water . Resour. Res, 26 (9): 2243-2244.

Tarboten, D. G., R. L. Bras, and I. Rodriguez-Iturbe. 1991. On the extraction of channel networks from digital elevation data. Hydrol. Process., 5: 81-100.

Tarboten, D. G., R. L. Bras, and I. Rodriguez-Iturbe. 1992. A physical basis for drainage density. Geomorphology, 5: 59-76.

Tribe, A. 1992. Problems in automated recognition of valley features from digital elevation models and a new method toward their resolution. Earth Surface Processes and Landforms, 17: 437-454.

Troutman, B. M., and M. R. Karlinger. 1984. Averaging properties of channel networks using methods in stochastic branching theory, paper presented at the Workshop on Scale Problems in Hydrology, Princeton Univ., Princeton, N. J., Oct. 31 to Nov. 2, 1984.

Troutman, B. M., and M. R. Karlinger. 1985. Unit hydrograph approximations assuming linear flow through topologically random channel networks, Water Resour. Res., 21 (5): 743-754.

Walker, M. D., D. A. Walker, and K. R. Everett. 1989. Wetland Soils and Vegetation, Arctic Foothills, Alaska. U.S. Department of the Interior Biological Report 89(7).

Walker, D. A., N. A. Auerbach, L. R. Lestak, S. V. Mueller, and M. D. Walker. 1996. A hierarchic GIS for studies of process, pattern, and scale in an arctic

ecosystem: The Arctic System Science Flux Study, Kuparuk Basin, Alaska. Presented at the 2nd circumpolar arctic vegetation mapping workshop, Arendal, Norway, May 20-23, 1996.

Weller, G., F. S. Chapin, K. R. Everett, J. E. Hobbie, D. Kane, W. C. Oechel, C. L. Ping, W.S. Reeburgh, D. Walker, and J. Walsh. 1995. The Arctic Flux Study: a regional view of trace gas release. Journal of Biogeography, 22: 365-374.

Wels, C., C.H. Taylor, and R.J. Cornet. 1991. Streamflow generation in a headwater basin on the Precambrian Shield. Hydrol. Processes, 5: 185-199.

Willgoose, G., R. L. Bras, and I. Rodriguez-Iturbe. 1991. A physical explanation of an observed link area-slope relationship. Water Resour. Res., 27(7): 1679-1702.

Wolman, M.G. 1955. The natural channel of Brandywine Creek, Pennsylvania, U.S. Geol. Surv. Prof. Pap., 271.

Wolock D. M., and G. J. McCabe Jr. 1995. Comparison of single and multiple flow direction algorithms for computing topographic parameters in TOPMODEL. Water Resour. Res., 31(5): 1315-1324.

Woo, M. K., and P. Marsh. 1978. Analysis of error in the determination of snow storage for small high arctic basins. Journal of Applied Meteorology, 17:1537-1541.

Woo, M. K., and P. Steer. 1982. Occurrence of surface flow on arctic slopes, southwestern Cornwallis Island. Canadian Journal of Earth Sciences, 19(12): 2368-2377.

Woo, M. K., and P. Steer. 1983. Slope hydrology as influenced by thawing of the active layer, Resolute, N.W.T. Canadian Journal of Earth Sciences, 20(6): 978-986.

Woo, M. K., Z. Yang, Z. Xia, and D. Yang. 1996. Streamflow processes in an alpine permafrost catchment, Tianshan, China. Permafrost and Periglacial Processes, 5: 71-85.

Woo, M. K. 1986. Permafrost hydrology in North America. Atmosphere-Ocean, 24(3): 201-234.

Wood, E. F., M. Sivapalan, K. J. Beven, and L. E. Band. 1988. Effects of spatial variability and scale with implications to hydrologic modeling. J. Hydrol., 102: 29-47.

Woodruff, J. F., and J. D. Hewlett. 1970. Predicting and mapping the average hydrologic response for the eastern United States. Water Resour. Res., 6: 1312-1326.

Wright, R. K. 1983. Relationships between runoff generation and active layer development near Schefferville, Quebec. Proc. Fourth International Conference on Permafrost, July 17-22, 1983, Fairbanks, AK. p. 1412-1417.